Strategies within predator-prey interactions
–
from individuals to ecosystems

Michael Raatz

Univ.-Diss.

zur Erlangung des akademischen Grades
"doctor rerum naturalium"
(Dr. rer. nat.)
in der Wissenschaftsdisziplin "Ökologie"

eingereicht an der
Mathematisch-Naturwissenschaftlichen Fakultät
Institut für Biochemie und Biologie
der Universität Potsdam

Ort und Tag der Disputation: Potsdam, 06.03.2019

Hauptbetreuer: Prof. Dr. Alexander Wacker
Zweit-Betreuerin: Prof. Dr. Ursula Gaedke
Externer Gutachter: Prof. Dr. Sebastian Diehl

https://doi.org/10.25932/publishup-42658
https://nbn-resolving.org/urn:nbn:de:kobv:517-opus4-426587

UNIVERSITY
OF POTSDAM

Strategies within predator-prey interactions – from individuals to ecosystems

PHD Thesis

for the degree of

Dr. rer. nat.

Biology

Submitted by:
Michael Raatz

Prepared at:
Institute of Biochemistry and Biology

Evaluation:
PD Dr. Alexander Wacker
Prof. Dr. Ursula Gaedke
Prof. Dr. Sebastian Diehl

Potsdam, November 2018

UNIVERSITÄT
POTSDAM

Strategien in Räuber-Beute Interaktionen – vom Individuum bis zum Ökosystem

DISSERTATION

zur Erlangung des akademischen Grades

Dr. rer. nat.

im Doktoratsstudium der

Biologie

Eingereicht von:
Michael Raatz

Angefertigt am:
Institut für Biochemie und Biologie

Beurteilung:
PD Dr. Alexander Wacker
Prof. Dr. Ursula Gaedke
Prof. Dr. Sebastian Diehl

Potsdam, November 2018

Contents

1 General introduction

Ecosystems are complex systems composed of biotic interactions between individual organisms, their populations and the communities to which they belong, all of which are embedded into and shaped by the abiotic, environmental conditions. Us humans rely on these ecosystems as we make use of a broad number of ecosystem services. The importance to sustainably use and manage these ecosystems is increasingly recognized, though the need to preserve central ecosystem functions does not match the actual conservation efforts (Fischer et al. 2018).

A detailed understanding of abiotic and biotic interactions forms the foundation that is required for successful conservation and sustainable ecosystem management. The ecosystem processes we investigate today are the result of optimization processes selecting for different strategies that organisms apply to cope with their surrounding. Understanding these strategies, their drivers, and how they shape the interactions between organisms and their environment sheds light on the ecosystem functions and processes and is therefore of major importance to many sustainability and conservation goals (Chapin et al. 1996).

1.1 Abiotic interactions

The abiotic environment can interact with organisms and shape their growth, reproduction, physiology and behaviour, often yielding different strategies. Among the abiotic factors, temperature is especially important as it heavily impacts physiological rates of organisms and affects their lifestyle (Pomeroy and Wiebe 2001; Kessler and Lampert 2004; Koussoroplis and Wacker 2016). In aquatic environments, salinity is an abiotic factor that limits the distribution of primary producers (Kirst 1990). Similarly, the availability of nutrients and light may limit growth and reproduction (performance), for example because of patchiness or temporal fluctuations of these abiotic resources. The physical structure of a landscape often generates heterogeneities in resource distributions and habitat suitability, and may limit the mobility of organisms (Tucker et al. 2018).

Abiotic resource distributions however predominantly affect autotrophs, as they consume their resources directly from the abiotic environment, and are therefore especially vulnerable to them. Heterotrophs in turn rely on already packaged energy sources from other organisms, finally making them dependent on autotrophs (and patchiness or fluctuations in their availability), but sparing them from sustaining a carbon-fixating machinery (Raven 1995; Jones 2000). Mixotrophy is a strategy that bridges these two extremes and enables organisms to perform photosynthesis and also acquire carbon by direct ingestion (Andersen et al. 2015).

Abiotic interactions may also give rise to feedbacks when organisms impact the above environmental factors, such as spatial distribution of abiotic resources or landscape structure. For example, organisms decrease the available resources by consumption or they may shape their environment to meet their needs, e.g. if they are ecosystem engineers.

1.2 Biotic interactions

Within this abiotic environment, organisms engage in a multitude of organism-organism interactions (Fig. 1.1). Prominent representatives of such biotic interactions are mutualism, commensalism, ammensalism, competition, predation and parasitism (Polis et al. 1989). While the result of mutualistic interactions is positive for both interaction partners, commensalism and ammensalism indicate interactions where only one partner benefits or loses, respectively, without negative effects for the other. Competition between two interaction partners implies negative impacts for both of them (Fig. 1.1a) (Connell 1983). Trophic interactions, such as predation and parasitism, are interactions where one partner benefits from the losses of the other, for example if one partner consumes the other (Holling 1959a,b). Trophic levels can be defined for predation and parasitism, whereas the benefiting partner forms the higher trophic level (Hairston and Hairston 1993). Within this work, I will focus on strategies that emerge in the context of predation.

Trophic interactions determine the structure of and energy fluxes within most food webs. They can mediate coexistence or extinctions of species and drive changes to their functional properties (traits), either by affecting the genetic diversity, the expressed phenotypes or the behaviour. An understanding of the mechanisms that determine these direct interactions and the indirect interactions that shape them is therefore at the heart of ecological research.

I will point out different strategies that organisms may apply to ensure their persistence and increase their fitness and abundance, while participating in predator-prey interactions. Often, persistence results in the permanent coexistence of multiple organisms employing different strategies. This coexistence is the foundation of biodiversity and is more and more realized to be the requirement for the preservation of many ecosystem services (Hooper et al. 2005; Oliver et al. 2015).

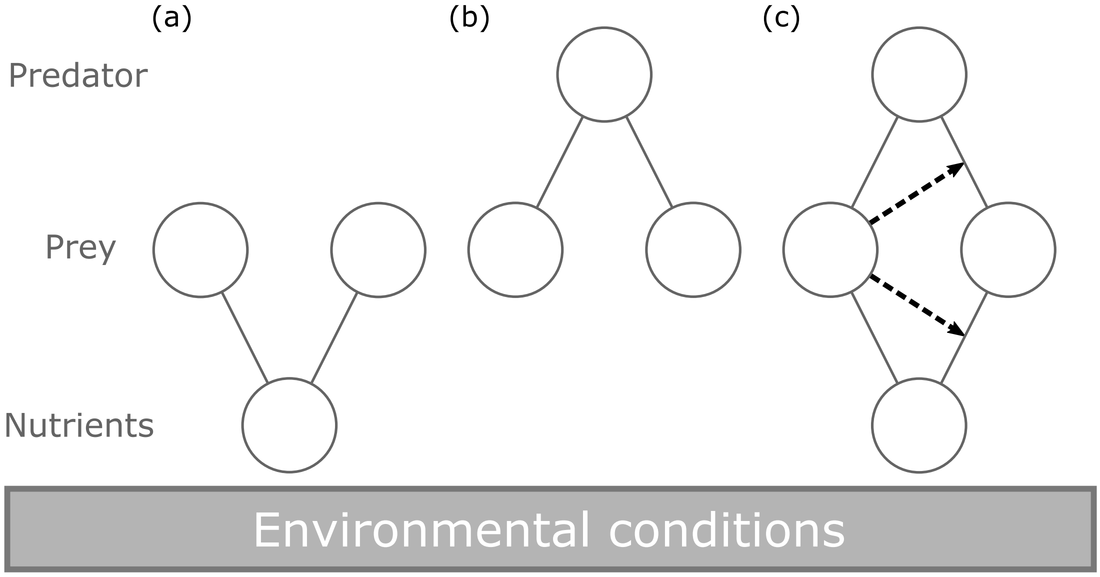

Figure 1.1 Examples of biotic interactions that are embedded into, and affected by, the abiotic environment. (a) Competition for abiotic nutrients by the prey. (b) Apparent competition of two prey types sharing one predator. (c) The combination of competition and apparent competition, which might be affected by indirect interactions, for example when one prey type affects the growth of, or predation on, the other prey type (black dashed arrows).

1.3 Indirect interactions

Besides the direct biotic interactions defined above, there are also indirect interactions between organisms that are of similar importance for ecosystems (Fig. 1.1c) (Werner and Peacor 2003; Jonsson et al. 2018). Just like direct interactions, these indirect interactions give rise to strategies that organisms may employ to ensure their persistence or supersede competitors. Such indirect relations can arise as soon as more than two partners interact and often manifest by shaping and altering the outcomes of direct interactions. If for example two species compete for the same food source, resulting in three interaction partners, their combined effect might be non-additive, with super-additivity and sub-additivity being termed facilitation (e.g. Sommer 1992) and interfence (Huisman and De Boer 1997), respectively. Another typical indirect interaction emerges as soon as two prey species share the same predator (apparent competition, Fig. 1.1b,c). Here, an increasing biomass of one prey species harms the other prey species not predominantly because of resource depletion, but by sustaining a higher predation pressure (Holt 1977; Holt and Lawton 1994; Abrams et al. 1998). Resource competition and apparent competition can also co-occur (Grover and Holt 1998), or vary temporally in their importance when populations cycle and either the resource concentration or the predator biomass is at high levels.

1.4 Strategies emerge from trait variation and optimization

Within food webs, organisms are situated at the network nodes and biotic and abiotic interactions form the edges (Fig. 1.1). These interactions are pathways that may be modified if the interaction partners select different strategies. The more complex a food web becomes, the more interactions shape the performance of organisms, allowing for more feasible strategies. If the web changes its structure (e.g. by the invasion of a new species) or the strengths of the interactions, different strategies may emerge and either coexist with or out-compete the resident strategy (Mack et al. 2000). Similarly, changes to the environment, in which the food web is embedded, can drive alterations in the optimal strategy.

The emergence of new strategies may be driven by selection from a pool of existing strategies (e.g. species or clonal sorting, phenotypic plasticity), or by the creation of entirely new ones (e.g. by mutations or recombination). The pool of existing strategies may be composed of inter-specific variation, i.e. functional differences between species, or intra-specific variation (Bolnick et al. 2011; Des Roches et al. 2018), i.e. trait variability within one species, for example if phenotype expression is plastic. The extent of food web or environmental changes determines the pressure to adapt existing strategies or to develop new ones (Merilä and Hendry 2014).

1.5 Thesis overview

There is a vast number of factors that impact trophic interactions on very different scales (Fig. 1.2). Within this thesis, I added to this list and went from smaller to larger scales, investigating the effects of (i) functioning of individual organisms, i.e. their physiology, (ii) nutritional composition of prey, (iii) adaptation of defense and offense traits, (iv) non-obvious interactions with other parts of the food web, i.e. effects of the food web structure. When viewed from the perspectives of either the predator, aiming for increasing its consumption, or the prey, trying to reduce the grazing pressure, these factors act as drivers for particular strategies, which benefit the organisms employing them (Fig. 1.3).

I studied these drivers, the strategies they give rise to, and the effects they bring about in aquatic phytoplankton-zooplankton systems. These model systems are representatives of plant-herbivore interactions, a broader class of predator-prey interactions. They provide a valuable basis for understanding interactions in larger food webs, as they are both experimentally testable and simple enough to encompass not too many details, see e.g. Boraas (1983). Their short generation time, together with the good manageability and convenient optical observation allows to obtain highly controlled, longterm experimental observations from chemostat systems, to which simulation models may be compared.

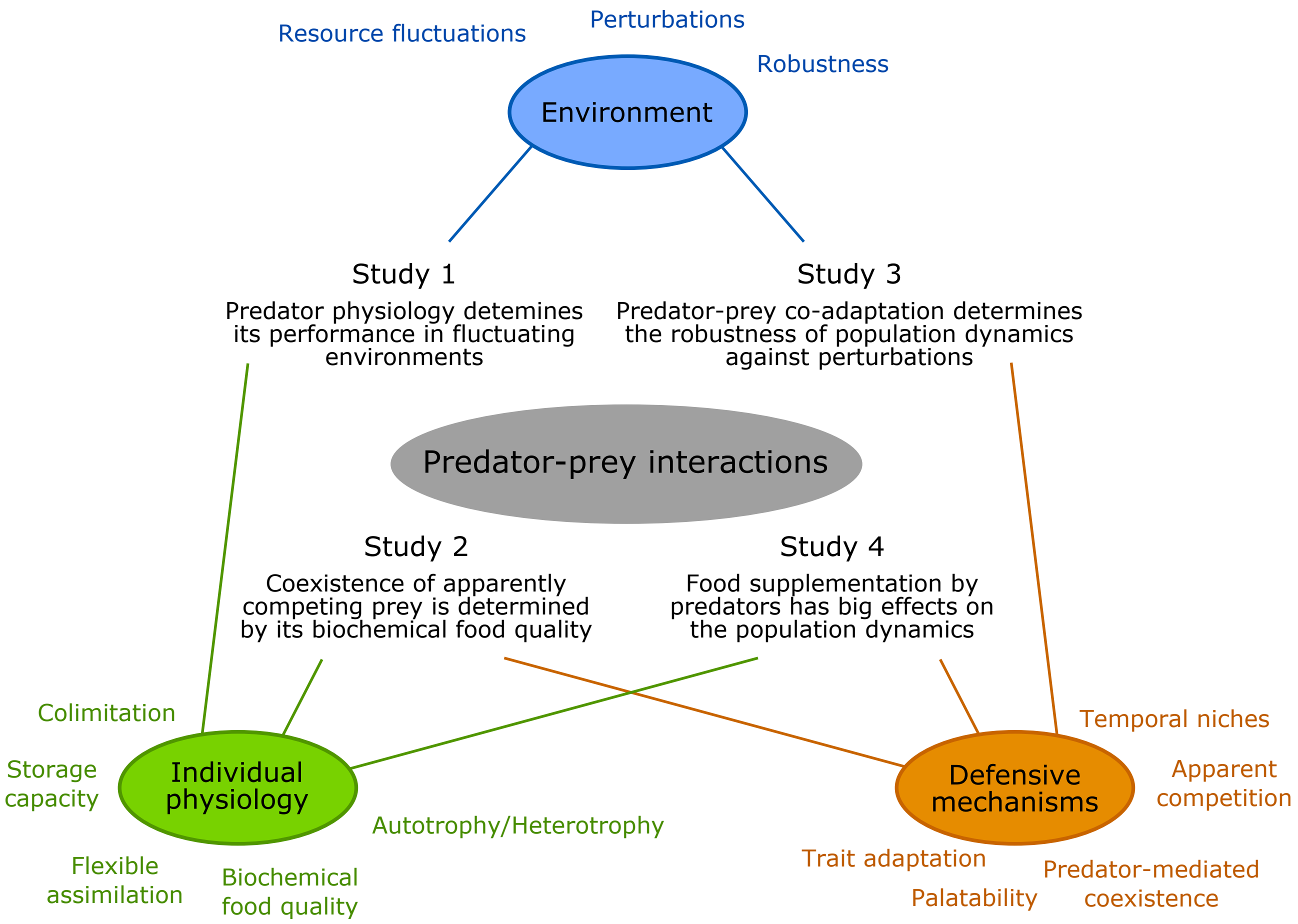

Figure 1.2 Conceptual frame of this thesis that centers around predator-prey interactions in aquatic food webs with different factors (given by the keywords) acting on these interactions. These factors may be grouped into the three larger categories individual physiology (green), defensive mechanisms (orange), or environment (blue). Some of these factors act as drivers for particular strategies that organisms may apply to ensure their persistence or increase their biomass.

Chapter 2

In the first study, which is under revision after an invitation to resubmit, I focus on individual predators and their physiology (Fig. 1.3a). We investigated how the juvenile growth rate of individual predators (in this study referred to as consumers) is affected by fluctuations in the availability of limiting nutrients within their prey (termed resources here). We hypothesized that different physiological strategies may increase performance under different fluctuation regimes. Accordingly, we set up a dynamic energy budget model that factorially includes storage of nutrients (mineral and biochemical) and acclimation of assimilation efficiencies, and experimentally tested the effects of nutrient fluctuations on *Daphnia magna*. As more than one nutrient may contemporaneously limit (co-limit) the growth of predators, we investigated also the effects of co-variance of such co-limiting nutrients. Throughout this study, we fixed the prey densities for single fluctuation periods, thus excluding feedbacks and allowing to only study specifically the predator level. We found that the temporal structure

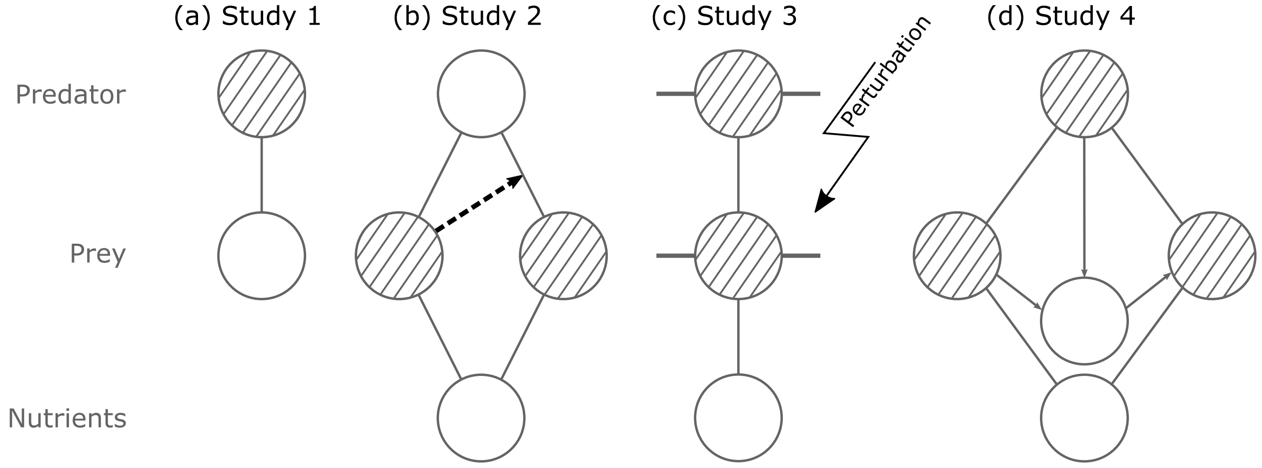

Drivers	Co-limitation Resource fluctuation	Competition Apparent competition Prey food quality	Press and pulse perturbations	Addition of bacteria (heterotrophic) to algae (autotrophic) prey
Strategies	Storage Acclimation	Defense Supply of essential nutrients	Adaptation of offense and defense	Degree of bacterivory Provision of essential resources to competitors Recycling
Effect variable	Growth rate	Coexistence Population dynamics	Robustness of pop. dynamics Coexistence	Predator biomass Prey coexistence Trophic transfer efficiency

Figure 1.3 Systems investigated in this thesis. Many of the factors shown in Fig. 1.2 act as drivers for certain strategies which may be applied by the prey or the predators. Application of strategies that were studied here is depicted by the grey hatching. These strategies impact different effect variables. The vertical bars in (c) represent trait adaptability.

of the fluctuation (frequency, phase, amplitude and covariance) has strong effects on the performance of *Daphnia*, which was in agreement with our model predictions. From the model we concluded that nutrient storage and acclimation of assimilation efficiencies are benefiting somatic growth in different regimes of the fluctuation spectrum.

Chapter 3

In the second study, which is published in Oikos, I included feedbacks by explicitly modelling nutrient and prey densities in a chemostat model (Fig. 1.3b). Here, I extended the focus on colimitation and investigated how this might affect coexistence in small food webs. I assumed that the predator feeds on two different prey species, which both deliver carbon as an energy source, but only one of them contains also an essential nutrient in sufficient amounts. I hypothesized that such food-quality differences between the prey species might directly affect the predator dynamics in the system and possibly feed back on the prey level. To allow for different scenarios of coexistence or dominance of either one prey species within the prey community, I assumed a defense-growth trade-off between them and studied how the trade-off–mediated coexistence pattern is affected by various food quality differences. I found that food quality can have strong effects on the population dynamics and coexistence patterns along the trade-off.

Chapter 4

I continued to investigate the effect of defense-growth trade-offs in predator-prey systems in chapter 4, which is submitted and currently under review. Now, however, I released the trait values of prey defense and predator offense, and studied the different predator-prey dynamics that may emerge from trait adaptation (Fig. 1.3c). I centered this project within the context of environmental perturbations that disturb food webs and investigated how the adaptive capacity of prey and predator affects the robustness of the predator-prey dynamics against such perturbations. I included pulse and press perturbations and measured different robustness properties (resilience, elasticity and resistance). Following a pulse perturbation, i.e. an instantaneous shift in biomasses or trait values, resilience determines whether the system returns to the pre-perturbation dynamics, and was measured by the extinction probability of the predator. Elasticity is the property governing how long this return takes and was measured as the return time. For the effect of press perturbations I developed a new measure for resistance, i.e. the distance between the pre- and post-perturbation attractors. In this study, faster co-adaptation tended to increase resilience and elasticity. However, I found complex effects of co-adaptation on the impact of press-perturbations, which may complicate predictions on the effect of environmental change for co-adaptive predator-prey systems.

Chapter 5

I increased the scope again in chapter 5, which is published in Limnology and Oceanography - Methods, and studied how adding a heterotrophic prey (bacteria), i.e. changing the food web structure, may affect the predator-prey dynamics (Fig. 1.3d). We tightly coupled this project to typical chemostat experiments with phyto- and zooplankton and investigated what effect bacteria as the additional prey species might have in this system. Different from chapter 2, now the bacteria are co-limited (by carbon and nitrogen), i.e. co-limitation occurs now on the trophic level of the prey. This results in a mixture of apparent competition between algae and bacteria and facilitation of bacteria by the algae, as they supply part of the carbon pool that is essential to the bacteria. I found that considering the microbial loop in phytoplankton-zooplankton chemostats may explain complex population dynamics that are sometimes observed experimentally. We proposed that by choosing the right predator species/traits experimenters may reduce the often unwanted impact of bacteria.

Bibliography

Abrams, P. A., Holt, R. D., and Roth, J. D. (1998). Apparent competition or apparent mutualism? Shared predation when populations cycle. *Ecology* 79: 201–212.

Andersen, K. H., Aksnes, D. L., Berge, T., Fiksen, Ø., and Visser, A. (2015). Modelling emergent trophic strategies in plankton. *J. Plankton Res.* 37: 862–868.

Bolnick, D. I., Amarasekare, P., Araújo, M. S., et al. (2011). Why intraspecific trait variation matters in community ecology. *Trends Ecol. Evol.* 26: 183–192.

Boraas, M. E. (1983). Population dynamics of food-limited two-stage chemostat culture. *Am. Soc. Limnol. Oceanogr.* 28: 546–563.

Chapin, F. S., Torn, M. S., and Tateno, M. (1996). Principles of Ecosystem Sustainability. *Am. Nat.* 148: 1016–1037.

Connell, J. H. (1983). On the Prevalence and Relative Importance of Interspecific Competition: Evidence from Field Experiments. *Am. Nat.* 122: 661–696.

Des Roches, S., Post, D. M., Turley, N. E., et al. (2018). The ecological importance of intraspecific variation. *Nat. Ecol. Evol.* 2: 57–64.

Fischer, M., Rounsevell, M., Rando, A. T.-M., et al. (2018). IPBES: Summary for policymakers of the regional assessment report on biodiversity and ecosystem services for Europe and Central Asia of the Intergovernmental Science-Policy Platform on Biodiversity and Ecosystem Services.

Grover, J. P. and Holt, R. D. (1998). Disentangling resource and apparent competition: Realistic models for plant-herbivore communities. *J. Theor. Biol.* 191: 353–376.

Hairston, N. G. and Hairston, N. G. (1993). Cause-Effect Relationships in Energy Flow, Trophic Structure, and Interspecific Interactions. *Am. Nat.* 142: 379–411.

Holling, C. S. (1959a). Some Characteristics of Simple Types of Predation and Parasitism. *Can. Entomol.* 91: 385–398.

Holling, C. S. (1959b). The Components of Predation as Revealed by a Study of Small-Mammal Predation of the European Pine Sawfly. *Can. Entomol.* 91: 293–320.

Holt, R. D. and Lawton, J. H. (1994). The Ecological Consequences of Shared Natural Enemies. *Annu. Rev. Ecol. Syst.* 25: 495–520.

Holt, R. D. (1977). Predation, apparent competition, and the structure of prey communities. *Theor. Popul. Biol.* 12: 197–229.

Hooper, D. U., Chapin, F. S., Ewel, J. J., et al. (2005). Effects of biodiversity on ecosystem functioning: A consensus of current knowledge. *Ecol. Monogr.* 75: 3–35.

Huisman, G. and De Boer, R. J. (1997). A formal derivation of the "Beddington" functional response. *J. Theor. Biol.* 185: 389–400.

Jones, R. I. (2000). Mixotrophy in planktonic protists: an overview. *Freshw. Biol.* 45: 219–226.

Jonsson, T., Kaartinen, R., Jonsson, M., and Bommarco, R. (2018). Predictive power of food web models based on body size decreases with trophic complexity. *Ecol. Lett.* 21: 702–712.

Kessler, K. and Lampert, W. (2004). Fitness optimization of Daphnia in a trade-off between food and temperature. *Oecologia* 140: 381–387.

Kirst, G. O. (1990). Salinity Tolerance of Eukaryotic Marine Algae. *Annu. Rev. Plant Physiol. Plant Mol. Biol.* 41: 21–53.

Koussoroplis, A.-M. and Wacker, A. (2016). Covariance modulates the effect of joint temperature and food variance on ectotherm life-history traits. *Ecol. Lett.* 19: 143–152.

Mack, R. N., Simberloff, D., Lonsdale, W. M., et al. (2000). Biotic invasions: causes, epidemiology, global consequences, and control. *Ecol. Appl.* 10: 689–710.

Merilä, J. and Hendry, A. P. (2014). Climate change, adaptation, and phenotypic plasticity: The problem and the evidence. *Evol. Appl.* 7: 1–14.

Oliver, T. H., Heard, M. S., Isaac, N. J., et al. (2015). Biodiversity and Resilience of Ecosystem Functions. *Trends Ecol. Evol.* 30: 673–684.

Polis, G. A., Myers, C. A., and Holt, R. D. (1989). The Ecology and Evolution of Intraguild Predation: Potential Competitors That Eat Each Other. *Annu. Rev. Ecol. Syst.* 20: 297–330.

Pomeroy, L. R. and Wiebe, W. J. (2001). Temperature and substrates as interactive limiting factors for marine heterotrophic bacteria. *Aquat. Microb. Ecol.* 23: 187–204.

Raven, J. A. (1995). “Comparative aspects of chrysophyte nutrition with emphasis on carbon, nitrogen and phosphorus”. In: *Chrysophyte Algae Ecol. Phylogeny Dev.* Cambridge, UK, Cambridge University Press, pp. 95–118.

Sommer, U. (1992). Phosphorus-limited Daphnia: Intraspecific facilitation instead of competition. *Limnol. Oceanogr.* 37: 966–973.

Tucker, M. A., Böhning-Gaese, K., Fagan, W. F., et al. (2018). Moving in the Anthropocene: Global reductions in terrestrial mammalian movements. *Science* 359: 466–469.

Werner, E. E. and Peacor, S. D. (2003). A review of trait-mediated indirect interactions in ecological communities. *Ecology* 84: 1083–1100.

1.6 Declaration of contributions

This thesis comprises four independent studies that are either published or undergoing peer-review.

Chapter 2

submitted as: Resource co-limited growth in fluctuating environments

Apostolos-Manuel Koussoroplis*, Svenja Schälicke*, Michael Raatz*, Moritz Bach and Alexander Wacker

* These authors contributed equally.

AK and AW designed the study. AK and SS performed the experiments. SS and AW provided the statistical analyses. AK and I developed the model and analyzed it with assistance by MB. I developed the acclimation model component and provided the final model results. AK, SS and I wrote the first draft of the manuscript. All authors contributed to later versions of it.

Chapter 3

published as: High food quality of prey lowers its risk of extinction, 2017, Oikos, 126: 1501-1510.

Michael Raatz, Ursula Gaedke and Alexander Wacker

AW designed the study. I developed the variable assimilation efficiency. I analyzed the model, with support by UG and AW. I wrote the first draft. UG and AW provided significant suggestions for later versions.

Chapter 4

submitted as: Co-adaptation impacts the robustness of predator-prey dynamics against perturbations

Michael Raatz, Ellen van Velzen and Ursula Gaedke

EV and UG conceived the study. EV and I developed the model. I performed the model analysis and wrote the first draft. All authors contributed to later versions of the manuscript.

Chapter 5

published as: One man's trash is another man's treasure - the effect of bacteria on phytoplankton-zooplankton interactions in chemostat systems, 2018, Limnology and Oceanography Methods, 16: 629-639.
Michael Raatz, Svenja Schälicke, Michael Sieber, Alexander Wacker, Ursula Gaedke
MS, UG and I conceived the study. I developed the static model, with help from UG. MS provided a first dynamic model version which was extended by UG and me. SS and AW provided practical information and measured model parameters. I performed the model analysis and wrote the first draft. All authors contributed to later versions of the manuscript.

Potsdam, 23 November 2018

Michael Raatz PD Dr. Alexander Wacker

2 Physiology determines predator performance under fluctuating food quality

Resource co-limited growth in fluctuating environments

Apostolos-Manuel Koussoroplis*[1,2], Svenja Schälicke*[1], Michael Raatz*[1], Moritz Bach[1] and Alexander Wacker[1]

[1] Institute of Biochemistry and Biology, University of Potsdam, Potsdam, Germany

[2] L.M.G.E. UMR CNRS 6023, Université Clermont Auvergne, Aubière, France

* These authors contributed equally.

Abstract

Theory predicts that resource variability often hinders consumer performance. Yet, how this effect depends on the temporal structure of resource fluctuations encountered within the lifetime of an individual remains poorly understood. We tackle this issue by combining a Dynamic Energy Budget model with feeding experiments of *Daphnia magna*. We decompose the complexity of natural resource fluctuations and tested the effect of fluctuation amplitude, resource peak timing (phase) and co-limiting resource covariance along different frequencies. Model and experiments show that resource storage enhances performance at high, but yields a sensitivity of growth to resource peak timing at low frequencies. Instead, digestive acclimation is beneficial at low frequencies. Negative covariance causes stronger growth depression at low, but might be beneficial at intermediate frequencies. Larger amplitudes exacerbate these effects. Viewed in the light of environmental change, we predict counterintuitive impacts of co-occurring perturbations to the temporal structure of resource supply for consumer performance.

Introduction

Climate change is expected to increase the frequency of extreme events (Meehl and Tebaldi 2004; Rahmstorf and Coumou 2011; Field et al. 2012). Providing local perturbations to established systems, these extreme events can promote environmental heterogeneity (Turner 2010). In contrast, anthropogenic impacts, such as pollution and industrialized agricultural practices, may induce biodiversity loss and simplify ecosystems thus decreasing environmental heterogeneity (Gámez-Virués et al. 2015). Within the tension of these two opposing scenarios the spatiotemporal variability perceived by organisms may either increase, decrease or remain unchanged.

The nutritional traits of plant or animal prey such as their composition of limiting resources or secondary metabolites strongly influence the organismal performance and consumer population dynamics (R. Sterner and Elser 2002; Simpson and Raubenheimer 2012; Hunter 2016; Sperfeld et al. 2016; Raatz et al. 2017). Spatiotemporal variability in the nutritional quality of food resources is inherent to natural consumer-resource systems (Orians and Jones 2001; Park 2004; Junker and Cross 2014; Grosbois et al. 2017), and most consumers face intense and frequent fluctuations in food quality during their lifetime. Accumulating evidence shows that such resource variability strongly influences consumers at the individual (Stockhoff 1993; Hood and R. W. Sterner 2010; Pearse et al. 2018), population, and community level (Underwood 2004; Riolo et al. 2015) and may have far-reaching ecological implications, e.g. for the control of herbivore pest populations in agroecosystems (McArt and Thaler 2013; Wetzel et al. 2016). The importance of resource variability results from the deviation between performance achieved at fluctuating resource supply and performance achieved at constant, average resource supply (variance effect, Fig. 2.1A). If performance follows a non-linear saturating function of resource concentration, performance decreases for higher resource variability (Jensen's inequality (Ruel and Ayres 1999; Wetzel et al. 2016)). However, developing a more mechanistic basis of resource variability effects would allow better predictions of consumer population dynamics in natural communities.

To date, studies on resource variability focused on single nutritional traits (Carlotti et al. 2010; Hood and R. W. Sterner 2010; Wagner et al. 2017). Yet, consumer performance can be simultaneously driven by several nutritional traits of their food (e.g. concentrations of various mineral and biochemical resources or secondary metabolites), a situation known as co-limitation (Sperfeld et al. 2012, 2016). Hence, when feeding in nutritionally variable environments, consumers need to acquire, store and use multiple resources which might, or might not, co-occur temporally and spatially. For example, many consumers need to mix different food items with imbalanced nutrient ratios to acquire a sufficient blend of the co-limiting resources (Simpson and Raubenheimer 2012). Such consumers typically experience negative covariance in the co-limiting resources if the availability of the different food items does not coincide in time. Co-limiting resources can also co-occur at high and balanced concentrations in only one food item while being low or absent in all other. Ecological factors such as patchiness, fear, territoriality, or physical constraints (Winder et al. 2004; Hebblewhite and Merrill 2009; Lasley-Rasher et al. 2011; Camp et al. 2015) may only allow intermittent access to the high quality food items, the rest of time being spent on low quality food. This leads to positive covariance in co-limiting resources since their availability for the consumer peaks and drops simultaneously over time.

When co-limiting resources act non-additively, the resource covariance pattern considerably influences consumer performance (Koussoroplis et al. 2017a). A consumer should therefore perform differently in positive and negative covariance scenarios although temporal means and variances of the co-limiting resources are the same (covariance effect sensu Koussoroplis and Wacker (2016); Fig. 1B). Given the propensity of co-limiting resources to interact (Simpson and Raubenheimer 2012; Sperfeld et al. 2016), the importance of resource variability for consumers cannot be addressed without considering the interplay of co-limitation and the spatiotemporal covariance of the co-limiting resources in the landscape.

Temporal and spatial resource variability are coupled and both translate to a perceived temporal fluctuation. Independently of whether the consumer is sessile in a dynamic environment (e.g. bivalves in tidal estuarine systems) or mobile in a heterogeneous landscape (e.g. daily vertically migrating zooplankton), nutritional variance and covariance are always experienced by the consumer as temporal fluctuations in resource supply. Changes in spatial or temporal contrasts of resource availability influence the amplitude of perceived resource fluctuation, whereas the grain-size of the environment (i.e. size or duration of food patches), the motility and life span, as well as the foraging behavior of the consumer influence the frequency and phase of the perceived fluctuations.

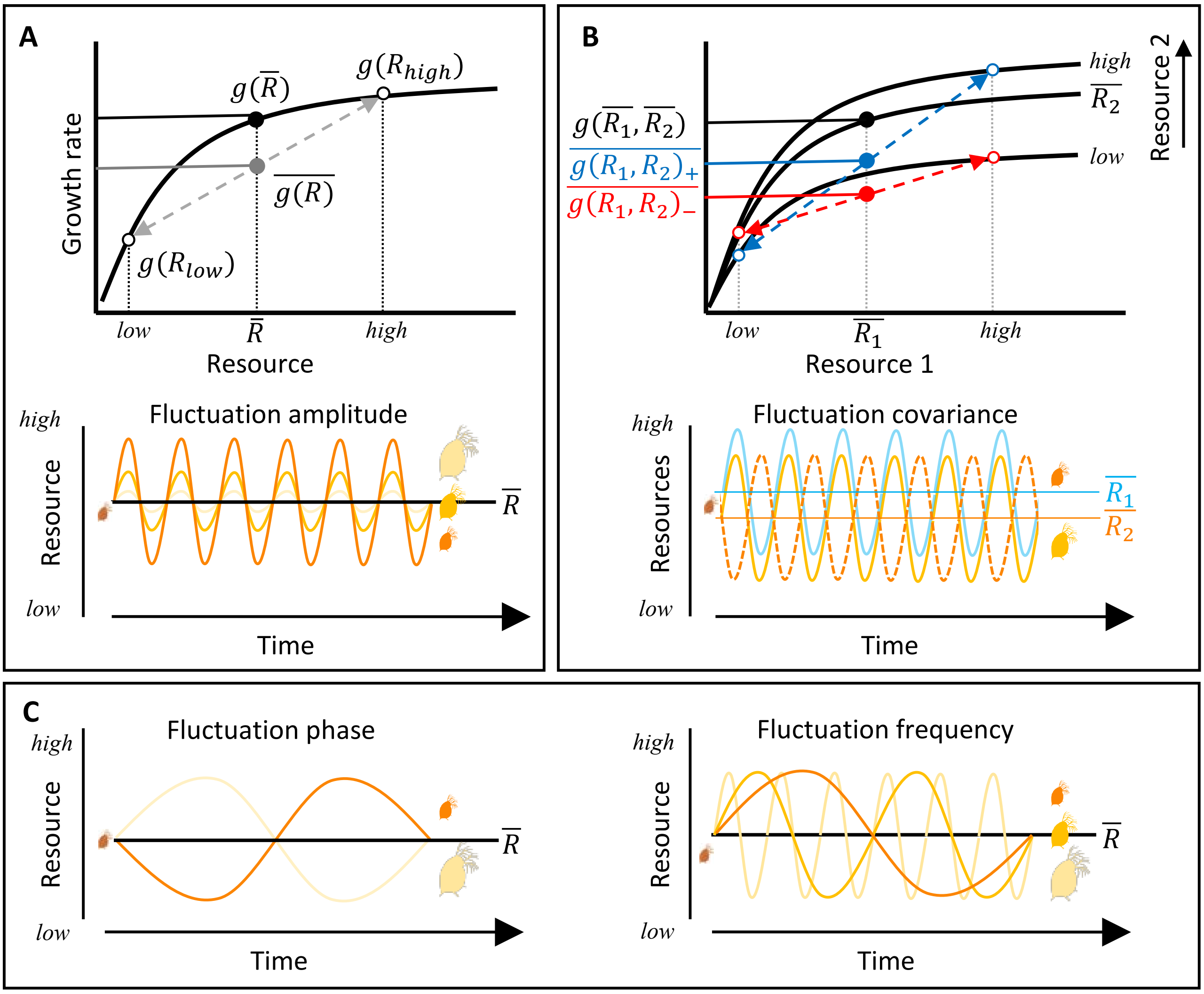

Figure 2.1 Hypotheses. (A) For single resource limitation, non-linear averaging predicts that the average growth rate of a consumer experiencing fluctuating supply in a limiting resource R, $\overline{g(R)}$, should be lower than the growth rate of a consumer experiencing a constant resource environment with same average resource conditions, $g(\overline{R})$. Consumer growth rate should decrease with increasing resource fluctuation amplitude. (B) When expanding to two synergistically co-limiting resources (R_1, R_2), the average growth rate of a consumer experiencing positively covarying co-limiting resources, $\overline{g(R_1, R_2)_+}$, should be higher than that of a consumer experiencing negative covariance, $\overline{g(R_1, R_2)_-}$. Note that an opposite covariance effect is expected if the co-limiting resources are antagonistic. (C) Because of reserve and acclimation effects (see text), the realized growth and therefore the exactitude of non-linear averaging predictions (panels A and B) should be modulated by the resource fluctuation phase and frequency (for simplicity, only single resource cases are depicted).

The performance of a consumer in a nutritionally variable environment can be empirically predicted from the resource-dependent responses generated under constant conditions (Sperfeld et al. 2016) using non-linear averaging methods (Wetzel et al. 2016; Denny 2017; Koussoroplis et al. 2017a). Yet, non-linear averaging needs to be regarded as a null-hypothesis based on the assumption that performance measured over longer time scales (typically several days) is a good approximation of the instantaneous performance in a fluctuating environment (Dowd et al. 2015). Obviously, this is not always the case as various physiological processes, which are not apparent under constant conditions, can manifest in a fluctuating environment. In this case, consumer performance in a variable environment deviates from that predicted by non-linear averaging (Niehaus et al. 2012; Kingsolver and Woods 2016; Koussoroplis et al. 2017a). For example, most living organisms first store recently acquired energy and nutrients into a metabolically inactive pool (hereafter reserves (Kooijman 2010)), which are subsequently mobilized and used for maintenance, growth, and reproduction. Such reserves may buffer the effects of environmental resource fluctuations on performance (hereafter reserve effect) (Muller and Nisbet 2000; Fujiwara et al. 2004; Hood and R. W. Sterner 2010). Furthermore, many organisms dynamically acclimate to fluctuating resources by e.g. adjusting nutrient extraction and transport through gut enzyme modifications (Karasov et al. 2011; Koussoroplis et al. 2017b), thereby improving assimilation efficiency of the resource that becomes most limiting (Clissold et al. 2010; Urabe et al. 2018). Acclimation processes may also have negative consequences if such processes are costly (Wetzel et al. 2016) or when acclimation lags behind the changes in environmental conditions (Kingsolver and Woods 2016). If acclimation is too slow compared to the fluctuations of the environment, organisms will underperform most of the time relative to non-linear average predictions (Niehaus et al. 2012; Koussoroplis et al. 2017a). This acclimation effect thus improves or decreases performance in fluctuating environments. Because of their innate physiological constraints, reserves and acclimation may operate at certain temporal scales, yielding a scale dependence of consumer performance, i.e. a different response to high and low frequencies at the same fluctuation amplitude (Koussoroplis et al. 2017a). Reserves and acclimation create a dependence of instantaneous growth on the nutritional history of an organism not only in terms of frequency, but also in terms of the phase of resource fluctuations.

Here, we test the hypothesis that for the same average and a fixed amplitude of resource quality fluctuations, environments with different temporal structures (i.e. resource supply fluctuation, covariance, frequency and phase, Fig. 2.1C) lead to altered consumer performances that do not necessarily comply with non-linear averaging predictions. We use a two-resource Dynamic Energy Budget (DEB) model (Fig. 2.2) to predict growth of a consumer in an environment with constant or fluctuating resource supply and compared the predictions to explore how the temporal structure of the environment mediates growth differences under fluctuating resources. Model predictions were experimentally reproduced by rearing juvenile *Daphnia magna* at variable phosphorus (P) and cholesterol supply. Our study offers both theoretical and empirical evidence that the temporal structure of resource availability can strongly decrease consumer performance in a fluctuating environment and provides a framework for modeling such negative effects. Using our model to predict the outcomes of combined changes in resource supply fluctuation amplitude and frequency enables novel insights on how landscape homogenization might affect local consumer species.

Materials and Methods

Design of the study

Within this study the organism is exposed either to a sequence of resource regimes with high and low concentrations of two co-limiting resources, which fluctuate in different frequencies, or to different constant conditions. Five constant treatments result from supplying constant concentrations of both resources either high or low, one high and the other low or both at the mean of high and low (Fig. 2.1A-B; open and black circles). Constant treatments were used to calculate non-linear averaging predictions for growth of the consumer (Fig. 2.1A-B). In treatments of fluctuating resources, concentrations (high or low) are arranged in variance scenarios, where only one of the two resources fluctuates, and in positive and negative covariance scenarios with high concentrations of the two resources coinciding or alternating, respectively, keeping the same average resource concentration as in constant conditions treatments. Different fluctuation frequencies (i.e. time spans of the resource regimes) and different phases (i.e. initial combinations of resource concentrations) were studied. The total duration of exposure was the same across treatments. This allows comparing growth responses to constant and to fluctuating resource supply at different fluctuation frequencies (Fig. 2.1).

Model structure

Based on General DEB Theory (Kooijman 2010) we constructed an ODE-model that predicts the juvenile somatic growth of an organism (Tab. 2.1). The three important aspects of the model are (i) co-limitation by two interactively essential resources (this constitutes the null-model), (ii) independent storage of these resources in two reserves and (iii) regulation of assimilation efforts depending on the relative filling of the reserves with a trade-off between the two resources.

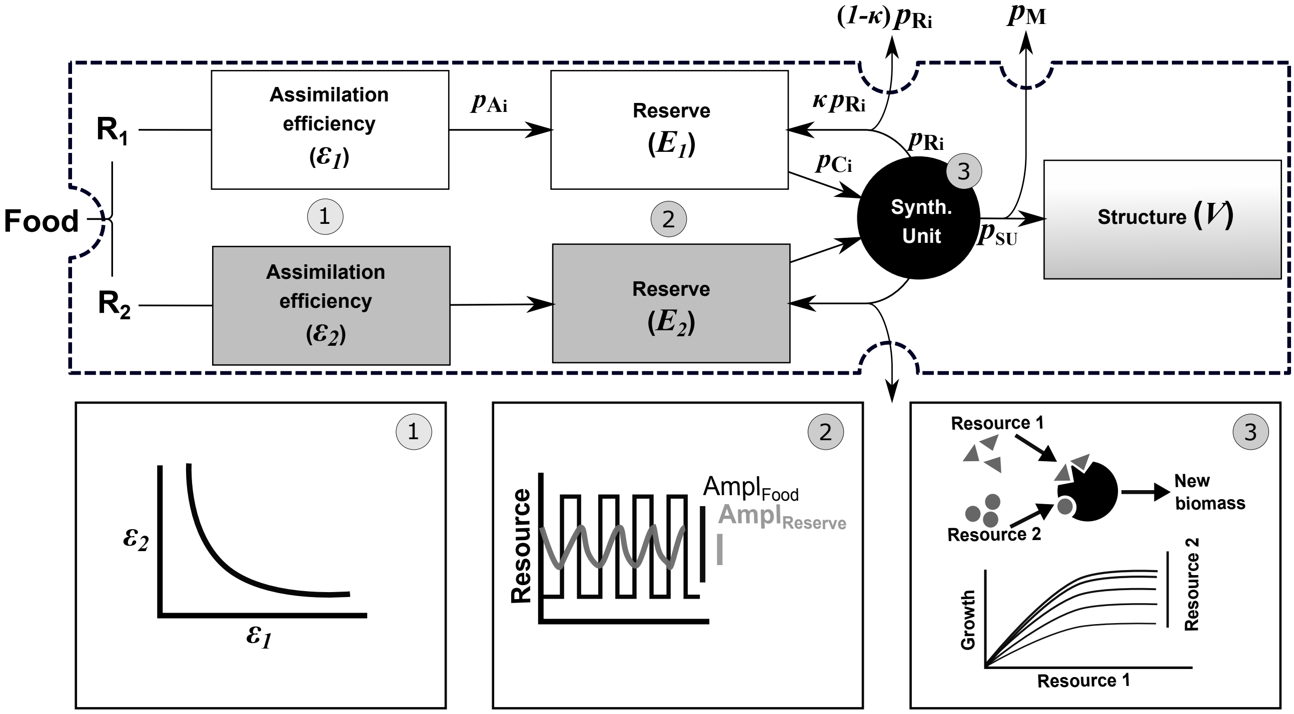

Figure 2.2 DEB model. Arrows indicate fluxes and rectangles indicate the state variables. Numbered circles indicate implemented physiological mechanisms: (i) The organism has the possibility to acclimate its assimilation efficiency to the resource that has the lower reserves (most limiting). The acclimation process involves a time lag and implies a trade-off shown in the left panel below. (ii) The organism has a reserve compartment for each resource that buffers the amplitude of higher frequency fluctuations in ingested resources (middle panel below). (iii) The synthesizing unit (SU) merges the resource fluxes that are liberated from the reserves into new biomass with a fixed resource ratio. The rate at which the SU produces biomass from the reserves depends on the intensity and the balance of the mobilized resources fluxes. The SU was implemented such that under constant resource conditions, the two resources act as interactively essential resources thereby enabling resource covariance effects.

The state variables of our model are the structural volume of the organism V, the respective resource density in the reserve E_i (i = resource 1 or 2) and assimilation effort ϕ which determines the assimilation efficiencies for the two resources A_i (Fig. 2.2). Resources are assimilated from the food proportionally to the available resource concentrations, the organism's surface and the assimilation efficiency for either resource. Assimilates are then added to the reserves at rates p_{Ai}. Reserves are consumed at rates p_{Ci}, proportionally to their density. The synthesizing unit (SU) (Kooijman 1998) combines the two consumption fluxes at rate p_{SU} which, after subtracting maintenance costs p_M, results in structural growth of the organism. Structural volume is created with a constant density of both resources. If influxes of the SU are imbalanced excessive resources are rejected at rate p_{Ri}, of which a fraction is recycled to the reserves while the rest is excreted. The resource density within the reserves is diluted by growth. Fluxes in and out of the reserves are expressed as resource density fluxes in units of resources per structural volume per time. We assume that the production of nutrient-specific digestive enzymes is energetically costly and that it involves trade-offs hindering the capacity of the consumer to maximize assimilation efficiency for all resources simultaneously (Zera and Harshman 2001). We therefore implemented a trade-off in the assimilation efficiency of the two co-limiting resources. Along this trade-off the organism allocates the assimilation effort (i.e. production of nutrient specific enzymes) towards the most limiting resource as a compensatory mechanism maintaining the nutrient uptake homeostasis (Clissold et al. 2010). Evidence suggests that in invertebrates such digestive processes are controlled by the nutrient status of the hemolymph (Bede et al. 2007). Accordingly, in the model, the allocation of assimilation effort is controlled by the balance of resources in the reserves. The adjustments of the assimilation effort are not immediate. We therefore implement a characteristic switching time that determines the speed at which an organism acclimates to changed resource conditions in the model (see Appendix A1, Figs. A1.1, A1.2 for further details). The model equations and parameter estimates are provided in Table 2.1.

Obtaining the modelled growth rates

The resulting system of ODEs is numerically integrated with the lsoda solver from the deSolve package in R (R Development Core Team 2014) for different fluctuation treatments. Starting from low initial volume and low, balanced reserve densities, the unsaturated increase in structural volume within the first four days yields an estimate for the somatic growth rate of juveniles that may be compared to experimental observations. Different parameter combinations, which represent limit cases of (i) no reserves, no variable assimilation, (ii) no variable assimilation, (iii) no reserves and (iv) the full model with reserves and variable assimilation, give rise to submodels that factorially combine the three important model components. Reserves are excluded by increasing the reserve conductance 1000-fold. Thus, the resources are not stored but directly passed on to the SU. Acclimation is excluded by fixing the assimilation efficiencies at the intermediate assimilation effort $\phi = 0.5$ along the trade-off curve. These submodels will be used to elucidate the interaction of the individual model components with the temporal resource structure. We provide a sensitivity analysis for the three most influential parameters in Appendix A1 (Fig. A1.3-A1.5).

Table 2.1 Model equations and parameter estimates. The model is loosely parametrized for *Daphnia*, when available, published values are given. All other values are set within reasonable biological ranges. [a] from (Vanoverbeke 2008); [b] inferred from (Koussoroplis et al. 2017b); [c] calculated from (Koussoroplis and Wacker 2016); [d] inferred from (Sperfeld and Wacker 2009) for cholesterol; [e] Authors' personal observation on the *D. magna* clone used; [f] slightly modified from AmP Daphnia magna version 2016/02/04 `bio.vu.nl/thb/deb/deblab/add_my_pet/`.

State variables

Symbol	Description	Differential equation	Initial condition	Unit
ϕ	Assimilation effort	$\frac{\mathrm{d}\phi}{\mathrm{d}t} = \frac{1}{\tau}\left(\phi_T(x) - \phi\right)$	0.5	1
E_i	Reserve density	$\frac{\mathrm{d}E_i}{\mathrm{d}t} = p_{Ai} - p_{Ci} + \kappa\, p_{Ri} - (p_{SU} - p_M)\, E_i$	10^{-11}	$\mathrm{mol\,mm^{-3}}$
V	Structual volumne	$\frac{\mathrm{d}V}{\mathrm{d}t} = (p_{SU} - p_M)\, V$	0.008	$\mathrm{mm^3}$

Functions

Symbol	Description	Equation
$\phi_T(x)$	Target assimilation effort at reserve balance $x = \frac{y_1\, E_1}{y_2\, E_2}$	$\phi_T(x) = \begin{cases} \frac{1}{2}x^{\gamma} + 1, & x \le 1 \\ \frac{1}{2}x^{-\gamma}, & x > 1 \end{cases}$
$\varepsilon_i(\phi)$	Assimilation effifiency	$\varepsilon_1 = \phi^{\alpha}(\varepsilon_{max} - \varepsilon_{min}) + \varepsilon_{min}$ $\varepsilon_2 = (1-\phi)^{\alpha}(\varepsilon_{max} - \varepsilon_{min}) + \varepsilon_{min}$

Fluxes

Name	Equation	Unit
Assimilation flux	$p_{Ai} = p_{Am}\, \varepsilon_i\, n_i\, V^{-\frac{1}{3}}$	$\mathrm{mol\,mm^{-3}d^{-1}}$
Catabolic flux	$p_{Ci} = u\, E_i\, V^{-\frac{1}{3}}$	$\mathrm{mol\,mm^{-3}d^{-1}}$
Outflow of SU	$p_{SU} = \frac{1}{\frac{1}{g_{max}} + \frac{1}{y_1\, p_{C1}} + \frac{1}{y_2\, p_{C2}} - \frac{1}{y_1\, p_{C1} + y_2\, p_{C2}}}$	$\mathrm{d^{-1}}$
Rejection flux	$p_{Ri} = \begin{cases} p_{Ci} - p_{SU}/y_i, & p_{Ci} - p_{SU}/y_i > 0 \\ 0, & p_{Ci} - p_{SU}/y_i \le 0 \end{cases}$	$\mathrm{mol\,mm^{-3}d^{-1}}$
Maintenance flux [a]	$p_M = 0.3\,\mathrm{d^{-1}}$	$\mathrm{d^{-1}}$

Parameters – fixed

Symbol	Description	Value
τ	characteristic switching time of assimilation [b]	$0.1\,\mathrm{d^{-1}}$
α	curvature of assimilation trade-off	3
γ	sensitivity for reserve balance	5
n_i	resource concentrations in the food	7×10^{-3} mol/molC (high cond.) 3×10^{-4} mol/molC (low cond.)
p_{Am}	maximum ingestion rate [c]	$4 \times 10^{-6}\,\mathrm{molC\,mm^{-2}\,d^{-1}}$
y_i	yield of structural volume per mole resource i [d]	$1.5 \times 10^{8}\,\mathrm{mm^3/mol}$
g_{max}	maximum volume-specific growth rate [e]	$0.6\,\mathrm{d^{-1}}$

Parameters – submodel-specific (null model, with storage, with acclimation, **full model**)

ε_{max}	maximum assimilation efficiency	0.2, 0.2, 0.9, **0.9**
ε_{min}	minimum assimilation efficiency	0.2, 0.2, 0.1, **0.1**
u	reserve conductance [f]	1000, 1, 1000, **1** $\mathrm{mm\,d^{-1}}$
κ	fraction of resources rejected by the SU and returned to the reserves	0, 0.3, 0, **0.3**

Experiments

Stock cultures of *D. magna* were kept in ADaM medium (Klüttgen et al. 1994) at 20°C with saturating amounts of the green algae *Acutodesmus* obliquus (SAG 276-3a, culture collection of algae, University of Göttingen, Göttingen, Germany). *Synechococcus elongatus* (SAG 89.79), a non-toxic cyanobacterium lacking essential sterols, was used as unialgal food in the experiments. P-replete *S. elongatus* (Syn P+) was cultured semi-continuously in aerated WC medium (Guillard and Lorenzen 1972) at dilution rates of $0.2\,\mathrm{d}^{-1}$. P-deficient *S. elongatus* (Syn P-) were cultivated without dilution using P-free WC medium. All cultures were kept at 20 °C at a light:dark cycle of 16:8 h. The details on determining C as well as P concentrations of Syn P- and Syn P+ cultures for the daily prepared food suspensions are published elsewhere (Lukas et al. 2011). By mixing Syn P+ and Syn P- cultures the appropriate P:C ratios of food suspensions were obtained. Cholesterol containing liposomes were produced following the protocol described in (Wacker and Martin-Creuzburg 2012) and supplemented to the food suspensions to obtain desired cholesterol concentrations. Third-clutch juveniles of *D. magna* (< 24 h old) were born on *S. elongatus* of limiting resource conditions ($1.25\,\mathrm{mmolP/molC}$, $0.25\,\mathrm{\mu g\ cholesterol/mgC}$). In the constant treatments daphnids experienced either constant high or low P (6.66 or $1.25\,\mathrm{mmol/molC}$) each in combination with constant high or low cholesterol (8; $0.25\,\mathrm{\mu g/mgC}$), or average conditions of high and low resource concentrations ($3.95\,\mathrm{mmolP/molC}$; $4.125\,\mathrm{\mu g\ cholesterol/mgC}$). In the variance treatments high and low concentrations of either P or cholesterol fluctuated, while the other resource (cholesterol or P, respectively) was constant at high concentration. In the covariance treatments high concentrations coincided or alternated, respectively for positive and negative covariance. Three different fluctuation frequencies of the resource supply ($0.25\,\mathrm{d}^{-1}$, $0.5\,\mathrm{d}^{-1}$, $1\,\mathrm{d}^{-1}$, for a total experimental duration of 4 days) were applied for variance and covariance treatments, where animals experienced either high or low concentrations of the respective varying resource(s) first (fluctuation phase). Each treatment consisted of four replicates with six juvenile *D. magna* per replicate. The cholesterol variance experiment was performed twice and the data was pooled resulting in eight replicates. The experiments were conducted at 20°C in the dark, using glass beakers filled with $200\,\mathrm{mL}$ of food suspensions prepared with ADaM medium. Food suspensions of *S. elongatus* ($2\,\mathrm{mgC/L}$) with targeted resource concentrations were prepared daily. Every 12 h (for $1\,\mathrm{d}^{-1}$ fluctuation treatments) but at least every 24 h (for constant, $0.25\,\mathrm{d}^{-1}$ and $0.5\,\mathrm{d}^{-1}$ fluctuation treatments) daphnids were transferred into renewed food suspensions to avoid food quantity limitation and to simulate (co)variance in P and cholesterol. Initial dry mass (M_0) of animals was determined at the beginning of the experiment using three subsamples of 10 juveniles dried for three days at 45°C and weighted on an electronic balance (± 1 µg, CP2P; Sartorius, Göttingen, Germany). After four days the final dry mass (M_T) of animals of each replicate was determined following the same procedure. Somatic growth rates g (d^{-1}) were calculated as increase in dry mass using the equation

$$g = \frac{\ln M_T - \ln M_0}{T},$$

where T is the duration of the experiment (4 days). To test for effects of fluctuation frequency and phase (variance experiments) or fluctuation frequency and covariance direction (covariance experiment) on growth, for each experiment a two-way ANOVA was applied followed by Tukey HSD post-hoc tests. A nested-design two-way ANOVA was used to additionally test for effects of fluctuation phase nested within positive and negative covariance in the covariance experiment. Here, only the lowest fluctuation frequency of $0.25\,\mathrm{d}^{-1}$ was considered. Means and associated 95% confidence intervals (CI) were estimated using a bootstrapping approach with 1000 repetitions (Efron and Tibshirani 1994). Regarding treatments of constant average resource supply ($g(\overline{R})$, $g(\overline{R_1}, \overline{R_2})$) and non-linear averaging predictions for variance ($\overline{g(R)}$), positive ($\overline{g(R_1, R_2)_+}$), and negative covariance ($\overline{g(R_1, R_2)_-}$), respectively, derived from constant resource condition treatments, a significant difference to observed growth rates under resource fluctuation was concluded in the absence of overlap between their respective CI.

Results

Model results

We find that the simulated somatic growth rate g of a consumer strongly changes with the fluctuation frequency of resource availability in both the variance and the covariance treatment, which confirms the temporal scale dependence (Fig. 2.3-2.4). Further, fluctuation phase and covariance of co-limiting resources impact growth of consumers and their effect depends on the frequency of fluctuations. This effect of the temporal structure of resource variability increases for larger fluctuation amplitudes (Fig. 2.5).

In the model, we included three central concepts of nutritional physiology (Fig. 2.2). By factorially combining these concepts we can study their impact on the relation between the structure of resource fluctuations and somatic growth of a consumer (Fig. 2.3A-D and Fig. 2.4A-D). Dynamic acclimation allows the consumer to regulate the assimilation efficiencies for co-limiting resources according to the balance of stored resources compared to internal requirements along a trade-off curve (Appendix A1, Fig. A1.1-A1.2). Reserves allow storage of the assimilated resources (Kooijman 2010). A synthesizing unit (SU (Kooijman 1998)) translates stored resources into structural growth. The SU is indispensable and forms the null model as the two limiting resources always have to be combined to create new biomass.

The SU comprises no frequency dependence (Figs. 2.3A and 2.4A). The inclusion of reserves, acclimation, or both into the model yields fluctuation frequency effects (Figs. 2.3B-D and 2.4B-D). Reserves increase growth across all fluctuation frequencies compared to the null model, but most dominantly for high frequencies (Figs. 2.3B and 2.4B). They thus create a transition of the simulated growth from the non-linear average prediction $\overline{g(R)}$ to the growth predicted under constant average resource conditions $g(\overline{R})$ in the variance treatment and from $\overline{g(R_1, R_2)_+}$ and $\overline{g(R_1, R_2)_-}$ to $g(\overline{R_1}, \overline{R_2})$ for positive and negative covariance, respectively. This increase of growth with increasing fluctuation frequency is steeper when the organism experiences a low resource concentration first, i.e. fluctuation phase effects are strongest at low fluctuation frequencies. Acclimation acts only when the two resources are fluctuating asynchronously, i.e. in the variance and negative covariance treatments (Fig. 2.3C and 2.4C). For low fluctuation frequencies, acclimation and the resulting specialization on assimilating one resource increases growth compared to the null model. For high fluctuation frequencies, simulated growth trends towards the null model as acclimation becomes too slow and assimilation efficiencies remain in an intermediate, non-specialized range.

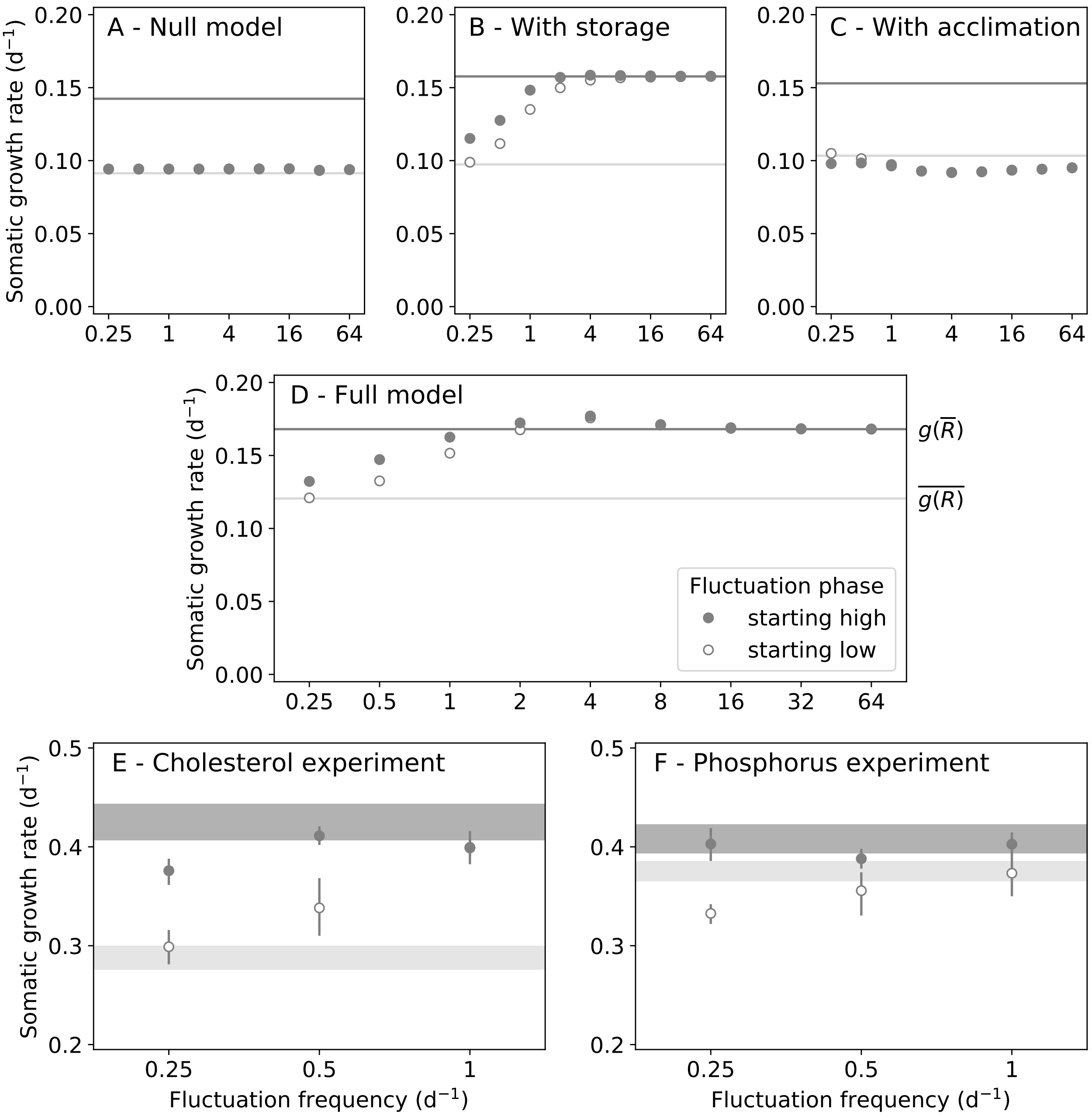

Figure 2.3 Effects of frequency and phase for fluctuations of one limiting resource. (A-D) Model results for the somatic growth rate of a consumer for the four different submodels. The dark grey horizontal lines are the predictions for growth under the same average constant resource supply, $g(\overline{R})$, whereas the lighter horizontal line is the non-linear averaging prediction of growth under variable resource supply, $\overline{g(R)}$ (see Fig. 2.1A). (E-F) Experimental observations of juvenile growth rate of *Daphnia magna* (mean ± 95% confidence interval, C.I.) under (E) fluctuating cholesterol or (F) phosphorus supply, with different starting conditions representing different fluctuation phases experienced after birth. The darker shaded area is the 95% C.I. of $g(\overline{R})$. The lighter shaded area is the 95% C.I. of $\overline{g(R)}$. The other (non-fluctuating) resource (phosphorus or cholesterol in the experiments) is kept at saturating supply.

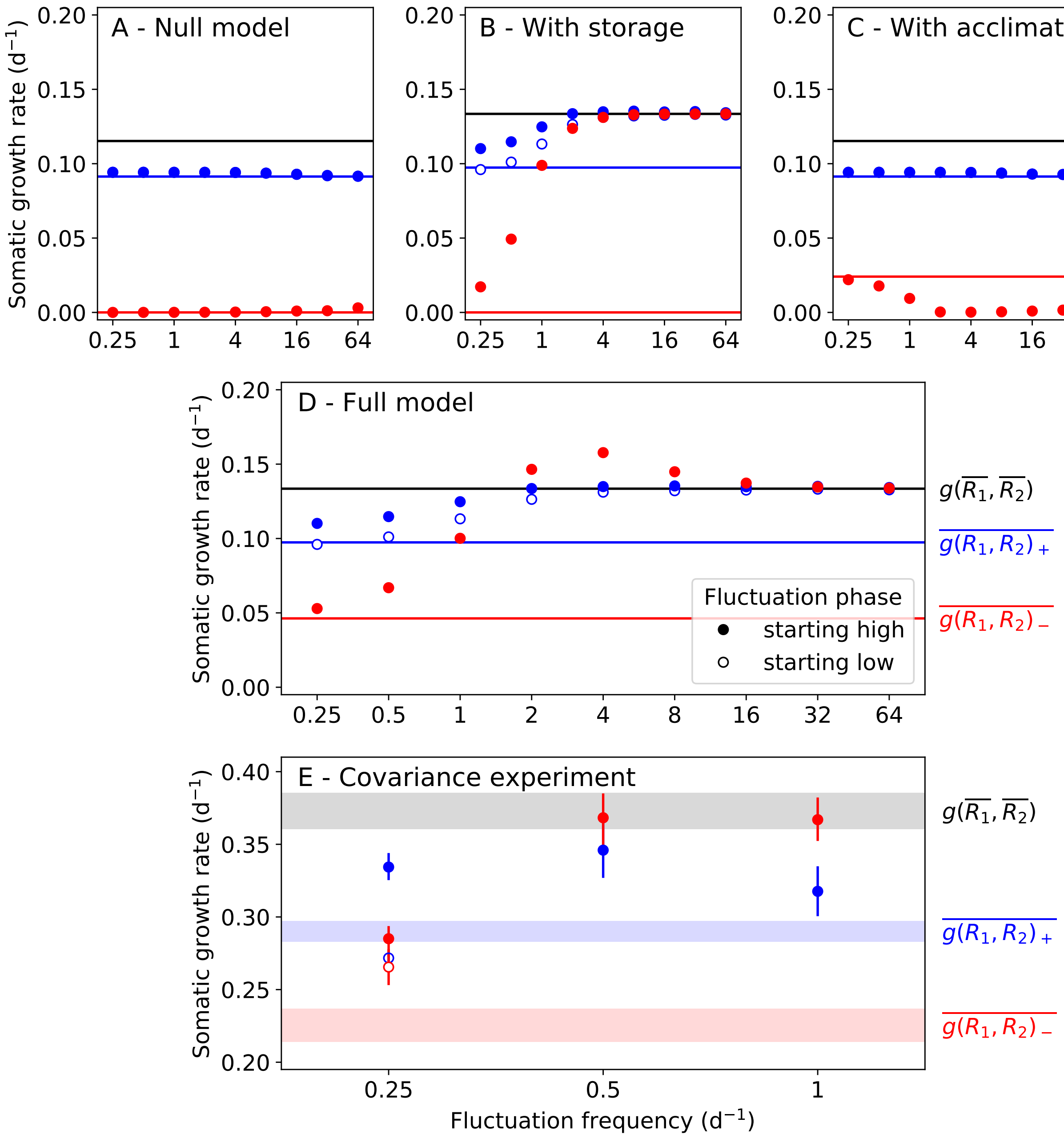

Figure 2.4 Effects of frequency, phase, and covariance for fluctuations of two co-limiting resources. (A-D) Modelled somatic growth rate of a consumer for the four different submodels with positively (blue) or negatively (red) co-varying supply in the two co-limiting resources. The black horizontal line shows the predicted growth under the same average constant resource supply, $g(\overline{R_1}, \overline{R_2})$, whereas the red and blue lines are the non-linear averaging predictions of growth under variable resource supply, $\overline{g(R_1, R_2)_{+/-}}$ (see Fig. 2.1B). (E) Experimentally observed juvenile growth rate of *Daphnia magna* (mean ± 95% C.I.) under positively or negatively covarying phosphorus and cholesterol supply. The combined effect of fluctuation phase and covariance was tested experimentally for $0.25\,\mathrm{d}^{-1}$ fluctuations. The grey shaded area is the 95% C.I. of $g(\overline{R_1}, \overline{R_2})$. Colored shaded areas are the 95% C.I. of $\overline{g(R_1, R_2)_+}$ (blue) and $\overline{g(R_1, R_2)_-}$ (red). Full circles denote high starting conditions, whereas open circles indicate low resource conditions experienced right after birth.

Adding both, storage and acclimation, to the null model increases growth rates even further across all fluctuation frequencies. Interestingly, this creates an inversion of the covariance effect at intermediate frequencies where storage and acclimation blend, i.e. the growth rates for negatively co-varying resources exceed those for positively co-varying ones (Fig. 2.3D and 2.4D). As we parametrized both resources identically, the phase of fluctuations does not affect growth in the negative covariance scenario and only under positive covariance, an initially low resource supply decreases growth at low fluctuation frequencies compared to initially high resources (Fig. 2.4D). These model observations are conserved for broad parameter ranges (Appendix A1, Fig. A1.3-A1.5).

As expected, reducing the amplitude of resource fluctuations decreases the deviations from the predictions for constant average resource conditions $g(\overline{R})$ or $g(\overline{R_1}, \overline{R_2})$ (Fig. 2.5). We thus find that reducing the fluctuation amplitude may increases the somatic growth rate of consumers, while reducing the fluctuation frequency may decrease it. Starting from the same reference frequency and amplitude, reducing both can create a complex mix of these partly opposing effects, which is affected by the covariance of the limiting resources (see insets Fig. 2.5).

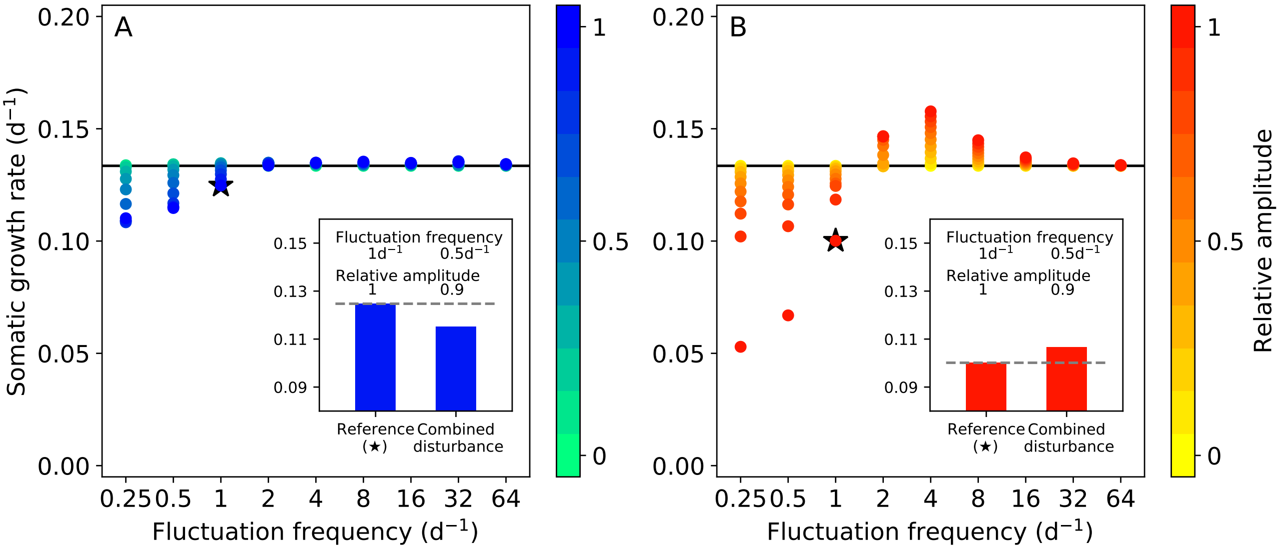

Figure 2.5 Impact of resource fluctuation amplitude. Modelled somatic growth of a consumer for decreasing fluctuation amplitudes relative to that assumed in Fig. 2.4 for positively (A) or negatively (B) co-varying co-limiting resources. Alterations to the temporal structure of resource variability perceived by consumers, e.g. caused by environmental disturbances, can occur via changed frequencies or amplitudes. For positively co-varying resources, reducing frequency and increasing amplitude decreases somatic growth rate. For negative covariance the effect of smaller frequencies and larger amplitudes is not consistent but depends on the reference frequency. The insets show that for identical reference situations (marked by the stars) the same alterations to the temporal structure may affect consumer performance in opposite directions if resources co-vary positively or negatively.

Experimental validation

We found a strong agreement between experimental results and the majority of predictions of the full model. In the experiment with fluctuating cholesterol supply, growth rates were affected both by fluctuation frequency (two-way ANOVA, $F_{2,41} = 20.21$, $p < 0.001$) and phase ($F_{1,41} = 41.17$, $p < 0.001$). As predicted, there were no growth differences between fluctuation phases at high frequencies (Fig. 2.3E), where growth rates were comparable to $g(\overline{R})$. At low frequencies, however, growth rates decreased stronger when exposed to low cholesterol concentrations first (interaction: $F_{2,41} = 9.56$, $p < 0.001$) and reached $\overline{g(R)}$ at the $0.25\,\mathrm{d}^{-1}$ frequency.

In the experiment with fluctuating P supply, growth rates were only marginally affected by fluctuation frequency (two-way ANOVA, $F_{2,18} = 2.63$, $p = 0.10$; Fig. 2.3F). In agreement with the model, growth rates were generally lower when animals experienced low P concentrations first (factor fluctuation phase, $F_{1,18} = 33.86$, $p < 0.001$). A marginal interaction between fluctuation frequency and phase ($F_{2,18} = 3.01$, $p = 0.07$) suggests the predicted increase in growth differences between the two fluctuation phases at lower frequencies. When exposed to high P supply first, growth rates were high across all tested fluctuation frequencies and did not differ from $g(\overline{R})$ (Fig. 2.3C). When experiencing low P supply first, growth rates decreased with decreasing fluctuation frequency as predicted by the model, but were generally lower than $g(\overline{R})$ at all frequencies and even lower than $\overline{g(R)}$ at the $0.25\,\mathrm{d}^{-1}$ frequency (Fig. 2.3C). Lower growth rates than $\overline{g(R)}$ are also predicted by the full model for certain parameter ranges (Appendix A1, Fig. A1.6).

The experiments also confirmed the majority of model predictions for the two resource covariance scenarios (Fig. 2.4E). Similar to the model predictions, frequency dependence was less pronounced for positive than for negative covariance, which is supported by a significant interaction of fluctuation frequency and covariance direction ($F_{2,18} = 15.14$, $p < 0.001$. As predicted, we observed an inversion of covariance effects; at the $0.25\,\mathrm{d}^{-1}$ frequency, negative covariance yielded a stronger growth decrease relative to $g(\overline{R_1}, \overline{R_2})$ than positive covariance (Tukey HSD, $p < 0.05$), whereas at the $1\,\mathrm{d}^{-1}$ frequency the decrease was stronger for positive covariance (Tukey HSD, $p < 0.05$). The overshoot of growth rates above $g(\overline{R_1}, \overline{R_2})$ was not observed at the frequencies that were used in the experiment. The effects of fluctuation phase were tested for the $0.25\,\mathrm{d}^{-1}$ frequency (Fig. 2.4E). Consistent with the model prediction, growth was affected by the fluctuation phase under positive covariance (nested ANOVA, $F_{2,12} = 38.07$, $p < 0.001$; Tukey HSD, $p < 0.001$), but was similar under negative covariance (Tukey HSD, $p = 0.09$. Amplitude effects were not tested experimentally.

Discussion

Our study combines theoretical and experimental approaches to explore how variability in nutritionally complex environments influences the growth of a consumer limited by the supply of one or multiple limiting resources. For the first time, we explored the growth constraints imposed by covariance of two co-limiting resources. We found that the phase and the (co-)variance of fluctuating resource supply strongly constrain consumer growth and that this effect depends on the frequency at which the consumer experiences resource fluctuations.

Our modeling approach sheds light on the way resource acquisition and storage physiology can determine consumer performance in nutritionally fluctuating environments. The model incorporates three central physiological processes linked to nutrition: the ability to (i) optimize the acquisition of the most limiting resource, (ii) store resources, and (iii) combine resources at the required ratios into new biomass.

The adjustment of resource assimilation efficiency is a universal trait (Yin and Johnson 2000; Ashley et al. 2006; Karasov et al. 2011) enabling the organisms to maintain their biochemical homeostasis by focusing their acquisition efforts on the resource in short supply (Clissold et al. 2010; Karasov et al. 2011; Wojewodzic et al. 2011; Bansemer et al. 2016). In metazoans, this can be achieved by various mechanisms such as plasticity in gut transit, length, and mass, or in types and concentration of digestive enzymes (Karasov et al. 2011). Our acclimation model focuses on the case of digestive enzyme plasticity, which in *Daphnia* has been observed for gut proteases, lipases and phosphatases (Schwarzenberger et al. 2010; Wojewodzic et al. 2011; Koussoroplis et al. 2017b). This adjustment of digestive enzymes may involve two types of costs. First, modifying the pool of digestive enzymes requires energy, which is then not available for other processes such as growth or reproduction. Second, full acclimation requires time during which the consumer underperforms, since the shape of the assimilation efficiency trade-off prevents an optimal acquisition of the most limiting resource. Hence, the consumer's growth may decrease below $\overline{g(R)}$. In the model simulations, when the resource fluctuations are slow enough (e.g. in a coarse grained environment), this delay becomes negligible compared to the time during which the organism benefits from full acclimation and specialization on the resource in short supply. As fluctuation frequency increases, the relative importance of the underperformance compared to the beneficial effect increases as the relative time spent at non-optimal assimilation efficiencies increases, thereby suppressing consumer growth. Eventually, the acclimation status will remain constant and adjust to the average nutritional conditions under which the organism assimilates both resources with suboptimal, reduced efficiency. In the model, acclimation is driven by imbalances of the resources in the reserves. Therefore, the underperformance, which indicates temporal costs for acclimation, occurs only when co-limiting resources are negatively covarying or under single resource variance.

Similar to acclimation, having reserves, i.e. a pool of assimilated resources stored in polymer form, is a universal trait in living organisms (Kooijman 2010). DEB theory assumes that assimilated resources first enter the reserves before being routed to growth and reproduction (Kooijman 2010). In our model reserves buffer high frequency fluctuations. This increases growth relative to the predictions for variable nutritional environments ($\overline{g(R)}, \overline{g(R_1, R_2)}$) for generally observed performance curves (Fig. 2.1A-B). Thus, high frequencies enable the consumer to grow as well as in a constant nutritional environment of the same average quality ($g(\overline{R}), g(\overline{R_1}, \overline{R_2})$), whereas under low frequencies performance converges towards $\overline{g(R)}$ or $\overline{g(R_1, R_2)}$ for variance and covariance scenarios, respectively (Koussoroplis et al. 2017a). The experimental observations are in agreement with the buffering effect. Including reserves in the model makes consumer growth depend not only on the frequency, but also on the phase of fluctuations, a pattern we also observed in our experiments. This indicates that in coarse-grained nutritional environments, where the temporal scale of resource fluctuations is large (i.e. low fluctuation frequency), timing is essential. Because initially accumulated reserves may be used during a subsequent phase of nutritional deprivation, experiencing a high quality nutritional environment creates a window of opportunity during early development and may dramatically improve performance (Malzahn and Boersma 2012).

We observed a strong covariance effect at low fluctuation frequencies. Growth under negative covariance is reduced compared to growth under positive covariance as the resource that is temporally in excess is rejected by the synthesizing unit and only partly recycled to the reserve compartment. Interestingly, combining reserves and acclimation dynamics (full model) cause an inversion in the direction of the covariance effect between high and low fluctuation frequencies, which also appears in our experimental results. Thus, not only the magnitude of the covariance effect but also its direction is determined by the resource fluctuation frequency. This illustrates the complexity of the challenges that consumers face when they need to acquire multiple resources in heterogeneous landscapes.

To tackle these challenges consumers may apply different physiological strategies, which become apparent in our model (see Fig. 2.3B,C and 2.4B,C). An intriguing route to follow would be to study whether different types of environments might select for different strategies and if trade-offs between them exist. Reserve specialists, i.e. organisms with large reserves that are used up only slowly, could withstand periods of nutritional deprivation, and thus benefit in fast fluctuating environments. Assimilation specialists, i.e. organisms directing their assimilation efforts to specific, most limiting resources, would be well adapted to slowly fluctuating environments with sequential availability of limiting resources.

Our study confirms that nutritionally heterogeneous environments are a challenge for consumers because they involve various physiological costs (Hood and R. W. Sterner 2010; Wetzel and Thaler 2016; Wetzel et al. 2016; Wagner et al. 2017). Resource heterogeneity can decelerate invasion fronts (Giometto et al. 2017) or limit the success of agricultural pests (Underwood 2004) and is therefore suspected to regulate the dynamics of natural or agricultural ecosystems. Nutritional heterogeneity depends on various natural or anthropogenic factors. In agroecosystems for example, herbivore attacks on plants induce the production of volatile chemical signals that prompt chemical defenses in undamaged plants (Morrell and Kessler 2017). Such induced responses increase nutritional heterogeneity of individual plants or groups of aggregated plants for herbivores (Karban 2017). On the other side, anthropogenic landscape homogenization or reduced plant species diversity decreases the nutritional heterogeneity experienced by herbivores. However, any attempt to predict effects of such changes on herbivores is difficult as long as resource heterogeneity is ill-defined. In both examples above, the changes concern the resource variance affecting the fluctuation amplitude as well as the resource grain size in the landscape affecting the fluctuation frequency perceived by the consumer. Our results contribute major insights here, as they show that fluctuation amplitude and frequency may act on consumer growth in opposite directions: decreased heterogeneity due to lower amplitude may increase consumer performance whereas decreased heterogeneity due to lower frequency may decrease it (Fig. 2.5). Hence, these two aspects of heterogeneity could compensate each other, e.g. a positive effect of landscape homogenization via the reduction of resource fluctuation amplitude could be weakened by a decrease in resource fluctuation frequency.

In nature, the physiological responses to environmental variability cannot be decoupled from behavior as these two aspects interact. Consumers permanently adjust their foraging behavior according to their nutritional status and their environment (e.g. resource peaks, predation risk, competitors or thermal preferences) (Kearney et al. 2010; Simpson and Raubenheimer 2012). Hence, even without a physical perturbation of the landscape, any alteration of the foraging behavior (e.g. staying longer in food patches, switching less often between complementary foods) (Lihoreau et al. 2017) modifies the perceived temporal structure of (co-)limiting resource supply. Understanding the linkages between foraging behavior, nutritional limitation and spatiotemporal distribution of (co-)limiting resources in the environment are clearly a fertile future field of research.

Given the multitude of factors shaping both the perceived variability of nutritional limitation as well as the physiological response of consumers, predicting their performance in a changing world is an intriguing yet challenging aspiration. Only an interdisciplinary approach allows to unravel the complex effects that may arise from the interplay of more frequent and drastic perturbations to the environment by extreme events on the one hand and anthropogenic environmental simplification on the other.

Acknowledgements

We thank Erik Sperfeld and Toni Klauschies for insightful comments on earlier versions of the manuscript. This study was supported by the German Research Foundation (KO5330/1-1 to AMK, WA2445/9-1 and WA2445/15-1 to AW).

Bibliography

Ashley, M. K., Grant, M., and Grabov, A. (2006). Plant responses to potassium deficiencies: a role for potassium transport proteins. *J. Exp. Bot.* 57: 425–436.

Bansemer, M. S., Qin, J. G., Harris, J. O., et al. (2016). Age-dependent response of digestive enzyme activities to dietary protein level and water temperature in greenlip abalone (Haliotis laevigata). *Aquaculture* 451: 451–456.

Bede, J. C., McNeil, J. N., and Tobe, S. S. (2007). The role of neuropeptides in caterpillar nutritional ecology. *Peptides* 28: 185–196.

Camp, M. J., Shipley, L. A., Johnson, T. R., et al. (2015). Modeling trade-offs between plant fiber and toxins: a framework for quantifying risks perceived by foraging herbivores. *Ecology* 96: 3292–3302.

Carlotti, F., Eisenhauer, L., and Calbet, A. (2010). Modelling the effect of constant and fluctuating food supply on egg production rates of Acartia grani. *Ecol. Modell.* 221: 495–502.

Clissold, F. J., Tedder, B. J., Conigrave, A. D., and Simpson, S. J. (2010). The gastrointestinal tract as a nutrient-balancing organ. *Proc. Biol. Sci.* 277: 1751–1759.

Denny, M. (2017). The fallacy of the average: on the ubiquity, utility and continuing novelty of Jensen's inequality. *J. Exp. Biol.* 220: 139–146.

Dowd, W. W., King, F. A., and Denny, M. W. (2015). Thermal variation, thermal extremes and the physiological performance of individuals. *J. Exp. Biol.* 218: 1956–1967.

Efron, B. and Tibshirani, R. (1994). An introduction to the bootstrap. Chapman and Hall/CRC press.

Field, C. B., Barros, V., Stocker, T. F., Qin, D., and Eds. (2012). Managing the risks of extreme events and disasters to advance climate change adaption: special report of the Intergovernmental Panel on Climate Change. Cambridge University Press.

Fujiwara, M., Kendall, B. E., and Nisbet, R. M. (2004). Growth autocorrelation and animal size variation. *Ecol. Lett.* 7: 106–113.

Gámez-Virués, S., Perović, D. J., Gossner, M. M., et al. (2015). Landscape simplification filters species traits and drives biotic homogenization. *Nat. Commun.* 6: 8568.

Giometto, A., Altermatt, F., and Rinaldo, A. (2017). Demographic stochasticity and resource autocorrelation control biological invasions in heterogeneous landscapes. *Oikos* 126: 1554–1563.

Grosbois, G., del Giorgio, P. A., and Rautio, M. (2017). Zooplankton allochthony is spatially heterogeneous in a boreal lake. *Freshw. Biol.* 62: 474–490.

Guillard, R. R. L. and Lorenzen, C. J. (1972). Yellow-green algae with chlorophyllide C. *J. Phycol.* 8: 10–14.

Hebblewhite, M. and Merrill, E. H. (2009). Trade-offs between predation risk and forage differ between migrant strategies in a migratory ungulate. *Ecology* 90: 3445–3454.

Hood, J. M. and Sterner, R. W. (2010). Diet Mixing: Do Animals Integrate Growth or Resources across Temporal Heterogeneity? *Am. Nat.* 176: 651–663.

Hunter, M. (2016). “Effects of primary producer chemistry on trophic interactions.” In: *Phytochem. Landsc.* Monographs. Princeton, NJ, Princeton University Press, pp. 39–137.

Junker, J. R. and Cross, W. F. (2014). Seasonality in the trophic basis of a temperate stream invertebrate assemblage: Importance of temperature and food quality. *Limnol. Oceanogr.* 59: 507–518.

Karasov, W. H., Martínez del Rio, C., and Caviedes-Vidal, E. (2011). Ecological Physiology of Diet and Digestive Systems. *Annu. Rev. Physiol.* 73: 69–93.

Karban, R. (2017). Plant communication increases heterogeneity in plant phenotypes and herbivore movement. *Funct. Ecol.* 31: 990–991.

Kearney, M., Simpson, S. J., Raubenheimer, D., and Helmuth, B. (2010). Modelling the ecological niche from functional traits. *Philos. Trans. R. Soc. B Biol. Sci.* 365: 3469–3483.

Kingsolver, J. G. and Woods, H. A. (2016). Beyond Thermal Performance Curves: Modeling Time-Dependent Effects of Thermal Stress on Ectotherm Growth Rates. *Am. Nat.* 187: 283–294.

Klüttgen, B., Dülmer, U., Engels, M., and Ratte, H. (1994). ADaM, an artificial freshwater for the culture of zooplankton. *Water Res.* 28: 743–746.

Kooijman, S. (1998). The Synthesizing Unit as model for the stoichiometric fusion and branching of metabolic fluxes. *Biophys. Chem.* 73: 179–188.

Kooijman, S. (2010). Dynamic Energy Budget theory for metabolic organisation. Third Edit. Cambridge University Press.

Koussoroplis, A.-M., Pincebourde, S., and Wacker, A. (2017a). Understanding and predicting physiological performance of organisms in fluctuating and multifactorial environments. *Ecol. Monogr.* 87: 178–197.

Koussoroplis, A.-M., Schwarzenberger, A., and Wacker, A. (2017b). Diet quality determines lipase gene expression and lipase/esterase activity in Daphnia pulex. *Biol. Open* 6: 210–216.

Koussoroplis, A.-M. and Wacker, A. (2016). Covariance modulates the effect of joint temperature and food variance on ectotherm life-history traits. *Ecol. Lett.* 19: 143–152.

Lasley-Rasher, R., Rasher, D., Marion, Z., Taylor, R., and Hay, M. (2011). Predation constrains host choice for a marine mesograzer. *Mar. Ecol. Prog. Ser.* 434: 91–99.

Lihoreau, M., Charleston, M. A., Senior, A. M., et al. (2017). Collective foraging in spatially complex nutritional environments. *Philos. Trans. R. Soc. B Biol. Sci.* 372: 20160238.

Lukas, M., Sperfeld, E., and Wacker, A. (2011). Growth Rate Hypothesis does not apply across colimiting conditions: cholesterol limitation affects phosphorus homoeostasis of an aquatic herbivore. *Funct. Ecol.* 25: 1206–1214.

Malzahn, A. M. and Boersma, M. (2012). Effects of poor food quality on copepod growth are dose dependent and non-reversible. *Oikos* 121: 1408–1416.

McArt, S. H. and Thaler, J. S. (2013). Plant genotypic diversity reduces the rate of consumer resource utilization. *Proc. R. Soc. B Biol. Sci.* 280: 20130639.

Meehl, G. A. and Tebaldi, C. (2004). More Intense, More Frequent, and Longer Lasting Heat Waves in the 21st Century. *Science* 305: 994–997.

Morrell, K. and Kessler, A. (2017). Plant communication in a widespread goldenrod: keeping herbivores on the move. *Funct. Ecol.* 31: 1049–1061.

Muller, E. and Nisbet, R. M. (2000). Survival and Production in Variable Resource Environments. *Bull. Math. Biol.* 62: 1163–1189.

Niehaus, A. C., Angilletta, M. J., Sears, M. W., Franklin, C. E., and Wilson, R. S. (2012). Predicting the physiological performance of ectotherms in fluctuating thermal environments. *J. Exp. Biol.* 215: 694–701.

Orians, C. M. and Jones, C. G. (2001). Plants as resource mosaics: a functional model for predicting patterns of within-plant resource heterogeneity to consumers based on vascular architecture and local environmental variability. *Oikos* 94: 493–504.

Park, S. (2004). Diel and vertical variability of seston food quality and quantity in a small subalpine oligomesotrophic lake. *J. Plankton Res.* 26: 1489–1498.

Pearse, I. S., Paul, R., and Ode, P. J. (2018). Variation in Plant Defense Suppresses Herbivore Performance. *Curr. Biol.* 28: 1981–1986.e2.

Raatz, M., Gaedke, U., and Wacker, A. (2017). High food quality of prey lowers its risk of extinction. *Oikos* 126: 1501–1510.

Rahmstorf, S. and Coumou, D. (2011). Increase of extreme events in a warming world. *Proc. Natl. Acad. Sci.* 108: 17905–17909.

Riolo, M. A., Rohani, P., and Hunter, M. D. (2015). Local variation in plant quality influences large-scale population dynamics. *Oikos* 124: 1160–1170.

Ruel, J. J. and Ayres, M. P. (1999). Jensen's inequality predicts effects of environmental variation. *Trends Ecol. Evol.* 14: 361–366.

Schwarzenberger, A., Zitt, A., Kroth, P., Mueller, S., and Von Elert, E. (2010). Gene expression and activity of digestive proteases in Daphnia: effects of cyanobacterial protease inhibitors. *BMC Physiol.* 10: 6.

Simpson, S. and Raubenheimer, D. (2012). The nature of nutrition: A unifying framework from animal adaptation to human obesity. Princeton University Press.

Sperfeld, E. and Wacker, A. (2009). Effects of temperature and dietary sterol availability on growth and cholesterol allocation of the aquatic keystone species Daphnia. *J. Exp. Biol.* 212: 3051–3059.

Sperfeld, E., Martin-Creuzburg, D., and Wacker, A. (2012). Multiple resource limitation theory applied to herbivorous consumers: Liebig's minimum rule vs. interactive co-limitation. *Ecol. Lett.* 15: 142–150.

Sperfeld, E., Raubenheimer, D., and Wacker, A. (2016). Bridging factorial and gradient concepts of resource co-limitation: Towards a general framework applied to consumers. *Ecol. Lett.* 19: 201–215.

Sterner, R. and Elser, J. (2002). Ecological Stoichiometry: The biology of elements from molecules to the biosphere. Princeton University Press.

Stockhoff, B. A. (1993). Diet Heterogeneity: Implications for Growth of a Generalist Herbivore, the Gypsy Moth. *Ecology* 74: 1939–1949.

Turner, M. G. (2010). Disturbance and landscape dynamics in a changing world. *Ecology* 91: 2833–2849.

Underwood, N. (2004). Variance and skew of the distribution of plant quality influence herbivore population dynamics. *Ecology* 85: 686–693.

Urabe, J., Shimizu, Y., and Yamaguchi, T. (2018). Understanding the stoichiometric limitation of herbivore growth: the importance of feeding and assimilation flexibilities. *Ecol. Lett.* 21: 197–206.

Vanoverbeke, J. (2008). Modeling individual and population dynamics in a consumer–resource system: Behavior under food limitation and crowding and the effect on population cycling in Daphnia. *Ecol. Modell.* 216: 385–401.

Wacker, A. and Martin-Creuzburg, D. (2012). Biochemical nutrient requirements of the rotifer Brachionus calyciflorus: Co-limitation by sterols and amino acids. *Funct. Ecol.* 26: 1135–1143.

Wagner, N. D., Prater, C., and Frost, P. C. (2017). Dynamic Responses of Phosphorus Metabolism to Acute and Chronic Dietary Phosphorus-Limitation in Daphnia. *Front. Environ. Sci.* 5: 1–10.

Wetzel, W. C. and Thaler, J. S. (2016). Does plant trait diversity reduce the ability of herbivores to defend against predators? the plant variability-gut acclimation hypothesis. *Curr. Opin. Insect Sci.* 14: 25–31.

Wetzel, W. C., Kharouba, H. M., Robinson, M., Holyoak, M., and Karban, R. (2016). Variability in plant nutrients reduces insect herbivore performance. *Nature* 539: 425–427.

Winder, M., Spaak, P., and Mooij, W. M. (2004). Trade-offs in daphnia habitat selection. *Ecology* 85: 2027–2036.

Wojewodzic, M. W., Kyle, M., Elser, J. J., Hessen, D. O., and Andersen, T. (2011). Joint effect of phosphorus limitation and temperature on alkaline phosphatase activity and somatic growth in Daphnia magna. *Oecologia* 165: 837–846.

Yin, Z. H. and Johnson, G. N. (2000). Photosynthetic acclimation of higher plants to growth in fluctuating light environments. *Photosynth. Res.* 63: 97–107.

Zera, A. J. and Harshman, L. G. (2001). The Physiology of Life History Trade-Offs in Animals. *Annu. Rev. Ecol. Syst.* 32: 95–126.

3 Biochemical food quality shapes coexistence of apparently competing prey

High food quality of prey lowers its risk of extinction

Michael Raatz, Ursula Gaedke and Alexander Wacker

Institute of Biochemistry and Biology, University of Potsdam, Potsdam, Germany

Abstract

The mineral and biochemical food quality of prey may limit predator production. This well-studied direct bottom-up effect is especially prominent for herbivore-plant interactions. Low-quality prey species, particularly when defended, are generally considered to be less prone to predator-driven extinction. Undefended high-quality prey species sustain high predator production thereby potentially increasing their own extinction risk. The food quality of primary producers is highly species-specific. In communities of competing prey species, predators thus may supplement their diets of low-quality prey with high-quality prey, leading to indirect horizontal interactions between prey species of different food quality. We explore how these predator-mediated indirect interactions affect species coexistence in a general predator-prey model that is parametrized for an experimental algae-rotifer system. To cover a broad range of three essential functional traits that shape many plant-herbivore interactions we consider differences in (i) the food quality of the prey species, (ii) their competitive ability for nutrient uptake and (iii) their defence against predation. As expected, low food quality of prey can, similarly to defence, provide protection against extinction by predation. Counterintuitively, our simulations demonstrate that being of high food quality also prevents extinction of that prey species and additionally promotes coexistence with a competing, low-quality prey. The persistence of the high-quality prey enables a high conversion efficiency and control of the low-quality prey by the predator and allows for re-allocation of nutrients to the high-quality competitor. Our results show that high food quality is not necessarily detrimental for a prey species but instead can protect against extinction and promote species richness and functional biodiversity.

Published as

Raatz, M., Gaedke, U., and Wacker, A. (2017). High food quality of prey lowers its risk of extinction. *Oikos* 126: 1501–1510.

Introduction

Organisms can directly interact in numerous ways, such as predation, parasitism or allelopathy. Besides direct interactions, the importance of indirect interactions between organisms such as competition for shared resources (MacArthur 1970; Chesson 1990; Abrams 1998) or apparent competition are increasingly recognized. Organismal properties which shape species abundances and interactions are commonly referred to as functional traits. Food quality is an important trait of prey that is determined by the degree of biochemical and mineral mismatch between prey and predators and may directly limit predator production. Especially at the plant-herbivore interface, nutritional imbalances between the provision of minerals and biochemicals in the prey and the demands of the predators are a common phenomenon (Elser et al. 2000; Elert et al. 2003). The food quality of plants for herbivores is often evaluated by the plants' composition of minerals (phosphorus and nitrogen) (Elser et al. 2007; Sterner 2008) or biochemical compounds such as essential amino acids, vitamins, polyunsaturated fatty acids and sterols, which herbivores cannot synthesize on their own (Müller-Navarra 1995; Martin-Creuzburg et al. 2009; Sperfeld et al. 2012; Wacker and Martin-Creuzburg 2012). These biochemicals are not homogeneously distributed among prey species. In fact, the biochemical composition of primary producers is highly species-specific (Ahlgren et al. 1992; Volkman 2003; Piepho et al. 2012; Martin-Creuzburg and Merkel 2016). This creates an indirect horizontal interaction between the prey species as the overall food quality of the prey community is determined by the differences in food quality among different prey species. Low food quality of a prey species may function as a protection against predation as the predator is constrained by a deficiency in essential nutrients. A sufficiently high share of a second, high-quality prey in the diet releases the predator from food quality limitation as it provides biochemical nutrients to supplement the low quality diet (Wacker and Martin-Creuzburg 2012). As the food is used with higher efficiency less nutrients are excreted and recycled.

Hence, this supplementation from a high quality to a low quality species increases predator production and decreases nutrient recycling. The balance between losses by predation and nutrient dependent growth determines the risk of a prey's extinction and therefore the prey community composition. Thus, we hypothesize that differences in food quality among prey species affect their coexistence. How exactly food quality affects coexistence (mediated by predation pressure and nutrient availability) is determined by the respective traits of the prey species. Consequently, we study the effect of food quality in the context of a variation in the prey's predation risk and competitiveness, which determine the prey's level of defence and its nutrient uptake ability at low nutrient concentrations, respectively. These two traits were shown to trade off against each other (Abrams and Matsuda 1997; Yoshida et al. 2004; Becks et al. 2012; Hiltunen et al. 2014), i.e. defence against predation may come at the cost of a lowered growth if resources are scarce.

Using numerical simulations, we evaluate how the indirect interactions between prey species of different food quality affect their coexistence and population dynamics at varying trade-off strengths between defence and competitiveness. The biochemical food quality, determined by the mismatch between the biochemical composition of predator and prey, and the predation risk, determined e.g. by structural defences, are considered to be functionally independent. Both factors can individually affect the performance of the predator and thus the future grazing pressure by the prey species investing their energy and organic compounds into defence structures and easily accessible essential compounds. We cover a wide range of predator-prey systems by considering three different scenarios in which two prey species have different combinations of food quality and defence: (1) *Equal food quality scenario* - both prey species are of high and identical food quality, thus eliminating the effects of food quality. This scenario was studied before (Abrams 1999; Jones and Ellner 2007) and serves as a reference. (2) *Undefended low quality scenario* - the undefended prey species is of low food quality compared to the defended prey. This is a plausible scenario since low quality food is often easily accessible and available in large quantities, e.g. grass and leaves. (3) *Defended low quality scenario* - the defended prey species is of low food quality compared to the undefended prey. This scenario is also ecologically reasonable as protective structures, such as thorns of terrestrial plants or thicker cell walls of algae mainly consist of carbon and thus decrease the food quality of the prey (van Donk 1997).

A meta-analysis showed that cyanobacteria are generally a bad food source for zooplankton (Wilson et al. 2006). The detrimental effects originated mostly from morphology or biochemical mismatches, whereas toxicity was less relevant. The above mentioned scenarios are therefore informative to the management of cyanobacterial blooms, depending on the level of defence and biochemical food quality of the cyanobacteria in focus relative to their competitors.

Although for better clarity we focus on the extreme cases where either one of the prey species is of very low quality, we present also intermediate cases to cover (i) the gradual transition between the scenarios and (ii) a broader range of natural predator-prey systems.

It is often assumed that low quality itself already provides protection against predation, and thus also against predator-mediated competition, as it prevents the predator to establish high grazing pressures (Moran and Hamilton 1980; Augner 1995). This reasoning suggests that high food quality is detrimental to a prey species as it increases predation pressure and may provide a niche for predator-mediated competitors. We show that high food quality of a prey species can instead increase its persistence and promote coexistence with low-quality prey. With this approach we study how trade-offs between functional traits of species and their biochemical composition, two prominent features in ecology, in concert shape community composition and population dynamics.

Model and Methods

Predator-prey model

We build on a predator-prey model that was first published by Fussmann et al. (2000) as an algae-rotifer chemostat model and its basic properties were discussed in Jones and Ellner (2004) and Jones and Ellner (2007). The basic model assumptions are nitrogen limitation, nitrogen homoeostasis and asexual reproduction of all species. Therefore, all state variables are scaled to nitrogen by the organisms' respective nitrogen content. Nitrogen N is taken up by two algal prey species A and B which are consumed by one herbivore species Z, e.g. a rotifer.

$$\frac{dN}{dt} = \delta N_{\mathrm{I}} + R - \delta N - \frac{\beta\, N}{K_{\mathrm{A}} + N}\, A - \frac{\beta\, N}{K_{\mathrm{B}} + N}\, B \tag{3.1}$$

$$\frac{dA}{dt} = \frac{\beta\, N}{K_{\mathrm{A}} + N}\, A - f_{\mathrm{A}}\, Z - \delta A \tag{3.2}$$

$$\frac{dB}{dt} = \frac{\beta\, N}{K_{\mathrm{B}} + N}\, B - f_{\mathrm{B}}\, Z - \delta B \tag{3.3}$$

$$\frac{dZ}{dt} = \varepsilon_{\mathrm{A}}\, f_{\mathrm{A}}\, Z + \varepsilon_{\mathrm{B}}\, f_{\mathrm{B}}\, Z - \delta Z \tag{3.4}$$

$$f_{\mathrm{A}} = \frac{\rho\, p_{\mathrm{A}}\, A}{K_{\mathrm{Z}} + p_{\mathrm{A}}\, A + p_{\mathrm{B}}\, B} \tag{3.5}$$

$$f_{\mathrm{B}} = \frac{\rho\, p_{\mathrm{B}}\, B}{K_{\mathrm{Z}} + p_{\mathrm{A}}\, A + p_{\mathrm{B}}\, B} \tag{3.6}$$

$$R = (1 - \varepsilon_{\mathrm{A}})\, f_{\mathrm{A}}\, Z + (1 - \varepsilon_{\mathrm{B}})\, f_{\mathrm{B}}\, Z \tag{3.7}$$

While the model is parametrised for an algae-rotifer chemostat, the model structure is applicable for many predator-prey systems. The parameters can be found in Table 3.1. An inflow concentration N_{I} constantly supplies nitrogen with a flow rate δ. At the same flow rate all nitrogen is washed out of the chemostat volume, be it dissolved in the medium or bound within organisms. Natural mortality of organisms is considered to be small compared to grazing losses or wash-out and therefore omitted. The substrate uptake by the algae is modelled with Monod functions. The functional responses of the grazer on the algal species A and B, f_{A} and f_{B}, are assumed to follow a Holling-type-II and extended

Table 3.1 Parametrization of our model for an algae-rotifer chemostat. [1] (see Tischner and Lorenzen 1979), [2] estimated for our system from (Fussmann et al. 2000) and (Becks et al. 2010), [3] estimated from own measurements, [4] set according to typical experimental conditions, [5] (see Gaedke et al. 2002).

Parameter	Description	Value	Unit
δ	Chemostat dilution rate [4]	0.5	d^{-1}
N_I	Chemostat inflow nitrogen concentration [4]	80	$\mu\mathrm{mol\ N/l}$
β	Maximum growth rate of algae	1	d^{-1}
K_A	Half-saturation constant of algal species A [1]	4.3	$\mu\mathrm{mol\ N/l}$
K_B	Half-saturation constant of algal species B [4]	4.3 - 43	$\mu\mathrm{mol\ N/l}$
p_A	Predation risk of algal species A (undefended) [4]	1	1
p_B	Predation risk of algal species B (defended) [4]	0 - 1	1
ρ	Maximum grazing rate of the predator [2]	1.76	d^{-1}
K_Z	Half-saturation constant of the predator [2]	28	$\mu\mathrm{mol\ N/l}$
ε_A	Conversion efficiency of A into Z	0 - 0.66	1
ε_B	Conversion efficiency of B into Z	0 - 0.66	1
$\frac{S_\mathrm{low}}{S_\mathrm{Z}}$	sterol conc. of low-quality prey relative to that of Z [3]	0	1
$\frac{S_\mathrm{high}}{S_\mathrm{Z}}$	sterol conc. of high-quality prey relative to that of Z [3]	0.8	1
e	Excretion factor [5]	0.33	1

to multiple prey species (Holling 1959). Due to potential food quality differences between the algal species we assume different conversion efficiencies ε_A and ε_B for each prey. The derivation of these conversion efficiencies can be found in the supplementaries and we argue that they are prey-density dependent (next section). An efficiency smaller than one implies that nitrogen is ingested by the herbivore but only partly converted into production. The remaining share is recycled via excretion and leads to the recycling rate R to ensure mass balance. As discussed by (Jones and Ellner 2007), a trade-off between defence and competitiveness of the prey is implemented for the two algal species A and B. The investment into a lowered predation risk p, e.g. by producing defensive structures, comes at the cost of an increased half-saturation constant K and thus a lowered competitive ability at low nutrient concentrations (*competitiveness*) $1/K$ (Yoshida et al. 2004). Algal species A is considered the *undefended* but better growing prey and B is *defended* against predation, but pays a cost for that defence, i.e. $p_\mathrm{B} \leq p_\mathrm{A}, 1/K_B \leq 1/K_A$. The position in trait-space of the defended prey will be varied to study the effect of the strength of the trade-off. Thus in our model we cover a broad range of defence, competitiveness and food quality; three key parameters that govern predator-prey systems in general and herbivore-plant interactions in particular.

Food quality of prey

The transfer of ingested prey biomass into predator biomass is governed by the predator's conversion efficiency. It can only be high if the demands for all essential biochemical nutrients (EBN) of the predator are met. Since the diet of a predator often consists of several prey species, with each of them having a different biochemical composition, its conversion efficiency depends on the community composition of the prey. A sufficiently high share of high-quality prey in the diet may provide the biochemical nutrients to also convert ingested low-quality prey into predator biomass. This links the conversion efficiency of the predator to population dynamics within the prey community and connects prey food quality with predator-prey interactions.

We vary the concentration of EBN among two prey species, resulting in either *high* or *low* food quality of a prey species. We assume that the EBN-to-nitrogen ratio of high quality food is well above the needs of the predator. Production from high quality food is therefore only nitrogen-limited. The EBN-to-nitrogen ratio of low-quality food is well below that of the predator. Thus, production from low-quality prey occurs with a low efficiency unless supplementary biochemical nutrients can be obtained from the ingestion of additional high-quality prey (see Fig. A2.1 in Supporting Information). The effect of these assumptions is captured by the conversion efficiencies ε_A and ε_B. Biochemical food quality thus affects only the numerical response of the predator but not its functional response. The conversion efficiency for the low-quality prey species ε_{low} is smaller than or equal to the conversion efficiency for the high-quality plant species $\varepsilon_{\text{high}}$. The following points thus hold for the conversion efficiency:

(i) If no high-quality prey is taken up, low-quality prey is consumed, but only leads to low production due to a limitation by EBN and ε_{low} is minimal.

(ii) If the predator ingests high-quality prey containing more EBN than it can use with the nitrogen from the high-quality prey, this surplus EBN enables further predator production from additionally consumed low-quality prey. The consumption of high-quality prey increases ε_{low}.

(iii) If a relatively large amount of high-quality prey is ingested, ε_{low} becomes maximal ($\varepsilon_{\text{low}} = \varepsilon_{\text{high}}$) and predator production from low-quality prey is not limited by EBN, but entirely nitrogen-limited.

This reasoning results in a formulation of the conversion efficiency of the low-quality prey species ε_{low} which depends on the biomass ratio of high-quality prey to low-quality prey (Fig. A2.2). For a formal derivation of equation (3.8) we refer to the supplementaries (see A2).

$$\varepsilon_{\text{low}} = \min\left(1 - e\,,\ \frac{S_{\text{low}}}{S_{\text{Z}}} + \frac{f_{\text{high}}}{f_{\text{low}}}\left(\frac{S_{\text{high}}}{S_{\text{Z}}} - (1 - e)\right)\right) \tag{3.8}$$

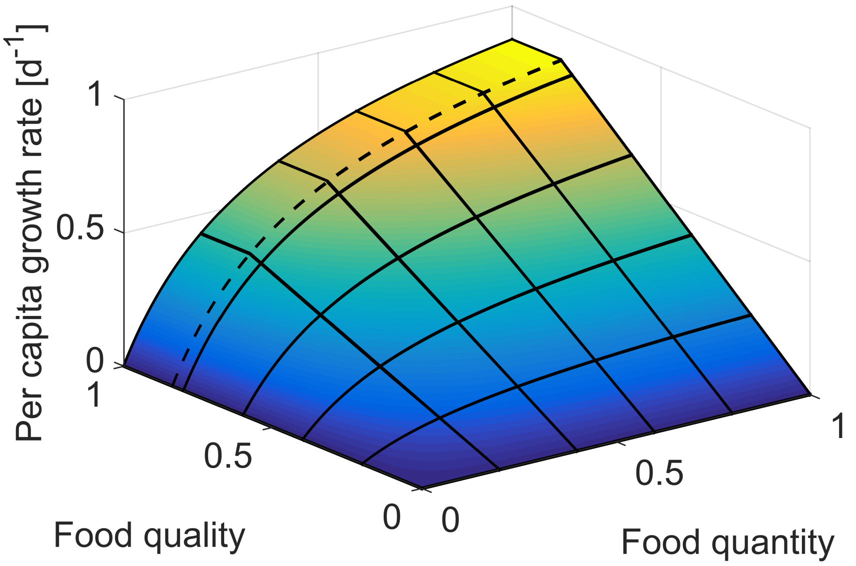

Figure 3.1 Co-limitation of predator growth by the quantity of available food, $(p_\mathrm{A}\,\mathrm{A}+p_\mathrm{B}\,\mathrm{B})/N_\mathrm{I}$, and its overall quality $\frac{p_\mathrm{A}\,\mathrm{A}}{p_\mathrm{A}\,\mathrm{A}+p_\mathrm{B}\,\mathrm{B}}$, assuming that A is the high-quality and B the low-quality prey. Parameters are $\frac{S_\mathrm{B}}{S_\mathrm{Z}}=0$, $\frac{S_\mathrm{A}}{S_\mathrm{Z}}=0.8$ and $e=0.33$.

The conversion efficiency of the high-quality prey species is constant and given by

$$\varepsilon_\mathrm{high}=1-e \tag{3.9}$$

Here, e is the excretion factor of the predator, S_{low}, S_{high} and S_Z are the EBN-to-nitrogen ratios of low-quality prey, high-quality prey and predator, respectively, and f_high and f_low are the functional responses of the predator on high- and low-quality prey, respectively. Since the biochemical nutrients are labile substances we assume that they are not recycled. The respective food quality scenario determines which prey species obtains which conversion efficiency:

Equal food quality scenario	$\varepsilon_\mathrm{A}=\varepsilon_\mathrm{high}$	$\varepsilon_\mathrm{B}=\varepsilon_\mathrm{high}$
Undefended low quality scenario	$\varepsilon_\mathrm{A}=\varepsilon_\mathrm{low}$	$\varepsilon_\mathrm{B}=\varepsilon_\mathrm{high}$
Defended low quality scenario	$\varepsilon_\mathrm{A}=\varepsilon_\mathrm{high}$	$\varepsilon_\mathrm{B}=\varepsilon_\mathrm{low}$

Our formulation of ε_B results in a partial co-limitation of predator growth by the quantity of available food, $(p_\mathrm{A}\,\mathrm{A}+p_\mathrm{B}\,\mathrm{B})/N_\mathrm{I}$, and its overall food quality, i.e. the relative portion of high-quality food among the available food. Fig. 3.1 shows the per capita growth rate of the predator for both quality and quantity of available food. If less than 80% of the available food are represented by the high-quality plant species, herbivore growth is co-limited by EBN and the quantity of available food. Above 80% of high-quality prey, food quality is not limiting and only food quantity determines predator growth via its functional response.

Simulations and determination of dynamics

By combining vectorization and parallel computing the system of ordinary differential equations (3.1) - (3.4) was integrated over a wide range of the trait space of the defended prey species B with the *ode23* algorithm in MatLab (The MathWorks, Natick, MA). The simulations were run for $400\,000$ time units (days) to overcome any transients. The simulations were initialized at $N(0) = 1/8\,N_{\mathrm{I}}$, $A(0) = 3/8\,N_{\mathrm{I}}$, $B(0) = 3/8\,N_{\mathrm{I}}$ and $Z(0) = 1/8\,N_{\mathrm{I}}$, except when we studied the dependence on initial conditions where different starting points were chosen. To distinguish between cycling and steady state dynamics, local peaks in herbivore density and the period length of cycles were determined using the *findpeaks* algorithm from the time-series toolbox in MatLab. Only the last $10\,000$ days were considered in this analysis and the period lengths were averaged. For peaks to be recognized, their relative size (prominence) had to exceed the simulation accuracy of 10^{-6}. The bifurcation between different dynamic states of the system were studied using the continuation and bifurcation software MatCont (Dhooge et al. 2003).

Results

Our simulations reveal how food quality influences species coexistence and population dynamics in a general predator-prey model. This holds in particular for the plant-herbivore interface as primary producers often differ in their biochemical composition from their consumers. We use an algae-rotifer system to examine three different combinations of prey food quality and defence: (1) *equal food quality scenario*, (2) *undefended low quality scenario* and (3) *defended low quality scenario*. Predator production is not limited by biochemical nutrients in the first scenario but potentially in the two others (Fig. 3.1). First, we evaluate species coexistence along the defence-competitiveness trade-off for the three different food quality scenarios (Fig. 3.2). Within each scenario, we vary the predation risk and the competitive ability at low nutrient concentrations of the defended prey species, relative to the undefended. Subsequently, the general types of species composition and population dynamics are discussed. Finally, we conclude by describing two ecologically relevant bistabilities between the system's long-term states. The results for the food quality scenarios are presented in detail for the extreme cases of prey food quality, as here the qualitative differences are clearest, but we present also the transition between these scenarios along a gradient of declining food quality.

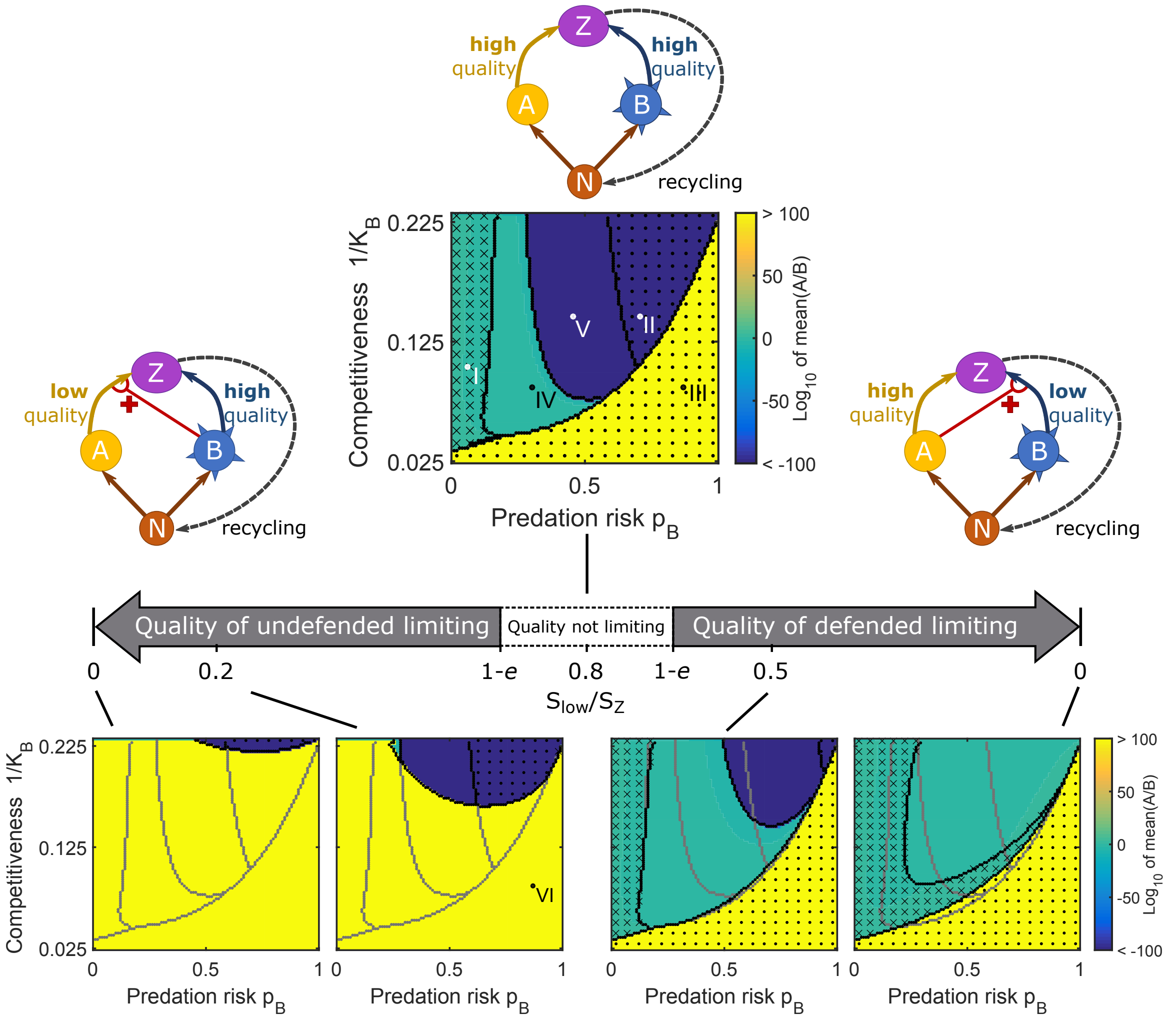

Figure 3.2 Competition outcome between the undefended prey A and the defended prey B growing on nitrogen N under predation by the predator Z for the three different food quality scenarios (above - *equal food quality*, far left - *undefended low quality*, far right - *defended low quality*) and the transitions. The trait differences between defended and undefended prey are varied by varying predation risk $p_\mathrm{B} \leq p_\mathrm{A}$ and competitiveness $1/K_B \leq 1/K_A$, $[(\mu\mathrm{mol\ N/l})^{-1}]$ of the defended prey. The colors depict the ratio between undefended and defended prey averaged over the last 10 000 days. Dotted and crossed regions show quarter phase lag and antiphase cycling dynamics, respectively. Regions without markers are in steady state. The boundaries of the different regions in the *equal food quality* scenario are shown in grey also in the other scenarios. Exemplary dynamics for parameter combinations **I-VI** are shown in Fig. 3.3. The predator goes extinct only in the yellow, unmarked region. Similar behaviour was found at a lower dilution rate of $\delta = 0.2\ \mathrm{d}^{-1}$ (Fig. A2.5).

Equally high food quality

The equal food quality scenario (Fig. 3.2, center) was studied before (Abrams 1999; Jones and Ellner 2007) and serves as a reference that excludes differences in food quality of prey. It exhibits three different final species compositions (Fig. 3.2). For high competitiveness and a moderately lowered predation risk of the defended prey species, the undefended prey is outcompeted (blue region, Fig.

3.2). This corresponds to low costs for relatively high gains in defence. The defence therefore pays off. If the competitiveness is too low, the defended prey species goes extinct as irrespective of the gain in defence the costs of maintaining the defensive strategy are too high (yellow region, Fig. 3.2). For very low predation risks both prey species coexist over a large range of the competitiveness of the defended prey (green region, Fig. 3.2). Here, the defended cannot sustain the predator alone as its defence is too high. Only if some undefended prey remains the predator is kept from extinction, which in turn ensures that the costs for defence pay off and the defended prey species persists.

Undefended prey is of low food quality

The outcome of prey competition changes drastically if the undefended prey is of low food quality (Fig. 3.2, left scenario). Only if the defended prey has a slightly lowered predation risk and a slightly lowered competitiveness compared to the undefended prey the competition outcome remains unchanged. Here, the defended prey is still able to dominate over the undefended prey as its defence pays off and costs are not too high (blue region, Fig. 3.2). Since the defended prey is of high food quality, it is able to sustain the predator. If the competitiveness of the defended prey is too low, the costs for defence become too high and the defended prey is outcompeted, as it was the case for equally high food quality in this region. However, now the undefended prey is of low food quality and cannot sustain the predator. Thus the predator goes extinct and only the undefended, low-quality prey remains (yellow region, Fig. 3.2). The same reasoning explains the outcome for a very low predation risk of the defended prey. In the equal food quality scenario, coexistence in this region was mediated by the predator, which was sustained only by the undefended prey as the defended prey was too defended. Since now the undefended prey is of low food quality, it does not sustain the predator which then cannot mediate coexistence. The resulting dominance of the undefended prey explains the spread of the yellow region over the steady state coexistence region and part of the region where the defended prey dominated in the equal food quality scenario. The extent of this overlap depends on the initial conditions and will be discussed later.

Defended prey is of low food quality

If the defended prey is of low food quality (Fig. 3.2, right scenario), we again see strong changes in the competition outcome compared to the other scenarios. The region in trait space where the defended prey outcompeted the undefended prey completely vanishes. In the equally high quality scenario the defence of the defended prey paid off while the defended prey was still able to sustain the predator on its own. Since it is now of poor nutritional value to the predator, it cannot sustain the predator which now depends on the high food quality of the undefended prey. If the undefended prey is grazed down to low biomasses the predator also decreases, thereby weakening the advantage of the defended over the undefended prey. This allows the undefended prey to withstand both competition with the defended prey as well as grazing from the predator. Consequently, the coexistence region which was only found for strong defences (low predation risk) in the equal food quality scenario now spreads across the entire range of predation risks (green region). If the costs of defence are too high for the defended prey, the undefended prey can persist with the predator due to its high food quality (yellow region). The upper boundary of this region, which defines at which competitiveness the defence pays off, is slightly shifted upwards. This implies that the defended prey needs an even higher competitiveness for its defence to pay off and to coexist with the undefended prey if it is of low food quality. Due to the increased coexistence of high and low-quality prey the effect of nutrient recycling is potentially large in this scenario. To study this effect we compared the prey competition outcome with (Fig. 3.2, right scenario) and without recycling (Fig. A2.3). We observed no qualitative changes in the coexistence pattern or the distribution of biomass (Fig. A2.4), but found less parameter combinations of cycling coexistence.

The outcome of prey competition is substantiated by the average biomasses of each species during the last $10\,000$ days of each simulation (Fig. A2.4). Within the coexistence region of the equal food quality scenario the defended prey on average reaches higher biomasses than the undefended prey. The predator attains high average biomasses for more parameter combinations in this scenario than in the other ones as it is never limited by food quality. The undefended prey has extremely high average biomasses in the undefended low quality scenario as it outcompetes its competitor and does not sustain the predator. Within the defended low quality scenario, the average biomasses are more evenly distributed across the parameter space compared to the other scenarios. Removing nutrient recycling reduces the average biomasses for most parameter combinations.

A central parameter in all chemostat studies is the dilution rate as it determines residence times of organisms and nutrients, and the relative importance of fresh nutrient supply versus recycling. Reducing the dilution rate from $0.5\ \mathrm{d}^{-1}$ to $0.2\ \mathrm{d}^{-1}$ enlarges the parameter space where defence pays off in the equal food quality scenario. Also the region in the defended low quality scenario where we predict coexistence mediated by the high quality of the undefended prey increases strongly (Fig. A2.5).

Population dynamics

Our system exhibits six different types of population dynamics for different parameter combinations of competitiveness and predation risk of the defended prey (Fig. 3.3). If both prey species coexist with the predator, the sum of the prey biomasses cycles antiphase with the predator biomass for lower predation risks (Fig. 3.2, crossed green region; Fig. 3.3, combination **I**). Within this antiphase cycling we observe temporal niching. If the predator biomass is high, the undefended prey is grazed down which releases the defended prey from nutrient competition. The predator declines as now the defended prey dominates the prey biomass. This releases the undefended prey from predation pressure and it outcompetes the defended prey. Therefore the temporal niche for the defended prey precedes the temporal niche of the undefended prey.

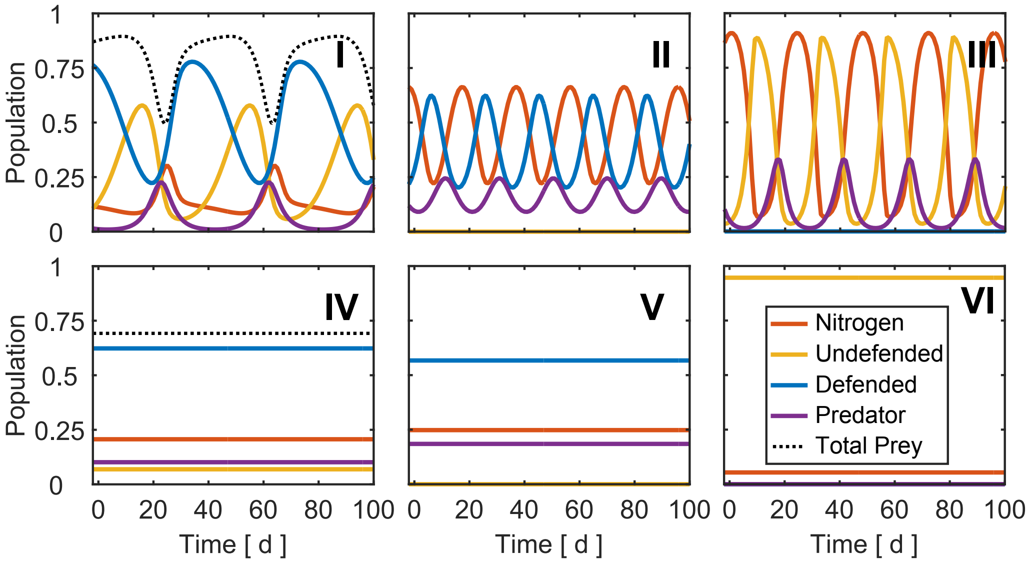

Figure 3.3 Population dynamics for the parameter combinations marked in figure 3.2. Populations are scaled to the inflow concentration of the chemostat and transients of 399900 days have been omitted. Combinations **I** and **IV** show coexistence of predator and both prey in antiphase cycling and steady state, respectively. In combinations **II** and **III** only one prey cycles with an approximately quarter phase lag with the predator. Combination **V** shows the steady state of the defended prey and the predator and in combination **VI** only the undefended prey, which is of low food quality in this case, remains in the system.

Prey coexistence in a steady state is attained for higher predation risks of the defended prey (Fig. 3.2, non-crossed green region; Fig. 3.3, combination **IV**). If one prey goes extinct and the remaining prey can sustain the predator population, prey and predator either cycle in a classic quarter-period phase lag (Fig. 3.2, dotted blue and dotted yellow region; Fig. 3.3, combinations **II** and **III**) or attain a steady state (Fig. 3.2, unmarked blue region; Fig. 3.3, combination **V**). If the predator is not sustained, the remaining prey grows to its steady-state capacity (Fig. 3.2, yellow unmarked region; Fig. 3.3, combination **VI**).

Bifurcations and bistability

We investigated the dependence of the dynamics on initial conditions and found a bistability in the undefended low quality scenario between dominance of the low-quality, undefended prey on the one hand and the species composition pattern found for equal food quality on the other hand (Fig. A2.6). Initially very low biomasses of the undefended, low-quality prey result in a smaller dominance region. If it has high initial biomasses, it dominates from the beginning and suppresses the establishment of either prey coexistence or the predator being sustained by the defended, high-quality prey, respectively.

We found a second bistability at the transition from cycling to steady state coexistence in the defended low quality scenario (Fig. 3.2, right scenario). In the reference model with equal biochemical food quality, coexistence in antiphase cycles and coexistence in steady state are connected by a supercritical Hopf-bifurcation (Fussmann et al. 2000; Jones and Ellner 2007). Within the defended low quality scenario, we find that the antiphase cycling at low predation risks of the defended prey and steady state prey coexistence are also connected by a supercritical Hopf-bifurcation. Interestingly, at intermediate predation risks, when decreasing the competitiveness of the defended prey, the transition from steady-state to antiphase cycling is instead mediated by a subcritical Hopf-bifurcation in combination with a cyclic-fold bifurcation (Fig. A2.7 and A2.8). This bifurcation pattern creates a bistability between steady state and antiphase cycling at the intersecting parameter region. This bistability becomes even more pronounced at lower dilution rates (Fig. A2.9).

Discussion

Food quality affects species coexistence

Under most natural conditions predators rely on a diverse community of prey species differing in their biochemical food quality. We show that these differences determine both prey species' coexistence and population dynamics. Our study reveals that within a diverse prey community, higher food quality does not necessarily imply a higher vulnerability to predation and extinction, but may favour survival under competition with a second defended prey species of lower food quality (Fig. 3.2, defended low quality scenario). In contrast, for a single prey species, low food quality is expected to serve as protection against extinction by predation (Moran and Hamilton 1980) as the predator cannot acquire enough biomass to graze down the prey population. Our results indicate that this protection is reduced as soon as there is a second, high-quality prey that can sustain a predator population (Fig. 3.2, undefended low quality scenario) and may thus be less relevant in nature.

The food quality of one prey species can modulate the growth of and predation on competing prey species and the resulting effect of food quality depends on differences and trade-offs between functional traits of the prey community. Consumption of a single individual directly decreases that species' density, but also impacts the whole prey community by two processes that directly depend on prey food quality: (i) additional predator production that increases the predation pressure on the whole prey community (numerical response) and (ii) nutrient recycling that makes nutrients from a consumed prey available to the whole prey community. These community effects of predation depend on both, the food quality of the consumed individual and the food quality composition of the whole prey community and are therefore highly context-dependent (Fig. 3.4).

Under high-quality conditions, i.e. in an environment dominated by high-quality prey, the predator production per consumed low-quality prey individual equals that of a high-quality prey since additionally consumed high-quality prey supplements the low-quality prey. Under low-quality conditions, however, an ingested individual of low-quality prey cannot be supplemented, leading to a low predator production. Under the same conditions an ingested high-quality prey allows for predator production from its own biomass and also delivers a surplus of biochemical nutrients that may be used to supplement additional predator production from low-quality prey.

Recycling behaves oppositely: under high-quality conditions only few of the nutrients bound within a consumed prey are recycled, irrespective of its own quality. The same holds for a high-quality prey that is consumed under low-quality conditions, while all of the nutrients from a low-quality prey are routed to the medium as there is no supplementation by high-quality prey (Fig. 3.4).

Whether and how the prey species are impacted by these indirect effects depends on their functional traits. The probability for a prey individual to be consumed and how it is affected by an increase in predation pressure are determined by its defence. Whether an increase of nutrient recycling matters depends on the competitiveness of the prey. Thus food quality gives rise to indirect species interactions between prey that shape the different competition outcomes within the trait space of the defended prey (Fig. 3.2).

Figure 3.4 implies that only strong competitors for nutrients can counteract predation with low food quality as most of their nutrients are recycled upon consumption and can only be regained if the low-quality prey is competitively superior. Therefore, under low-quality conditions, implying high recycling, low food quality is rather detrimental for a defended prey. Consumption of a low-quality

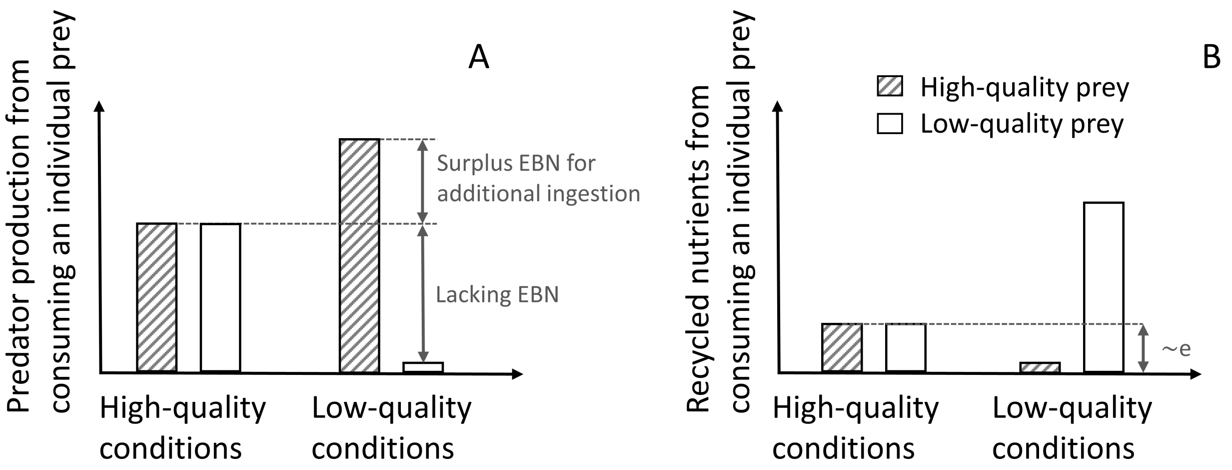

Figure 3.4 Predator production and nutrient recycling depend on both the ingested individual's food quality and the food quality of the whole prey community, i.e. the food quality conditions. (A) - Under high-quality conditions the predator can grow equally well on high- and low-quality prey due to supplementation. Under low-quality conditions, i.e. the predator is generally quality-limited, a high-quality prey individual can be converted efficiently into predator biomass. Also, it contributes surplus essential biochemical nutrients (EBN) that allow for additional predator production from low-quality prey. Under the same conditions an ingested low-quality prey individual is not supplemented and predator production is low. (B) - Under high-quality conditions nutrient recycling is proportional to the excretion factor e. Under low-quality conditions surplus EBN from an ingested high-quality prey individual reduce the net recycled nutrients below normal excretion as nitrogen from additional ingestion can also be converted, while most of the nutrients from a low-quality prey are recycled.

prey individual does not increase the predation pressure on the prey community. This prevents a competitive advantage for the defended prey. Instead, most of the nutrients from the ingested low-quality prey are recycled and made accessible to competitors, allowing for growth of an undefended prey species that is a better competitor for nutrients. If this species is of high food quality it increases the predator production by dietary supplementation of the low-quality species. Eventually, the supplementation limits its further net growth since now the defence of the defended prey pays off. Thus, the combination of limitation of predator production and recycling shifts biomass from the low-quality to the high-quality prey and promotes the persistence of the undefended high-quality prey species.

We assumed a rather high dilution rate typical for experimental systems studying predator-prey relationships (Fussmann et al. 2000). However, lower dilution rates in fact increase the significance of our results (Fig. A2.5). At low dilution prey growth is more bottom-up limited which makes being defended even more valuable as it protects already established biomasses. This allows the defended prey to outcompete the undefended prey already at lower competitiveness in the equal food quality scenario. As a consequence, also the coexistence region is enlarged which is mediated by quality limitation of the predator in the defended low quality scenario (Fig. A2.5). Additionally, lower dilution increases the importance of recycled nutrients relative to fresh supply (Vadstein et al. 2012).

This impedes the competitive ability of a low-quality species of which a higher portion is recycled by grazing (Fig. 3.4) and these recycled nutrients remain longer available to competitors due to the lower dilution rate.

Food quality affects population dynamics

Populations tend to switch from steady state to predator-prey cycles if the energy flux to the predators increases and food chains become more top-heavy (Abrams 1999; Rip and McCann 2011) and we observed corresponding patterns in our simulations. These switches are of ecological importance as within the cycles, populations may reach very small numbers making them vulnerable to stochastic extinctions (Rosenzweig 1971). Depending on the strength of the defence-competitiveness trade-off we found two types of population dynamics that enable both prey species to coexist with the predator (Fig. 3.3). Within the antiphase cycles of total prey and predator biomass, the niches that both prey occupy are temporally separated as the prey competes for a single nutrient (Gilpin 1975; Armstrong and McGehee 1980). At high competitiveness and high predation risk of the defended prey (weak trade-off) both prey species become more similar. This tends to increase the competition of the prey species as their temporal niches overlap to a larger extent. Therefore, prey growth becomes more bottom-up limited and its density dependence increases, which promotes steady-state dynamics. Similarly, competition between the two prey species increases without recycling. The amount of substrate in the system is reduced as a nitrogen export is created which becomes high at high grazing and low prey food quality. Thus, without recycling, we find cycling coexistence only for half as many parameter combinations (Fig. A2.3). At the transition from steady state of defended prey and predator to quarter phase lag cycling an increasing predation risk of the defended prey results in a higher prey availability for the predator and higher predator production, promoting predator-prey cycles.

Food quality may cause a bistability

In our system, the coexistence in antiphase cycles and the coexistence in steady-state is partly bistable giving rise to two possible long-term dynamics for the same species. This bistability is ecologically important for two reasons: (i) The mean biomasses of the species differ between the two states (Fig. A2.7). This affects system properties such as the mean food quality of the prey trophic level, but also the biomass of the predator is different. This can for example determine the system's invasibility for a top-predator or potential ecosystem services, e.g. production of essential biochemicals. (ii) Due to the non-linear dependence of grazing on prey biomass mean clearance rates differ between a cycling system and a system at steady state, even if the mean biomasses were equal (Jensen's inequality). This again can cause different energy fluxes between trophic levels for the same species or impact possible top-predators that may average over fluctuating biomasses due to their larger body size. Which of these states is attained depends on the initial conditions. Switching between the two attractors by directed perturbations can occur, e.g. by loss of a certain amount of the high-quality prey. Knowledge of such bistabilities in natural systems is important as it impacts their long-term predictability and may explain regime shifts (Andersen et al. 2009).

Biological relevance of our results

Intuitively, one expects low food quality of prey to be an indirect protection against predation as it prevents the predator to thrive and we can confirm this hypothesis for the undefended low quality scenario for a substantial parameter range. Counterintuitively, we also found that combining low food quality with a defence against predation can be unfavourable for that species. In this case, low food quality promotes coexistence with a second species that is especially vulnerable to predation as it is both undefended and of high food quality. This unexpected result is ecologically relevant as the underlying scenario is supported by experimental findings. Defensive physiological structures, such as thicker cell walls (van Donk 1997; Hamm et al. 2003) or spines and thorns (Milewski et al. 1991; Tollrian and Harvell 1999) are mainly made of carbon (e.g. cellulose) and therefore, by increasing the carbon-to-nutrient ratio, decrease the food quality of the defended prey. The defended low quality scenario that comprises the coexistence promoting effect of food quality thus may regularly occur in natural systems.

While in general our approach makes no assumptions of a distinct ecosystem, an intriguing and economically relevant example where our model may be informative are cyanobacterial blooms. Firstly, reports of the low biochemical quality of cyanobacteria for grazers accumulate (Martin-Creuzburg et al. 2009; Wacker and Martin-Creuzburg 2012). Secondly, the morphology of cyanobacteria is diverse ranging from single-celled forms over colonies to filamentous species and largely affects zooplankton performance analogous to the predation risk we defined (Wilson et al. 2006). Thus, both the undefended low quality scenario and the defended low quality scenario are realistic situations for pelagic ecosystems as predation risk and food quality are always measured relative to the respective competitors of the cyanobacteria. The undefended low quality scenario (Fig. 3.2, left side) is representative for cyanobacterial blooms when no better competitor for nutrients is present, and grazers and competitors go extinct. The defended low quality scenario (Fig. 3.2, right side) holds for defended cyanobacteria (e.g. by colony-forming or mat-building) which are worse competitors for nutrients than other high quality algal species due to their defense (e.g. by limited diffusion through the clumps). For this situation, our study predicts that the complete take-over of the cyanobacteria is prevented by the high quality of the competitor which fits with observations (Nixdorf and Hoeg 1993).

The nutritional imbalance at the plant-herbivore interface is a general feature in nature (Elser et al. 2000). Thus, food quality plays an important role across scales and ecosystems and supplementary feeding might be a prominent strategy of many herbivores. Our work shows that food quality can determine species coexistence and population dynamics and that a prey species can shape the predation on the whole prey community. Together with other species' traits and trade-offs among these traits, low food quality can reduce predation pressure while high food quality can promote predator-mediated coexistence of prey. Nature comprises more than direct species interactions and food quality should be considered an important factor that mediates indirect interactions and shapes functional biodiversity.

Acknowledgements

We thank Apostolos-Manuel Koussoroplis, Elias Ehrlich, Dominik Martin-Creuzburg and Teppo Hiltunen for helpful discussions and insightful comments on the manuscript. Also we thank the reviewers who improved the manuscript significantly. This work was funded by DFG (WA 2445/8-1, WA 2445/11-1, GA 401/26-1) as part of the Priority Programme 1704 (DynaTrait).

Bibliography

Abrams, P. A. (1998). High Competition with Low Similarity and Low Competition with High Similarity: Exploitative and Apparent Competition in Consumer-Resource Systems. *Am. Nat.* 152: 114–128.

Abrams, P. A. (1999). Is Predator-Mediated Coexistence Possible in Unstable Systems? *Ecology* 80: 608–621.

Abrams, P. A. and Matsuda, H. (1997). Prey Adaptation as a Cause of Predator-Prey Cycles. *Evolution* 51: 1742–1750.

Ahlgren, G., Gustafsson, I.-B., and Boberg, M. (1992). Fatty acid content and chemical composition of freshwater microalgae. *J. Phycol.* 28: 37–50.

Andersen, T., Carstensen, J., Hernández-García, E., and Duarte, C. M. (2009). Ecological thresholds and regime shifts: approaches to identification. *Trends Ecol. Evol.* 24: 49–57.

Armstrong, R. A. and McGehee, R. (1980). Competitive Exclusion. *Am. Nat.* 115: 151–170.

Augner, M. (1995). Low nutritive quality as a plant defense: effects of herbivore-mediated interactions. *Evol. Ecol.* 9: 605–616.

Becks, L., Ellner, S. P., Jones, L. E., and Hairston Jr, N. G. (2010). Reduction of adaptive genetic diversity radically alters eco-evolutionary community dynamics. *Ecol. Lett.* 13: 989–997.

Becks, L., Ellner, S. P., Jones, L. E., and Hairston, N. G. (2012). The functional genomics of an eco-evolutionary feedback loop: Linking gene expression, trait evolution, and community dynamics. *Ecol. Lett.* 15: 492–501.

Chesson, P. (1990). MacArthur's consumer-resource model. *Theor. Popul. Biol.* 37: 26–38.

Dhooge, A., Govaerts, W., and Yu. A. Kuznetsov (2003). matcont: A matlab package for numerical bifurcation analysis of ODEs.

van Donk, E. (1997). Defenses in phytoplankton against grazing induced by nutrient limitation, UV-B stress and infochemicals. *Aquat. Ecol.* 31: 53–58.

Elert, E. v., Martin-Creuzburg, D., and Le Coz, J. R. (2003). Absence of sterols constrains carbon transfer between cyanobacteria and a freshwater herbivore (Daphnia galeata). *Proc. R. Soc. B Biol. Sci.* 270: 1209–1214.

Elser, J. J., Bracken, M. E. S., Cleland, E. E., et al. (2007). Global analysis of nitrogen and phosphorus limitation of primary producers in freshwater, marine and terrestrial ecosystems. *Ecol. Lett.* 10: 1135–1142.

Elser, J. J., Fagan, W. F., Denno, R. F., et al. (2000). Nutritional constraints in terrestrial and freshwater food webs. *Nature* 408: 578–580.

Fussmann, G. F., Ellner, S. P., Shertzer, K. W., and Hairston, N. G. J. (2000). Crossing the Hopf Bifurcation in a Live Predator-Prey System. *Science* 290: 1358–1360.

Gaedke, U., Hochstädter, S., and Straile, D. (2002). Interplay between energy limitation and nutritional deficiency: empirical data and food web models. *Ecol. Monogr.* 72: 251–270.

Gilpin, M. E. (1975). Limit Cycles in Competition Communities. *Am. Nat.* 109: 51–60.

Hamm, C. E., Merkel, R., Springer, O., et al. (2003). Architecture and material properties of diatom shells provide effective mechanical protection. *Nature* 421: 841–843.

Hiltunen, T., Hairston, N. G., Hooker, G., Jones, L. E., and Ellner, S. P. (2014). A newly discovered role of evolution in previously published consumer-resource dynamics. *Ecol. Lett.* 17: 915–923.

Holling, C. S. (1959). The Components of Predation as Revealed by a Study of Small-Mammal Predation of the European Pine Sawfly. *Can. Entomol.* 91: 293–320.

Jones, L. E. and Ellner, S. P. (2004). Evolutionary tradeoff and equilibrium in an aquatic predator-prey system. *Bull. Math. Biol.* 66: 1547–1573.

Jones, L. E. and Ellner, S. P. (2007). Effects of rapid prey evolution on predator–prey cycles. *J. Math. Biol.* 55: 541–573.

MacArthur, R. (1970). Species packing and competitive equilibrium for many species. *Theor. Popul. Biol.* 1: 1–11.

Martin-Creuzburg, D. and Merkel, P. (2016). Sterols of freshwater microalgae: potential implications for zooplankton nutrition. *J. Plankton Res.* 38: 865–877.

Martin-Creuzburg, D., Sperfeld, E., and Wacker, A. (2009). Colimitation of a freshwater herbivore by sterols and polyunsaturated fatty acids. *Proc. R. Soc. B Biol. Sci.* 276: 1805–1814.

Milewski, A. V., Young, T. P., and Madden, D. (1991). Thorns as induced defenses: experimental evidence. *Oecologia* 86: 70–75.

Moran, N. and Hamilton, W. (1980). Low nutritive quality as defense against herbivores. *J. Theor. Biol.* 86: 247–254.

Müller-Navarra, D. C. (1995). Biochemical versus mineral limitation in Daphnia. *Limnol. Oceanogr.* 40: 1209–1214.

Nixdorf, B. and Hoeg, S. (1993). Phytoplankton — Community Structure, Succession and Chlorophyll Content in Lake Müggelsee from 1979 to 1990. *Int. Rev. der gesamten Hydrobiol. und Hydrogr.* 78: 359–377.

Piepho, M., Arts, M. T., and Wacker, A. (2012). Species-specific variation in fatty acid concentrations of four phytoplankton species: Does phosphorus supply influence the effect of light intensity or temperature? *J. Phycol.* 48: 64–73.

Rip, J. M. K. and McCann, K. S. (2011). Cross-ecosystem differences in stability and the principle of energy flux. *Ecol. Lett.* 14: 733–740.

Rosenzweig, M. L. (1971). Paradox of Enrichment: Destabilization of Exploitation Ecosystems in Ecological Time. *Science* 171: 385–387.

Sperfeld, E., Martin-Creuzburg, D., and Wacker, A. (2012). Multiple resource limitation theory applied to herbivorous consumers: Liebig's minimum rule vs. interactive co-limitation. *Ecol. Lett.* 15: 142–150.

Sterner, R. W. (2008). On the phosphorus limitation paradigm for lakes. *Int. Rev. Hydrobiol.* 93: 433–445.

Tischner, R. and Lorenzen, H. (1979). Nitrate uptake and nitrate reduction in synchronous Chlorella. *Planta* 146: 287–292.

Tollrian, R. and Harvell, C. D. (1999). The Ecology and Evolution of Inducible Defenses. Princeton University Press.

Vadstein, O., Olsen, L. M., and Andersen, T. (2012). Prey-predator dynamics in rotifers: Density-dependent consequences of spatial heterogeneity due to surface attachment. *Ecology* 93: 1795–1801.

Volkman, J. K. (2003). Sterols in microorganisms. *Appl. Microbiol. Biotechnol.* 60: 495–506.

Wacker, A. and Martin-Creuzburg, D. (2012). Biochemical nutrient requirements of the rotifer Brachionus calyciflorus: Co-limitation by sterols and amino acids. *Funct. Ecol.* 26: 1135–1143.

Wilson, A. E., Sarnelle, O., and Tillmanns, A. R. (2006). Effects of cyanobacterial toxicity and morphology on the population growth of freshwater zooplankton: Meta-analyses of laboratory experiments. *Limnol. Oceanogr.* 51: 1915–1924.

Yoshida, T., Hairston, N. G., and Ellner, S. P. (2004). Evolutionary trade-off between defence against grazing and competitive ability in a simple unicellular alga, Chlorella vulgaris. *Proc. R. Soc. B Biol. Sci.* 271: 1947–1953.

4 Co-adaptation impacts robustness of predator-prey dynamics facing perturbations

Co-adaptation impacts the robustness of predator-prey dynamics against perturbations

Michael Raatz, Ellen van Velzen and Ursula Gaedke

Institute of Biochemistry and Biology, University of Potsdam, Potsdam, Germany

Abstract

Global change threatens the maintenance of ecosystem functions that are shaped by the persistence and dynamics of populations. It has been shown that the persistence of species increases if they possess larger trait adaptability. Here, we investigate whether this adaptability also affects the robustness of population dynamics of interacting species and thereby shapes the reliability of ecosystem functions that are driven by these dynamics. We model co-adaptation in a predator-prey system as changes to predator offense and prey defense due to evolution or phenotypic plasticity. We investigate how trait adaptation affects the robustness of population dynamics against press perturbations to environmental parameters, and against pulse perturbations targeting species abundances and their trait values. Robustness of population dynamics is characterized by resilience, elasticity and resistance. In addition to employing established measures for resilience and elasticity against pulse perturbations (extinction probability and return time), we propose the warping distance as a new measure for resistance against press perturbations which compares the shapes and amplitudes of pre- and post-perturbation population dynamics. As expected, we find that the robustness of population dynamics depends on the speed of adaptation, but in non-trivial ways. Elasticity increases with speed of adaptation as the system returns more rapidly to the pre-perturbation state. The pattern for resilience is more complex, as resilience is enhanced by intermediate speeds of adaptation, as here adaptation dampens biomass oscillations. The resistance of population dynamics strongly depends on the target of the press perturbation, which prevents a simple relationship with the adaptation speed. We often find that low robustness coincides with high amplitudes of population dynamics. Hence, amplitudes may indicate the robustness against perturbations also in other natural systems with similar dynamics. Our findings show that besides counteracting extinctions, trait adaptation indeed strongly affects the robustness of population dynamics against press and pulse perturbations.

Introduction

Environmental perturbations are likely to occur more frequently in many ecosystems as local conditions for many communities are altered permanently, e.g. due to climate and land-use changes, and instantaneously, e.g. by harvesting or extreme weather events (Meehl and Tebaldi 2004; Rahmstorf and Coumou 2011; Fischer et al. 2018). Population dynamics are a key determinant of many ecosystem functions (Lovett et al. 2002; Yang 2004; Bauer et al. 2014; Barraquand et al. 2017). To evaluate the stability of ecosystem functions facing global change it is therefore of crucial importance to understand how population dynamics are impacted by such perturbations.

These population dynamics are strongly influenced by the functional traits that determine the interactions between organisms. It is by now well-established that these traits are often flexible and may adapt to new biotic and abiotic conditions through evolution or phenotypic plasticity (West-Eberhard 1989; Kovach-Orr and Fussmann 2013). If strong enough, such adaptation may prevent extinctions of populations subject to strong environmental changes (Hughes et al. 2008; Oliver et al. 2015). We hypothesize that, similar to decreasing the extinction risk, the potential for adaptation may increase the robustness of population dynamics against perturbations and thereby buffer the degree of change to the dynamics.

Prominent examples for rapid, contemporary trait adaptation are changes in offense and defense traits in predator-prey or host-parasite systems (Kopp and Tollrian 2003; Yoshida et al. 2003; Mougi and Iwasa 2010; Cortez and Weitz 2014; Frickel et al. 2016). Here, trait changes increase individual fitness and can induce complex population dynamics through feed-backs between the co-adapting offense and defense traits. Trade-offs between the offense (defense) trait and other growth-related traits, such as maximum growth rate, half-saturating prey (resource) concentration or conversion efficiency of the predator (prey) restrict an arms race and allow for cyclic trait dynamics. In such systems, organisms are torn between optimizing their fitness with respect to environmental conditions on the one hand but also with respect to the interaction between trophic levels on the other. Traits adapt to optimally balance between these fitness components. External perturbations could therefore have a strong impact on the population dynamics, which might however be mediated by trait adaptation, resulting in complex population and trait dynamics.

We study how different types of perturbations affect the dynamics of a predator-prey system, and how their robustness is mediated by offense-defense co-adaptation. Not only the type of the perturbation, but also its target (e.g. biomasses or trait values) may affect the robustness of the dynamics, i.e. how the population and trait dynamics are altered by the perturbations. We therefore investigate whether the ability to adapt within ecologically relevant timescales affects the robustness of predator-prey systems and how this relationship is impacted by the perturbation type and target.

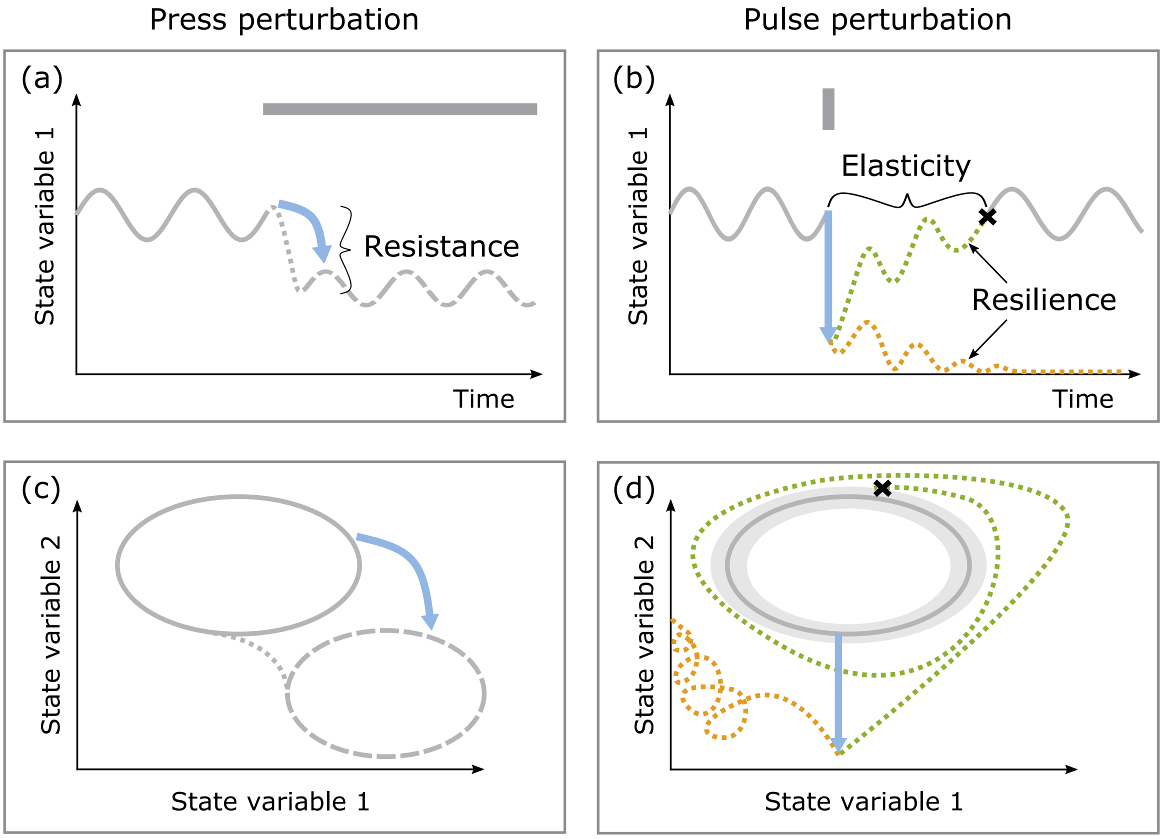

Figure 4.1 Sketch illustrating the types of perturbations and the different aspects of robustness of the population dynamics. Time series (top) and state space representations (bottom) of a system targeted by a press perturbation, i.e. permanent change in a system parameter, panels (a) and (c), or a pulse perturbation, i.e. an instantaneous change in one or more state variables, panels (b) and (d). Perturbations are represented by grey bars in (a) and (b), their effect is depicted by the blue arrows. A press perturbation changes the shape and location of the attractor. The distance between the pre- and post-perturbation attractor (full and dashed lines in panel c) is a measure for the resistance. A pulse perturbation deflects the trajectory away from the attractor. Resilience determines whether the trajectory remains in the basin of attraction of the pre-perturbation attractor and returns to it in a transient (dotted green line) or moves to an alternative stable state (dotted orange line). For a resilient system, elasticity determines how quickly the trajectory returns to the attractor. It is measured by the return time that passes until the trajectory enters a narrow state space volume around the attractor. This event is marked by the crosses in (b) and (d).

We will consider *press* and *pulse* perturbations as perturbation types and *resistance* (against press perturbations) and *resilience* and *elasticity* (after pulse perturbations) as corresponding robustness measures. Press perturbations permanently change the population and trait dynamics (Bender et al. 1984). Resistance measures the magnitude of this change (Fig. 4.1a,c) (Grimm and Wissel 1997), i.e. the dynamics of a more resistant system will change less strongly. Instantaneous perturbations are termed pulse perturbations (Fig. 4.1b,d) (Bender et al. 1984). Whether the system recovers from a pulse perturbation is governed by its resilience. How quickly the pre-perturbation state is reached depends on the elasticity of the system (Grimm and Wissel 1997), but is equivalent to engineering resilience as defined by Holling (1996). Trait adaptability may provide organisms with means to buffer the effects of press and pulse perturbations and preserve, potentially after a transient, the original population dynamics.

First, we characterize the effect of the speed of adaptation and the two most decisive environmental parameters on the dynamics themselves from bifurcation diagrams. These diagrams allow us to identify different regimes of biomass-trait dynamics along the speed of adaptation. We use the different robustness measures (resistance or resilience and elasticity) to characterize how robust these dynamics are when faced with press and pulse perturbations, respectively. We find that robustness tends to increase for faster adaptive systems, although this tendency is not exclusive but depends on further details, such as the perturbation target. From recurrent similarities between the different regimes and the robustness measures we can infer a correlation between them and conclude that the population and trait dynamics themselves already signal their robustness against environmental perturbations. The counter-intuitive nature of some of our results shows the need for detailed analyses such as ours, to guide conservation efforts and predict the impact of perturbations on the dynamics of adaptive consumer-resource systems.

Methods

Model description

We investigate a predator-prey chemostat ODE model with substrate s, prey x and predator y. The chemostat presents a tractable simplification of natural food webs, where the fluxes are balanced and the overall number of parameters is rather low (Smith and Waltman 1995). Many of the numerous environmental factors that act on food webs in nature reduce to two parameters in the chemostat, the inflow concentration of substrate and the chemostat dilution rate. As a result, it is mainly these two parameters that determine the balance between bottom-up and top-down limitation, which is a strong determinant of the population dynamics.

Our model is parameterized for an algae-rotifer system, the parameters are provided in Tab. 4.1. The substrate is modelled as nitrogen ($\mu\mathrm{mol}\,\mathrm{L}^{-1}$). Prey and predator are scaled to carbon ($\mathrm{mg}\,\mathrm{L}^{-1}$).

Table 4.1 Parameter values and their biological meaning. References: [1]varied within this study, [2]Raatz et al. (2018) and references therein, [3]van Velzen and Gaedke (2017), [4]van Velzen and Gaedke (2018)

Parameter	Biological meaning	Value
δ	Chemostat dilution rate[1]	$0.4\ \mathrm{d}^{-1}$, if not stated otherwise
s_I	Inflow resource concentration[1]	80 µmolN/L, if not stated otherwise
$\omega_{A,N}$	N content in an algal cell[2]	4.6×10^{-8} µmolN
$\omega_{A,C}$	C content in an algal cell[2]	6×10^{-9} mgC
r_0	Maximum algal growth rate[2]	$1.9\,\mathrm{d}^{-1}$
K	Algal half-saturation[2]	49 µmolN/L
a_0	Maximum attack rate of rotifers[2]	$3.6/2.34\,\mathrm{mgC}^{-1}\,\mathrm{d}^{-1}$
ε_0	Maximum conversion efficiency of rotifers[3]	1
h	Handling time of rotifers[2]	$1/3.6\,\mathrm{d}$
G	Speed of adaptation[1]	10^{-3} - $10^{-0.5}$
c_x	Costs for defense[3]	3
c_y	Costs for offense[3]	2
θ	Slope of attack rate function[4]	7
α	Lower boundary for trait values[4]	0.001

The model reads as follows

$$\begin{aligned}\frac{\mathrm{d}s}{\mathrm{d}t} &= \delta\,(s_I - s) - \frac{\omega_N}{\omega_C}\,r\,\frac{s}{K+s}\,x\\ \frac{\mathrm{d}x}{\mathrm{d}t} &= r\,\frac{s}{K+s}\,x - \frac{a\,x}{1+a\,h\,x}\,y - \delta\,x\\ \frac{\mathrm{d}y}{\mathrm{d}t} &= \varepsilon\,\frac{a\,x}{1+a\,h\,x}\,y - \delta\,y\end{aligned} \tag{4.1}$$

Substrate is supplied to the chemostat system and washed out by the dilution rate δ, s_I is the substrate concentration in the inflow medium. Prey growth reduces the substrate following a Monod term with maximum growth rate r and half-saturation constant K. The growth of prey is rescaled to substrate consumption from carbon to nitrogen by the ratio of the respective per-capita contents ω_N/ω_C. Prey is grazed by the predator following a Type II functional response with attack rate a and handling time h, and washed out by dilution. Predator growth is converted from grazing by the conversion efficiency ε. Washout decreases predator density and is assumed to be large compared to natural mortality, which is thus omitted for simplicity.

We implemented co-adaptation between prey defense u and predator offense v (Iwasa et al. 1991; Yamauchi and Yamamura 2005; Mougi and Iwasa 2010; van Velzen and Gaedke 2017), (Eq. 4.2). Defense and offense traits are dimensionless. This formulation makes no assumptions on the type of adaptation and therefore corresponds to both evolution or adaptation driven by phenotypic plasticity. Trait changes are scaled relative to the ecological dynamics by the speed of adaptation G (Abrams 1992), which corresponds to the additive genetic variation in the prey and predator populations divided by their generation time in the case of evolutionary adaptation (Iwasa et al. 1991; Mougi and Iwasa 2010, 2011). The traits change proportionally to the respective gradient of per-capita net growth rates along the traits. The exponential functions in Eq. 4.2 are boundary functions restricting the dynamics of u and v to positive values by decreasing the speed of trait changes when u or v approach zero ($\alpha = 0.001$) (Abrams and Matsuda 1997; van Velzen and Gaedke 2017).

$$\begin{aligned} \frac{\mathrm{d}u}{\mathrm{d}t} &= G\,\frac{\partial \frac{1}{x}\frac{\mathrm{d}x}{\mathrm{d}t}}{\partial u}\; e^{-\frac{\alpha}{u}} \\ \frac{\mathrm{d}v}{\mathrm{d}t} &= G\,\frac{\partial \frac{1}{y}\frac{\mathrm{d}y}{\mathrm{d}t}}{\partial v}\; e^{-\frac{\alpha}{v}} \end{aligned} \tag{4.2}$$

The accessible trait range is constrained by trade-offs between prey defense u and maximum growth rate r, and predator offense v and conversion efficiency ε (Eq. 4.3). The difference between defense and offense determines the attack rate the predator can exert on the prey, which is implemented as a sigmoidal function. The maximum slope of the attack rate function is scaled by θ. The maximum growth rate of prey in the Monod term r and the conversion efficiency of predators ε decrease with increasing trait values, i.e. higher defense or offense, according to Gaussians with heights r_0 and ε_0, and standard deviations $1/c_x$ and $1/c_y$. These standard deviations can be interpreted as the inverses of the costs for trait changes. For given trait values higher costs correspond to stronger decreases in maximum growth rate and conversion efficiency (Mougi and Iwasa 2011; van Velzen and Gaedke 2017).

$$\begin{aligned} a &= \frac{a_0}{1 + e^{\theta(u-v)}} \\ r &= r_0\, e^{-c_x u^2} \\ \varepsilon &= \varepsilon_0\, e^{-c_y\, v^2} \end{aligned} \tag{4.3}$$

It has been shown that the biomass-trait dynamics in this model can be understood by examining the effective prey biomass, which is given by the product of the normalized conversion efficiency and attack rate of the predator and the prey density, $\frac{\varepsilon}{\varepsilon_0}\,\frac{a}{a_0}\,x$ (van Velzen and Gaedke 2017, 2018). This quantity informs not only about the total prey density, but also about how accessible the prey is to predator and how efficiently it can be converted into predator growth

The system of ordinary differential equations (Eq. 4.1) was integrated using the NDSolve function in Mathematica (Wolfram Research Inc. 2014). Bifurcations of the model were studied using the continuation and bifurcation software MatCont (Dhooge et al. 2003).

Obtaining a discretized attractor

The dynamics of the biomass-trait system (Eqs. 4.1 and 4.2) give rise to a trajectory, i.e. a curve, that is described by the system's movement through the state space spanned by the state variables (s, x, y, u, v) as time passes (Fig. 4.1). For a given parameter set the trajectory tracks an attractor through the state space, which can be a limit cycle. The shape and size of this attractor characterize the biomass-trait dynamics and may be used to study changes to these dynamics. To allow further investigation, a discretized representation of this attractor consisting of 500 points was obtained by simulating exactly one period length of the population dynamics from initial conditions on the attractor. To determine these initial conditions, the system was simulated for $10\,000$ days, starting from $s_0 = 10\,\mu\mathrm{mol\,L^{-1}}$, $x_0 = 1\,\mathrm{mgC/L}$, $y_0 = 0.8\,\mathrm{mgC/L}$, $u_0 = 0.3$, $v_0 = 0.35$. The endpoint of this simulation then served as the initial condition for the attractor. To exclude the transient the period length was determined from the last $1\,000$ days of this simulation, which was discretized with a temporal resolution of 0.001 days. Using the FindPeaks function in Mathematica the maxima in these last $1\,000$ days were determined. The period length was then obtained from the average time span between these maxima, excluding the edges of the observation period, which yield trivial maxima.

Robustness measures

Resistance to press perturbations

Press perturbations cause permanent changes to the size, shape and location of this attractor, by permanently changing one or more of the environmental parameters that determine the dynamics of the system. Resistance determines the sensitivity to such permanent changes. A less resistant system exhibits stronger changes for small changes in the environmental parameters. In a chemostat system, many of the natural environmental factors acting on the system can be captured by the parameters for inflow concentration s_I and dilution rate δ.

We determined the resistance of our system by assessing the dissimilarity of pre- and post-perturbation attractors that arise from a permanent change in one of these two parameters (Fig. 4.1a,c). The direction of the parameter change can be freely chosen as the dissimilarity is symmetric with respect to the choice of which attractor is the pre- or post-perturbation attractor. The dissimilarity might however depend on the parameter region in which the perturbations occur. Thus, we created the pre- and post-attractors from parameter changes relative to a reference parameter set p_r and varied this reference. The two attractors that correspond to the pre- and post-perturbation states of the system A_1 and A_2 are then the attractors for $p_{1,2} = p_r \pm \Delta p$.

Two arbitrary, open curves can be compared by dynamic time warping (Berndt and Clifford 1994). We slightly adapted this concept and used it to measure the dissimilarity between the two attractors A_1 and A_2, by assigning each point on one attractor to the nearest point on the other attractor. To do so, we have to define a distance measure. The Euclidean distance between two points in state space can only be calculated if the units of all coordinates, i.e. vector components, are equal. To compare all components of the two attractors, i.e. all five dimensions (s, x, y, u, v) which have different units, one way would be to rescale the attractor and set the minimum and maximum along every axis to zero and one, respectively. While doing so, we however lose the information on the size and location of the attractor, as well as change the shape strongly, both of which would render this kind of comparison little informative. Instead, we converted the substrate s, which is in units of nitrogen concentration, to the equivalent carbon concentration if all that nitrogen would be built into prey biomass, using the prey's carbon-to-nitrogen ratio. This allows us to compare substrate, prey and predator components, i.e. the projections of the attractors on three dimensions from the five-dimensional state space. Also, the traits for defense and offense have the same units and the attractor projections into trait-space are also directly comparable.

By comparing only the converted substrate, prey and predator (all $\mathrm{mgC/L}$) or defense and offense (both dimensionless) we can thus define two measures of attractor dissimilarity using the Euclidean distance: (i) the average warping distance (AWD), which is the average over all shortest distances from the points on one attractor to any nearest point on the other attractor, and (ii) the maximum warping distance (MWD), which is the maximum of these shortest distances. The MWD is similar to the Fréchet distance (Fréchet 1906; Eiter and Mannila 1994). It increases strongly if only a few points on one attractor move away from the other attractor, assuming both are limit cycles. The AWD is therefore more conservative and averages the dissimilarities that occur over the whole length of the attractors. An example of how the two measures are obtained is presented in Fig. 4.2. It nicely shows that the AWD is dominated by the many small distances at smaller biomasses where the trajectory moves slowly. The MWD however captures the short excursions in state space, which yield large distances between the attractors. Using AWD and MWD we determined the resistance of the predator-prey system in a chemostat (Eqs. 4.1, 4.2) against press perturbations to the environmental parameters of dilution rate δ and inflow concentration s_I.

Resilience and elasticity after pulse perturbations

Resilience and elasticity are measured after pulse perturbations to the state variables. These perturbations can target the resource, biomasses and traits either individually or simultaneously (Fig. 4.1b,d).

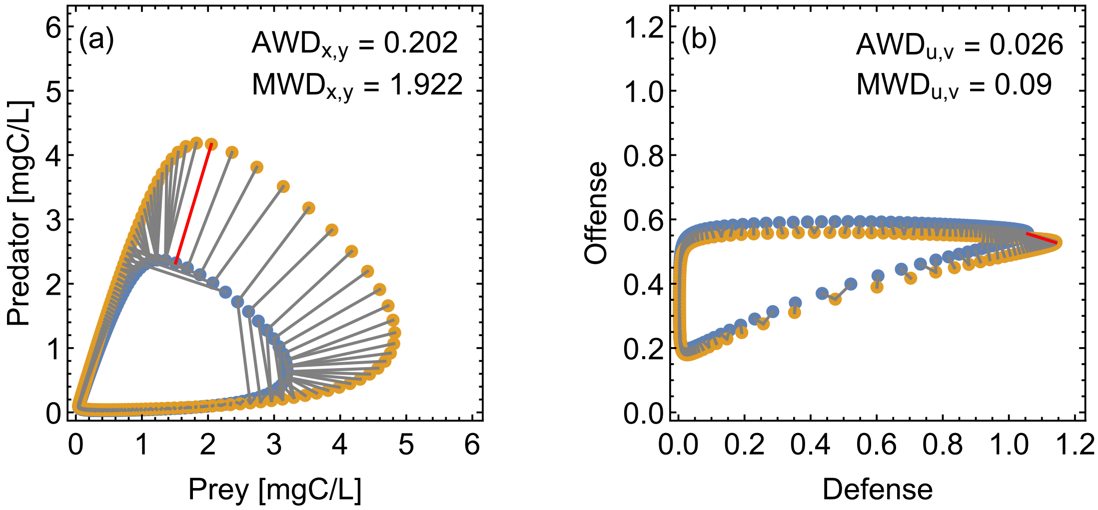

Figure 4.2 Visualization of two discretized attractors (yellow and blue dots) that correspond to pre- and post perturbation attractors of a press-perturbation to the inflow concentration, $s_I = (1 \pm 0.2)s_r$, and their average and maximum warping distance (AWD and MWD) for (a) the biomass components and (b) the trait components of the attractors. Because of their different units, the distances can only be defined separately for the biomass space or the trait space. For calculating the AWD and MWD, each point on one discretized attrator is connected to its nearest point on the other attractor (grey lines). For symmetry reasons these connections start from both attractors. Therefore, one point on one attractor can be linked to more than one point on the other attractor. The AWD is the average length of these connections, the MWD is the length of the longest connection (red line). Parameters are $s_r = 80\,\mu\mathrm{mol\,L}^{-1}$, $\delta = 0.4\,\mathrm{d}^{-1}$ and $G = 10^{-0.5}$.

In nature, perturbations to the substrate can be caused by flooding events or fertilization. Extinction events, e.g. due to draughts or fires, emigration and immigration waves can lead to instantaneous changes in the biomasses. Pulse perturbations to the traits can either be correlated to biomass changes or be decoupled from them. For example, an environmental cue may appear that causes instantaneous trait changes but then dissolves and releases the traits again, e.g. kairomones that induce zooplankton defense (Kopp and Tollrian 2003).

The perturbations are applied to the state variables by drawing random starting conditions for the solution of the differential equations (Eqs. 4.1, 4.2) from uniform distributions across reasonable intervals of the state variables (Tab. 4.2). These starting conditions represent the first time point of the trajectory after a pulse perturbation displaced it away from the attractor, which itself is not changed by the perturbation. We ran $10\,000$ simulations to sample the whole state space of initial conditions. We tested different perturbation targets by perturbing either all state variables, only substrate and biomasses or only the traits. Unperturbed state variables were set to a randomized location on the attractor.

Table 4.2 Boundaries for the uniform distribution from which the random initial conditions were drawn to simulate pulse perturbations. The minima and maxima are set to cover the typical and reasonable ranges that the state variables attain.

State variable	Minimum	Maximum
s	$10^{-12}\,\mu\mathrm{molN/l}$	$80\,\mu\mathrm{molN/l}$
x	$10^{-12}\,\mathrm{mgC/l}$	$10\,\mathrm{mgC/l}$
y	$10^{-12}\,\mathrm{mgC/l}$	$10\,\mathrm{mgC/l}$
u	10^{-12}	1
v	10^{-12}	0.75

Resilience, i.e. whether or not a system returns to its pre-perturbation attractor, is determined for each random perturbation by checking whether the predator biomass drops below an extinction threshold of $1\,\mathrm{Ind}\,/\mathrm{L}$ after the perturbation. This excludes multistability, i.e. the existence of multiple stable attractors with positive predator biomasses, which holds for almost the entire parameter range in our system (Suppl. Fig. A3.1 and A3.2).

Elasticity is measured by the return time t_r that passes until the trajectory moves into a vicinity of $\pm\,3\%$ around the pre-perturbation attractor for the first time after the perturbation (Fig. 4.1b, d). This vicinity is determined from the shortest distance $\mathrm{d_{CP}}$ between the discretized representation of attractor A and a point P of the trajectory. This distance is rescaled to the individual coordinates of the curve in state space (Eq. 4.4).

$$\mathrm{d_{CP}}(A,P) = \min_{i\in\{0,\ldots,n\}} \left(\sqrt{\sum_{j=1}^{m} \left(\frac{A_{i,j} - P_j}{A_{i,j}} \right)^2} \right) \tag{4.4}$$

Here, $n = 500$ is the number of points on the attractor and $m = 5$ is the number of dimensions of the system of differential equations (Eqs. 4.1, 4.2).

Results

We find that the potential for trait adaptation in a predator-prey system, as characterized by the speed of adaptation (Eq. 4.2), strongly affects the population dynamics and three different measures for their robustness against perturbations. We quantified (i) the resistance of population dynamics against press perturbations to environmental parameters, and (ii) the resilience and (iii) the elasticity of the system against pulse perturbations to the state variables (i.e. substrate, biomasses and/or traits). We will start by presenting the unperturbed population and trait dynamics and then turn to how adaptation shapes the robustness of these dynamics under the impact of either press or pulse perturbations.

Different regimes of system dynamics

We can classify four different regimes of biomass-trait dynamics (R1 - R4) from the bifurcation diagram along the speed of adaptation G (Fig. 4.3a). The amplitude of the trait oscillations increases for higher G, with the defense starting to oscillate already at lower values of G compared to the offense. The offense trait thus requires a higher speed of adaptation to change its value within a population cycle. The oscillation amplitudes of substrate and biomasses are large for low and high G, but small at intermediate speeds of adaptation.

Looking closer into the dynamics, we see that for low G only the predator and prey biomasses oscillate while the traits remain constant (R1), (Fig. 4.3b). R1 therefore represents a regime where trait adaptation is negligible compared to the biomass oscillations, i.e. a non-adaptive reference state. As G increases, this regime transits to a regime R2 where defense oscillations start to appear without significant changes in the biomass oscillations. The maxima of the effective prey biomass, and therefore also the predator maxima increase slightly (Fig. 4.3c). If G increases further, also the offense starts to oscillate (R3), although at smaller amplitudes than the defense. Interestingly, in this regime of trait oscillations the biomass oscillations are buffered by changes in the traits. This results in shorter oscillation periods and smaller amplitudes of predator, prey and effective prey biomass (Fig. 4.3d). For even higher G, the offense is fast enough to immediately track changes in the defense. This decreases the effect of the defense and increases the maximum effective prey biomass again, causing strong simultaneous biomass and trait oscillations (R4). Here, the basic dynamical pattern remains, but the oscillation amplitudes of all state variables increase, together with an again increasing period (Fig. 4.3e). While their boundaries change slightly, these regimes are preserved for broad ranges of the dilution rate δ and inflow concentration s_I, representing the relevant environmental factors in our system (Suppl. Fig. A3.3).

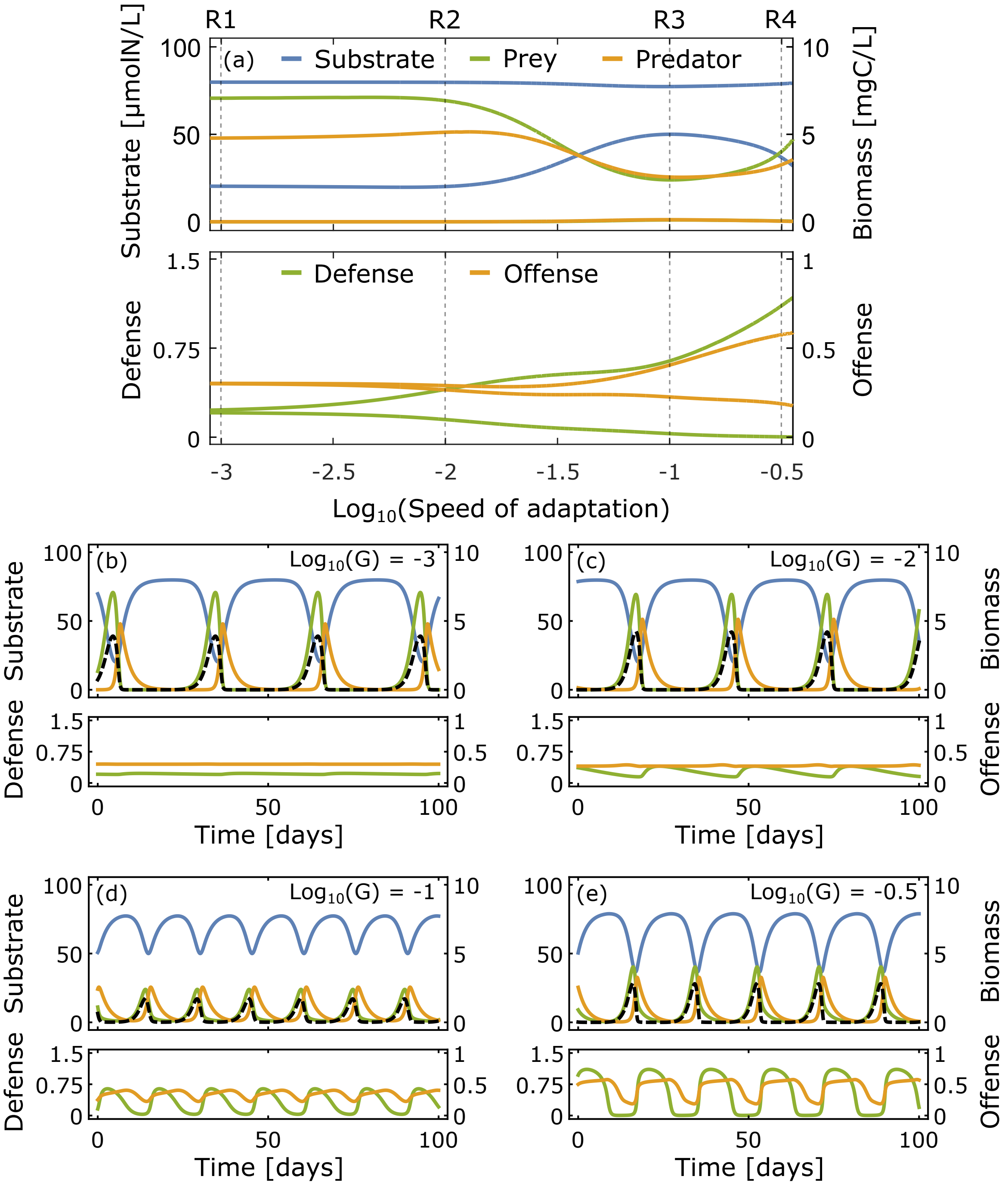

Figure 4.3 Regimes of system dynamics for an intermediate dilution rate $\delta = 0.4\,\mathrm{d}^{-1}$ and inflow concentration $s_I = 80\,\mathrm{\mu mol\,L^{-1}}$. (a) Bifurcation diagram along the speed of adaptation G showing the maxima and minima of the substrate (blue), the prey and its defense (green) and the predator and its offense (orange). (b-e) System dynamics at the vertical dashed grey lines in panel (a) following the same color coding. The black dashed line shows the effective prey biomass. (b) For small G biomasses oscillate while trait oscillations are minor (Regime R1). (c) For slightly larger G the prey defense oscillates stronger (Regime R2). (d) At larger G also the offense oscillates and the trait oscillations buffer the biomass oscillations (Regime R3). (e) At very high G both biomasses and traits oscillate strongly (Regime R4).

Resistance of predator-prey dynamics

In the following, we will quantify the resistance of the predator-prey system by measuring the dissimilarity between the pre- and post-perturbation attractors which arise from a press perturbation, i.e. a permanent change to either the inflow concentration or the dilution rate (Fig. 4.1a, c). The dissimilarity is determined by comparing the two attractors at $\pm 20\%$ of the reference parameter value (Figs. 4.2, 4.4, 4.5). We employ two different measures, the average and maximum warping distance (AWD and MWD), which represent the averaged and maximum distance between the two attractors and are small for high resistance. A large AWD between pre- and post-perturbation attractors indicates that the perturbation changes the dynamics over a large range of the population cycle, whereas a large MWD points to only a short, but strong delineation from the original dynamics. We find that adaptation has often strong effects on both measures, but the specific results also depend on (i) whether the inflow concentration or the dilution rate are perturbed, (ii) the value of the reference parameter around which the perturbations occurs, and (iii) the subset of state variables, for which the attractor dissimilarities are computed.

When the inflow concentration is perturbed, the AWD between the two attractors decreases when going from low (R1, R2) to intermediate (R3) speeds of adaptation G demonstrating an enhanced resistance (Fig. 4.4a, c, e). Increasing G further increases the AWD again (R4), when only biomasses or trait components of the attractors are considered. The MWD follows a similar pattern for substrate, prey and predator (Fig. 4.4b, d), while the traits behave differently (Fig. 4.4f). Here, the MWD has a maximum at intermediate G while the AWD decreases, implying that the trait dynamics become overall more similar, but strong differences arise in a small region of the attractor.

If the dilution rate is perturbed, only the behaviour of AWD and MWD of the trait components resembles the one observed for perturbations to the inflow concentration (Fig. 4.5e, f). The patterns for dissimilarities in substrate and biomasses are instead more complex and strongly depend on the reference dilution rate. While going from R1 to R3 increases AWD and MWD for small reference dilution rates, these quantities decrease for large reference dilution rates. Increasing the speed of adaptation further from R3 to R4 then decreases AWD for all reference dilution rates. From these findings we can conclude that the resistance of this predator-prey system tends to increase with faster adaptation if the substrate inflow is perturbed, but no simple relationship can be found if the press perturbation targets the dilution rate.

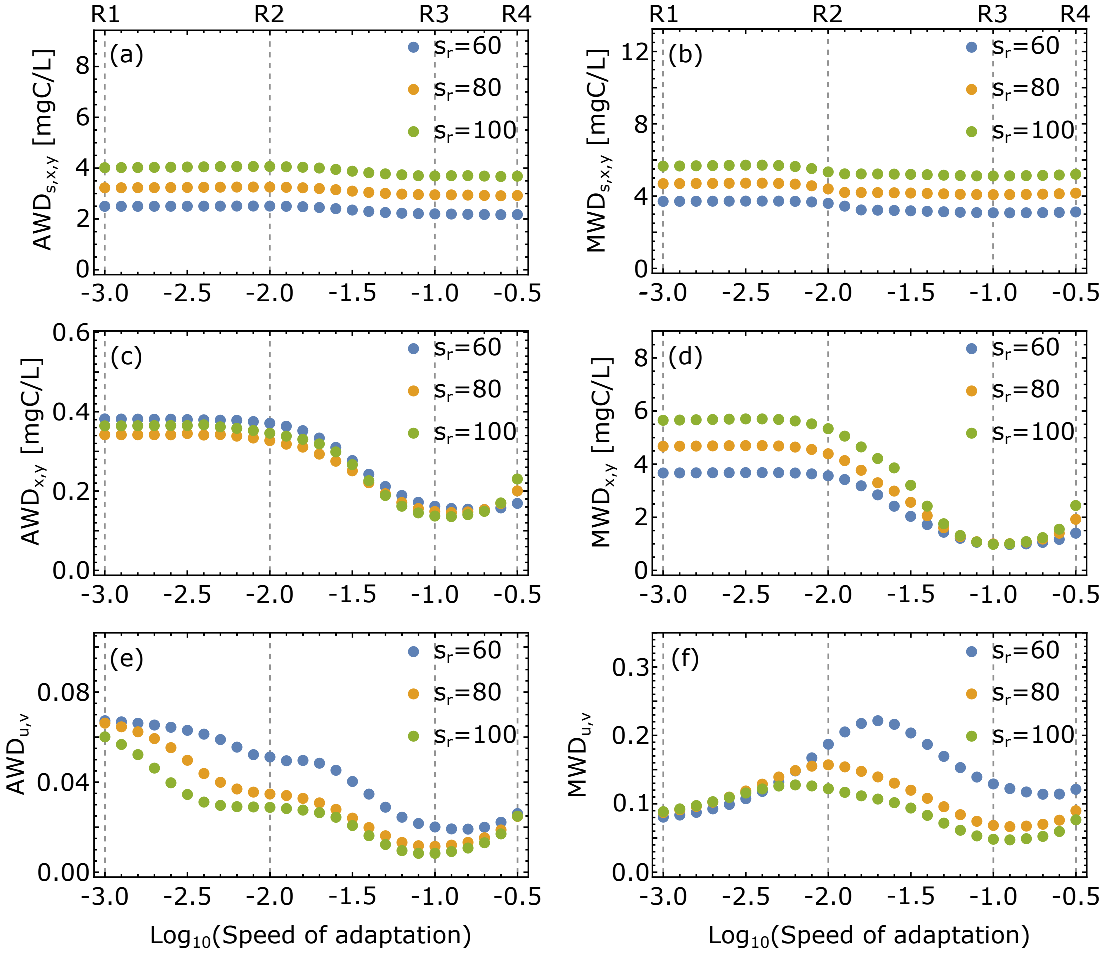

Figure 4.4 Resistance of dynamics in response to environmental press perturbations measured by the dissimilarity between the pre- and post-perturbation attractors at inflow concentrations $\pm 20\%$ around the reference inflow concentration s_r (see Fig. 4.2). (a) Average warping distance (AWD) of the attractor projection onto substrate, prey and predator. The substrate is scaled to carbon equivalents by the prey's carbon-to-nitrogen ratio. (b) Maximum warping distance (MWD) of substrate, prey and predator, (c-d) AWD and MWD between only the prey and predator components of the two attractors, (e-f) AWD and MWD between the trait components of the attractors. Smaller dissimilarities correspond to larger resistance.

The bifurcation diagrams along the dilution rate and the inflow concentration show why the reference dilution rate has a stronger impact on the attractor dissimilarities than the value of the reference inflow concentration (Suppl. Figs. A3.1 and A3.2). The AWD of two attractors at slightly different values around the reference parameter is similar to the slope of the difference between maxima and minima in these bifurcation diagrams. This slope measures how the longest axis of the attractor in one dimension changes if the environmental parameter is changed, although it does not inform about changes in attractor shape and location. If the inflow concentration increases, the predator-prey system is enriched and the minima and maxima of all state variables respond mainly monotonically with a similar behaviour for different speeds of adaptation (Suppl. Figs. A3.1). While the inflow concentration only governs the substrate input into the system, the dilution rate additionally controls the outflow,

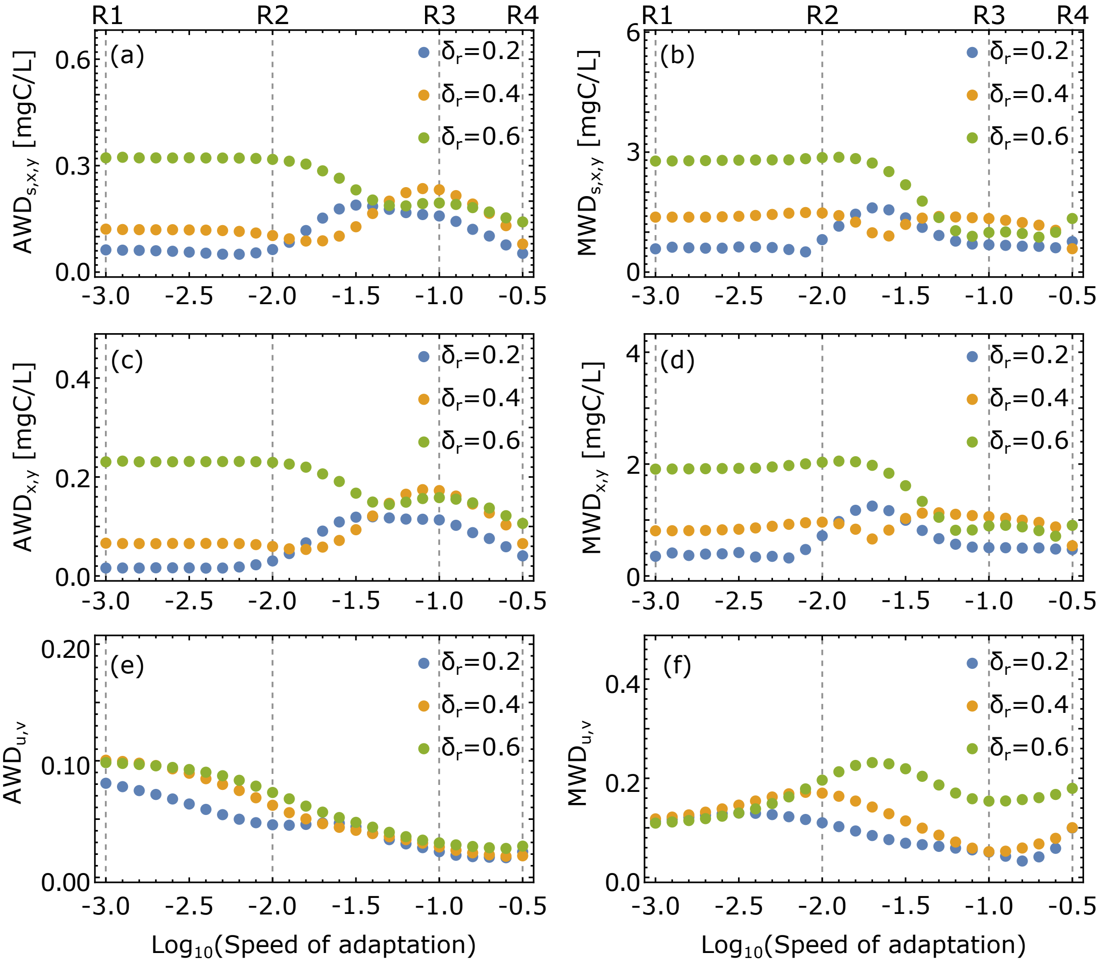

Figure 4.5 Resistance of dynamics in response to environmental press perturbations measured by the dissimilarity between two attractors at dilution rates $\pm 20\%$ around the reference dilution rate δ_r. Further plot specifics are equal to those in Fig. 4.4.

i.e. the losses of substrate, prey and predator. Therefore, the minima and maxima of substrate, prey and predator depend non-monotonically on the dilution rate and this dependence differs strongly for different speeds of adaptation (Suppl. Fig. A3.2). The slope of the difference between maxima and minima therefore depends strongly on the location along the bifurcation axis, i.e. the reference dilution rate, and the speed of adaptation, yielding the complex patterns found for AWD and MWD in Fig. 4.4. Following this comparison, we also see that large slopes in bifurcation diagrams indicate low resistance to press perturbations along the bifurcation parameter as already small parameter changes induce strong changes in the state variables. From the bifurcation diagrams we can also conclude that the speed of adaptation does not affect species coexistence along the environmental parameters that were targeted by press perturbations in our system. Nevertheless, it slightly affects the location of the Hopf-bifurcation at low inflow concentrations and high dilution rates. For fast speeds of adaptation the Hopf-bifurcation becomes sub-critical, creating a bistability between steady state and limit cycle (Figs. A3.1 and A3.2).

Resilience of predator-prey dynamics

We will now present how the speed of adaptation affects the system's response to pulse perturbations (Fig. 4.1b,d). The speed of adaptation governs whether trait adaptation can operate on ecological time scales and ranges from almost non-adaptive (R1) to highly adaptive (R4) regimes. We mimicked the pulse perturbations by setting the targeted state variables to random values drawn from a uniform distribution, thereby deflecting the system's trajectory away from the attractor.

The resilience of the system, as characterized by the extinction probability of the predator, is determined by the speed of adaptation G, the identity of the state variables that are targeted by the perturbation pulse, and the perturbation strength (left column in Fig. 4.6). The highest number of extinctions occurs if all state variables are perturbed at the same time (Fig. 4.6a). The extinction probability follows a u-shaped trend across the speed of adaptation with a minimum at intermediate $G = 10^{-1}$, corresponding to dynamics regime R3. This pattern is also present if only substrate and biomasses or only the traits are perturbed (Figs. 4.6c, e), although the total number of extinctions is lower here.

We find that two conditions increase the likelihood of extinctions: (i) The pulse perturbation moves the system to a region of high biomasses in combination with high trait values (panels a in Suppl. Figs. A3.4 - A3.6) and (ii) Trait adaptation is either very slow (R1) or very fast (R4). The first condition, i.e. a strong perturbation, moves the trajectory far away from the attractor, causing a rapid decrease of biomasses towards very small values after the perturbation, similar to an oscillator that is heavily excited. If also the trait values are high, the prey's maximum growth rate and the predator's conversion efficiency are low due to the trade-offs, which further accelerates the biomass decline (see exemplary dynamics in Suppl. Fig. A3.7).

If only a subset of the state variables is perturbed, the non-targeted state variables are set to a random location on the attractor. This location also affects the extinction risk, as for example choosing higher biomasses, if the traits are perturbed to high values, increases the extinction risk (Suppl. Fig. A3.8). This pattern is further determined by the second condition, i.e. higher extinction risks for non-adaptive or rapidly adaptive regimes (R1 and R4). If adaptation is slow the traits remain at unfavourably high values and the predator goes extinct. If trait adaptation is very fast the prey cannot decrease the grazing pressure it is exposed to by increasing its defense as the predator can directly co-adapt and increase its offense. Thereby the predator further decreases the prey biomass while paying the costs of a reduced conversion efficiency. Consequently, predator growth cannot compensate the losses by dilution, and the predator drives itself to extinction by co-adapting too quickly. For intermediate speeds of adaptation, however, the biomass oscillations are buffered by trait adaptations, indicating slower rates of biomass change. This prevents strong biomass decreases during the transient after the perturbation and reduces the number of extinctions.

Elasticity of predator-prey dynamics

Following a pulse perturbation, the system's elasticity determines the return time, i.e. the time it takes until the system's trajectory arrives back in the vicinity of the attractor. For perturbations of different strength, different return times are expected, which results in a broad return time distribution. We find that these distributions are shifted towards smaller return times as the speed of adaptation increases and are in some cases bimodal (right column in Fig. 4.6). The shift to faster returns, i.e. higher elasticity, for faster adaptation is strongest if all state variables or only the traits are perturbed (panels b and f in Fig. 4.6), which is also where the spread in return times is largest. If only substrate and biomasses are targeted (Fig. 4.6d), the maximum return times are smaller, but still we see noticeable decreases in the return times for fast speeds of adaptation from $\overline{t_{r,\ G=10^{-3}}} = 35.7\,\mathrm{d}$ and $\overline{t_{r,\ G=10^{-2}}} = 37.3\,\mathrm{d}$ to $\overline{t_{r,\ G=10^{-1}}} = 24.8\,\mathrm{d}$ and $\overline{t_{r,\ G=10^{-0.5}}} = 19.7\,\mathrm{d}$. This shows that even if only the biomasses of the species are changed, their trait dynamics still impact the return to the attractor.

The bimodality manifests as a clustering into faster and slower returns, with a separation around $t_r = 10$ days if only substrate and biomasses are perturbed (Fig. 4.6d). We find that in these cases the peak for shorter return times stems from weaker perturbations that deflected the trajectory not too far away from the attractor (panels b and c in Suppl. Figs. A3.4 - A3.6). Here, the trajectory returns back to the attractor already within the first transient cycle. If this is not the case, the trajectory has to perform at least another excursion through the state space before it can come closer to the attractor again and eventually penetrate the predefined 3% vicinity around the attractor.

Discussion

In this study, we find that trait diversity and adaptability arising from phenotypic plasticity and genetic diversity can, similar to species diversity, increase the robustness of food webs to perturbations. Earlier research has mainly focused on the effect of adaptation on species coexistence (Hughes and Stachowicz 2004; Chevin et al. 2010; Gonzalez et al. 2012; Kovach-Orr and Fussmann 2013; Merilä and Hendry 2014; Oliver et al. 2015; Bell 2017) or investigated the population dynamics of adaptive predator-prey systems without external influences (Abrams and Matsuda 1997; Mougi and Iwasa

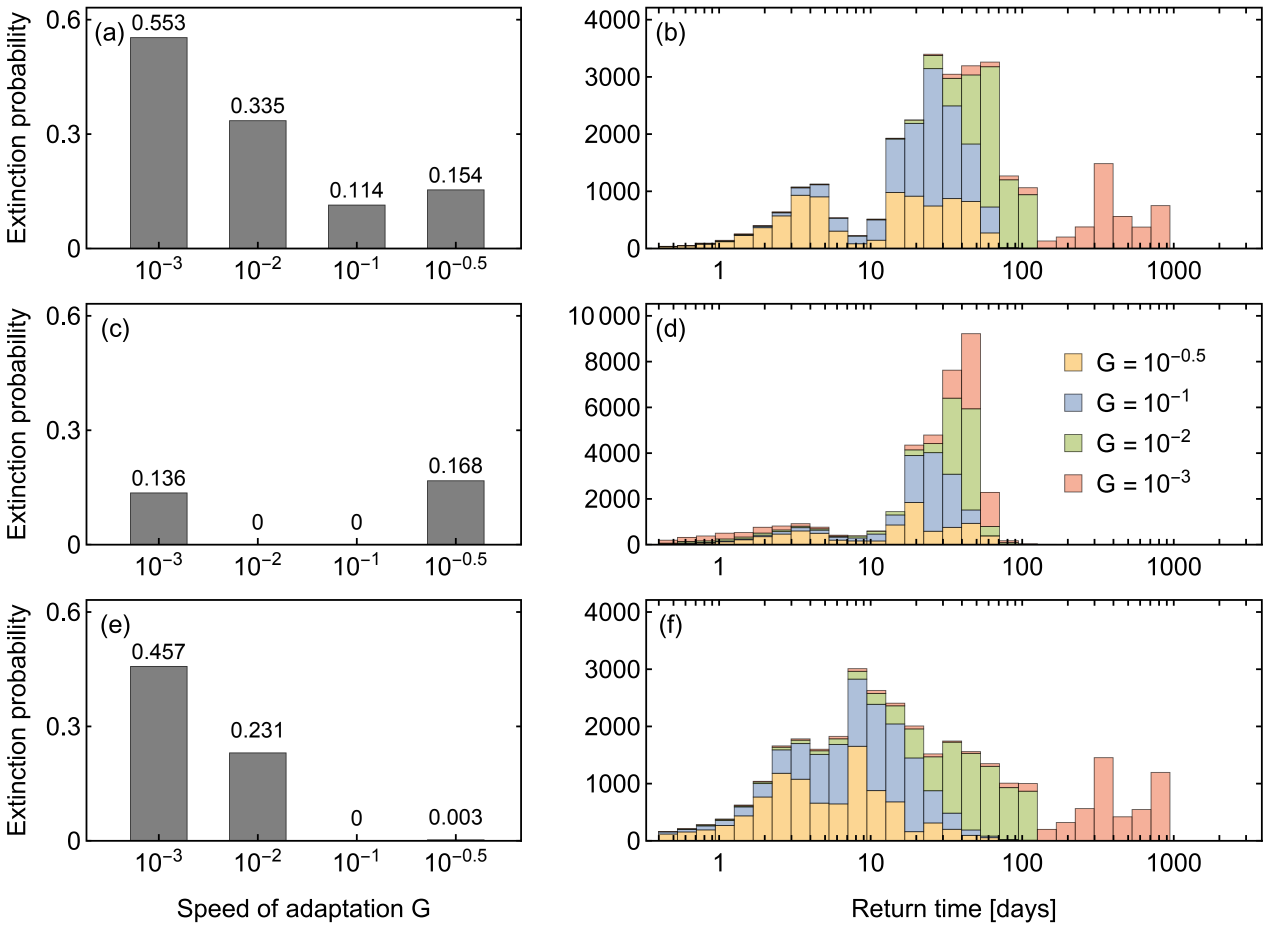

Figure 4.6 Resilience and elasticity of the predator-prey dynamics in response to random pulse perturbations, characterized by the extinction probability of the predator (left column) and the return time distributions of system trajectories (right column). The perturbations target all state variables (panels a and b), the substrate and the biomasses (panels c and d) and the traits (panels e and f). The different speeds of adaptation G correspond to the four regimes of dynamics R1-R4 (Fig. 4.3).

2010, 2011; Klauschies et al. 2016; van Velzen and Gaedke 2017). We connected these two fields and investigated how, via inducing different regimes of population dynamics, adaptation affects robustness properties like resistance, resilience and elasticity. We have shown that trait adaptation may increase the robustness of population dynamics of co-adapting prey and predators against press and pulse perturbations, but that these results depend on the speed of adaptation and the type and target of the perturbation. Most importantly our results show that the expectation of faster adaptation necessarily yielding larger robustness is not true. Instead we find that different speeds of adaptation yield different population dynamics, which then are more or less robust against perturbations.

For press perturbations, we have seen that via affecting the population dynamics (cycle amplitude and location of the Hopf-bifurcation), the speed of adaptation strongly impacts the resistance of the predator-prey system but the direction of the impact is variable. This manifests in an altered deformation and translocation of the attractor under press perturbations. For pulse perturbations, we have shown that resilience is highest in intermediately adaptive systems, as indicated by a lower extinction probability of the predator. Elasticity, i.e. the speed of return back to the pre-perturbation attractor, increased in more adaptive systems where the speed of adaptation is higher. We observed that changes in the robustness measures along the speed of adaptation coincide with changes in the amplitudes of the population dynamics that mark the transitions between different regimes of dynamics. From this we can conclude that the population dynamics themselves already signal their robustness against perturbations; and co-adaptation, via creating these different regimes of dynamics, therefore determines this robustness.

This relation is very apparent for the resistance of population dynamics against press perturbations. The speed of adaptation affects how the amplitude and shape of the population cycle, i.e. the attractor, changes along other parameters, such as the inflow concentration and the dilution rate. If these environmental parameters are targeted by press perturbations, the dissimilarities between pre- and post-perturbation attractors are therefore also shaped by the speed of adaptation. A first and intuitive estimate of how the predator-prey system responds to these perturbations could be the slope of maxima and minima in bifurcation diagrams for the perturbed parameter or the slope of the amplitudes. Accordingly, we found the reason for the complex relationship between speed of adaptation and perturbation target already in these diagrams. If the amplitudes change non-monotonically along the perturbed parameter, as for the dilution rate in our system, and if the speed of adaptation deforms these amplitudes in a complex way, it is obvious that resistance will show no simple dependence on adaptation speed. Taking a more comprehensive approach, we proposed the average warping distance AWD and the maximum warping distance MWD to measure the distance between the pre- and post-perturbation attractors and quantify the resistance of the system against press perturbations. These account also for more complex changes in the shape of the attractor, which otherwise could unnoticedly become highly complex, e.g. multiple local maxima of one species within one population cycle could arise (as e.g. in Raatz et al. 2017).

Differences of AWD and MWD indicate whether perturbations have on average a large effect, or whether this effect becomes pronounced only for a short period of the whole population cycle. Figs. 4.4e and f reveal that the AWD decreases when increasing the speed of adaptation from R1 to R2 while the MWD increases. This indicates that the pre- and post-perturbation attractors become more similar on average, but differences in a short region of the two attractors increase. Translated to perturbations of natural systems this may yield different management implications. If management aims to minimize the maximum effect of perturbations, e.g. an outbreak of a pest for a limited time within one vegetation period, a lower MWD may be more desirable and compensate for a higher

AWD. While in our system we applied these measures only to limit cycles, they can also be used to quantify the translation of stable fixed points along an environmental parameter, where the AWD would equal the MWD.

The system's response to pulse perturbations is also affected by the amplitude and shape of the biomass-trait oscillations, and how these are impacted by adaptation. Here, the relationship between robustness and trait adaptation is more straightforward. If the system exhibits strong biomass oscillations already in the unperturbed state, the oscillations following a pulse perturbation will also be strong and make extinctions more likely. This explains the higher extinction risk for slow (R1) and very fast adaptation (R4). For intermediate adaptation speeds the biomass oscillations are dampened and buffered by trait oscillations which reduces extinctions. This dampening of biomass oscillations is caused by especially efficient prey adaptation, as prey defense can be up-regulated without the predator offense immediately following in this parameter region.

If the unperturbed system shows strong trait oscillations (i.e. fast adaptation), this indicates that trait changes are possible on ecological time scales and therefore also allow the species to respond quickly to perturbations by changing their traits. Accordingly, we have seen that faster speeds of adaptation allow a faster return from changed population densities and traits back to the pre-perturbation attractor.

Mathematically, the shift towards smaller return times with larger speeds of adaptation G is expected as G directly scales the speed at which the trajectory can move through state space, at least in the coordinates of prey defense and predator offense. For small speeds of adaptation, trait dynamics are much slower than biomass dynamics and the return to the attractor is slowed down by slow changes in the traits. However, it is interesting and rather unexpected that we also find the shift towards smaller return times with increasing adaptation speed if only substrate and biomasses are perturbed. Here, a biomass-trait feedback manifests where faster trait adaptation enables the predator-prey system to respond more rapidly to instantaneous biomass perturbations. This faster return is ecologically relevant as it decreases the time the system spends in transient phases, with potentially larger cycle amplitudes, which were found to increase the extinction risk (Pimm et al. 1988; Inchausti and Halley 2003).

As stated above, the impact of co-adaptation on predator-prey population dynamics seems to be of central importance for their robustness against perturbations. In our system, we encountered four regimes of dynamics where biomasses and trait values oscillated with different amplitudes. The transitions between these regimes coincided with changes in the robustness measures. Predator-prey systems that differ from ours might comprise only some of these regimes or have them differently ordered. Nevertheless also in these systems, the speed of adaptation should strongly affect the robustness of population dynamics, with similar dynamics-robustness correlations.

How co-adaptation shapes different regimes of population dynamics has been investigated before (see e.g. Abrams and Matsuda 1997; Yamauchi and Yamamura 2005; Mougi and Iwasa 2010, 2011; Tien and Ellner 2012; van Velzen and Gaedke 2017; Cortez 2018; Patel et al. 2018). The particular findings, i.e. whether faster trait adaptation decreases the amplitudes of species' biomasses and increases the amplitudes of trait oscillations, are not conclusive but seem to depend on the system under investigation. Also in our system these patterns are rather complex. Comparing the four different regimes of population dynamics shows that, as the speed of adaptation increases from slow to intermediate values, biomass oscillations decrease while trait oscillations increase. This was also observed by Mougi and Iwasa (2010), although the models differ slightly in their structure (Rosenzweig-MacArthur vs. chemostat here), trade-off shape (linear vs. Gaussian here) and parameterization. In contrast to their study, however, we find that biomass oscillations increase again towards even faster adaptation and occur together with pronounced trait oscillations. This overall pattern manifests in both resistance and resilience and determines the system's response to the perturbations. Interestingly, it agrees with the principle of energy flux (Rip and McCann 2011) which states that a higher energy flux to the highest trophic level in a food chain causes stronger oscillations and is nicely captured by the effective prey biomass in our system. If mainly the defense of the prey adapts during a population cycle (R3), the energy flux to the predator decreases as the effective prey biomass is low. The effective prey biomass increases if adaptation is too slow for defense to increase effectively within a population cycle (R1 and R2), or fast enough for the offense to also be up-regulated in response to an increased defense (R4). This corresponds to a higher energy flux to the predator at slow and fast speeds of adaptation and coincides with stronger biomass cycles.

Typically, the robustness of populations or ecosystems against perturbations is measured for traits that are directly linked to environmental parameters, e.g. maximum critical temperatures or nutrient affinities, and adaptability of such traits to changing conditions provides obvious fitness advantages (Bell and Gonzalez 2009; Agashe et al. 2011; Ramsayer et al. 2013). Moving beyond that, we considered trait adaptability in defense and offense, where advantages are not that obvious as these two traits are not directly related to environmental impacts but determine interspecific, i.e. trophic, interactions. We showed that adaptability of such trophic traits may also strongly impact the robustness of populations and their interactions against perturbations, as accounting for all factors that impact growth and loss is key. In our system, this includes growth and wash-out for prey and predators and grazing for the prey. Adaptation of defense and offense allows to alter the maximum growth rate of the prey and the conversion efficiency of the predator along the trade-offs. This provides a flexibility to optimize the fitness of both predator and prey facing perturbations, which results from adaptability in defense and offense, even if these traits are not obviously mediating environmental impacts.

To conclude, we found that trait adaptation has strong effects on the robustness of population dynamics in a predator-prey system. We have shown that varying the potential for co-adaptation creates different regimes of biomass-trait dynamics, which are differently impacted by press and pulse perturbations. We found that faster trait adaptation (from rapid evolution or phenotypic plasticity) can increase the robustness of population dynamics against perturbations, but in some cases also achieves the exact opposite. This shows that details such as the perturbation type, target and strength matter. As our model makes only few assumptions on the system under investigation, it is applicable to many predator-prey, but also host-parasite and other plant-herbivore systems, all of which provide often dynamic key linkages in many ecosystems. Interestingly, the results for press perturbations, which could result from long-term environmental changes, such as anthropogenic landscape modifications or climate change, are less conclusive than those for pulse perturbations. This strengthens the need for ecosystem-specific investigations of the robustness of population dynamics in changing environments to allow an ecosystem management that ensures sustained ecosystem functions and stable provisioning of ecosystem services. Our study shows that co-adaptation should be regarded a key component in this process.

Acknowledgements

This work was funded by DFG (WA 2445/11-1, GA 401/26-1) as part of the Priority Programme 1704 (DynaTrait). We thank Alice Boit for constructive comments during the writing process.

Bibliography

Abrams, P. A. (1992). Adaptive foraging by predators as a cause of predator-prey cycles. *Evol. Ecol.* 6: 56–72.

Abrams, P. A. and Matsuda, H. (1997). Prey Adaptation as a Cause of Predator-Prey Cycles. *Evolution* 51: 1742–1750.

Agashe, D., Falk, J. J., and Bolnick, D. I. (2011). Effects of founding genetic variation on adaptation to a novel resource. *Evolution* 65: 2481–2491.

Barraquand, F., Louca, S., Abbott, K. C., et al. (2017). Moving forward in circles: challenges and opportunities in modelling population cycles. *Ecol. Lett.* 20: 1074–1092.

Bauer, B., Vos, M., Klauschies, T., and Gaedke, U. (2014). Diversity, Functional Similarity, and Top-Down Control Drive Synchronization and the Reliability of Ecosystem Function. *Am. Nat.* 183: 394–409.

Bell, G. (2017). Evolutionary Rescue. *Annu. Rev. Ecol. Evol. Syst* 48: 605–27.

Bell, G. and Gonzalez, A. (2009). Evolutionary rescue can prevent extinction following environmental change. *Ecol. Lett.* 12: 942–948.

Bender, E. A., Case, T. J., and Gilpin, M. E. (1984). Perturbation Experiments in Community Ecology: Theory and Practice. *Ecology* 65: 1–13.

Berndt, D. and Clifford, J. (1994). Using dynamic time warping to find patterns in time series. *Work. Knowl. Discov. Databases* 398: 359–370.

Chevin, L.-M., Lande, R., and Mace, G. M. (2010). Adaptation, Plasticity, and Extinction in a Changing Environment: Towards a Predictive Theory. *PLoS Biol.* 8: e1000357.

Cortez, M. H. (2018). Genetic variation determines which feedbacks drive and alter predator-prey eco-evolutionary cycles. *Ecol. Monogr.* 88: 353–371.

Cortez, M. H. and Weitz, J. S. (2014). Coevolution can reverse predator-prey cycles. *Proc. Natl. Acad. Sci.* 111: 7486–7491.

Dhooge, A., Govaerts, W., and Yu. A. Kuznetsov (2003). matcont: A matlab package for numerical bifurcation analysis of ODEs.

Eiter, T. and Mannila, H. (1994). *Computing discrete Fréchet distance*. Tech. rep. Information Systems Department, Technical University of Vienna.

Fischer, M., Rounsevell, M., Rando, A. T.-M., et al. (2018). IPBES: Summary for policymakers of the regional assessment report on biodiversity and ecosystem services for Europe and Central Asia of the Intergovernmental Science-Policy Platform on Biodiversity and Ecosystem Services.

Fréchet, M. M. (1906). Sur quelques points du calcul fonctionnel. *Rend. del Circ. Mat. di Palermo* 22: 1–72.

Frickel, J., Sieber, M., and Becks, L. (2016). Eco-evolutionary dynamics in a coevolving host-virus system. *Ecol. Lett.* 19: 450–459.

Gonzalez, A., Ronce, O., Ferriere, R., and Hochberg, M. E. (2012). Evolutionary rescue: an emerging focus at the intersection between ecology and evolution. *Philos. Trans. R. Soc. B Biol. Sci.* 368: 20120404.

Grimm, V. and Wissel, C. (1997). Babel, or the ecological stability discussions: an inventory and analysis of terminology and a guide for avoiding confusion. *Oecologia* 109: 323–334.

Holling, C. (1996). “Engineering resilience versus ecological resilience”. In: *Eng. within Ecol. constraints*. Washington (DC), National Academies Press, pp. 31–44.

Hughes, A. R. and Stachowicz, J. J. (2004). Genetic diversity enhances the resistance of a seagrass ecosystem to disturbance. *Proc. Natl. Acad. Sci.* 101: 8998–9002.

Hughes, A. R., Inouye, B. D., Johnson, M. T. J., Underwood, N., and Vellend, M. (2008). Ecological consequences of genetic diversity. *Ecol. Lett.* 11: 609–623.

Inchausti, P. and Halley, J. (2003). On the relation between temporal variability and persistence time in animal populations. *J. Anim. Ecol.* 72: 899–908.

Iwasa, Y., Pomiankowski, A., and Nee, S. (1991). The Evolution of Costly Mate Preferences II. The ’Handicap’ Principle. *Evolution* 45: 1431–1442.

Klauschies, T., Vasseur, D. A., and Gaedke, U. (2016). Trait adaptation promotes species coexistence in diverse predator and prey communities. *Ecol. Evol.* 6: 4141–4159.

Kopp, M. and Tollrian, R. (2003). Reciprocal phenotypic plasticity in a predator-prey system: Inducible offences against inducible defences? *Ecol. Lett.* 6: 742–748.

Kovach-Orr, C. and Fussmann, G. F. (2013). Evolutionary and plastic rescue in multitrophic model communities. *Philos. Trans. R. Soc. B Biol. Sci.* 368: 20120084.

Lovett, G. M., Christenson, L. M., Groffman, P. M., et al. (2002). Insect Defoliation and Nitrogen Cycling in Forests: Laboratory, plot, and watershed studies indicate that most of the nitrogen released from forest foliage as a result of defoliation by insects is redistributed within the ecosystem, whereas only a small f. *Bioscience* 52: 335–341.

Meehl, G. A. and Tebaldi, C. (2004). More Intense, More Frequent, and Longer Lasting Heat Waves in the 21st Century. *Science* 305: 994–997.

Merilä, J. and Hendry, A. P. (2014). Climate change, adaptation, and phenotypic plasticity: The problem and the evidence. *Evol. Appl.* 7: 1–14.

Mougi, A. and Iwasa, Y. (2010). Evolution towards oscillation or stability in a predator-prey system. *Proc. Biol. Sci.* 277: 3163–3171.

Mougi, A. and Iwasa, Y. (2011). Unique coevolutionary dynamics in a predator-prey system. *J. Theor. Biol.* 277: 83–89.

Oliver, T. H., Heard, M. S., Isaac, N. J., et al. (2015). Biodiversity and Resilience of Ecosystem Functions. *Trends Ecol. Evol.* 30: 673–684.

Patel, S., Cortez, M. H., and Schreiber, S. J. (2018). Partitioning the Effects of Eco-Evolutionary Feedbacks on Community Stability. *Am. Nat.* 191: 381–394.

Pimm, S. L., Jones, H. L., and Diamond, J. (1988). On the Risk of Extinction. *Am. Nat.* 132: 757–785.

Raatz, M., Schälicke, S., Sieber, M., Wacker, A., and Gaedke, U. (2018). One man's trash is another man's treasure-the effect of bacteria on phytoplankton-zooplankton interactions in chemostat systems. *Limnol. Oceanogr. Methods* 16: 629–639.

Raatz, M., Gaedke, U., and Wacker, A. (2017). High food quality of prey lowers its risk of extinction. *Oikos* 126: 1501–1510.

Rahmstorf, S. and Coumou, D. (2011). Increase of extreme events in a warming world. *Proc. Natl. Acad. Sci.* 108: 17905–17909.

Ramsayer, J., Kaltz, O., and Hochberg, M. E. (2013). Evolutionary rescue in populations of Pseudomonas fluorescens across an antibiotic gradient. *Evol. Appl.* 6: 608–616.

Rip, J. M. K. and McCann, K. S. (2011). Cross-ecosystem differences in stability and the principle of energy flux. *Ecol. Lett.* 14: 733–740.

Smith, H. L. and Waltman, P. (1995). The theory of the chemostat: dynamics of microbial competition. 13th ed. Vol. 13. Cambridge university press.

Tien, R. J. and Ellner, S. P. (2012). Variable cost of prey defense and coevolution in predator-prey systems. *Ecol. Monogr.* 82: 491–504.

van Velzen, E. and Gaedke, U. (2017). Disentangling eco-evolutionary dynamics of predator-prey coevolution: the case of antiphase cycles. *Sci. Rep.* 7: 17125.

van Velzen, E. and Gaedke, U. (2018). Reversed predator-prey cycles are driven by the amplitude of prey oscillations. *Ecol. Evol.* 8: 6317–6329.

West-Eberhard, M. J. (1989). Phenotypic Plasticity and the Origins of Diversity. *Annu. Rev. Ecol. Syst.* 20: 249–278.

Wolfram Research Inc. (2014). Mathematica. Champaign, Illinois.

Yamauchi, A. and Yamamura, N. (2005). Effects of defense evolution and diet choice on population dynamics in a one-predator-two-prey system. *Ecology* 86: 2513–2524.

Yang, L. H. (2004). Periodical cicadas as resource pulses in North American forests. *Science* 306: 1565–1567.

Yoshida, T., Jones, L. E., Ellner, S. P., Fussmann, G. F., and Hairston, N. G. (2003). Rapid evolution drives ecological dynamics in a predator-prey system. *Nature* 424: 303–306.

5 Addition of heterotrophic to autotrophic prey alters predator-prey dynamics

One man's trash is another man's treasure - the effect of bacteria on phytoplankton-zooplankton interactions in chemostat systems

Michael Raatz[1], Svenja Schälicke[1], Michael Sieber[2], Alexander Wacker[1] and Ursula Gaedke[1]

[1] Institute of Biochemistry and Biology, University of Potsdam, Potsdam, Germany

[2] Department Evolutionary Theory, Max-Planck Institute for Evolutionary Biology, Plön, Germany

Abstract

Chemostat experiments are employed to study predator-prey and other trophic interactions, frequently using phytoplankton-zooplankton systems. These experiments often use population dynamics as fingerprints of ecological and evolutionary processes, assuming that the contributions of all major actors to these dynamics are known. However, bacteria are often neglected although they are frequently present. We argue that even without external carbon input bacteria may affect the experimental outcomes depending on experimental conditions and the physiological traits of bacteria, phytoplankton and zooplankton. Using a static carbon flux model and a dynamic simulation model we predict the minimum and maximum impact of bacteria on phytoplankton-zooplankton population dynamics. Under bacteria-suppressing conditions, we find that the effect of bacteria is indeed negligible and their omission justified. Under bacteria-favouring conditions, however, bacteria may strongly affect average biomasses of phytoplankton and zooplankton. The population dynamics may become highly complex, which may result in wrong interpretations when inferring processes (e.g. trait changes) from population dynamic patterns without considering bacteria. We provide suggestions to reduce the bacterial impact experimentally. Besides optimizing experimental conditions (e.g. the dilution rate) the appropriate choice of the zooplankton predator is decisive. Counterintuitively, bacteria have a larger impact if the predator is not bacterivorous as high bacterial biomasses and complex population dynamics arise via competition for nutrients with the phytoplankton. Only at least partial bacterivory minimizes the impact of bacteria. Our results help to improve the design of chemostat experiments and their interpretation, and advance the study of ecological and evolutionary processes in aquatic food webs.

Published as

Raatz, M., Schälicke, S., Sieber, M., Wacker, A., and Gaedke, U. (2018). One man's trash is another man's treasure-the effect of bacteria on phytoplankton-zooplankton interactions in chemostat systems. *Limnol. Oceanogr. Methods* 16: 629–639.

Introduction

Highly controllable and easy to handle laboratory experimental approaches are a useful tool to understand complex trophic interactions in natural systems. A prominent representative of these are phytoplankton-zooplankton chemostat experiments which have proven themselves in multiple studies of basic ecological and evolutionary concepts, see e.g. (Novick and Szilard 1950; Fussmann et al. 2000; Yoshida et al. 2003; Becks et al. 2012; Hiltunen et al. 2013; Declerck et al. 2015). Aside from biomass levels, these experiments often focus on patterns in population dynamics, which are fingerprints of interactions between the organisms. While they are undoubtedly able to provide proof-of-concept-like dynamics, chemostat experiments occasionally lack reproducibility, with unexpected experimental runs often not being published, and inference from individual chemostat experiments may be difficult (Bengfort et al. 2017). We hypothesize that bacteria may be one cause of such experimental irregularities.

In numerous chemostat experiments bacteria are an unwanted but often unavoidable and inherent part of the system. While phytoplankton cultures may be run axenically, most zooplankton cultures contain at least parts of the microbiome of the animals (Ishino et al. 2012; Seah et al. 2017). Due to the usually long duration of chemostat experiments also an unintended introduction of bacteria may eventually occur. Phytoplankton exudation and zooplankton excretion drive production of dissolved and particulate organic carbon, providing resources for these bacteria even without an organic carbon source in the growth medium (Vadstein et al. 2003). Bacteria may hamper algal growth by competition for nutrients (Bratbak and Thingstad 1985) and bacterivory can constitute a substantial portion of zooplankton production (Starkweather et al. 1979; Arndt 1993; Ooms-Wilms 1997). Nevertheless, bacteria are often neglected in chemostat studies. Motivated by earlier experimental investigations (Starkweather et al. 1979; Aoki and Hino 1996; Hino et al. 1997), we challenge this omission and study under which conditions bacteria can substantially influence phytoplankton growth and contribute to zooplankton production, and thereby affect the shape of predator-prey cycles in a typical chemostat experiment.

First we show that already a simple carbon flux model based on a few assumptions without population dynamics predicts that the impact of bacteria may become large. We therefore include a carefully parametrized microbial loop into a standard phytoplankton-zooplankton chemostat model (Fussmann et al. 2000) (Fig. 5.1) and study changes in mean biomasses and population dynamics. We analyse how the response of the system to the presence of bacteria depends on experimental conditions, whether the physiological traits of bacteria, phytoplankton and zooplankton favour or suppress bacteria, and how well the zooplankton is able to ingest the bacteria, i.e. its degree of bacterivory. The experimental conditions determine the relative importance of nutrient inflow and losses of nutrients and organisms due to washout on the one hand versus the internal recycling of nutrients and grazing-induced mortality on the other hand. The physiological traits of phytoplankton and zooplankton determine the rate at which organic carbon is produced and the fierceness of the competition for limiting nutrients between algae and bacteria. The degree of bacterivory of the zooplankton determines the grazing pressure on the bacteria. Experimental conditions, physiology and degree of bacterivory thus define the conditions under which bacteria may or may not thrive and impact the system.

To sharpen the focus of chemostat experiments on the phytoplankton-zooplankton interaction the question arises how the unwanted but unavoidable effect of bacteria can be minimized. One intriguing strategy to follow could be choosing zooplankton species with a low degree of bacterivory, assuming that non-ingested bacteria would hardly affect the system. Thus, rotifers, which are often less bacterivorous than ciliates (Arndt 1993), may be favoured for phytoplankton-zooplankton chemostat experiments. Instead, we find that the effect of bacteria is low at high degrees of bacterivory. By considering bacteria as inherent actors in phytoplankton-zooplankton experiments we are able to predict conditions when the effect of bacteria is large and provide means to minimize it.

Materials and Procedures

We employ two models to study the effect of bacteria on phytoplankton-zooplankton interactions. We start with a simple static carbon flux model (Fig. 5.1a) to estimate how much predator production may result from bacterial production and how this depends on algal exudation, predator excretion and bacterial growth efficiency. Then, we develop a dynamic chemostat model that provides insights into the mean biomasses and population dynamics of all species, which comes at the costs of requiring more assumptions (Fig. 5.1b).

In both models the rate of organic carbon production depends on the physiological parameters for maximal algal exudation $e_{\max}$ and predator excretion $(1-\varepsilon)$, ε being the predator assimilation efficiency. How efficiently this carbon pool can be used by the bacteria is set by their growth efficiency $(1-r_B)$, with the bacterial respiration r_B. Bacteria are suppressed by low carbon supply, which occurs at low algal exudation and low predator excretion, and inefficient use of that carbon by the bacteria. Bacteria are favoured by high carbon supply, i.e. at high algal exudation, predator excretion and bacterial growth efficiency. Using the lower and upper end of the broad ranges of published values for these parameters (Tab. 1, Appendix 1) we construct a minimum and a maximum impact scenario

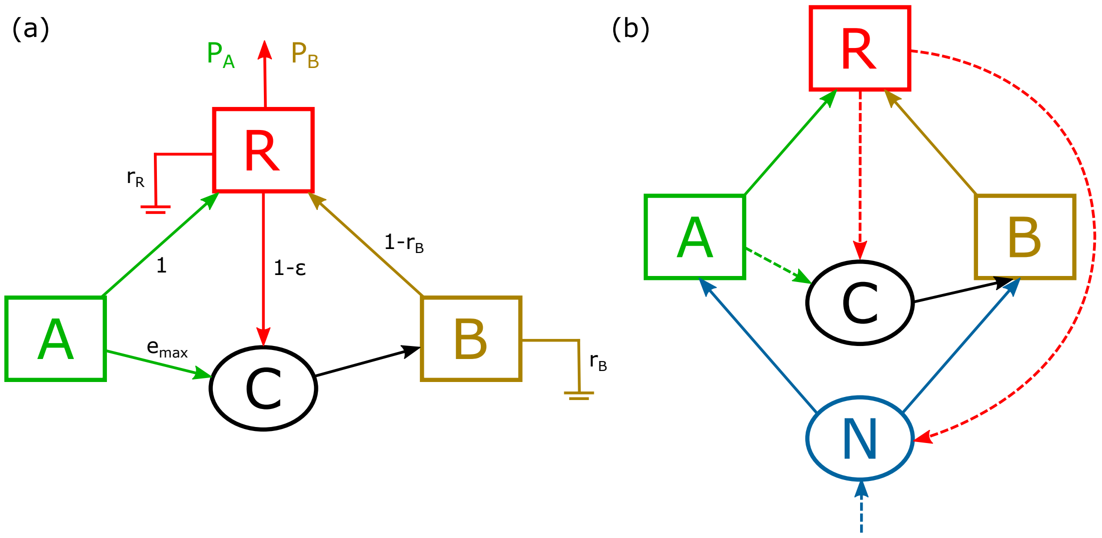

Figure 5.1 Food web sketches with the limiting resource nitrogen (N), organic carbon pool (C), algae (A), bacteria (B) and rotifers (R). (a) Static carbon flux model with parameters as used in Eqs. 5.1. One unit of algal production directly sustains predator excretion, respiration and production (P_A), but also entails additional carbon. These exudates fuel a pool of organic carbon that allows for bacterial production. This bacterial production per unit algal production also increases predator production (P_B). Respiratory losses are depicted by earth ground symbols. (b) Dynamic phytoplankton-zooplankton chemostat model as given by Eqs. 5.2. Here, solid arrows represent consumption, substance flows are shown in dashed arrows and respiratory fluxes are omitted for clarity.

of conditions suppressing or favouring bacteria, respectively.

Suppressing conditions

$$e_{max} = 0.2 \quad (1-\varepsilon) = 0.3 \quad (1-r_B) = 0.3$$

Favouring conditions

$$e_{max} = 0.4 \quad (1-\varepsilon) = 0.6 \quad (1-r_B) = 0.6$$

In the following, we investigate the effect of bacteria by employing these two extreme scenarios, which account for the great variability of observed bacterial growth conditions. We focus on typical chemostat experiments with obligatory autotrophic algae. We do not include bacterial toxicity, which might become important at high bacterial densities that are less likely to occur without additional carbon sources. Such high densities of toxic bacteria would result in predator extinction and the chemostat experiments would be stopped.

Static carbon flux model

A first estimate of the effect of bacteria for the two extreme cases of suppressing and favouring conditions for bacterial growth can be obtained from a static model of the carbon fluxes between algae, bacteria and predators. We constructed a model similar to those presented by Anderson and Ducklow (2001) and Gaedke et al. (2002) to compute the predator production that originates from bacterial production for different physiological parameters, i.e. bacteria-suppressing or -favouring conditions (Fig. 5.1a). We assume a steady state for all species. This translates to maximal algal exudation, as nitrogen limitation is high. Algal exudation is assumed to be proportional to algal production. Thus, every unit of algal production increases the organic carbon pool by exudates of e_{max}. A unit of algal net biomass production is completely ingested by the predator and converted either to predator excretion of $(1-\varepsilon)$, respiration r_R or production P_A. Additionally to algal exudation, predator excretion supplies the carbon pool, which is consumed by bacteria. The bacteria respire parts of this carbon while they invest the rest into biomass production, which is completely taken up by the predator at steady state. Parts of this ingested bacterial production returns to the carbon pool by excretion. We resolve this loop by a geometric series. After respiratory losses, this results in a predator production from bacteria (P_B) which originated from one unit of algal production. The predator production per unit algal production from algae (P_A) and bacteria (P_B) thus becomes

$$\begin{aligned} P_A &= \varepsilon(1 - r_R) \\ P_B &= \frac{e_{max} + (1 - \varepsilon)}{1 - (1 - r_B)(1 - \varepsilon)}\,(1 - r_B)\,\varepsilon\,(1 - r_R) \end{aligned} \tag{5.1}$$

From Eqs. 5.1 we can compute the fraction of predator production that originates from bacteria $P_B/(P_A + P_B)$ and the ratio of predator production with and without bacteria $(P_A + P_B)/P_A$, which gives the increase of predator production caused by the consumption of bacteria additionally to phytoplankton. Notably, these quantities become independent of predator respiration as it cancels out. This reduces the number of influential parameters to the physiological parameters that characterize the favouring and suppressing conditions, which makes these estimates of predator production even more robust and applicable to many species. However, this static model conveys no feed-back on the prey and thus no information on actual biomasses or population dynamics. Thus, we consider below a mechanistic differential equation model (Eqs. 5.2) to obtain a full picture of the effects of bacteria on phytoplankton-zooplankton interactions.

Dynamic phytoplankton-zooplankton model with organic carbon pool and bacteria

Using a well-established model presented by Fussmann et al. (2000) and Yoshida et al. (2003), we describe the predator-prey interaction of the rotifer *Brachionus calyciflorus* (R, Ind /L) feeding on its natural prey, the unicellular green algae *Monoraphidium minutum* (A, cells/L) in a chemostat (Fig. 5.1b). We simplify the original model slightly by assuming that every rotifer individual is fertile, i.e. we neglect the short periods of juvenile growth and senescence, but extend it by adding a pool of organic carbon C (μmol L^{-1}) and bacteria B (cells/L). Nitrogen N (μmol L^{-1}) is the limiting resource for algal growth. Bacterial growth is assumed to be multiplicatively co-limited by nitrogen and carbon. The full model reads

$$\begin{aligned}
\frac{\mathrm{d}N}{\mathrm{d}t} &= \delta\, N_I + (1-\varepsilon)\,\omega_{R,N}\,(F_{R,A} + F_{R,B})\,R \\
&\qquad - \omega_{A,N}\,F_A\,A - \omega_{B,N}\,F_B\,B - \delta\,N \\
\frac{\mathrm{d}C}{\mathrm{d}t} &= \frac{e_{\mathrm{dyn}}}{1-e_{\mathrm{min}}}\,\omega_{A,C}\,\beta_A\,A \\
&\qquad + (1-\varepsilon)\,\omega_{R,C}\,(F_{R,A} + F_{R,B})\,R \\
&\qquad - \frac{1}{1-r_B}\,\omega_{B,C}F_B\,B - \delta\,C \\
\frac{\mathrm{d}A}{\mathrm{d}t} &= F_A\,A - \frac{\omega_{R,C}}{\omega_{A,C}}\,F_{R,A}\,R - \delta\,A \\
\frac{\mathrm{d}B}{\mathrm{d}t} &= F_B\,B - \frac{\omega_{R,C}}{\omega_{B,C}}\,F_{R,B}\,R - \delta\,B \\
\frac{\mathrm{d}R}{\mathrm{d}t} &= (1-r_R)\,\varepsilon\,(F_{R,A} + F_{R,B})\,R - \delta\,R
\end{aligned} \tag{5.2}$$

All parameter values are listed in Tab. 1 along with their biological meaning (for a detailed discussion see Appendix 1). We will now describe the terms of the model in the order as they appear in Eqs. 5.2. The nitrogen pool in the chemostat is supplied by the inflow of fresh medium, which is given by the product of chemostat dilution rate δ and nitrogen concentration in the medium N_I, and the excretion of the predators from feeding on algae and bacteria. Algal and bacterial growth, at per capita rates F_i (Eqs. 5.3), and wash-out reduce the nitrogen pool.

Exudation by algae is assumed to be proportional to algal carbon fixation, whereas the proportionality factor increases linearly towards a maximum as the algal nutrient limitation increases (e_{dyn}, see Appendix 2 and Suppl. Fig. A4.1). This dynamic, nutrient dependent exudation by algae, together with the excretion by predators maintains the carbon pool. Carbon is diminished by bacterial consumption and wash-out. The interactions of species i with the carbon and nutrient pools are scaled by the respective carbon ($\omega_{i,C}$) and nitrogen ($\omega_{i,N}$) content of an individual.

Algae and bacteria grow at per capita growth rates [d^{-1}] of

$$\begin{aligned}
F_A &= \beta_A \frac{1-e_{\mathrm{dyn}}}{1-e_{\mathrm{min}}}\,\frac{N}{H_A + N} \\
F_B &= \beta_B \frac{C}{H_{B,C} + C}\,\frac{N}{H_{B,N} + N}
\end{aligned} \tag{5.3}$$

where β_i is the maximum growth rate of species i, $e_{\min}$ is the minimum exudation and H_i is the half saturation constant. Algal and bacterial densities are reduced by predator grazing and wash-out. The predator per capita grazing rates on algae and bacteria $[\mathrm{d}^{-1}]$ follow a multi-species Holling Type-II shape (Eqs. 4).

$$\begin{aligned} F_{R\,A} &= G\,\frac{\omega_{A,C}\,A}{H_R + \omega_{A,C}\,A + p_B\,\omega_{A,C}\,B} \\ F_{R\,B} &= G\,\frac{p_B\,\omega_{B,C}\,B}{H_R + \omega_{A,C}\,A + p_B\,\omega_{B,C}\,B} \end{aligned} \tag{5.4}$$

Here, G is the maximum grazing rate of a predator and H_R is the half saturation constant scaled to carbon. The bacteria are potentially less edible than the algae, depending on the degree of bacterivory of the predators p_B which provides the part of the bacterial population that is accessible to the predator. Effectively, this scales up the half-saturation constant of the predator for feeding on bacteria. Grazing is converted into bacterial or algal losses by the ratio of carbon contents per individual. The predators assimilate only a part of the ingested food. What is not assimilated is excreted and enters the carbon pool. The assimilates are further reduced by respiration, the remainders are used for production of new predator biomass. The only loss-term of predators is wash-out.

Numerical simulations and determination of dynamics

To achieve a broad picture of the effects of bacteria, we examined the parameter space spanned by the dilution rate of the chemostat δ and the degree of bacterivory of the predator p_B, thereby considering the two scenarios suppressing or favouring bacteria. The dilution rate is an important parameter for the performance of the individual species as it determines the rate of nutrient input and the loss rates of all species. The degree of bacterivory is important as it shapes the interspecific interactions via the apparent competition between algae and bacteria mediated by the predator. A third important system parameter is the nutrient inflow concentration N_I, which we included in our analysis at an intermediate dilution rate for favouring conditions. The system of ordinary differential equations Eqs. 5.2 was integrated with the *odeint* package from the Scipy library (Jones et al. 2001) in Python (version 3.5). The presence of bacteria in an algae-rotifer system may have two ecologically important effects, first on the mean biomasses, which can directly be obtained from the model outputs, and second on the population dynamics. To distinguish between steady state, regular cycles and irregular dynamics, local peaks in the normalized autocorrelation function (nACF) of the algal density were detected using the *argrelmax* algorithm from Scipy. A time series was classified as being at steady state if no peaks with prominence above the accuracy of the solver were detected. If the first peak of the nACF was above 0.95 the dynamics are periodic and were classified as regular. We termed the population dynamics of one such period the *repetitive unit* and extracted the number of algal maxima from it. If all peaks of the nACF were below 0.95 the dynamics show no clear repetitive pattern and thus were classified as irregular.

Table 5.1 Parameters and their biological meaning. Ranges are given for parameters that were varied within this study. Parameter values are either estimated from unpublished chemostat runs (Guntram Weithoff, Svenja Schälicke, personal communication) or taken from literature. See also the description of parameter choice in Appendix 1.

Parameter	Biological meaning	Value	Reference
$e_{\max}$	Maximum carbon exudation of algae	0.2 .. 0.4	varied, Baines and Pace (1991)
$e_{\min}$	Minimum carbon exudation of algae	0.1	varied, Baines and Pace (1991)
r_B	Carbon respiration by bacteria	0.4 .. 0.7	varied, del Giorgio and Cole (1998)
r_R	Carbon respiration by rotifers	0.5	Humphreys (1979)
ε	Carbon assimiliation efficiency of rotifers	0.4 .. 0.7	varied, Straile (1997)
δ	Chemostat dilution rate	0.07 .. 0.7 d^{-1}	varied within standard experimental ranges, see e.g. Vadstein et al. (2003) or Fussmann et al. (2000)
N_I	Inflow resource concentration	$160\,\mu\mathrm{molN/L}$	set to standard experimental conditions, see e.g. Becks et al. (2010)
$\omega_{A,N}$	N content in an algal cell	$4.6 \times 10^{-8}\,\mu\mathrm{molN}$	estimated from unpublished data, G. Weithoff
$\omega_{B,N}$	N content in a bacterial cell	$8.8 \times 10^{-10}\,\mu\mathrm{molN}$	from $\omega_{B,C}$ with C:N = 5.65 (Vrede et al. 2002)
$\omega_{R,N}$	N content in a rotifer	$1.2 \times 10^{-3}\,\mu\mathrm{molN}$	stimated from unpublished data, G. Weithoff
$\omega_{A,C}$	C content in an algal cell	$5 \times 10^{-7}\,\mu\mathrm{molC} \,\widehat{=}\, 6\,\mathrm{pgC}$	stimated from unpublished data, G. Weithoff
$\omega_{B,C}$	C content in a bacterial cell	$5 \times 10^{-9}\,\mu\mathrm{molC} \,\widehat{=}\, 60\,\mathrm{fgC}$	set to 1/100 of $\omega_{A,C}$ in agreement with Vrede et al. (2002)
$\omega_{R,C}$	C content in a rotifer	$6.7 \times 10^{-3}\,\mu\mathrm{molC} \,\widehat{=}\, 80\,\mathrm{ngC}$	from $\omega_{R,N}$ with C:N = 5.6 (Jensen et al. 2006), in agreement with Dumont et al. (1975) and Rothhaupt (1990)
β_A	Maximum algal growth rate	$1.9\,\mathrm{d}^{-1}$	estimated from unpublished data, S. Schälicke
β_B	Maximum bacterial growth rate	$1\,\mathrm{d}^{-1}$	Morris and Lewis (1992)
G	Rotifer maximum ingestion rate	$3.6\,\mathrm{d}^{-1} \,\widehat{=}\, 288\,\mathrm{ngC/d}$	Rothhaupt (1990)
H_A	Algal half-saturation	$49\,\mu\mathrm{molN/L}$	estimated from unpublished data, S. Schälicke
$H_{B,N}$	Bacterial half-saturation for nitrogen	$4.9\,\mu\mathrm{molN/L}$	set to 1/10 of the algal half-saturation
$H_{B,C}$	Bacterial half-saturation for carbon	$0.83\,\mu\mathrm{molC/L}$	Tittel et al. (2012)
H_R	Rotifer half-saturation	$195\,\mu\mathrm{molC/L} \,\widehat{=}\, 2.34\,\mathrm{mgC/L}$	set, in approximate agreement with Fussmann et al. (2000)
p_B	Edibility of bacteria	0 .. 1	varied

Assessment

Effect of bacteria on predator production

The static carbon flux model predicts a dependence of predator production on maximal algal exudation $e_{\max}$, predator assimilation efficiency ε and bacterial respiration r_B (Fig. 5.2). The model justifies the rationale behind the maximum and minimum impact scenarios, i.e. bacteria-favouring and –suppressing conditions, respectively. Predator production is least strongly affected by the presence of bacteria at low algal exudation, low predator excretion and low bacteria growth efficiency. The model predicts that under these bacteria-suppressing conditions 14% of the total predator production originate from ingesting bacteria. This results in an increase of total predator production by 16%. In contrast, under bacteria-favouring conditions bacteria constitute 48% of total predator production, which almost doubles with an increase by 94%. From this simplified model, we already see that bacteria may have a large effect under certain physiological conditions.

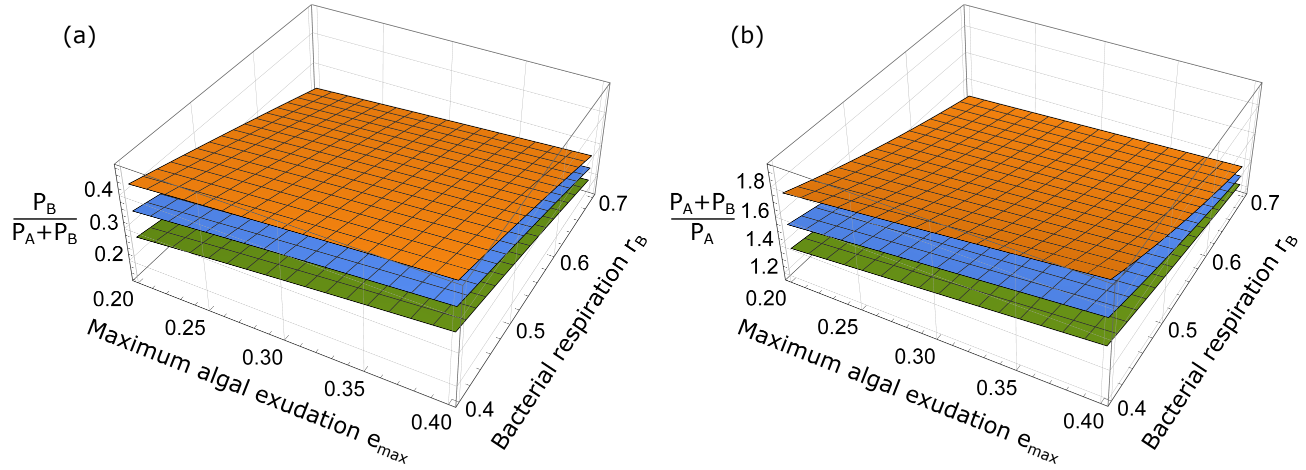

Figure 5.2 Impact of bacteria on predator production as predicted by the static model. Depending on the exudation, i.e. the fraction of carbon that is maximally exudated by algae $e_{\max}$, the bacterial respiration, i.e. the fraction of carbon taken up by bacteria that is respired r_B, and the assimilation efficiency of predators ε, bacteria can contribute a significant portion to predator production. The assimilation efficiency is set to 0.4 (orange, top), 0.55 (blue, middle) and 0.7 (green, bottom). (a) Predator production derived from bacteria (P_B) relative to total predator production ($P_A + P_B$). (b) Total predator production with bacteria present relative to the predator production without bacteria.

Effect of bacteria on mean biomass

Using the mechanistic model, we compare the effect of bacteria in chemostat experiments under suppressing and favouring conditions for large ranges of the chemostat dilution rate δ and the degree of bacterivory of the predator p_B. These two key parameters, which govern the fluxes in the system, may strongly affect the mean biomasses of all species (Fig. 5.3). Comparing the two extreme cases of bacteria-suppressing versus bacteria-favouring conditions shows that under suppressing conditions bacterial biomass remains mostly negligible and algal and predator biomass is thus independent of the degree of bacterivory by the predator (Fig. 5.3a). With little bacteria present algal mean biomass increases and predator biomass decreases as the dilution rate increases. Only at very low degrees of bacterivory and high dilution rates the bacteria can achieve non-negligible biomasses, which is reflected by a slightly lower algal biomass in this parameter region. In contrast, under bacteria-favouring conditions bacteria reach considerable mean biomasses, which are highest at low degrees of bacterivory and high dilution rates (Fig. 5.3b). An increasing degree of bacterivory results in lower bacterial and higher predator biomass. The algal biomass increases due to a release from competition. At very strong bacterivory and low dilution rate bacterial mean biomass becomes negligible in favour of the algae. The predator goes extinct if the dilution rate exceeds its maximal realized per capita growth rate. The dilution rates that the predator can withstand increase with stronger bacterivory.

The effect size of bacteria represented by the logarithmic ratio of mean biomasses in simulations with and without bacteria provides a direct measure of the impact of bacteria on mean biomasses (Fig. 5.4, Suppl. Fig. A4.2). While for suppressing conditions the bacterial biomass and thus the effect size of bacteria is negligible throughout the parameter space (Suppl. Fig. A4.2), interesting patterns emerge for favouring conditions (Fig. 5.4). Here, the total biomass in the chemostat, i.e. the sum of algae, predators and bacteria in units of carbon per litre decreases strongly if bacterivory and dilution rates are at intermediate levels, which originates from low algal biomasses that are not compensated by the bacteria and the biomass increase of the predator.

Effect of bacteria on population dynamics

Population dynamics are often used as fingerprints of biological interactions. To study how they are affected by the presence of bacteria, we evaluated the type of population dynamics in the parameter space of Fig. 5.3 and Fig. 5.4 for the bacteria-favouring scenario where bacteria have a significant effect on the mean biomasses (Fig. 5.5, Fig. 5.6). We found a complex pattern of alternating regions of regular and non-regular dynamics (Fig. 5.5).

At low dilution rates and high to intermediate degrees of bacterivory the population dynamics are fairly simple (panels i and ii in Fig. 5.6). Within a cycle the algae establish first, nitrogen declines and organic carbon accumulates which allows the bacteria to increase as well. Finally, the predator reaches high biomasses by grazing down both algae and bacteria. This releases the nitrogen, the

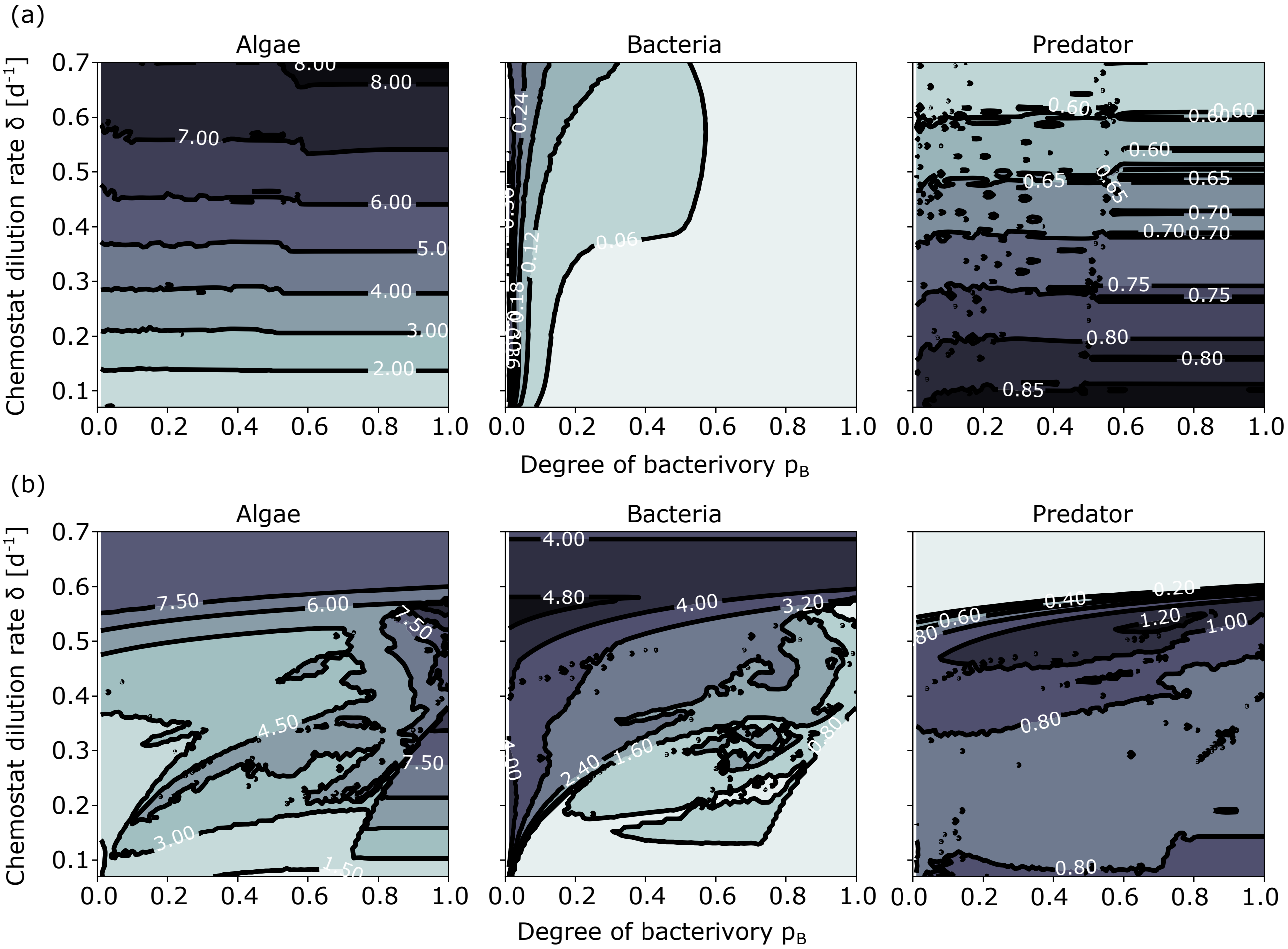

Figure 5.3 Mean biomasses for (a) suppressing conditions (algal exudation, predator excretion and bacterial growth efficiency are low) and (b) favouring conditions for bacteria (algal exudation, predator excretion and bacterial growth efficiency are high) for the parameter space spanned by the chemostat dilution rate δ and the degree of bacterivory of the predator p_B. Colours correspond to different biomass levels $[\mathrm{mgC/L}]$ in the individual plots as the biomass ranges vary largely.

predator declines and the whole cycle starts again. However, if the degree of bacterivory is too high, the bacteria go extinct (as in panel i). These classic predator-prey cycles can easily become highly complex, driven by the interaction of direct and indirect competition between algae and bacteria (panels iii, iv, and v). For a fairly low degree of bacterivory and a low dilution rate, the predators increases for a second time within one cycle of the overall population dynamics (termed repetitive unit) even though algal densities are already too low to enable predator net growth (panel iii). This second predator peak is mainly realized from grazing on bacteria and shows that the presence of bacteria can strongly alter the shape of the predator population dynamics.

For broad parameter ranges multiple algal maxima occur within one repetitive unit (panel iv) and partly the dynamics become irregular, i.e. no repetitive unit can be found in the time-series of the biomasses (panel v). Here, algae and bacteria alternate during the increase of the predator. Bacteria are the better competitors for nitrogen, but rely on the carbon exudates from the algae. Thus, the algal

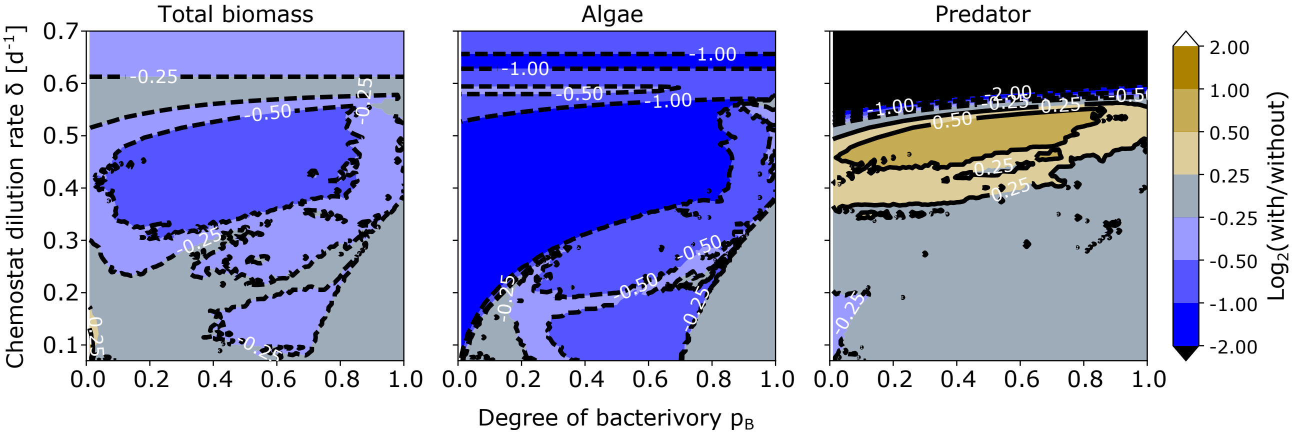

Figure 5.4 Effect size of bacterial presence under bacteria-favouring conditions. The effect size is defined as the logarithmic ratio to base 2 of the mean biomasses with and without bacteria. The presence of bacteria often decreases algal and total biomass but mostly increases predator biomass. Under suppressing conditions, the bacteria have only little effect (see Suppl. Fig. A4.2).

biomass increases first, but is soon reduced mainly by washout since predation pressure is still very low due to the low predator biomass. Algae are washed out at higher nitrogen concentrations than bacteria given their higher half-saturation constants. The bacteria, however, are washed out when the carbon is depleted. This increases the nitrogen concentration and allows the algae to increase again. Eventually, the predator has accumulated enough biomass to graze down both algae and bacteria. Without further food, the predator is now washed out and the whole cycle starts again. At high dilution rates the cycle amplitude decreases (panel vi) and eventually the dynamics reach a steady state (panel vii). If the predator goes extinct, algae and bacteria continue to coexist in a steady state (panel viii).

Explanation of results

The combined effect of dilution rate and degree of bacterivory can be understood by shifts in the balance between bottom-up and top-down control (Fig. 5.5 and Fig. 5.6). At high dilution rates and low degrees of bacterivory the predator is strongly limited in its net growth and the prey becomes more bottom-up limited (Fig. 5.6, panels vi, vii and viii). Thus, its cycle amplitudes decrease and mean biomasses increase. The low top-down control allows the prey to first deplete the resources before being washed out, in parts of the parameter space for multiple times during one predator cycle, before the predator has caught up and finally grazes down the prey (Fig. 5.6, panels iv and v). Within this first phase of low top-down control competition between algae and bacteria alternates with algae supporting bacterial growth through the release of organic carbon, which explains the complex multi-cycle patterns. At low dilution rates and high degrees of bacterivory the top-down control increases as

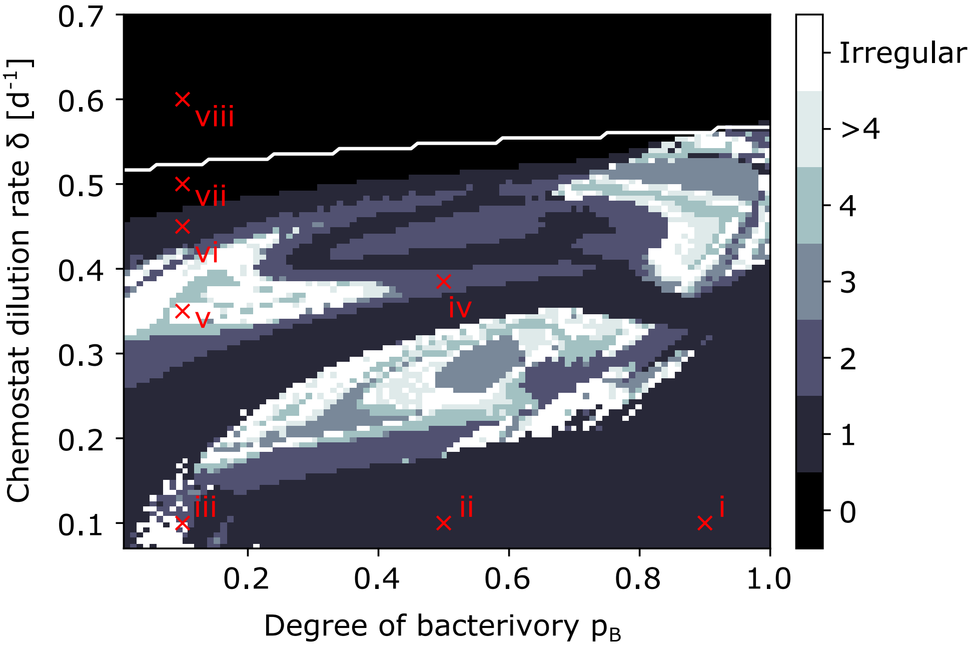

Figure 5.5 Population dynamics under favouring conditions determined by the number of algal peaks within a repetitive unit, i.e. the shortest periodic element. If no such unit was found the dynamics are classified as irregular, or steady state if no oscillations occurred at all. Mean predator biomass drops below $10^{-30}\,\mathrm{mgC/L}$ above the white line. The dynamics can become highly complex, unless bacteria are grazed down by the predator, which happens for high degrees of bacterivory p_B and low chemostat dilution rates δ.

the predator is able to exert a considerable predation pressure on both algae and bacteria, thus forcing the system into more regular predator-prey cycles (Fig. 5.6, panels i and ii). The second predator peak (Fig. 5.6, panel iii) arises if the predation pressure is strong enough to quickly reduce algal biomass, while exudates are not yet washed out. This remaining carbon, together with the low degree of bacterivory, creates a short window of opportunity of high bacterial biomass, which then results in a peak in the predator's biomass without high algal biomasses.

Effect of nutrient inflow concentration

Similar to the above results, also the parameter space spanned by nutrient inflow concentration and degree of bacterivory is composed of regions of different bottom-up – top-down balances. As the inflow concentration increases the chemostat system is enriched and all mean biomasses increase (Suppl. Fig. A4.3a). An increasing degree of bacterivory has a similar effect for the predator as it broadens its food spectrum. Also, higher degrees of bacterivory suppress bacteria and favour algae in their apparent competition. Thus, if both parameters are low there is strong bottom-up control and the effect size of bacteria on the total biomass and the algae is small (Suppl. Fig. A4.3b). If nutrient inflow

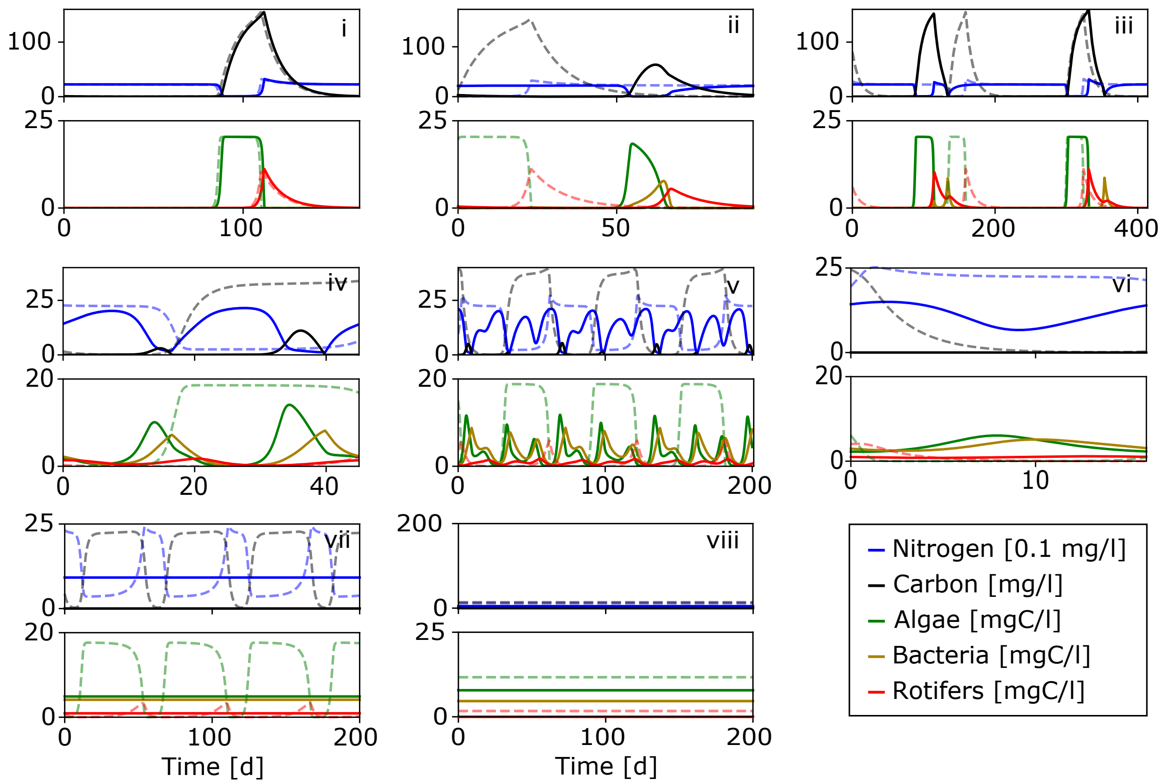

Figure 5.6 Time series for the marked parameter combinations in Fig. 5.5. Solid and dashed lines correspond to simulation runs with and without bacteria present, respectively. The drastic differences between the simulations with and without bacteria show that bacteria can strongly affect the population dynamics. The dynamics were characterized from the dynamics with bacteria included. If a periodicity could be determined, the repetitive unit is shown, otherwise the dynamics are plotted for 200 days. Periodic dynamics contain either one (panels i, ii, vi) or multiple prey maxima within a repetitive unit (panels iii and iv). Steady states are shown in panels vii, where all species coexist, and viii, where the predator went extinct. Non-periodic dynamics were termed irregular and are shown in panel v. In panel iii, the predator reaches a first maximum from grazing down algae and bacteria. This results in excretions from which the bacteria increase a second time, allowing also the predator to increase again. It is only possible to explain this second predator peak by also considering bacteria.

concentration and degree of bacterivory are high this results in a strong top-down control which again decreases the effect size of bacteria on the total biomass and the algae. At intermediate parameter ranges, however, both total biomass and algae are strongly negatively affected by bacteria. The effect size of bacteria on the predator behaves contrary. In the parameter regions of high bottom-up control and high top-down the predator is affected negatively, whereas it largely benefits from the bacteria in the intermediate region. The dynamic pattern approximately reflects these three regions with simpler dynamics at strong forcing and more complex dynamics in the intermediate regime (Suppl. Fig. A4.3c).

Discussion

Chemostat experiments, particularly with phytoplankton-zooplankton systems, are often employed to resolve ecological and evolutionary questions regarding predator-prey interactions. However, bacteria are omnipresent actors in nature. In this paper we argue that it may be indispensable to either include bacteria in the interpretation of study results or to take applicable measures to minimize their effect. Using a simplified, static carbon-flux model as well as a mechanistic, dynamic chemostat model, which has been parametrized closely to typical experimental systems, we show that bacteria are able to strongly impact predator production, biomass levels and population dynamics in chemostat experiments. Under bacteria-suppressing conditions, i.e. if specific physiological properties of the organisms reduce the production and utilization of organic carbon, we expect bacteria to generally play only a minor role, if at all. Under bacteria-favouring conditions, however, predator production is substantially increased by the presence of bacteria. It is important to note that the contribution of bacteria to predator ingestion varies in time and thus temporally exceeds the mean values predicted by the static carbon-flux model. From the dynamic model we see that the effect of bacteria on the biomasses and particularly the population dynamics in the chemostat strongly depends on the experimental conditions, i.e. the dilution rate and nutrient inflow concentration, as well as the degree of bacterivory of the predators.

Impact of the bacterial pathway on the food web structure

The shift of biomass from algae to bacteria at intermediate dilution rates and bacterivory decreases the total biomass in the chemostat when comparing systems with and without bacteria present. Here, the biomass of the bacteria and the biomass increase of the predator are not sufficient to compensate for the biomass losses of the algae as the bacterial pathway in the food web includes bacterial respiration as an additional loss-term along which biomass is irretrievably lost. This may obstruct predictions for biomass yield and energy balances in aquatic mass cultures if bacteria were not considered (Hino et al. 1997). On the other hand, this pathway increases the predator biomass as now algal exudates and predator excretion, which are lost without bacteria, are recycled by the bacteria and may be used by the predator, thus increasing the efficiency by which primary production is transferred to the predator.

Importance of bacteria for population dynamics

While for high degrees of bacterivory and low dilution rates we observed regular predator-prey cycles, the dynamics can become highly complex for intermediate parameter regions. Within one pronounced and experimentally detectable cycle of the predator multiple cycles of algae and bacteria can occur. At low bacterivory and low dilution rates the overall dynamics resemble those without bacteria at first glance. The only indication of bacteria having an effect in this region is the second predator peak, which cannot be explained without considering bacteria in an experimental chemostat system and instead might lead to wrong conclusions.

A recent model study showed that already small changes in food web structure, such as introducing a second predator with a slightly different prey preference, may result in intermittent cycles (Bengfort et al. 2017). We showed that including bacteria in a chemostat model may cause similar deviations from the expected predator-prey interactions. Population dynamics observed in chemostat experiments are occasionally quite irregular (personal communication Guntram Weithoff; (Bengfort et al. 2017)) and it remains to be studied whether this irregularity is just a more complex attractor similar to the ones observed in this study. Bacteria could thus be an overlooked actor in chemostat experiments responsible for unexpected complexity of population dynamics.

Impact of bacteria when inferring processes from patterns

A prominent example of eco-evolutionary feedbacks is the evolution of defense in prey populations under predation, resulting in a temporal niche for a defended, less palatable clone when the predation pressure is high (Becks et al. 2012). As long as the defended prey dominates predator biomass decreases and a niche opens for the undefended prey if it is more competitive for nutrients than the defended prey. These interactions result in dynamics similar to those presented in Fig. 5.6, panels ii and iv. Here, the algae increase first and their exudation provides a temporal niche for bacteria. Thus, bacteria depend on the algae, even though algae and bacteria also compete for nitrogen. Recently, we showed that a similar combination of facilitation and competition between two prey species can ensure their coexistence (Raatz et al. 2017). Such sustained coexistence by temporal niching results in a prolonged total prey biomass peak (here the sum of algae and bacteria) and a delayed predator response, which both are characteristic for eco-evolutionary dynamics (Yoshida et al. 2003; van Velzen and Gaedke 2017). Thus, by merely inferring a process from a pattern without acknowledging the presence of bacteria may overestimate the importance of eco-evolutionary dynamics.

Implications for improvement of experimental design

Our study enables us to propose means for reducing the impact of bacteria in chemostat studies that explicitly focus on phytoplankton-zooplankton interactions by adjusting their design accordingly. Aside from the easily implemented measure to reduce the dilution rate, which enables a stronger response by the predator, also the ability to ingest bacteria should be taken into account when the predator species is selected. Instead of intuitively using species incapable of ingesting bacteria (e.g. numerous rotifers, (Arndt 1993)), predator species with a high degree of bacterivory could be the preferred choice (e.g. many ciliates, (E. B. Sherr and B. F. Sherr 1987)).

Bacteria can affect phytoplankton-zooplankton interactions in a chemostat by two mechanisms: (i) by competing for nutrients with the algae and (ii) by contributing to predator production. When we considered the effect sizes as a measure of the ratio of average biomasses with and without bacteria the zero-bacterivory limit corresponds to the case when only competition is at play. A high degree of bacterivory, however, includes the effect of both competition and predator divergence. Since the effect sizes do not vanish towards low degrees of bacterivory we see that bacteria have a considerable competitive impact on the algae and thus affect the food web even if they do not contribute to the production of the predator. A high degree of bacterivory of the predator minimizes the competitive impact of bacteria and thus decreases the effect of bacteria in chemostat experiments.

Here we argue that bacteria are an unavoidable and inherent actor in phytoplankton-zooplankton chemostats, whose impact may be minimized by choosing the right experimental setup. Thereby we should keep in mind that – up to now overlooked – bacteria might have some impacts on population dynamics and species coexistence that are comparable to the previously overlooked effects of rapid evolution (Yoshida et al. 2003).

Our study shows that only with an appropriate choice of the predator species and an appreciation for the presence and role of all important actors we can correctly interpret phytoplankton-zooplankton chemostats and use them to study complex predator-prey interactions.

Acknowledgements

This work was funded by DFG (WA 2445/8-2, WA 2445/11-1, GA 401/26-1) as part of the Priority Programme 1704 (DynaTrait).

Bibliography

Anderson, T. R. and Ducklow, H. W. (2001). Microbial loop carbon cycling in ocean environments studied using a simple steady state model. *Aquat. Microb. Ecol.* 26: 37–49.

Aoki, S. and Hino, A. (1996). Nitrogen flow in a chemostat culture of the rotifer Brachionus plicatilis. *Fish. Sci.* 62: 8–14.

Arndt, H. (1993). Rotifers as predators on components of the microbial web (bacteria, heterotrophic flagellates, ciliates) ? a review. *Hydrobiologia* 255-256: 231–246.

Baines, S. B. and Pace, M. L. (1991). The production of dissolved organic matter by phytoplankton and its importance to bacteria: Patterns across marine and freshwater systems. *Limnol. Oceanogr.* 36: 1078–1090.

Becks, L., Ellner, S. P., Jones, L. E., and Hairston Jr, N. G. (2010). Reduction of adaptive genetic diversity radically alters eco-evolutionary community dynamics. *Ecol. Lett.* 13: 989–997.

Becks, L., Ellner, S. P., Jones, L. E., and Hairston, N. G. (2012). The functional genomics of an eco-evolutionary feedback loop: Linking gene expression, trait evolution, and community dynamics. *Ecol. Lett.* 15: 492–501.

Bengfort, M., van Velzen, E., and Gaedke, U. (2017). Slight phenotypic variation in predators and prey causes complex predator-prey oscillations. *Ecol. Complex.* 31: 115–124.

Bratbak, G. and Thingstad, T. (1985). Phytoplankton-bacteria interactions: an apparant paradox? Analysis of a model system with both competition and commensalism. *Mar. Ecol. Prog. Ser.* 25: 23–30.

Declerck, S. A. J., Malo, A. R., Diehl, S., et al. (2015). Rapid adaptation of herbivore consumers to nutrient limitation: eco-evolutionary feedbacks to population demography and resource control. *Ecol. Lett.* 18: 553–562.

Dumont, H. J., Van de Velde, I., and Dumont, S. (1975). The dry weight estimate of biomass in a selection of Cladocera, Copepoda and Rotifera from the plankton, periphyton and benthos of continental waters. *Oecologia* 19: 75–97.

Fussmann, G. F., Ellner, S. P., Shertzer, K. W., and Hairston, N. G. J. (2000). Crossing the Hopf Bifurcation in a Live Predator-Prey System. *Science* 290: 1358–1360.

Gaedke, U., Hochstädter, S., and Straile, D. (2002). Interplay between energy limitation and nutritional deficiency: empirical data and food web models. *Ecol. Monogr.* 72: 251–270.

del Giorgio, P. A. and Cole, J. J. (1998). Bacterial growth efficiency in natural aquatic systems. *Annu. Rev. Ecol. Syst.* 29: 503–541.

Hiltunen, T., Jones, L. E., Ellner, S. P., and Hairston, N. G. (2013). Temporal dynamics of a simple community with intraguild predation: an experimental test. *Ecology* 94: 773–779.

Hino, A., Aoki, S., and Ushiro, M. (1997). Nitrogen-flow in the rotifer Brachionus rotundiformis and its significance in mass cultures. *Hydrobiologia* 358: 77–82.

Humphreys, W. F. (1979). Production and respiration in animal populations. *J. Anim. Ecol* 48: 427–453.

Ishino, R., Iehata, S., Nakano, M., et al. (2012). Bacterial Diversity Associated with the Rotifer Brachionus plicatilis sp. Complex Determined by Culture-Dependent and -Independent Methods. *Biocontrol Sci.* 17: 51–56.

Jensen, T. C., Anderson, T. R., Daufresne, M., and Hessen, D. O. (2006). Does excess carbon affect respiration of the rotifer Brachionus calyciflorus Pallas? *Freshw. Biol.* 51: 2320–2333.

Jones, E., Oliphant, T., Peterson, P., et al. (2001). SciPy: Open source scientific tools for Python.

Morris, D. P. and Lewis, W. M. (1992). Nutrient limitation of bacterioplankton growth in Lake Dillon, Colorado. *Limnol. Oceanogr.* 37: 1179–1192.

Novick, A. and Szilard, L. (1950). Description of the Chemostat. *Science* 112: 715–716.

Ooms-Wilms, A. L. (1997). Are bacteria an important food source for rotifers in eutrophic lakes? *J. Plankton Res.* 19: 1125–1141.

Raatz, M., Gaedke, U., and Wacker, A. (2017). High food quality of prey lowers its risk of extinction. *Oikos* 126: 1501–1510.

Rothhaupt, K. O. (1990). Differences in particle size-dependent feeding efficiencies of closely related rotifer species. *Limnol. Oceanogr.* 35: 16–23.

Seah, B. K. B., Schwaha, T., Volland, J.-M., et al. (2017). Specificity in diversity: single origin of a widespread ciliate-bacteria symbiosis. *Proc. R. Soc. B Biol. Sci.* 284: 20170764.

Sherr, E. B. and Sherr, B. F. (1987). High rates of consumption of bacteria by pelagic ciliates. *Nature* 325: 710–711.

Starkweather, P. L., Gilbert, J. J., and Frost, T. M. (1979). Bacterial feeding by the rotifer Brachionus calyciflorus: Clearance and ingestion rates, behavior and population dynamics. *Oecologia* 44: 26–30.

Straile, D. (1997). Gross growth efficiencies of protozoan and metazoan zooplankton and their dependence on food concentration, predator-prey weight ratio, and taxonomic group. *Limnol. Oceanogr.* 42: 1375–1385.

Tittel, J., Büttner, O., and Kamjunke, N. (2012). Non-cooperative behaviour of bacteria prevents efficient phosphorus utilization of planktonic communities. *J. Plankton Res.* 34: 102–112.

Vadstein, O., Olsen, L. M., Busch, A., Andersen, T., and Reinertsen, H. R. (2003). Is phosphorus limitation of planktonic heterotrophic bacteria and accumulation of degradable DOC a normal phenomenon in phosphorus-limited systems? A microcosm study. *FEMS Microbiol. Ecol.* 46: 307–316.

van Velzen, E. and Gaedke, U. (2017). Disentangling eco-evolutionary dynamics of predator-prey coevolution: the case of antiphase cycles. *Sci. Rep.* 7: 17125.

Vrede, K., Heldal, M., Norland, S., and Bratbak, G. (2002). Elemental Composition (C, N, P) and Cell Volume of Exponentially Growing and Nutrient-Limited Bacterioplankton. *Appl. Environ. Microbiol.* 68: 2965–2971.

Yoshida, T., Jones, L. E., Ellner, S. P., Fussmann, G. F., and Hairston, N. G. (2003). Rapid evolution drives ecological dynamics in a predator-prey system. *Nature* 424: 303–306.

6 General discussion

In the previous chapters 2 to 5 I have presented four case studies with a scope broadening from the physiology of individual predators towards the structure of small food webs. Within each of these chapters, I studied the effect of different traits, and variations in these traits, within or between species, and how this affected the respective predator-prey interactions. This trait variation, be it static as in chapters 2, 3 and 5, or variable as in chapter 4, gives rise to different strategies along the respective trait axes. Within the following, I want to examine the former results with a focus on these strategies, and highlight how such strategies are beneficial under certain circumstances to the organisms applying them.

6.1 Acclimation and storage are beneficial strategies under certain fluctuation regimes

In chapter 2, I presented acclimation of assimilation and resource storage as two different physiological strategies that allow a predator to increase its growth rate in environments of fluctuating prey quality. However, I found that these two strategies are beneficial in different parts of the spectrum of fluctuations that the predator perceives. Acclimation of the assimilation apparatus probably involves a time lag, during which for example a different set of digestive enzymes is produced in order to increase the assimilation efficiencies for one nutrient. In the presence of a trade-off between the assimilation of different nutrients, this acclimation comes at the cost of lowering the assimilation efficiencies for the other nutrient. This yields high gains from acclimation if resource fluctuations are slow, i.e. if the fluctuation frequency is low. Fast fluctuations, however, cannot be tracked by the acclimation and benefits cease. Storage of nutrients involves no such lag and provides the bigger advantage when fluctuations are fast. Here, nutrients that become depleted at one point in time, reappear quickly before the stored nutrients are emptied, thus increasing growth rates for fast fluctuations.

Thinking in terms of strategies, the ability to acclimate the assimilation efficiencies to the internal nutritional requirements, without being able to store these nutrients, creates acclimation specialists (as in Figs. 2.3C and 2.4C). These are favoured in environments where fluctuations occur on larger temporal or spatial scales. Such large scale fluctuations could be induced for example by weather events or seasonal changes.

If acclimation is excluded, but predators are able to store nutrients (Figs. 2.3B and 2.4B), such storage specialists perform well in frequently fluctuating environments, where nutrient fluctuations are for example created by fast movement across spatial heterogeneities. If a trade-off exists between acclimation and storage, different scales of fluctuations would select for different physiological adaptations, either towards acclimation in slowly, or storage in fast fluctuating environments. Without such a trade-off (as in Fig. 2.4D), intermediate frequencies and uncorrelated resource fluctuations yield the highest growth rates.

The lifetime of an organism determines the characteric time spans in which the organism is susceptible to nutritional fluctuations. Similarly, it governs whether such fluctuations are perceived as slow or fast. Therefore, the combination of physiological strategy (acclimation and/or storage) and lifetime determines the fluctuation regime in which a predator performs best. Investigations into different systems and regions across the globe could elucidate whether this hypothesized selection indeed occurred. For example, temperate aquatic systems are exposed to strong seasonalities, whereas resource distributions in tropical regions should be less variable throughout the year (Acevedo-Trejos et al. 2015). Therefore, adaptations to variability in resources should be more prominent in temperate regions for organisms with life spans large enough to be affected by such fluctuations.

A strategy to actively influence the perceived fluctuation pattern is movement (Kearney et al. 2010). Mobile organisms may therefore adapt their foraging behaviour according to their preferred fluctuation regime and select habitats (resource patches) or food sources (prey species) that fit their nutritional physiology. Optimizing movement decisions for beneficial nutrient fluctuation regimes however has to be balanced with other fitness-related factors, such as predation risk by other predators or encounter rates with mating partners; see section B for a description of a study on movement patterns in rotifers that I was involved in (Obertegger et al. 2018).

Within this project, we assumed that the consumption of the predator does not affect the prey density. Of course, this assumption is highly unrealistic. A promising future avenue could thus be to include such feedbacks and model an explicit predator-prey interaction. A straightforward way of doing so would be to employ a chemostat model as in chapter 3 with two different prey species. Each of these prey species would then contain one of the co-limiting resources in large amounts. The consequences on the population dynamics could be highly complex. Competition for nutrients would favour negative covariance of the two prey species, while the colimitation of the predator might favour positive covariance and their coexistence, similar to chapter 3. The different physiological strategies of the predator may then render the outcomes even more intriguing.

6.2 Food quality provides strategies to compensate for lacking defense

In contrast to the previous discussion, the physiology of the predator was fixed in chapter 3, but I investigated the effect of different strategies within the prey community. As the foundation, I assumed that two different prey species may be more or less defended against a shared predator and investigated the effect of the strength of a trade-off between predation risk and competitiveness. In similar work, it was found that such a trade-off may enable coexistence of defended and undefended prey (Abrams 1999; Jones and Ellner 2007; Ehrlich and Gaedke 2018). To this reference situation I added the third trait axis of food quality differences within the prey species. This yields two extreme scenarios where either the defended or the undefended prey is the low-quality prey within the apparent competition and creates an indirect interaction between the two prey species.

Interestingly, I found that, compared to the reference situation without food quality limitation, the undefended prey benefits in both extreme scenarios. Being either of poor or high quality is beneficial for an undefended prey species in competition with defended prey of high or poor quality, respectively. In this line, food quality yields strategies to compensate for lacking defense against predation.

In the reference scenario without food quality limitation, coexistence or dominance of either prey species may be observed in the trait space spanned by predation risk and competitiveness of the defended prey (Fig. 3.2). If the undefended prey is of low quality, it however dominates for most of the parameter combinations within the trait space. Only if the undefended, low quality prey is initially at low biomasses, larger regions of dominance of the defended prey may be found (see Fig. A2.6 for this bistability). The coexistence region, where the undefended prey would have to share the abiotic resources with the defended prey, vanishes almost completely. Accordingly, also the average biomasses of the undefended prey increase strongly (Fig. A2.4b). If the defended prey is of low quality, being of high quality is beneficial for the undefended prey instead. Here, the region of dominance by the defended prey vanishes and gives room to an enlarged region of coexistence. This prevents the extinction of the undefended prey and raises its average biomass compared to the reference scenario (Fig. A2.4c). Overall, I showed that food quality is an important trait that may introduce indirect interactions within the prey community, with the possibility to heavily impact the outcomes of apparent competition.

In natural systems, co-limitation is a common characteristic of predator-prey interactions (Guo et al. 2016; Sperfeld et al. 2016). Thus, also particularly low or high food quality could be a widespread strategy to prevent exclusion from food webs. Cyanobacterial blooms are a very apparent example for the dominance of less edible, low quality prey (Wilson et al. 2006). During this period, being of high food quality might prevent the extinction of other phytoplankton species, as they are required to sustain the predator species. These strategies, however, remain beneficial for a prey species only as long as there is no source for compensatory feeding available to remedy the limitation by particular (bio-)chemical nutrients. If there is already a lot of high quality food available to the predator, its quality limitation drops and the effect of food quality differences vanishes (Fig. 3.4).

If having a certain food quality is a strategy that may enhance the performance of a prey species, the question of course arises how variable this quality is. As I considered the concentration of essential biochemical nutrients as the food quality determinant of a species, this translates to variability in exactly these nutrients, which was found to be quite high (Martin-Creuzburg and Merkel 2016). This supports the hypothesis that different food-quality-related strategies might be applied to ensure the persistence of certain prey species. It was suggested that food quality might be affected by anthropogenic disturbances (Guo et al. 2016), implying that food-quality-mediated persistence may be vulnerable to perturbations. Future research should target these issues.

6.3 Trait adaptation may be a strategy to enhance resilience

Instead of being restricted to fixed trait values, prey and predator populations are often observed to possess a strong flexibility in their traits, which allows them to adapt to enhance their performance (West-Eberhard 1989; Kopp and Tollrian 2003; Yoshida et al. 2003; Frickel et al. 2016). Often, this flexibility is found to be beneficial when dealing with environmental perturbations, i.e. in traits that determine the individual-environment (abiotic) interactions. In chapter 4, however, I investigated how adaptation of traits that shape the predator-prey interaction may similarly affect different robustness properties when facing perturbations. Here, I found that being adaptive may, in some cases, increase the robustness but no general pattern became apparent.

Within the model, we explicitly included the strategy to adapt along a trait axis. The prey is able to increase a defensive trait, while the predator may increase its offense. Both of these processes are restricted by trade-offs that decrease the gross growth rates for increasing defense and offense. Individual trait adaptation is driven by the first derivative of the per-capita growth rate with respect to the trait, i.e. the fitness gradient. In the time series in Fig. 4.3 we saw examples of how an increasing defense allows the prey to buffer the increase of predator biomass and still gain more biomass. In turn, increasing its offense allows the predator eventually to overcome the defense and graze down the prey.

We showed that the consequences of this adaptive strategy, that operates between predator and prey, go beyond these pairwise interactions and affect also the robustness of the population dynamics against environmental perturbations. The effects of seemingly restricted strategies may thus reach further then intuitively expected.

6.4 A broader food spectrum maximizes fitness

In chapter 5, I investigated how the direct predator-prey interaction between phytoplankton and zooplankton changes if a competitor to the prey is introduced into the food web (bacteria), i.e. the food web structure changes. While in the earlier chapters strategies of predator and prey could be selected based on the pairwise interaction, now further strategies along the microbial loop as a separate pathway are possible.

Including heterotrophic bacteria in the system allowed us to study the competition between these and the autotrophic algae. Without an additional carbon source, we saw that the bacteria can never outcompete the algae, even though they are better competitors for nutrients (Azam et al. 1983) (nitrogen in our example), as they rely on the carbon fixation by the algae. I identified this process as the origin of the complex population dynamics with multiple algae and bacteria maxima within one predator cycle (Figs. 5.5, 5.6). As long as the predator biomass is low during a cycle, only the competition for nutrients determines the dynamics of the prey community. The bacteria first deplete the nutrients, but can do so only as long as there is organic carbon available. Once the carbon is depleted, the bacteria cannot increase their biomass further and the algae take up the nitrogen. During their growth, they release exudates which then allow the bacteria to grow again, stopping the increase of the algae. Once the predator biomass finally increases enough to exert a considerable grazing pressure both prey biomasses reduce. This pattern is thus evidence for the temporal commensalism of bacteria by the algae through the carbon supply (Azam et al. 1983). As soon as the bacterial nutrient consumption starts to limit the growth of the algae this commensalism switches to a detrimental interaction for the algae. Accounting also for the effect of the predator, this results in a net-negative interaction between algae and bacteria (Fig. 5.4b). However, the algae cannot go extinct by competition, as they are indispensable for their competitors.

A strategy that we explicitly investigated in this study is the predator's ability to ingest bacteria, i.e. its degree of bacterivory. Here, I found that average biomasses of the predator are largest for intermediate bacterivory (Fig. 5.3). Even though the bacteria reduce the original food source of the predator by competition, their net-effect is still beneficial to the predator (Fig. 5.4), as they also recycle parts of the algal exudates and excretions of the predator. This carbon would be lost without bacteria. An at least partly bacterivorous predator is able to access this recycled carbon and increases the transfer efficiency within this small food web.

All of the above processes and feedbacks are heavily impacted by the physiological parameters that control algal exudation, bacterial carbon use efficiency and predator excretion. Within this study, we investigated the extremes at the edges of the broad parameter ranges reported by earlier publications (bacteria-suppressing and -favouring conditions, Appendix A4). However, it would also be a reasonable assumption that these physiological parameters may not be static, but instead evolve, depending for example on current nutritional constraints. If algae could control the form in which they exudate the carbon, potentially at a certain cost, this would allow them to choose a form that is less accessible to the bacteria if the algae are nutrient-limited and bacterial biomasses are high. Such non-accessible compounds were hypothesized by Ietswaart and Flynn (1995) and could pose as one promising direction of future research by including trait adaptation into algae-bacteria interactions, a field constantly being of interest (Bratbak and Thingstad 1985; Grover 2000; Ramanan et al. 2016).

6.5 Relation of drivers, strategies and traits

Within this thesis I investigated different factors that can affect different effect variables within predator-prey interactions, ranging from individual physiology to environmental impacts (Figs. 1.2 and 1.3). These factors can act as drivers for the application of a number of strategies by either predators or prey (Fig. 6.1, Tab. 6.1).

The application of these strategies however relies on the flexibility in the functional traits that are connected to the strategies (Fig. 6.1). For example, storing resources can only be applied as a strategy if an organism has the physical capacity of doing so. Similarly, only mobile organisms can select a habitat that fulfills their optimal nutrient fluctuation pattern; see chapter B for a summary of a project where we determined the accessible trait ranges from predator-prey time series data (Rosenbaum et al. 2018).

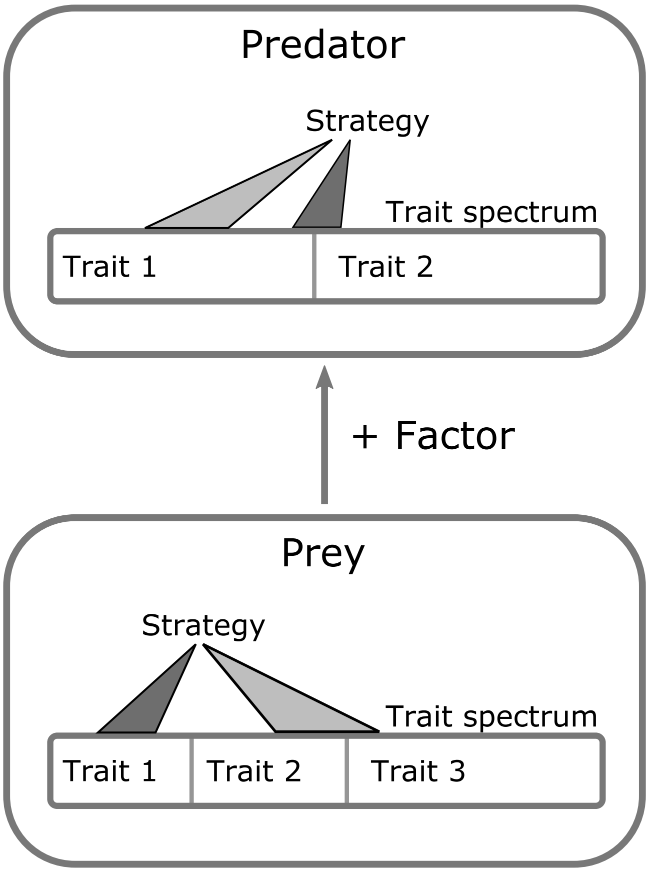

Figure 6.1 Factors that affect the predator-prey interaction allow prey and predator to apply different strategies. These strategies require certain traits and trait ranges to be present in the trait spectrum of prey or predator. A single factor might allow the application of multiple strategies. One strategy might be realized by optimizations of different traits, potentially even a concerted optimization of multiple traits (differently shaded grey triangles). Multiple factors might interact and give rise to strategies not available if only single factors were affecting the predator-prey interaction.

Often, multiple traits may bring about the same strategy. For example, a large variety of defense mechanisms exist in phytoplankton, ranging from thicker cell walls over enlarged body size to colony formation (van Donk et al. 1997; van Donk 1997). While different defense mechanisms may affect the predator at different stages of the predation process (Ehrlich and Gaedke 2018), most of them result in a similar strategy of being the defended prey that competes apparently with a less defended prey type. Therefore, strategies are the translation of traits to processes (i.e. the defense strategy determines how well an algal prey individual with a certain cell wall thickness is ingested by a rotifer). Also, one successful strategy can be the outcome of different trait optimization pathways (Fig. 6.1). Studying strategies thus allows to abstract from specific traits and translate them into ecological processes and patterns, such as temporal niches and predator-mediated coexistence.

Similarly, the set of strategies within predator-prey interactions, that is made available by a set of factors (the drivers), is linked to the concept of ecological niches (Grinnell 1917; Hutchinson 1957;

Leibold 1995; Holt 2009). If a certain strategy allows a species to persist, the application of this strategy corresponds to occupying a certain niche. The larger the number of factors that are considered becomes, the more different strategies are possible. More strategies enable species to occupy more niches, which allows for increased diversity. Thus, accounting for a multitude of drivers may ultimately enable to understand larger than expected diversity, as for example the paradox of the plankton (Hutchinson 1961).

6.6 Implications – From food web modules to ecosystems

I have shown that the different strategies pointed out in this work impact many ecosystem processes. On the species level, they affect the growth rates and average biomasses of prey and predators and therefore shift the bottom-up–top-down balance. On the community level, these strategies affect the coexistence of different species, which, elevated to a larger scale, forms the basis for biodiversity. Biodiversity, in turn, may maintain ecosystem processes (Hooper et al. 2005). Studying the relation between these strategies, their drivers, and the traits that realize them therefore enhances our understanding of important ecosystem functions, with the possibility to enable predictions into the future. Within this study, I investigated rather simple food web modules. However, already these gave rise to elaborate population dynamics and multistable coexistence patterns. Natural food webs are composed of combinations of different modules (mainly tri-trophic food chains, exploitative and apparent competition, and omnivory/intraguild predation) (Milo 2002; Bascompte 2009). They are therefore far more complex, as the sum of different modules (also called network motifs) may be greater than its parts (Kondoh 2008). However, it was reported that food webs and their modules were selected for high persistence and stability, thus decreasing the apparent dynamical complexity (Allesina and Pascual 2008; Kondoh 2008; Borrelli et al. 2015). Therefore, it remains to be tested whether the strategies I investigated occur frequently in nature – and if so have a big effect – or whether they are compensated for by additional food web interactions. Translating from food web modules to complex food webs and ecosystems remains a challenge (Bascompte 2009). However, only the investigation of these smaller sub-systems allows us to eventually scale up our predictions, from the physiology of individual organisms to the functioning of whole ecosystems.

Table 6.1 Conceptual summary: Factors from different categories can act as drivers for strategies with different effects on predator-prey interactions.

Category	Factor/Driver	Strategy	Effect	Chapter
Individual physiology	Storage capacity	Storage of resources	Increased performance at fast fluctuations	2
	Flexible assimilation	Acclimation of assimilation efficiencies	Increased performance at slow fluctuations	2
	Biochemical food quality	Provision of essential resources in a food web	Promotion of predator-mediated coexistence	3
			Modification of apparent competition to prevent extinction	5
	Autotrophy/ Heterotrophy	Recycling of waste products	Increase of transfer efficiency in the food web	5
Defensive mechanisms	Different levels of palatability	Defense against predation	Temporal niche partitioning creates predator-mediated coexistence of defended and undefended prey	3, 4, 5
		Broad foraging spectrum of the predator	Increase of predator biomass	5
	Trait adaptation	Adaptation of offense and defense traits	Maximization of instantaneous growth rates	4
			Reduction of biomass amplitudes	4
			Partial reduction of mean biomasses	4
Environmental factors	Resource fluctuations	Habitat selection	Optimization of perceived resource fluctuation patterns	2
	Perturbations	Trait variability	Provision of trait flexibility that may increase robustness	4

Bibliography

Abrams, P. A. (1999). Is Predator-Mediated Coexistence Possible in Unstable Systems? *Ecology* 80: 608–621.

Acevedo-Trejos, E., Brandt, G., Bruggeman, J., and Merico, A. (2015). Mechanisms shaping size structure and functional diversity of phytoplankton communities in the ocean. *Sci. Rep.* 5: 17–20.

Allesina, S. and Pascual, M. (2008). Network structure, predator–prey modules, and stability in large food webs. *Theor. Ecol.* 1: 55–64.

Azam, F., Fenchel, T., Field, J., et al. (1983). The Ecological Role of Water-Column Microbes in the Sea. *Mar. Ecol. Prog. Ser.* 10: 257–263.

Bascompte, J. (2009). Disentangling the Web of Life. *Science* 325: 416–419.

Borrelli, J. J., Allesina, S., Amarasekare, P., et al. (2015). Selection on stability across ecological scales. *Trends Ecol. Evol.* 30: 417–425.

Bratbak, G. and Thingstad, T. (1985). Phytoplankton-bacteria interactions: an apparant paradox? Analysis of a model system with both competition and commensalism. *Mar. Ecol. Prog. Ser.* 25: 23–30.

van Donk, E., Lürling, M., Hessen, D. O., and Lokhorst, G. M. (1997). Altered cell wall morphology in nutrient-deficient phytoplankton and its impact on grazers. *Limnol. Oceanogr.* 42: 357–364.

van Donk, E. (1997). Defenses in phytoplankton against grazing induced by nutrient limitation, UV-B stress and infochemicals. *Aquat. Ecol.* 31: 53–58.

Ehrlich, E. and Gaedke, U. (2018). Not attackable or not crackable – How pre- and post-attack defenses with different competition costs affect prey coexistence and population dynamics. *Ecol. Evol.* 8: 6625–6637.

Frickel, J., Sieber, M., and Becks, L. (2016). Eco-evolutionary dynamics in a coevolving host-virus system. *Ecol. Lett.* 19: 450–459.

Grinnell, J. (1917). The Niche-Relationships of the California Thrasher. *Auk* 34: 427–433.

Grover, J. P. (2000). Resource competition and community structure in aquatic micro-organisms: experimental studies of algae and bacteria along a gradient of organic carbon to inorganic phosphorus supply. *J. Plankton Res.* 22: 1591–1610.

Guo, F., Kainz, M. J., Sheldon, F., and Bunn, S. E. (2016). The importance of high-quality algal food sources in stream food webs - current status and future perspectives. *Freshw. Biol.* 61: 815–831.

Holt, R. D. (2009). Bringing the Hutchinsonian niche into the 21st century: Ecological and evolutionary perspectives. *Proc. Natl. Acad. Sci.* 106: 19659–19665.

Hooper, D. U., Chapin, F. S., Ewel, J. J., et al. (2005). Effects of biodiversity on ecosystem functioning: A consensus of current knowledge. *Ecol. Monogr.* 75: 3–35.

Hutchinson, G. E. (1961). The Paradox of the Plankton. *Am. Nat.* 95: 137–145.

Hutchinson, G. E. (1957). Concluding Remarks. *Cold Spring Harb. Symp. Quant. Biol.* 22: 415–427.

Ietswaart, T. and Flynn, K. (1995). Modelling interactions between phytoplankton and bacteria under nutrient-regenerating conditions. *J. Plankton Res.* 17: 1395–1395.

Jones, L. E. and Ellner, S. P. (2007). Effects of rapid prey evolution on predator–prey cycles. *J. Math. Biol.* 55: 541–573.

Kearney, M., Simpson, S. J., Raubenheimer, D., and Helmuth, B. (2010). Modelling the ecological niche from functional traits. *Philos. Trans. R. Soc. B Biol. Sci.* 365: 3469–3483.

Kondoh, M. (2008). Building trophic modules into a persistent food web. *Proc. Natl. Acad. Sci.* 105: 16631–16635.

Kopp, M. and Tollrian, R. (2003). Reciprocal phenotypic plasticity in a predator-prey system: Inducible offences against inducible defences? *Ecol. Lett.* 6: 742–748.

Leibold, M. A. (1995). The Niche Concept Revisited: Mechanistic Models and Community Context. *Ecology* 76: 1371–1382.

Martin-Creuzburg, D. and Merkel, P. (2016). Sterols of freshwater microalgae: potential implications for zooplankton nutrition. *J. Plankton Res.* 38: 865–877.

Milo, R. (2002). Network Motifs: Simple Building Blocks of Complex Networks. *Science* 298: 824–827.

Obertegger, U., Cieplinski, A., Raatz, M., and Colangeli, P. (2018). Switching between swimming states in rotifers – case study Keratella cochlearis. *Mar. Freshw. Behav. Physiol.* 51: 159–173.

Ramanan, R., Kim, B.-H., Cho, D.-h., Oh, H.-m., and Kim, H.-s. (2016). Algae–bacteria interactions: Evolution, ecology and emerging applications. *Biotechnol. Adv.* 34: 14–29.

Rosenbaum, B., Raatz, M., Weithoff, G., Fussmann, G. F., and Gaedke, U. (2018). Estimating parameters from multiple time series of population dynamics using Bayesian inference. biorXiv.

Sperfeld, E., Raubenheimer, D., and Wacker, A. (2016). Bridging factorial and gradient concepts of resource co-limitation: Towards a general framework applied to consumers. *Ecol. Lett.* 19: 201–215.

West-Eberhard, M. J. (1989). Phenotypic Plasticity and the Origins of Diversity. *Annu. Rev. Ecol. Syst.* 20: 249–278.

Wilson, A. E., Sarnelle, O., and Tillmanns, A. R. (2006). Effects of cyanobacterial toxicity and morphology on the population growth of freshwater zooplankton: Meta-analyses of laboratory experiments. *Limnol. Oceanogr.* 51: 1915–1924.

Yoshida, T., Jones, L. E., Ellner, S. P., Fussmann, G. F., and Hairston, N. G. (2003). Rapid evolution drives ecological dynamics in a predator-prey system. *Nature* 424: 303–306.

Summary

Predator-prey interactions provide central links in food webs. These interaction are directly or indirectly impacted by a number of factors. These factors range from physiological characteristics of individual organisms, over specifics of their interaction to impacts of the environment. They may generate the potential for the application of different strategies by predators and prey. Within this thesis, I modelled predator-prey interactions and investigated a broad range of different factors driving the application of certain strategies, that affect the individuals or their populations. In doing so, I focused on phytoplankton-zooplankton systems as established model systems of predator-prey interactions.

At the level of predator physiology I proposed, and partly confirmed, adaptations to fluctuating availability of co-limiting nutrients as beneficial strategies. These may allow to store ingested nutrients or to regulate the effort put into nutrient assimilation. We found that these two strategies are beneficial at different fluctuation frequencies of the nutrients, but may positively interact at intermediate frequencies. The corresponding experiments supported our model results. We found that the temporal structure of nutrient fluctuations indeed has strong effects on the juvenile somatic growth rate of *Daphnia*.

Predator colimitation by energy and essential biochemical nutrients gave rise to another physiological strategy. High-quality prey species may render themselves indispensable in a scenario of predator-mediated coexistence by being the only source of essential biochemical nutrients, such as cholesterol. Thereby, the high-quality prey may even compensate for a lacking defense and ensure its persistence in competition with other more defended prey species.

We found a similar effect in a model where algae and bacteria compete for nutrients. Now, being the only source of a compound that is required by the competitor (bacteria) prevented the competitive exclusion of the algae. In this case, the essential compounds were the organic carbon provided by the algae. Here again, being indispensable served as a prey strategy that ensured its coexistence.

The latter scenario also gave rise to the application of the two metabolic strategies of autotrophy and heterotrophy by algae and bacteria, respectively. We found that their coexistence allowed the recycling of resources in a microbial loop that would otherwise be lost. Instead, these resources were

made available to higher trophic levels, increasing the trophic transfer efficiency in food webs.

The predation process comprises the next higher level of factors shaping the predator-prey interaction, besides these factors that originated from the functioning or composition of individuals. Here, I focused on defensive mechanisms and investigated multiple scenarios of static or adaptive combinations of prey defense and predator offense. I confirmed and extended earlier reports on the coexistence-promoting effects of partially lower palatability of the prey community. When bacteria and algae are coexisting, a higher palatability of bacteria may increase the average predator biomass, with the side effect of making the population dynamics more regular. This may facilitate experimental investigations and interpretations. If defense and offense are adaptive, this allows organisms to maximize their growth rate. Besides this fitness-enhancing effect, I found that co-adaptation may provide the predator-prey system with the flexibility to buffer external perturbations.

On top of these rather internal factors, environmental drivers also affect predator-prey interactions. I showed that environmental nutrient fluctuations may create a spatio-temporal resource heterogeneity that selects for different predator strategies. I hypothesized that this might favour either storage or acclimation specialists, depending on the frequency of the environmental fluctuations.

We found that many of these factors promote the coexistence of different strategies and may therefore support and sustain biodiversity. Thus, they might be relevant for the maintenance of crucial ecosystem functions that also affect us humans. Besides this, the richness of factors that impact predator-prey interactions might explain why so many species, especially in the planktonic regime, are able to coexist.

Zusammenfassung

Organismen interagieren miteinander und mit ihrer Umwelt. Innerhalb dieses Netzwerks von Interaktionen sind Fraßbeziehungen zwischen Räubern und ihrer Beute von zentraler Bedeutung. Sie werden auf verschiedenen Ebenen von unterschiedlichen Faktoren beeinflusst, was zur Ausprägung von diversen Strategien von Räuber oder Beute führen kann. Diese Faktoren und die Strategien die sie hervor bringen sind Gegenstand dieser Doktorarbeit.

In mehreren Modellierungsstudien habe ich vielseitige Faktoren untersucht, die sich dem Aufbau einzelner Organismen, Verteidigungs- und Angriffsmechanismen sowie Umwelteinflüssen zuordnen lassen. Dabei konzentrierte ich mich auf ein etabliertes Modellsystem zur Erforschung von Räuber-Beute-Dynamiken und untersuchte die Fraßbeziehung zwischen Phytoplankton als Beute und Zooplankton als Räuber.

Ich fand heraus, dass die Bereitstellung von essentiellen Ressourcen für Konkurrenten oder Räuber eine Strategie sein kann, mit der Beutearten sich vor dem Aussterben schützen können. Auch die direkte Verteidigung gegen den Räuber ist eine häufige Strategie zur Verringerung des Fraßdrucks und kann ebenfalls Koexistenz fördern. Für anpassungsfähige Verteidigung der Beute und Angriffsstärke des Räubers konnte ich zeigen, dass dies sowohl die Fitness erhöhen, als auch die Robustheit der Räuber-Beute-Dynamiken gegen äußere Störungen erhöhen kann. Weiterhin fand ich heraus, dass physiologische Anpassungsmechanismen wie Speicherung oder anpassungsfähige Aufnahme von Nährstoffen die Wachstumsrate des Räubers verbessern können, wenn die Qualität der verfügbaren Beute in der Umwelt des Räubers fluktuiert.

Viele der Strategien, die ich in dieser Arbeit herausgestellt habe, können die Koexistenz von verschiedenen Arten fördern und damit zu erhöhter Biodiversität beitragen, welche wiederum entscheidend ist für die Stabilität von Ökosystemen und deren Nutzbarkeit.

A Supplementaries

A1 Chapter 2 - Appendix

Assimilation trade-off

Organisms face the challenge of reconciling external resource availability and internal nutritional needs. This can be achieved by storing or egesting excess resources. An energetically more efficient route would be to prevent unnecessary ingestion in the first place and thus be able to spend that energy on the assimilation of resources in short supply. Here, we will present how we modelled the adaptive assimilation of resources that is driven by the internal resource requirements.

The internal requirements are set as the ratio of resource concentrations in the structural volume of the organism. The deviation between these requirements and the balance of resources in the reserves determines how much energy should be allocated to favour the assimilation of the more limiting resource over the other. The resource balance is given by $x = \frac{y_1}{y_2}\frac{E_1}{E_2}$, where E_i are the reserve densities and y_i are the resource yields, i.e. the inverse resource concentrations. The resources are thus balanced for $x = 1$ and unbalanced otherwise.

Using an assimilation effort function ϕ this balance symmetrically translates into an estimate of whether energy investment should go into the assimilation of resource 1 (for $\phi \to 1$) or resource 2 (for $\phi \to 0$). The sensitivity for small imbalances γ, i.e. around $x = 1$, determines how drastic changes to the assimilation apparatus should be even for minor deviations (Fig. A1.1).

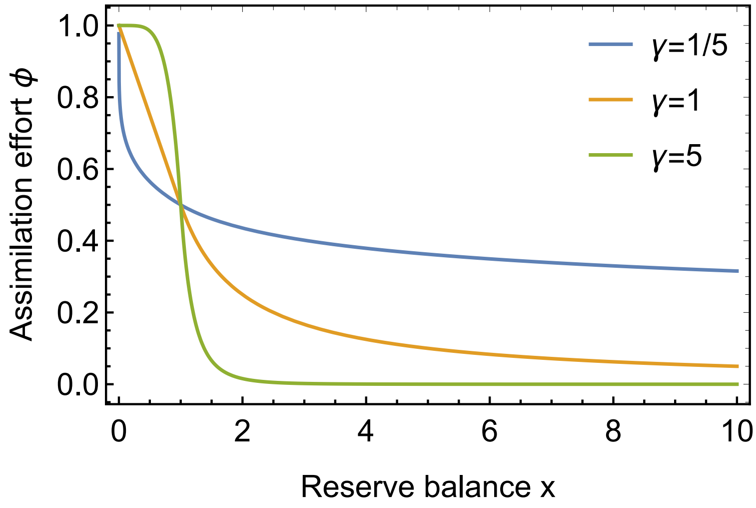

Figure A1.1 Assimilation effort. If reserves are highly unbalanced ($x < 1$ or $x > 1$) more assimilation effort is allocated to either one nutrient. If reserves are balanced ($x = 1$) both nutrients are assimilated equally. The sensitivity parameter γ gives the slope at $x = 1$. Throughout this study we assumed high sensitivity with $\gamma = 5$.

We assume that a trade-off exists between the assimilation efficiencies of the two resources, which can generally be linear, concave or convex. This trade-off arises if energy or enzymes allocated to assimilate one resource lack to assimilate the other. The exact shape of the trade-off is determined by (i) whether the two resources are assimilated independently of each other and (ii) how the individual assimilation efficiencies depend on the allocated energy or enzymes. For independent resource assimilation, a linear trade-off is expected if the assimilation efficiencies increase linearly with allocation, while a concave (convex) trade-off arises if the assimilation efficiencies are concave (convex) functions of allocation. This concave relationship could result for example from a saturation of assimilation efficiencies for higher investments, i.e. the denser membrane proteins are packed, the more they inhibit each other and operate less efficiently. A convex trade-off could be caused by cooperative enzymes, which disproportionately increase their activity at higher densities. The shape of the trade-off curve in the model is set by the shape parameter α (Fig. A1.2). If now the reserves become imbalanced the organism can change its target assimilation effort along this trade-off curve. The target assimilation effort is given by

$$\phi_T(x) = \begin{cases} -\frac{1}{2}x^{\gamma} + 1, & x \leq 1 \\ \frac{1}{2}x^{-\gamma}, & x > 1 \end{cases}$$

for reserve balance x. The assimilation effort then tracks the effort target in time.

$$\frac{\mathrm{d}\phi}{\mathrm{d}t} = \frac{1}{\tau}\left(\phi_T(x) - \phi\right)$$

τ is the characteristic switching time of the assimilation apparatus and thus scales the speed at which the organism is able to acclimate.

Sensitivity analysis

In this section, we will study the model behavior for the three most important parameters in the covariance treatments. These parameters for which our model shows the highest sensitivity are the characteristic switching time of assimilation τ (Fig. A1.3), the reserve conductance u (Fig. A1.4), and the shape parameter of the assimilation trade-off α (Fig. A1.5). Overall, we see that the observed patterns are robust against changes in these parameters.

The switching time τ sets the speed at which the assimilation effort can be changed. This acclimation is driven by the balance of reserves. τ does therefore only affect growth rates in variable resource conditions where the two resources do not co-vary positively (Fig. A1.3). Smaller τ allows for very fast changes of the assimilation effort allocation, which results in a sustained reserve balance. This

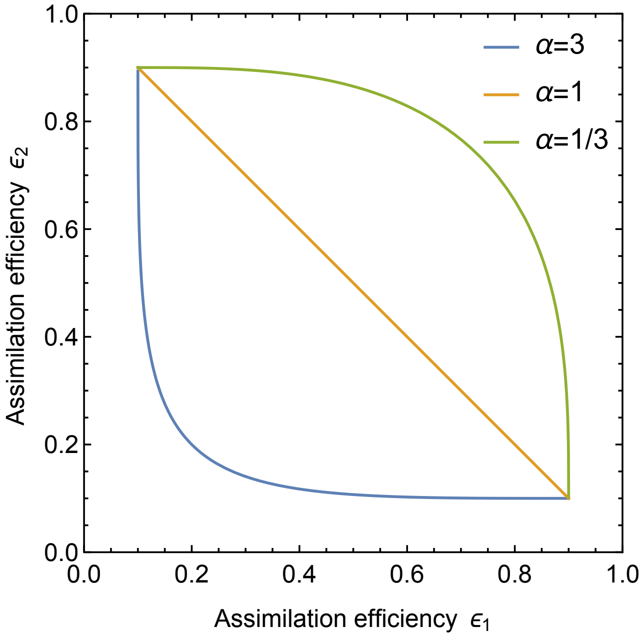

Figure A1.2 Shape of the assimilation trade-off curve. The trade-off curve determines the possible combinations of assimilation efficiencies. For $\alpha < 1$ the assimilation trade-off is concave, at $\alpha = 1$ linear and convex for $\alpha > 1$. Throughout this study, we focused on cooperative enzymatic assimilation pathways and thus used a shape parameter of $\alpha = 3$.

increases growth for slow and intermediate fluctuation frequencies as no resource becomes "too" limiting. The overshoot of simulated growth rates above the predictions for constant, average resources, which occurs where benefits from acclimation and storage blend, accordingly only emerges for intermediate and fast accilimation, i.e. small and intermediate τ. For smaller τ this peak is shifted towards higher frequencies as acclimation is fast enough to react also to these fluctuations. The general patterns of increasing growth with increasing fluctuation frequency, an inversion of the effect of covariance and growth rates above the predictions from constant conditions are present for a broad range of τ.

The reserve conductance u affects two processes, which may affect growth rates in opposite directions in fluctuating environments. First, it controls the outflow of resources out of the reserves towards the SU. A lower conductance thus decreases the overall resource flow to the SU and therefore also the growth rate under constant conditions, both for positive and negative covariance (Fig. A1.3). Second, if resources are fluctuating, the reserves allow for storage of resources obtained during high resource phases, which then can be used during phases of low resources. Smaller conductances therefore increase the storage capacity but also limit the supply rate to the SU. Accordingly, we observe higher growth rates for intermediate conductances, which balance these two opposing effects, for most fluctuation frequencies (Fig. A1.4). Only for very fast fluctuations, where also smaller storage capacity allows efficient buffering, larger conductances yield the highest growth rates. Under positive covari-

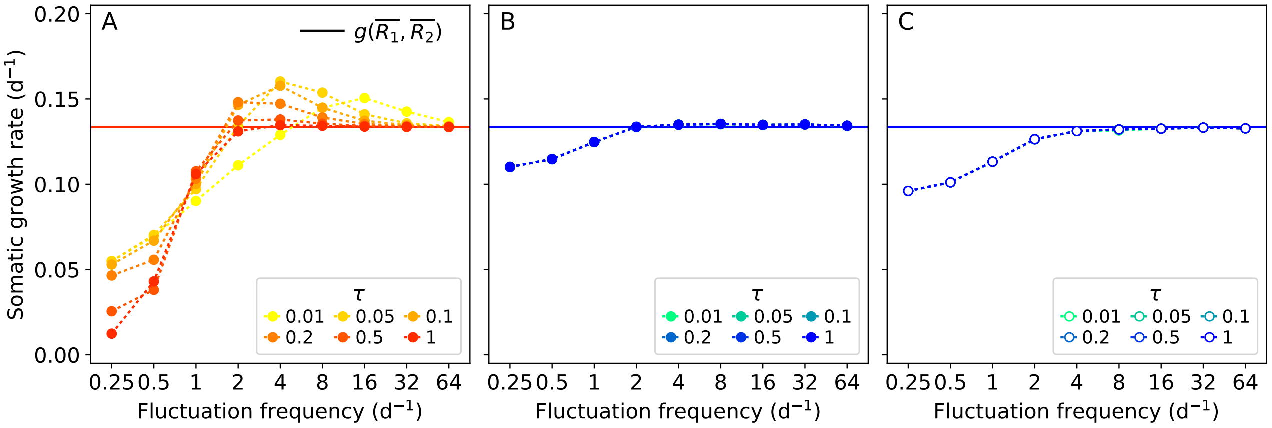

Figure A1.3 Full model sensitivity to the characteristic switching time τ. (A) Negative covariance. (B) Positive covariance and starting with high resources. (C) Positive covariance and starting with low resources.

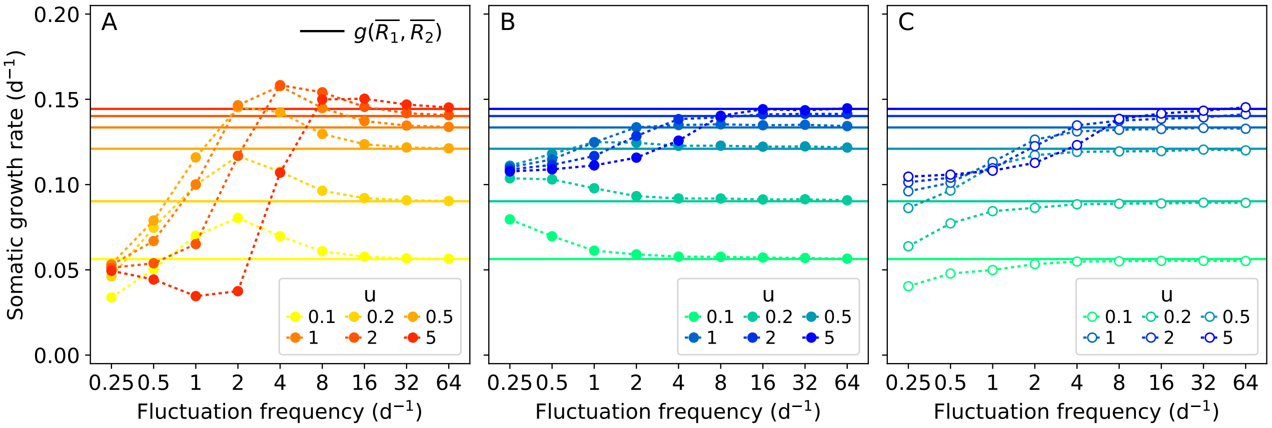

Figure A1.4 Full model sensitivity to the reserve conductance u. (A) Negative covariance. (B) Positive covariance and starting with high resources. (C) Positive covariance and starting with low resources.

ance the effect of fluctuation phase becomes stronger for smaller u. Here, the growth rates at small conductances, i.e. large storage capacity, overshoot the predictions from constant conditions for low fluctuation frequencies if high concentrations are initially provided as these resources can be efficiently stored and used later. Again, the observed patterns are robust for broad parameter ranges in u. For faster positively co-varying fluctuations the phase effect vanishes and growth rates trend towards the constant condition predictions. For negative covariance, growth rates exceed these predictions at intermediate frequencies.

The trade-off shape α defines the non-linearity of the assimilation trade-off. For $\alpha < 1$ the second derivative of the trade-off curve is negative, zero for $\alpha = 1$ and positive for $\alpha > 1$. In Fig. A1.5 we see that this non-linearity controls the inversion of the covariance effect, including the overshoot above constant condition predictions. For $\alpha < 1$ the trade-off curve is concave and the trade-off is weak. This results in on average higher assimilation efficiencies and increases growth, both under

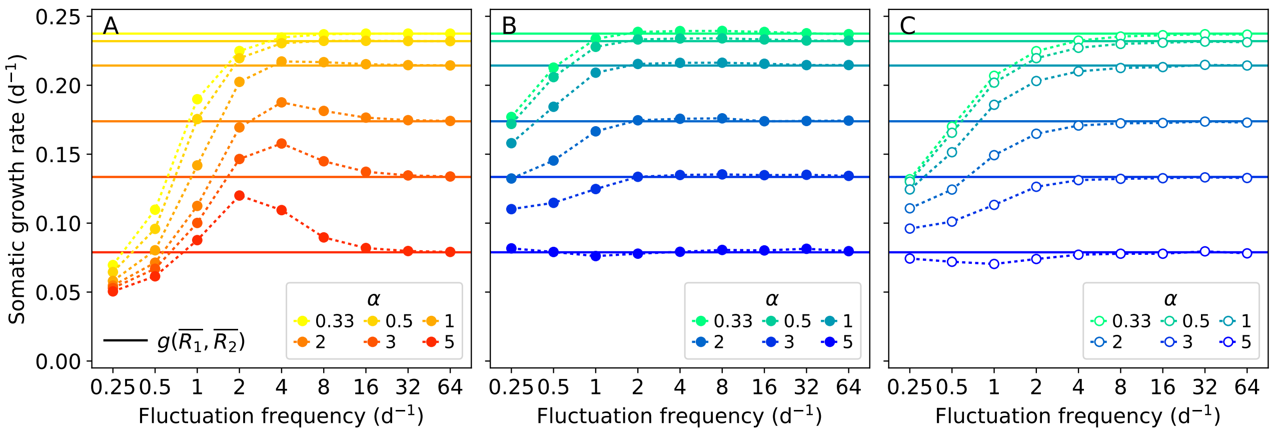

Figure A1.5 Full model sensitivity to the trade-off shape α. (A) Negative covariance. (B) Positive covariance and starting with high resources. (C) Positive covariance and starting with low resources.

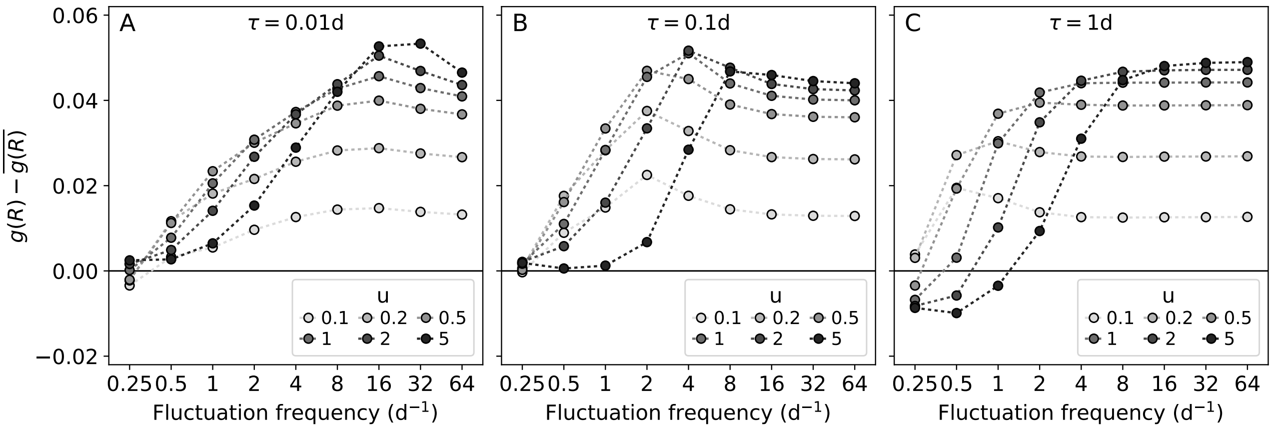

Figure A1.6 Transient underperformance in the full model: Sensitivity to reserve conductance u and characteristic switching time τ. Single resource fluctuation starting with low resources. Underperformance is defined as the situation where modelled growth rate under fluctuating conditions, $g(R)$, is lower than the growth predicted by non-linear averaging, $\overline{g(R)}$.

constant and variable conditions. Growth rates for positive and negative covariance converge for fast fluctuation frequencies. If α is large, the trade-off curve is convex and the trade-off is strong. This increases the effect of assimilation acclimation towards specializing on one resource. On average, the assimilation efficiencies are smaller here, thus, growth rates are also generally lower. The specialization on the assimilation of one resource increases the total resource assimilation if the resources are provided sequentially. Thus, we observe here the inversion of the covariance effect and growth rates become higher for negative than for positive covariance at fast fluctuation frequencies.

For certain combinations of τ and u we observe a modelled growth rate below the predictions from non-linear averaging (Fig. A1.6), especially for large τ, i.e. slow acclimation of the assimilation efficiencies, and large u, i.e. small storage capacity. Here, a mixture of mal-adaptation and lacking compensation by storage causes an underperformance of the organism relative to the predictions from non-linear averaging under fluctuating resource supply.

A2 Chapter 3 - Appendix

Derivation of the conversion efficiency

Within the following we will present the derivation of the conversion efficiency for the food quality scenario where the defended prey B has low food quality (defended low quality scenario), see also Fig. A2.1 in Supporting Information. For the opposite case, the same arguments hold and only the prey species A and B need to be interchanged, as this derivation makes no assumptions on growth or defence of the respective prey species. Also, we assume the essential biochemical nutrients to be sterols, though the derivation equally holds for similar substances. For a compilation of symbols used in the following derivation we refer to Table A2.1.

The conversion efficiency determines how much nitrogen is invested into production at a certain time point if a certain amount of nitrogen is consumed. Predator production in our model is co-limited by the amount of sterols in the diet and the amount of biomass that is consumed. Since we assume homoeostasis in all organisms, we use nitrogen as a measurable surrogate for biomass. The amount of available prey nitrogen then shapes the functional response curve (Holling type II) which gives the amount of ingestion at a given point in time. Only part of the ingested nitrogen n^I is assimilated, the rest of the ingested nitrogen will be excreted. The amount of excretion is determined by the excretion constant e. At what efficiency the assimilated nitrogen can be transferred into new predator biomass depends on the amount of sterols σ^I that were ingested together with the nitrogen from each prey species, since new biomass can only be created at the sterol-to-nitrogen ratio S_Z of the predator. Here we assume that sterols are not excreted but completely assimilated as this should usually be the case. Also, neither nitrogen nor sterols are used up within respiration. The overall conversion efficiency ε measured in nitrogen (as a surrogate for biomass) will thus not only depend on excretion, but also on the available amount of sterols in the diet.

Our model assumes, that the two prey species differ in their sterol content, whereas prey A contains more sterols per nitrogen than what would be needed to produce predator biomass and the other contains less. Therefore there will be surplus sterols left over from the high-quality prey A that can be used together with surplus nitrogen that was left over from the low-quality prey B. Altogether, this means that the lacking sterols in B reduce the conversion efficiency of Z from B, but can be complemented by sterols delivered by A.

We will now derive the conversion efficiency of Z from feeding on B by considering nitrogen and sterol balances for all processes described above. We will start with the sterol and nitrogen balances for independent reproduction on either of the two food sources. If an amount of nitrogen n_A^I is ingested by consuming prey species A, then $(1-e)\,n_A^I$ nitrogen is assimilated and therefore available for either reproduction (n_A^P) or to be left-over as surplus (n_A^S). The remaining nitrogen $e\,n_A^I$ will be recycled and added to the surrounding medium. The same should hold for sterols from A except they are not excreted and thus not recycled. Therefore we can formulate the basic mass balances for nitrogen and sterols from the two prey species A and B.

$$n_A^I - n_A^{Recycling} = (1-e)\,n_A^I = n_A^P + n_A^S \tag{A2.1}$$

$$\sigma_A^I = \sigma_A^P + \sigma_A^S \tag{A2.2}$$

$$n_B^I - n_B^{Recycling} = (1-e)\,n_B^I = n_B^P + n_B^S \tag{A2.3}$$

$$\sigma_B^I = \sigma_B^P + \sigma_B^S \tag{A2.4}$$

With S, the amount of sterols per nitrogen unit in an organism, we can connect sterols and nitrogen used in reproduction ($\sigma_A^P = n_A^p\,S_A$, $\sigma_B^P = n_B^p\,S_B$). Thus, the sterol balances become

$$n_A^I\,S_A = n_A^P\,S_Z + \sigma_A^S \tag{A2.5}$$

$$n_B^I\,S_B = n_B^P\,S_Z + \sigma_B^S \tag{A2.6}$$

Now we can derive conditions for the sterol to nitrogen ratios of the three species so that there is no surplus nitrogen coming from A and no surplus sterols coming from B. What this means is that all nitrogen from A is used up with the sterols from A and all sterols from B are used up with the nitrogen from B. If we call for $n_A^S = 0$ we see in equation A2.5 that σ_A^S vanishes exactly at $S_A = (1-e)\;S_Z$. Therefore σ_A^S becomes larger than zero if $S_A > (1-e)\;S_Z$ resulting in surplus sterols which were not used in reproduction from A. Following the same rationale we see that for $(1-e)\;S_Z > S_B$ there will be no surplus sterols from B but left-over nitrogen that was not used up in reproduction from B. If we put these two conditions together we arrive at an expression for the sterol-to-nitrogen ratios of the three organisms that fulfils our requirements and allows for surplus nitrogen from B to be used with surplus sterols from A:

$$S_A > (1-e)\;S_Z > S_B \tag{A2.7}$$

which also represents our claim of one high-quality prey and one low-quality prey species. This ensures $n_A^S = 0$ and $\sigma_B^S = 0$ and turns equations A2.5 and A2.6 to

$$n_A^I\,S_A = (1-e)\,n_A^I\,S_Z + \sigma_A^S \tag{A2.8}$$

$$n_B^I\,S_B = n_B^P\,S_Z \tag{A2.9}$$

Now we can connect the surplus sterols σ_A^S from A with the surplus nitrogen n_B^S from B and define the amount of sterols (σ_A^{SP}) and nitrogen (n_B^{SP}) that will additionally lead to growth and reproduction due to supplementation. Since still not all sterols or nitrogen might be used up in reproduction, we will allow for nitrogen to be recycled and sterols to go to waste, as sterols are usually not recycled.

$$\sigma_A^S = \sigma_A^{SP} + \sigma_A^{Waste} \tag{A2.10}$$

$$n_B^S = n_B^{SP} + n_B^{S,\ Recycling} \tag{A2.11}$$

The conversion efficiency now can be defined as the ratio of nitrogen from B used for reproduction and the amount of ingested nitrogen from B:

$$\varepsilon_B = \frac{n_B^P + n_B^{SP}}{n_B^I} \tag{A2.12}$$

From here on there are two possible outcomes, either there are too many sterols left over which cannot be used up with the surplus nitrogen, or there is too much nitrogen left over which cannot be used up with the surplus sterols. Which option is chosen depends on whether the ratio of surplus sterols over surplus nitrogen is larger or smaller than the body content ratio of sterols to nitrogen in the predator S_Z.

In option one no nitrogen is recycled and some sterols will go to waste. In the second case no sterols will go to waste but some nitrogen is recycled. Since we are computing the conversion efficiency in nitrogen units the first scenario with zero recycling leads to maximum efficiency, whereas the latter will result in a reduced conversion efficiency in nitrogen units as sterols are lacking.

Case I - $\sigma_A^S / n_B^S > S_Z$

In this case, there are enough sterols available and no additional nitrogen has to be recycled, which means $\sigma_A^{Waste} > 0$ and $n_B^{S,\ Recycling} = 0$ in equations A2.10 and A2.11. Therefore $n_B^S = n_B^{SP}$ and equation A2.3 becomes

$$(1-e)\, n_B^I - n_B^P = n_B^{SP}$$

and we arrive at a conversion efficiency of

$$\begin{aligned} \varepsilon_{B1} &= \frac{n_B^P + (1-e)\, n_B^I - n_B^P}{n_B^I} \\ &= 1 - e \end{aligned} \tag{A2.13}$$

which is exactly the maximum possible efficiency if only excretion reduces the amount of nitrogen used for reproduction.

Case II - $\sigma_A^S / n_B^S < S_Z$

In the second scenario, sterols are limiting the amount of nitrogen to be used for reproduction, which translates to $\sigma_A^{Waste} = 0$ and $n_B^{S,\ Recycling} > 0$ in equations A2.10 and A2.11. Thus we have $\sigma_A^S = \sigma_A^{SP}$ which we can rewrite with equation A2.8 to

$$\begin{aligned} \sigma_A^S &= n_B^{SP}\, S_Z \\ &= n_A^I (S_A - (1-e)\, S_Z) \end{aligned}$$

With equation A2.9 the conversion efficiency for the case of limiting sterols becomes

$$\begin{aligned} \varepsilon_{B2} &= \frac{n_B^P + n_B^{SP}}{n_B^I} \\ &= \frac{S_B}{S_Z} + \frac{n_A^I}{n_B^I} \left(\frac{S_A - (1-e)\, S_Z}{S_Z} \right) \end{aligned} \tag{A2.14}$$

Connecting the two cases

The condition for the second case can be rewritten to obtain an upper limit of the conversion efficiency that equals the conversion efficiency of the first case.

$$\begin{aligned} \sigma_A^S &< n_B^S\, S_Z \\ n_A^I (S_A - (1-e)\, S_Z) &< S_Z \left((1-e)\, n_B^I - n_B^P \right) \\ n_A^I (S_A - (1-e)\, S_Z) &< S_Z ((1-e)\, n_B^I - n_B^I \frac{S_B}{S_Z}) \\ n_A^I (S_A - (1-e)\, S_Z) &< n_B^I ((1-e)\, S_Z - S_B) \end{aligned}$$

$$\frac{n_A^I}{n_B^I} < \frac{(1-e)\, S_Z - S_B}{S_A - (1-e)\, S_Z} \tag{A2.15}$$

Equation A2.15 can now be inserted into equation A2.14 to obtain the upper limit of ε_{B2} since the term within the brackets is always positive after condition A2.7.

$$\varepsilon_{B2} < \frac{S_B}{S_Z} + \frac{(1-e)\, S_Z - S_B}{S_A - (1-e)\, S_Z} \left(\frac{S_A - (1-e)\, S_Z}{S_Z} \right) = 1 - e$$

Therefore whenever the condition of the second case holds, the conversion efficiency will stay below that of the first case and we can use the minimum function to bring the two formulations of the conversion efficiency together.

$$\begin{aligned} \varepsilon_B &= \min(\varepsilon_{B1}, \varepsilon_{B2}) \\ &= \min \left(1 - e\ ,\ \frac{S_B}{S_Z} + \frac{n_A^I}{n_B^I} \left(\frac{S_A - (1-e)\, S_Z}{S_Z} \right) \right) \end{aligned} \tag{A2.16}$$

to obtain an expression of the conversion efficiency in units of nitrogen which holds for all n_A^I and n_B^I if the species' sterol to nitrogen ratios fulfil condition A2.7.

As we have seen, the conversion efficiency from feeding on A under condition A2.7 is

$$\varepsilon_A = 1 - e \tag{A2.17}$$

and the amount of recycled nitrogen from A and B becomes

$$n_A^{Recycling} = (1 - \varepsilon_A)\, n_A^I \tag{A2.18}$$

$$n_B^{Recycling} = (1 - \varepsilon_B)\, n_B^I \tag{A2.19}$$

where $n_A^{Recycling}$ is only determined by excretion but $n_B^{Recycling}$ is given by excretion together with unused nitrogen due to sterol limitation.

If we now define a certain time unit τ over which a nitrogen amount of n^I was consumed by one predator unit Z we can relate the ingested nitrogen to the functional responses f which gives the rate of nitrogen ingestion at a given time point by writing

$$f = \frac{n^I}{\tau}$$

and the conversion efficiency can be expressed in terms of the functional responses f_A and f_B given in the ordinary differential equations 3.2-3.4 (Fig. A2.2).

$$\varepsilon_B = \min\left(1 - e\,,\ \frac{S_B}{S_Z} + \frac{f_A}{f_B}\left(\frac{S_A - (1-e)\, S_Z}{S_Z}\right)\right) \tag{A2.20}$$

and the total recycling term R becomes the sum already given in equation 3.7.

$$R = (1 - \varepsilon_A)\, f_A\, Z + (1 - \varepsilon_B)\, f_B\, Z$$

Table A2.1 List of symbols used for the derivation of the conversion efficiency.

Parameter	Description	Unit
ε_A	conversion efficiency of Z on A with respect to *N*	1
ε_B	conversion efficiency of Z on B with respect to *N*	1
f_A	Functional response of Z on A	µmol N/s
f_B	Functional response of Z on B	µmol N/s
S_A	Sterol to *N* ratio of prey A	nmol Sterol/µmol N
S_B	Sterol to *N* ratio of prey B	nmol Sterol/µmol N
S_Z	Sterol to *N* ratio of predator Z	nmol Sterol/µmol N
e	Excretion factor	1
τ	Arbitrary time relating functional responses to consumed *N*	day
n_A^I	Ingested amount of *N* from A at a given time per unit predator	µmol N
$n_A^{Recycling}$	Ingested *N* from A not assimilated but immediately recycled	µmol N
n_A^P	*N* from A directly used up for reproduction with sterols from A	µmol N
n_A^S	Surplus *N* from A not used up for reproduction with sterols from A	µmol N
σ_A^I	Ingested amount of sterols from A at a given time per unit predator	nmol Sterols
σ_A^P	Sterols from A that are directly used up for reproduction with *N* from A	nmol Sterols
σ_A^S	Surplus sterols from A not used up for reproduction with *N* from A	nmol Sterols
n_B^I	Ingested amount of *N* from B at a given time per unit predator	µmol N
$n_B^{Recycling}$	Ingested *N* from B that is not assimilated but immediately recycled	µmol N
n_B^P	*N* from B that is directly used up for reproduction with sterols from B	µmol N
n_B^S	Surplus *N* from B not used up for reproduction with sterols from B	µmol N
σ_B^I	Ingested amount of sterols from B at a given time per unit predator	nmol Sterols
σ_B^P	Sterols from B directly used up for reproduction with *N* from B	nmol Sterols
σ_B^S	Surplus sterols from B not used up for reproduction with *N* from B	nmol Sterols
σ_A^{SP}	Surplus sterols from A enabling reproduction with surplus *N* from B	nmol Sterols
n_B^{SP}	Surplus *N* from B enabling reproduction with surplus sterols from A	µmol N
σ_A^{Waste}	Surplus sterols from A for which no surplus *N* from B is left	nmol Sterols
$n_B^{S,Recycling}$	Surplus *N* from B for which no surplus sterols from A are left	µmol N

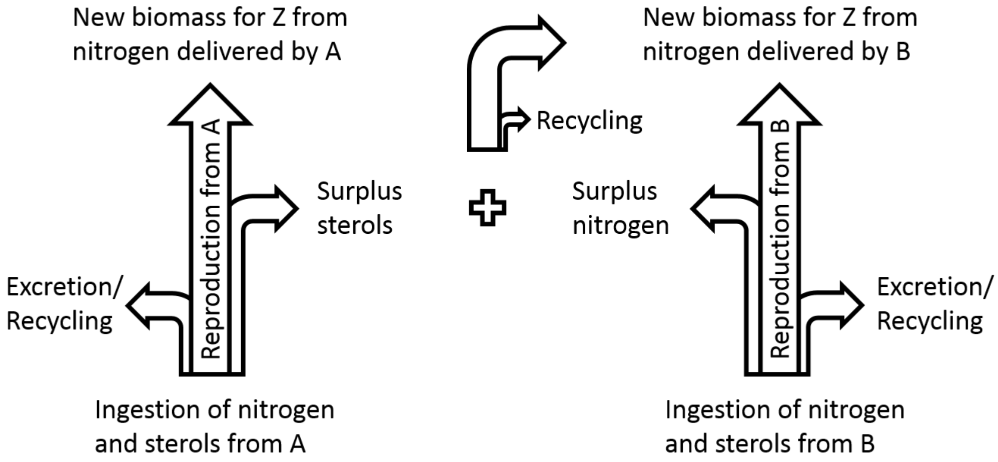

Figure A2.1 Illustration of the flow of mass from the producers A and B to the consumer Z and the concept of surplus nitrogen and surplus EBN (here sterols) to increase the nitrogen flow from B to Z. The ratio of A to B determines the relative amounts of surpluses. How those are processed determines the conversion efficiency of feeding on B. Here, it is assumed that the defended prey B has low food quality (defended low quality scenario). For the opposite case A and B can be interchanged deliberately within this derivation.

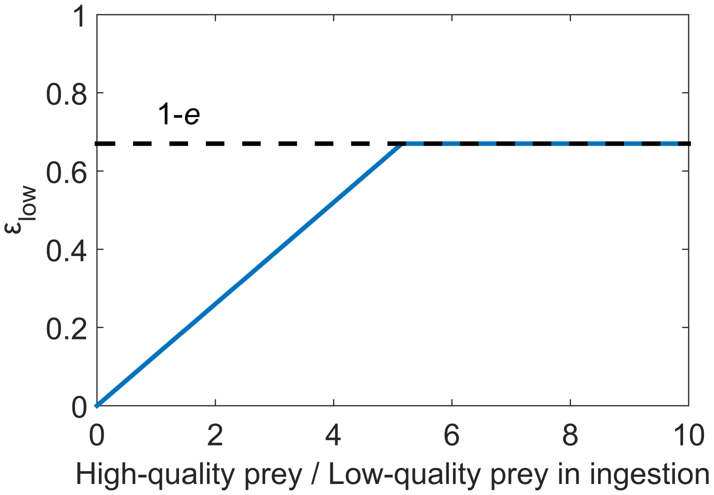

Figure A2.2 The conversion efficiency of the predator for the low-quality prey depends on the functional responses for low-quality and high-quality prey as given in equation 3.8. Parameters that determine the shape of the conversion efficiency are chosen as $\frac{S_{\text{low}}}{S_{\text{Z}}} = 0$, $\frac{S_{\text{high}}}{S_{\text{Z}}} = 0.8$ and $e = 0.33$
.

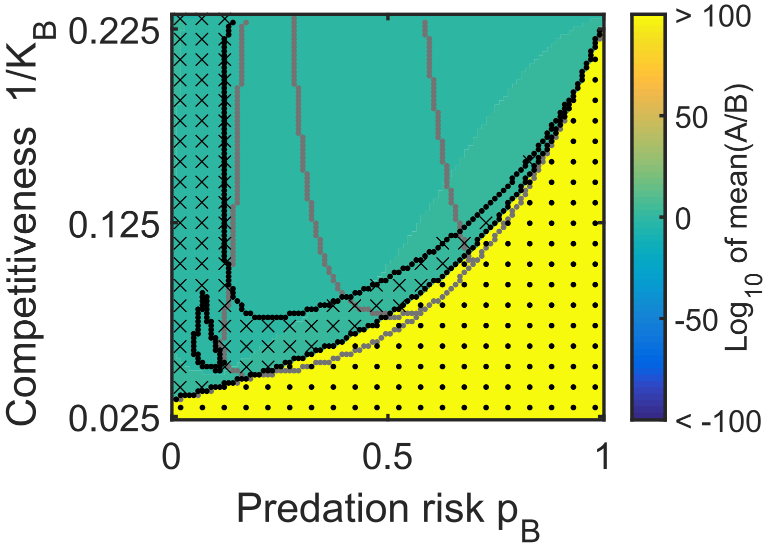

Figure A2.3 Coexistence without recycling at high food quality of undefended prey. Plot specifics are the same as in Fig. 3.2.

(a) Equal food quality scenario

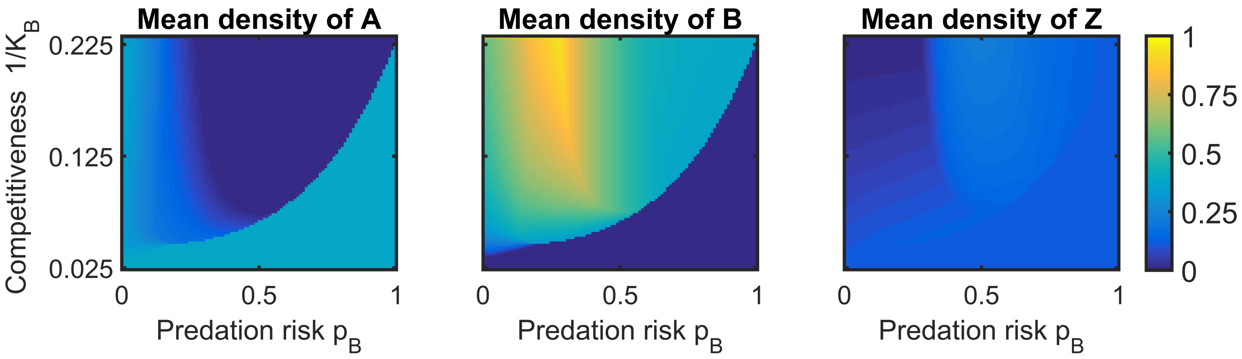

(b) Undefended low quality scenario

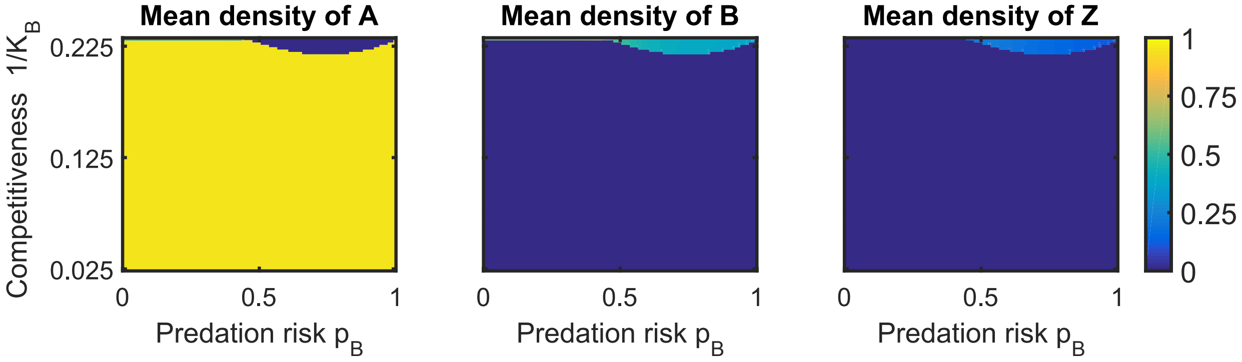

(c) Defended low quality scenario

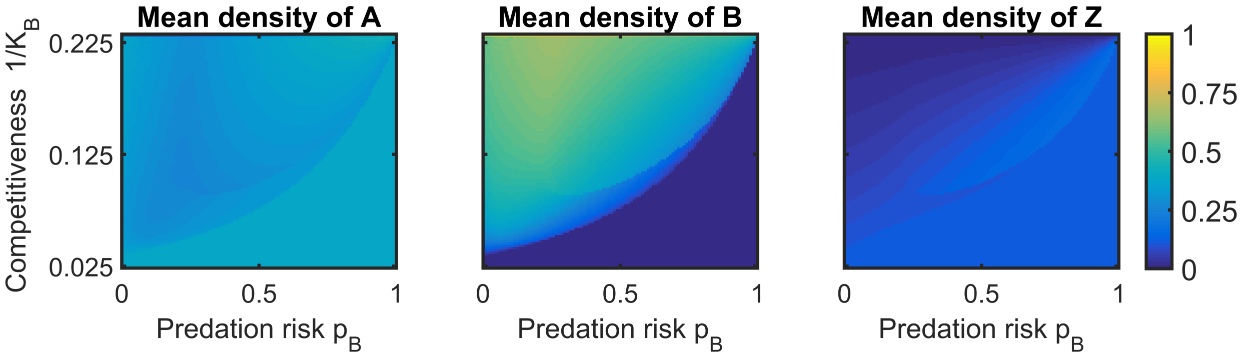

(d) Defended low quality scenario with recycling term R set to zero

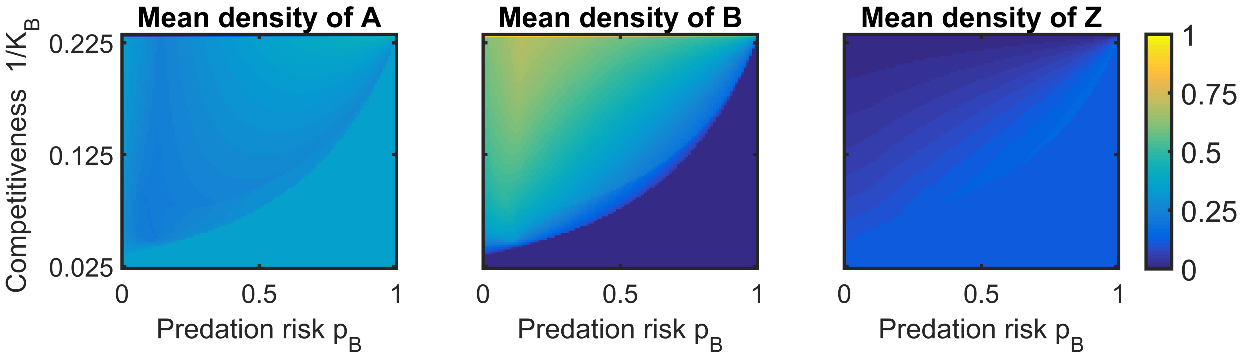

Figure A2.4 Biomasses of the undefended prey A (left), the defended prey B (middle) and the predator Z (right) relative to the inflow concentration, averaged over the last 10 000 days of the simulations.

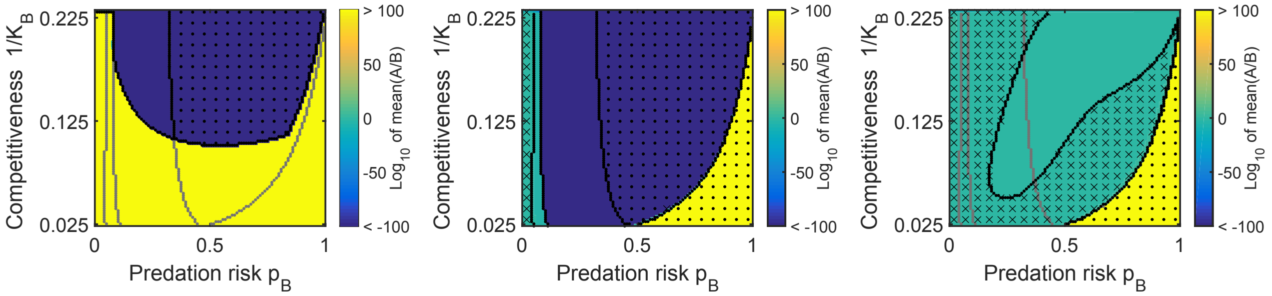

(a) Undefended low quality (b) Equal food quality (c) Defended low quality

Figure A2.5 Competition outcome at lower dilution rate $\delta = 0.2\ \mathrm{d}^{-1}$. Plot specifics are the same as in Fig. 3.2. A dilution rate of $\delta = 0.3\ \mathrm{d}^{-1}$produces intermediate results compared to Fig. 3.2.

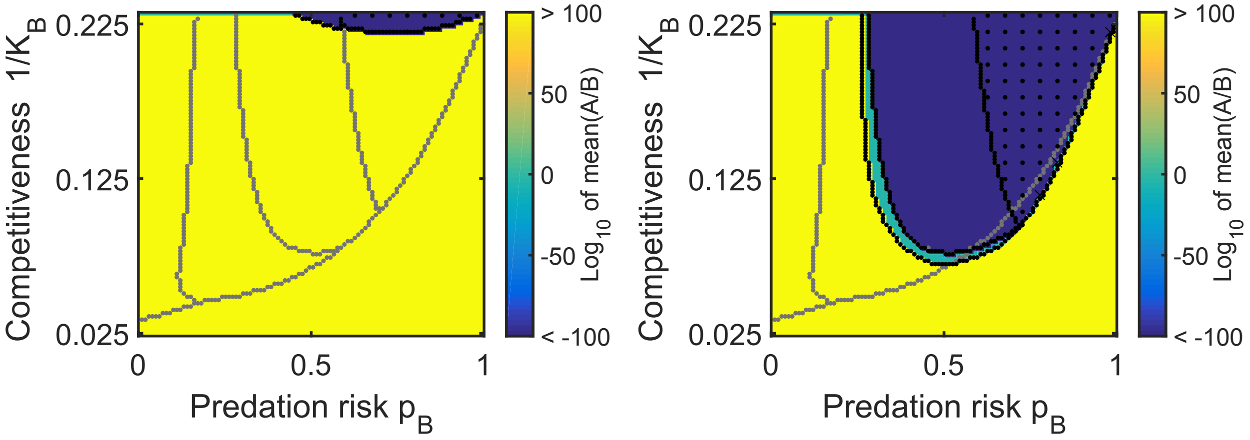

(a) $A_0 = 3/8\,N_{\mathrm{I}}$ (b) $A_0 = 1/80\,N_{\mathrm{I}}$

Figure A2.6 Bistability in the system where the undefended prey A has the low food quality, shown by using different initial conditions for the undefended prey A and the same plot as in Fig. 3.2.

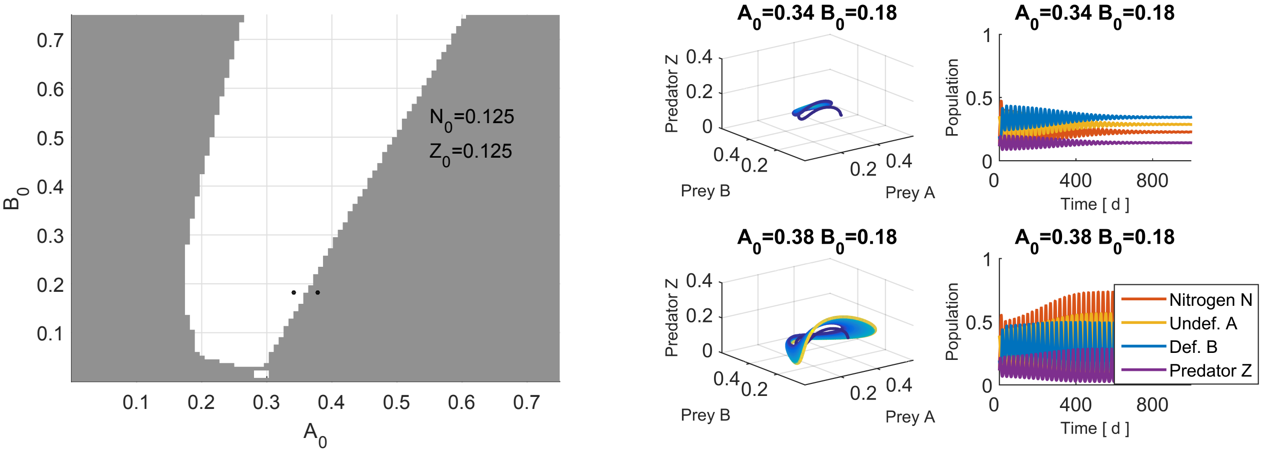

(a) Bistability check

(b) Population dynamics at the bistability boundary

Figure A2.7 Bistability in the dynamics of the system with an undefended high-quality prey was found by varying the initial conditions for a given parameter set. Densities are given relative to inflow concentration N_I. (a) Bistability at $1/K_B = 0.1042(\mathrm{\mu mol\ N/l})^{-1}$ and $p_\mathrm{B} = 0.5$. In the grey regions the population is cycling, the white region depicts steady state. (b) Visualization of the two basins of attraction and the corresponding population dynamics at the boundary between steady state dynamics and cycling. The colouring in the phase-space plots moves from blue to yellow in time. Mean biomasses differ between both states, e.g. $\overline{Z_{ss}} = 0.14\,N_\mathrm{I} > \overline{Z_{cycl}} = 0.11\,N_\mathrm{I}$.

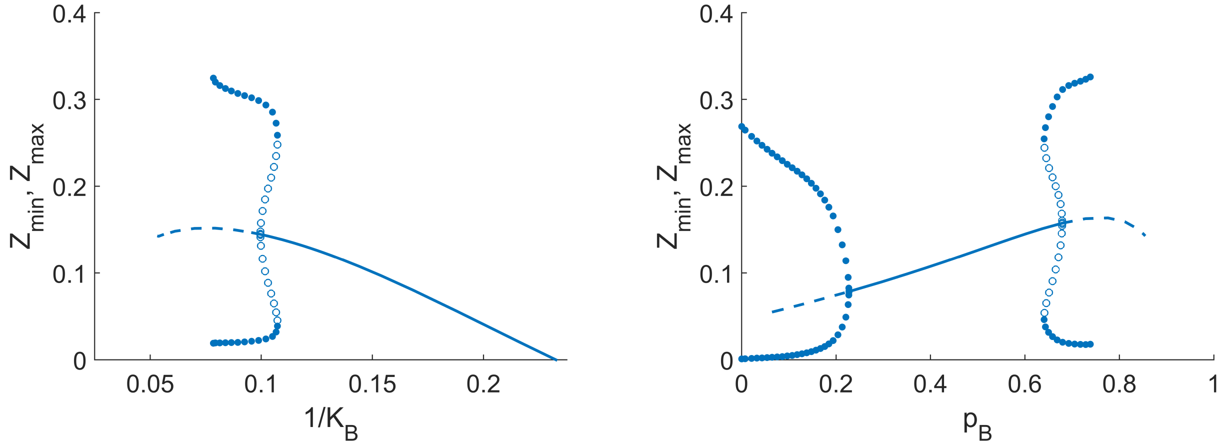

(a) Fixed predation risk $p_\mathrm{B} = 0.5$, variation along the competitiveness $1/K_B$

(b) Fixed competitiveness $1/K_B = 0.125\,(\mu\mathrm{mol\,N/l})^{-1}$, variation along the predation risk p_B

Figure A2.8 Bifurcation plots of the transitions between steady state coexistence and cycling coexistence with an undefended high-quality prey along (a) the competitiveness $1/K_B$ and (b) the predation risk p_B. (a) Above $1/K_B = 0.1\,(\mu\mathrm{mol\,N/l})^{-}1$ the steady state is stable. Between $1/K_B = 0.1\,(\mu\mathrm{mol\,N/l})^{-}1$ and $1/K_B = 0.11\,(\mu\mathrm{mol\,N/l})^{-1}$ both steady state and large amplitude antiphase limit cycle are stable. They are separated by an unstable limit cycle, which emerges from the steady state in a subcritical Hopf-bifurcation and falls onto the stable limit cycle in a cyclic-fold bifurcation. Below $1/K_B = 0.1\,(\mu\mathrm{mol\,N/l})^{-1}$ the steady state is unstable and below $1/K_B = 0.075\,(\mu\mathrm{mol\,N/l})^{-1}$ reaches the region where B goes extinct and the coexistence attractor therefore becomes unstable. (b) Below $p_B = 0.22$ only the antiphase cycling is stable, above the steady state becomes stable in a supercritical Hopf bifurcation. Between $p_B = 0.62$ and $p_B = 0.68$ both steady state and large amplitude antiphase limit cycle are stable. They are separated by an unstable limit cycle emerging from the steady state in a subcritical Hopf-bifurcation and falling onto the stable limit cycle in a cyclic-fold bifurcation. Above $p_B = 0.75$ the steady state reaches the region where B goes extinct and the coexistence attractor therefore becomes unstable.

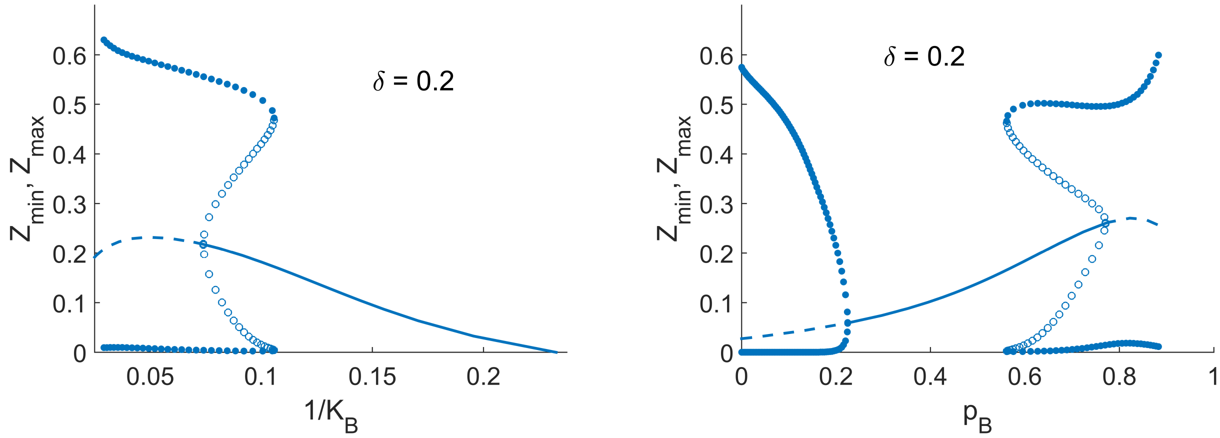

(a) Fixed predation risk $p_\mathrm{B} = 0.5$, variation along the competitiveness $1/K_B$

(b) Fixed competitiveness $1/K_B = 0.125\,(\mu\mathrm{mol\,N/l})^{-1}$, variation along the predation risk p_B

Figure A2.9 Plot specifics as in Fig. A2.8, but at a dilution rate of $\delta = 0.2\ \mathrm{d}^{-1}$.

A3 Chapter 4 - Appendix

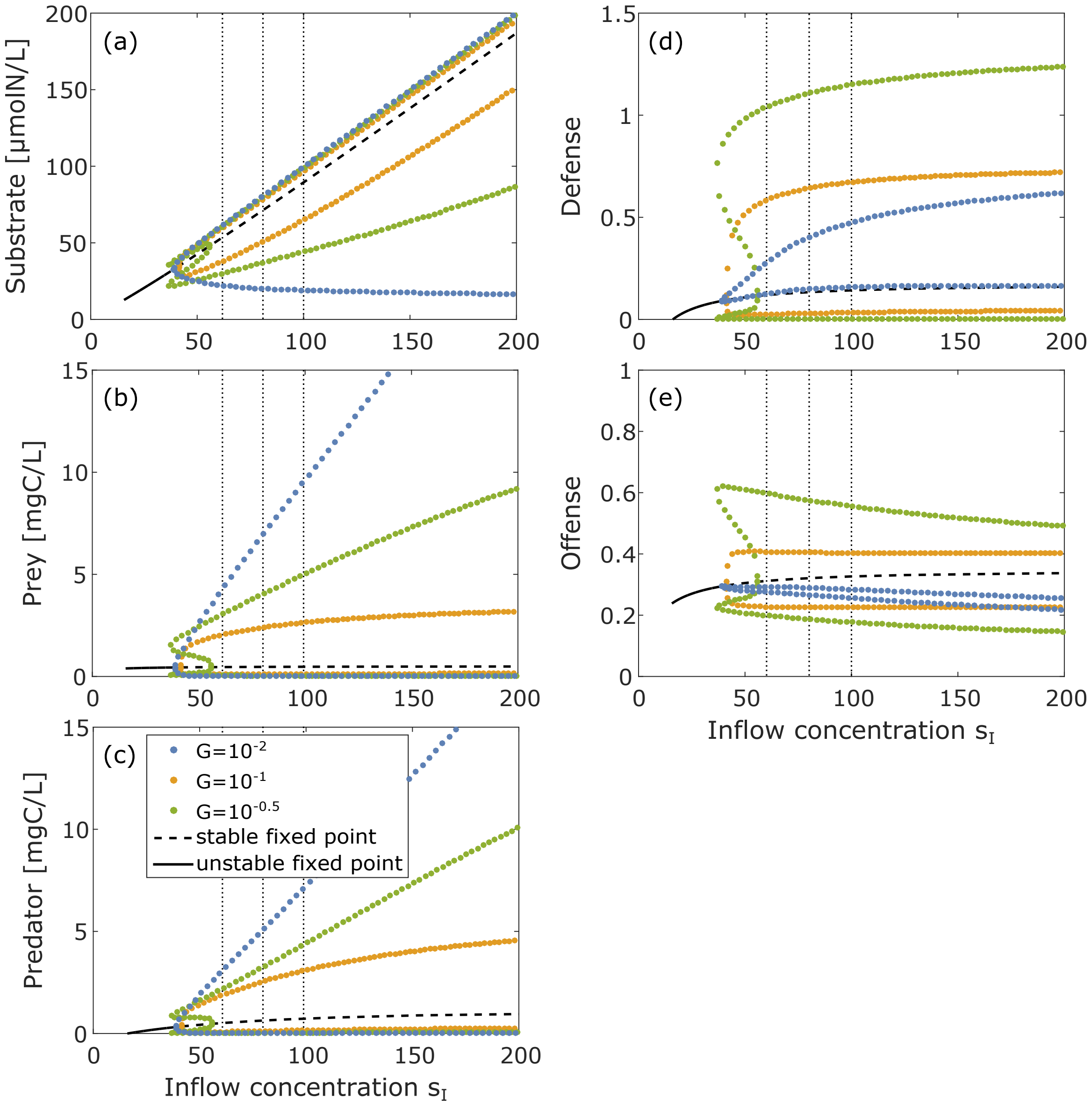

Figure A3.1 Bifurcation diagrams along the chemostat inflow concentration s_I as the bifurcation parameter for an intermediate dilution rate of $\delta = 0.4\,\mathrm{d}^{-1}$ for (a) substrate, (b) prey, (c) predator, (d) prey defense and (e) predator offense with different speeds of adaptation G. The stability of the fixed point is drawn for $G = 10^{-2}$, while the location of the Hopf bifurcation along s_I changes with G. $G = 10^{-3}$ is omitted for clarity. The dotted lines mark the reference inflow concentration s_r around which the press perturbations occur in Fig. 4.4 with $\pm 20\%$.

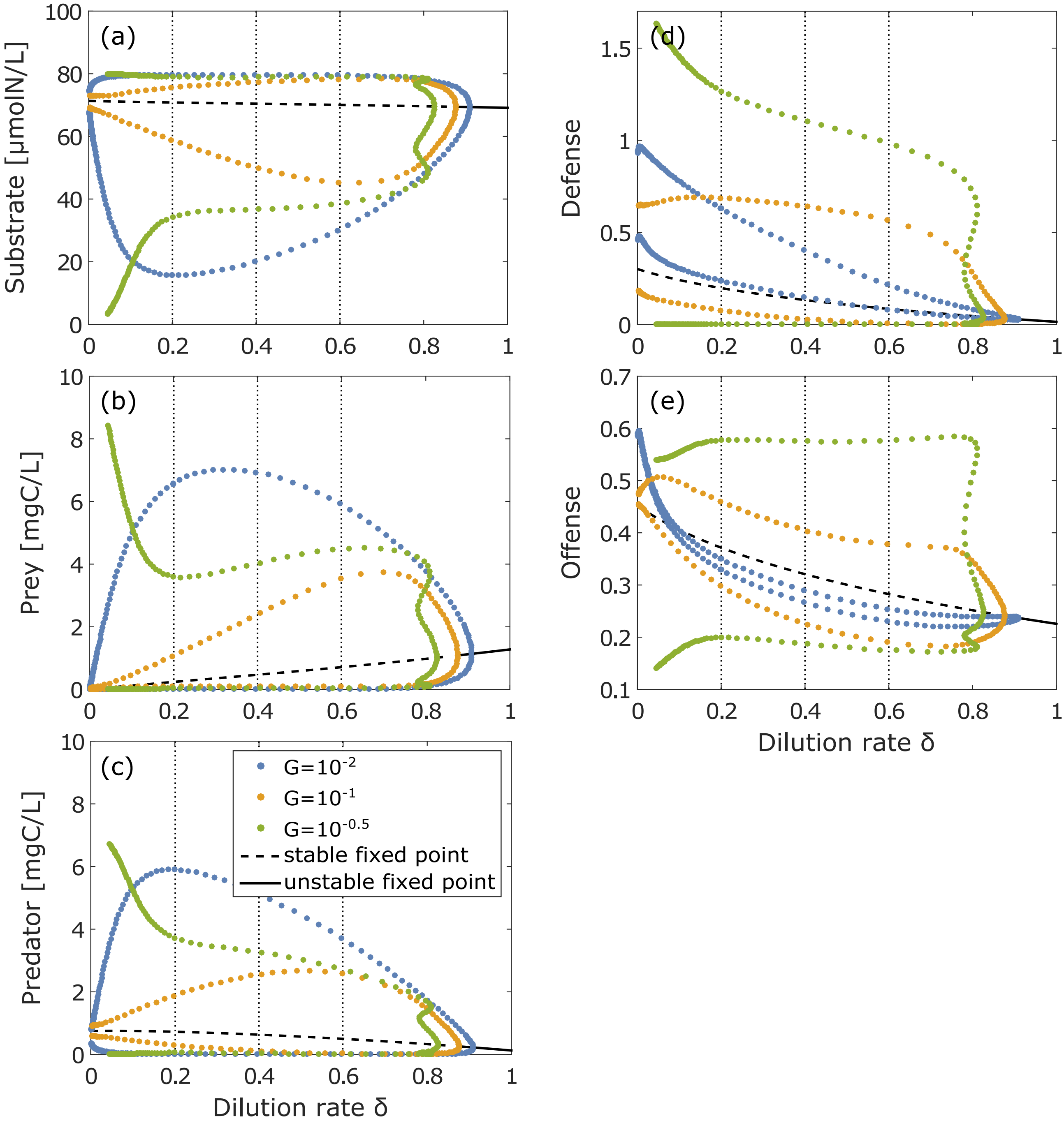

Figure A3.2 Bifurcation diagrams along the chemostat dilution rate δ as the bifurcation parameter for an intermediate inflow concentration of $s_I = 80\,\mu\mathrm{mol\,L}^{-1}$. Further plot specifics as in Suppl. Fig. A3.1.

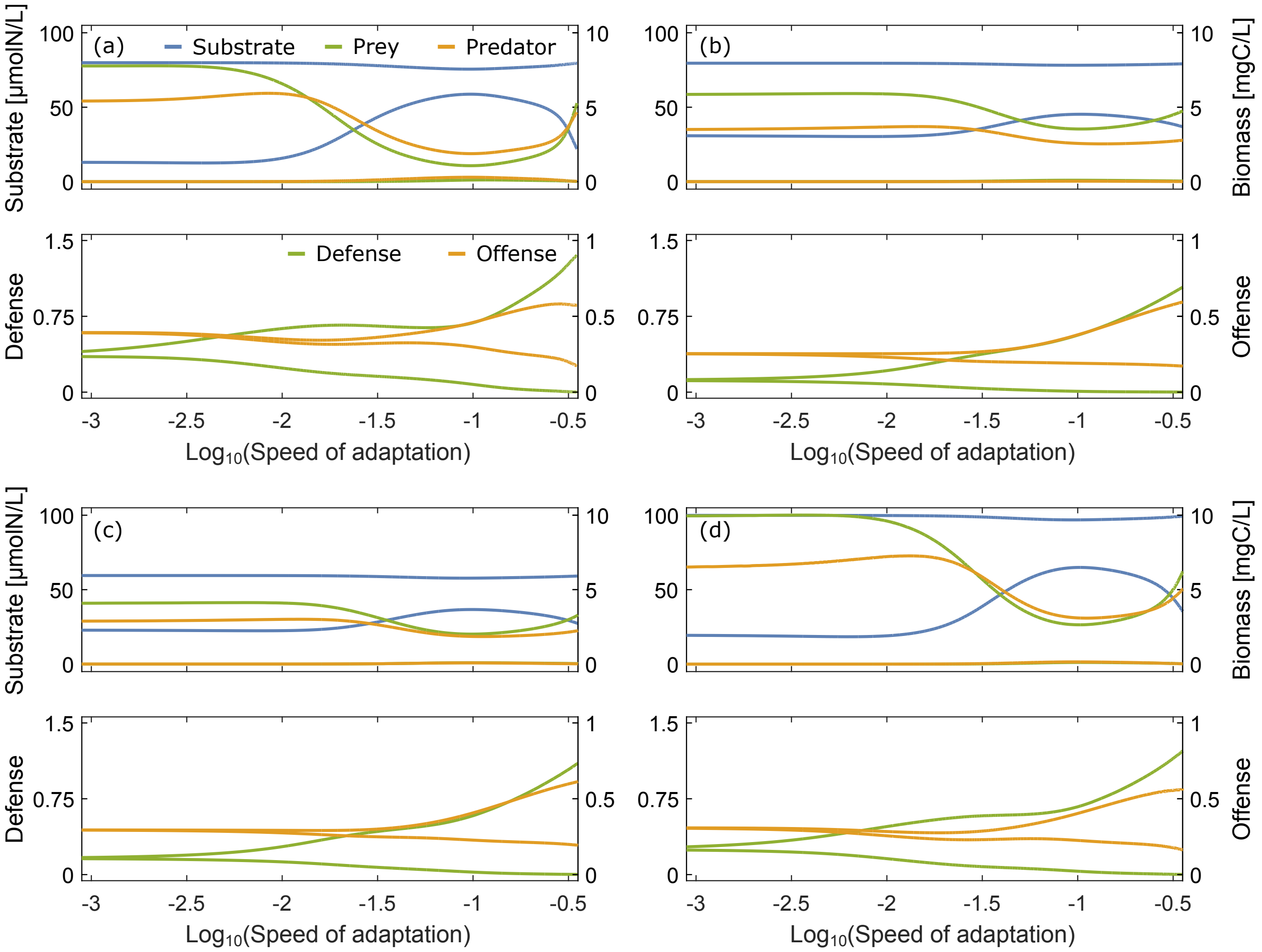

Figure A3.3 Bifurcation diagrams along the speed of adaptation G as the bifurcation parameter to cover different combinations of dilution rates δ and inflow concentrations s_I. Low and high dilution rates are combined with intermediate inflow concentrations and intermediate dilution rates are combined with low and high inflow concentrations, to complement Fig. 4.3, where both parameters are at intermediate values. (a) $\delta = 0.2\,\mathrm{d}^{-1}$ and $s_I = 80\,\mathrm{\mu mol\,L}^{-1}$, (b) $\delta = 0.6\,\mathrm{d}^{-1}$ and $s_I = 80\,\mathrm{\mu mol\,L}^{-1}$, (c) $\delta = 0.4\,\mathrm{d}^{-1}$ and $s_I = 60\,\mathrm{\mu mol\,L}^{-1}$, (d) $\delta = 0.4\,\mathrm{d}^{-1}$ and $s_I = 100\,\mathrm{\mu mol\,L}^{-1}$. The four different regimes (R1-R4) defined in Fig. 4.3 are apparent for all parameter combinations.

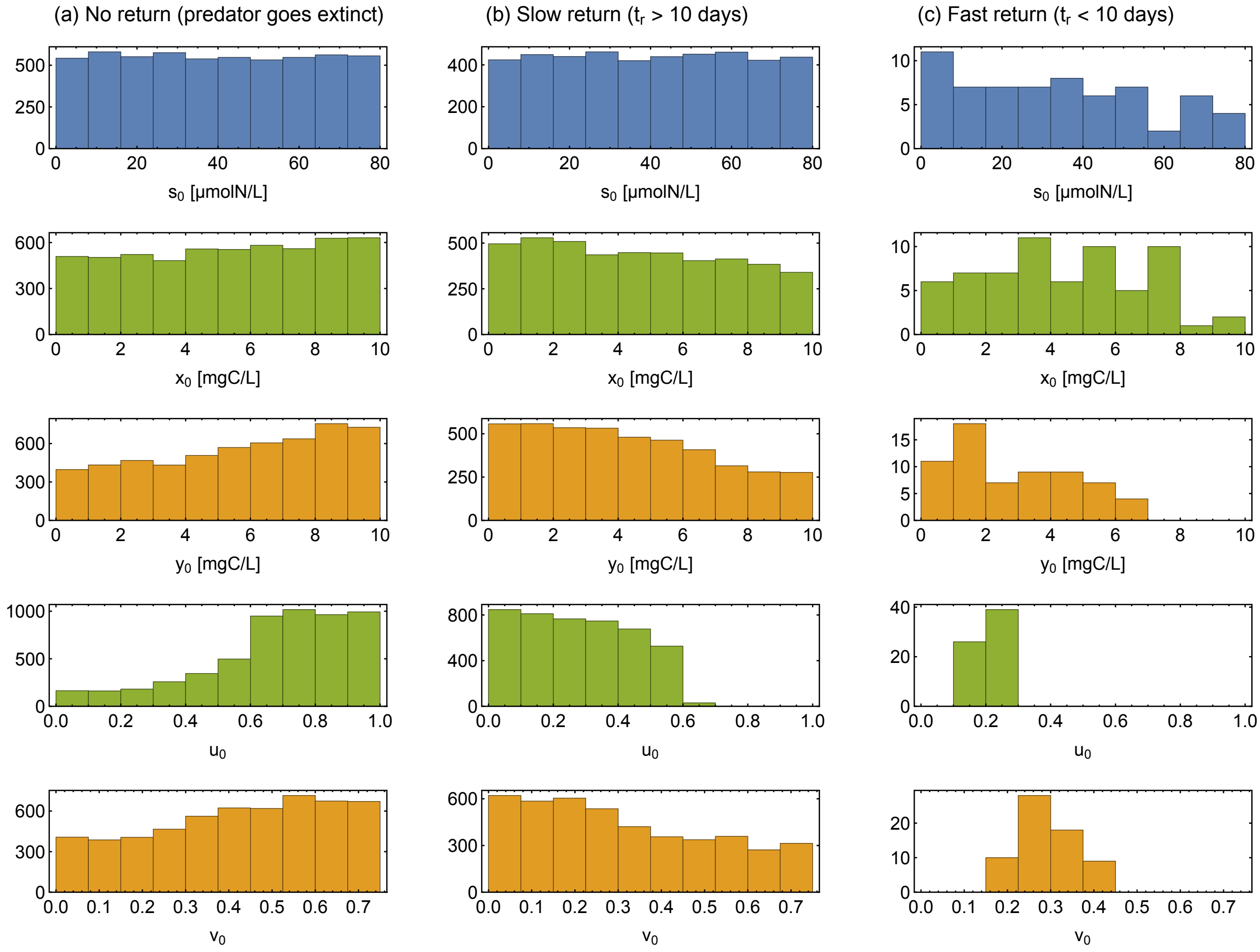

Figure A3.4 Histograms of the pulse perturbations, i.e. the random initial conditions for substrate s_0, prey x_0, predator y_0, defense u_0 and offense v_0, in regime R1 if all state variables are targeted, separated by extinctions (left column), slower returns (middle column) and faster returns (right column). Fast returns occur only if the traits are only slightly perturbed. Extinctions are more likely if the trajectory is perturbed to high biomasses and high trait values. Substrate perturbation is of minor importance.

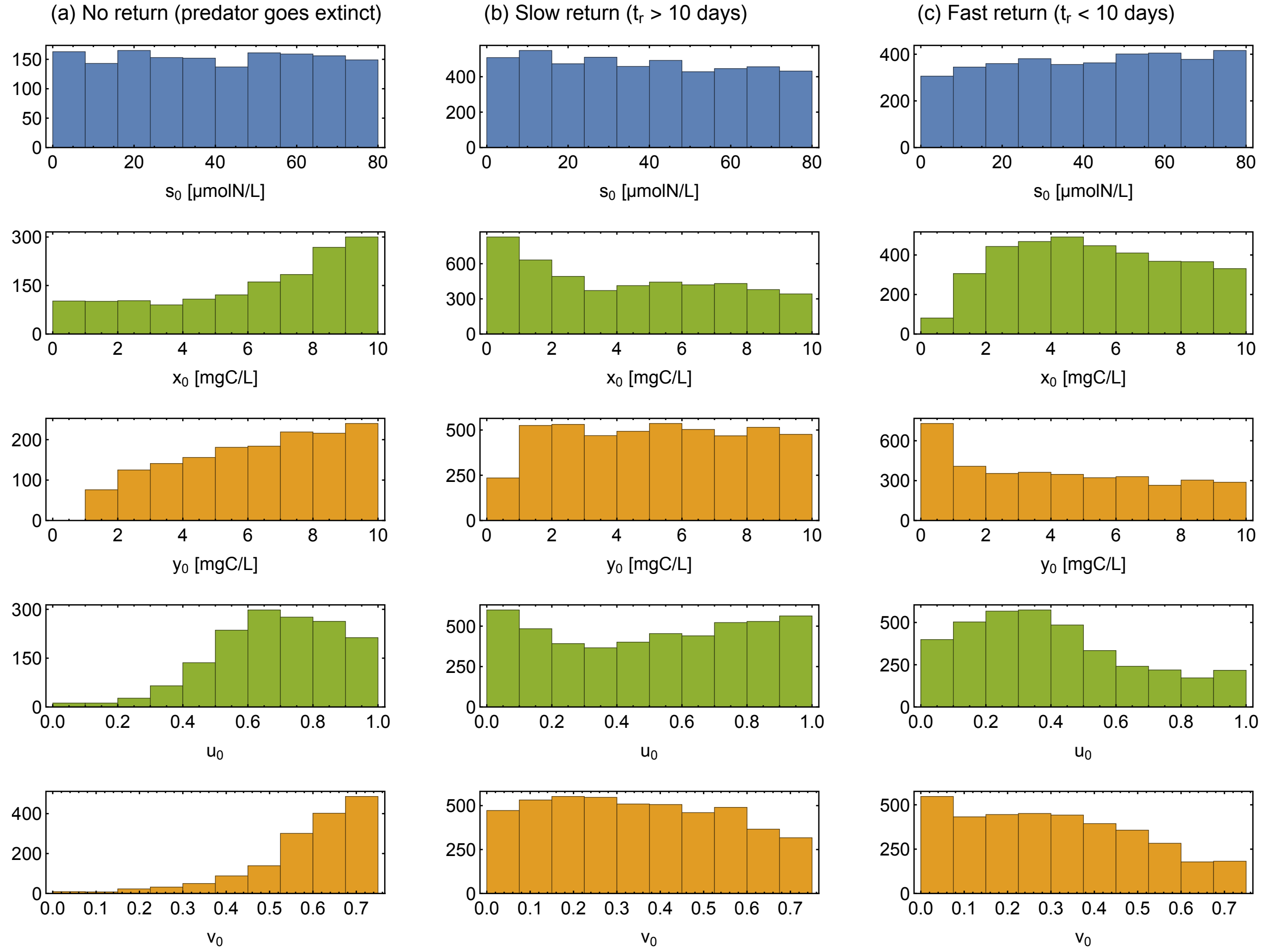

Figure A3.5 Histograms of the pulse perturbations, i.e. the random initial conditions, in regime R4 if all state variables are targeted. Further specifics as in Suppl. Fig. A3.4. Also here, faster returns are more likely for small perturbations. Extinctions are more likely if the trajectory is perturbed to high biomasses and high trait values.

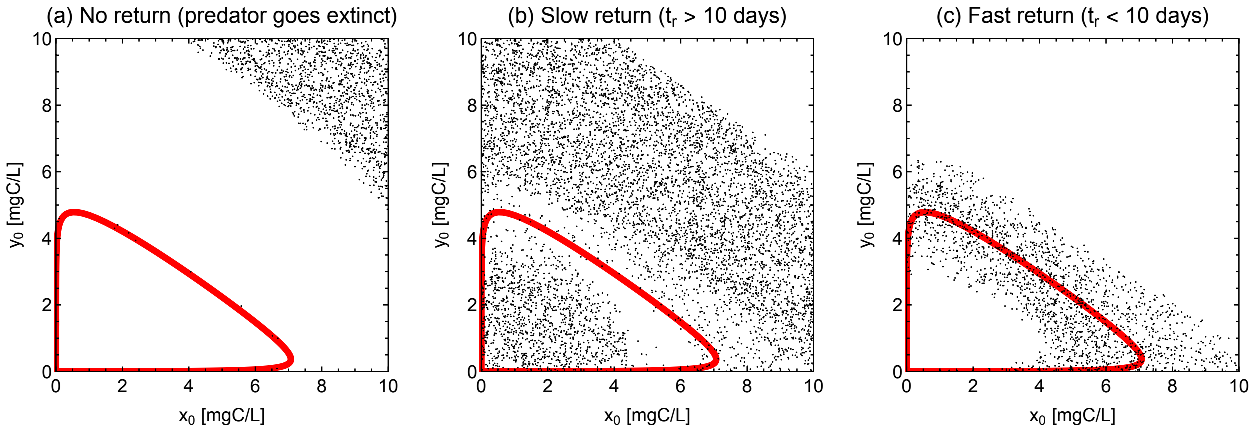

Figure A3.6 Scatter plots of the perturbed prey and predator biomasses x_0 and y_0 from pulse perturbations to substrate, prey and predator at $G = 10^{-3}$ (Fig. 4.6c-d). The respective attractor is shown in red. The perturbation results in either (a) predator extinction, (b) large or (c) small return times t_r. Extinctions occur if the trajectory is perturbed to high biomasses. Returns are faster if the displacement from the attractor is small.

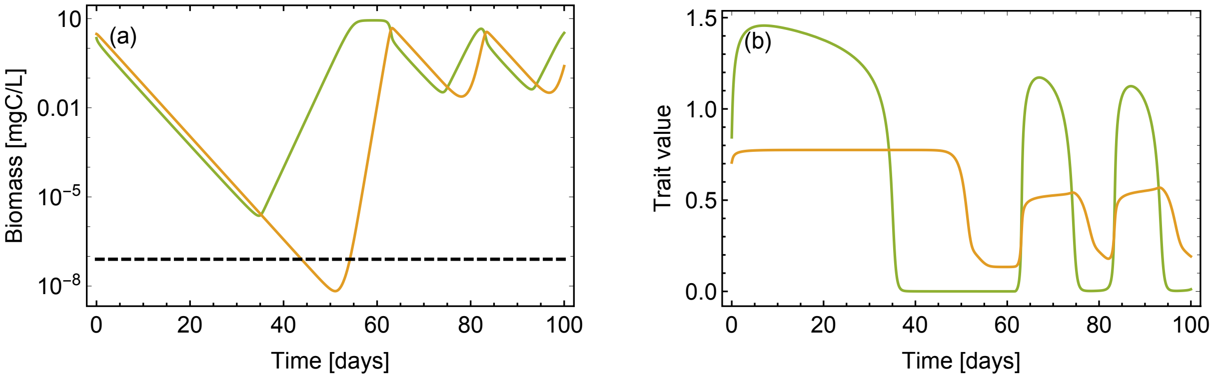

Figure A3.7 Dynamics of an exemplary extinction event after a pulse perturbation to the traits ($u_0 = 0.844$ and $v_0 = 0.706$) at $G = 10^{-0.5}$, showing the transient after the perturbation. The initial conditions of the biomasses, which are not targeted by the perturbation, are marked in black in Suppl. Fig. A3.8. (a) Prey (green) and predator biomasses (orange) and (b) defense (green) and offense (orange) move far away from the attractor following the perturbation. Eventually, the predator biomass drops below the black dashed line in (a) marking the extinction treshold.

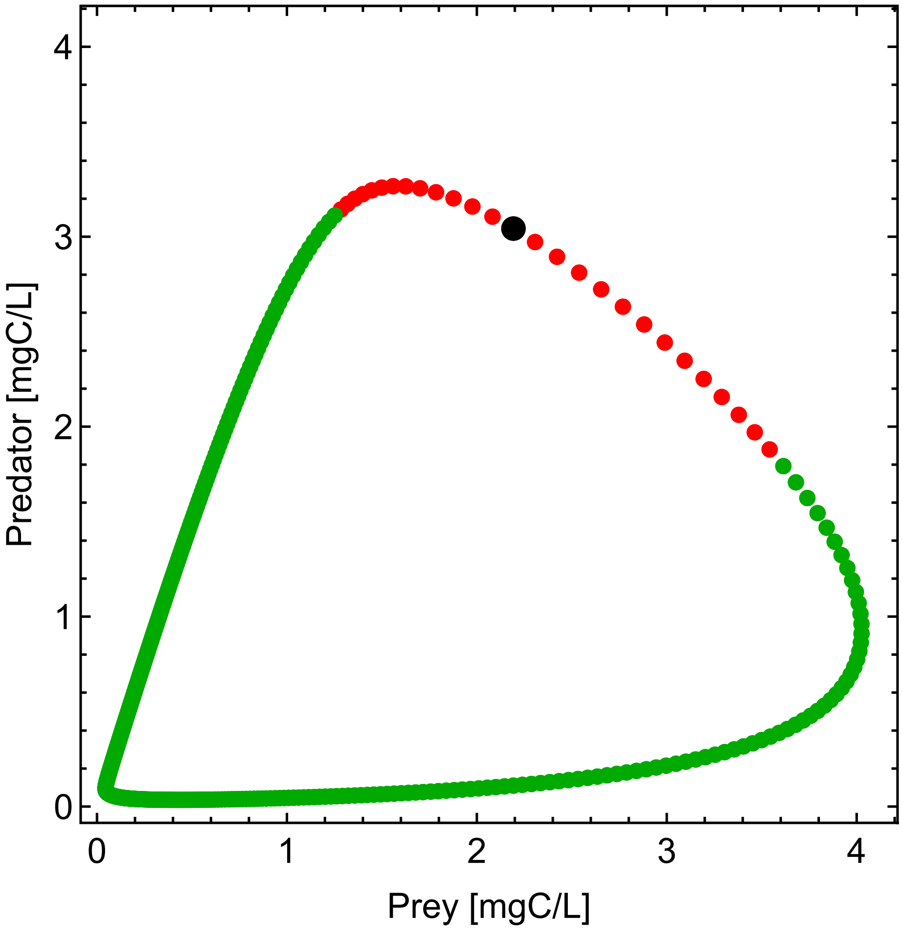

Figure A3.8 Effect of the choice of the position of non-targeted state variables on the attractor on the extinction risk following a pulse perturbation to a subset of the state variables. Here, defense and offense were perturbed to $u_0 = 0.844$ and $v_0 = 0.706$ at $G = 10^{-0.5}$. Green points mark choices for the biomasses where the predator persists, for red points it goes extinct. The transient dynamics for the combination marked by a black point are shown in Suppl. Fig. A3.7.

A4 Chapter 5 - Appendix

Parameter choice

Parameters for the maximum and minimum impact scenarios

Reports on algal exudation are highly variable. A meta-analysis found that the ratio of exudates relative to primary production varies between 2.82% and 42.1%, whereas 10 out of 16 systems that were included in the analysis had values above 10% (Baines and Pace 1991). Thus, we set the minimum exudation to $e_{\min} = 0.1$. For bacteria-suppressing conditions we set a maximum exudation of $e_{\max} = 0.2$, under favouring conditions, we assumed $e_{\max} = 0.4$. In another meta-analysis bacterial growth efficiencies on carbon that was excreted by phytoplankton were found to range from 0.3 to 0.8 (del Giorgio and Cole 1998). This corresponds to values for the respiration parameter r_B between 0.2 and 0.7. Accordingly, we set the bacterial respiration to $r_B = 0.7$ for the bacteria-suppressing conditions, but remain conservative and only set $r_B = 0.4$ for the bacteria-favouring scenario, as the carbon pool in our study also consists of rotifer excretion which is typically not as easily processible as algal exudates. Rotifer gross growth efficiency was found to range from 0.1 to 0.4 (Straile 1997). This also includes rotifer respiration r_R, which we set to 0.5 (Humphreys 1979), and therefore corresponds to carbon assimilation efficiencies between 0.2 and 0.8. Again, we remain conservative and choose $\varepsilon = 0.4$ for bacteria-suppressing conditions and $\varepsilon = 0.7$ for bacteria-favouring conditions.

Chemostat parameters

In an experiment, the parameters for dilution rate and resource nitrogen concentration in the inflow medium have to be set according to the needs of the species under study. The setting for the dilution rates should be reasonable in comparison to the typical prey and predator growth rates, so that both are able to achieve substantial positive net growth. For fast growing prey, such as *Chlorella* in Fussmann et al. (2000), higher dilution rates are possible, but also examples of very low dilution rates exist and are equally valid (Vadstein et al. 2003). The same reasoning applies to the inflow concentration where also different values are regularly used and adjusted to the species and research goals (Fussmann et al. 2000; Becks et al. 2010). Hence, we cover a large range of δ and N_I in our analysis.

Algae parameters

Generally, algal morphology is divers and results in broad possible parameter ranges. We chose to parametrize the algae according to *Monoraphidium minutum*, which is used as food to sustain our lab cultures of *Brachionus calyciflorus* and has also been used by others as prey in experiments with zooplankton (Rothhaupt 1990b; Rothhaupt 1992). It is generally similar to other small green algae like *Chlorella* or *Chlamydomonas*, which are also commonly used in chemostat experiments (Yoshida et al. 2003; Becks et al. 2010). Typically, when grown alone in a chemostat with an inflow concentration of $N_I = 80\,\mu\mathrm{molN/L}$ and a dilution rate of $\delta = 0.55\,\mathrm{d}^{-1}$ *Monoraphidium* will achieve maximum biomass densities around $10\,\mathrm{mgC/L}$ and cell densities of $1.75 \times 10^9\,\mathrm{cells/L}$ (unpublished data, personal communication G. Weithoff, S. Schälicke). This results in an approximate per-cell carbon content of $\omega_{A,C} = 6\,\mathrm{pgC}$. Making the simplifying assumption that all free nitrogen in the chemostat is taken up by the algae, this results in a per-cell nitrogen content of $\omega_{A,N} = 4.6 \times 10^{-8}\,\mu\mathrm{molN}$. Under the same assumption, the algal growth rate and half-saturation constant were estimated from the initial growth phase in a chemostat to $\beta_A = 1.9\,\mathrm{d}^{-1}$ and $H_A = 49\,\mu\mathrm{molN/L}$ (unpublished data, Svenja Schälicke).

Bacteria parameters

Also bacteria are highly diverse in the traits that determine growth under chemostat conditions. Large size ranges were reported for bacteria from a eutrophic lake (Gaedke et al. 2004). We chose the average on the log-scale of this study, which results in a carbon content per cell of $\omega_{B,C} = 60\,\mathrm{fgC}$, which also agrees with marine bacterioplankton grown in batch cultures (Vrede et al. 2002). Here, depending on nutrient limitation, the bacteria contained between $39 \pm 3\,\mathrm{fgC}$ per cell under carbon limitation and $92 \pm 5\,\mathrm{fgC}$ per cell under nitrogen limitation. In a chemostat that is run under nitrogen-limiting conditions the bacteria are co-limited by carbon and nitrogen. When the bacterial biomass is low and the carbon pool is high, nitrogen limitation will prevail. While the bacteria consume the carbon pool, nitrogen limitation will become dominant. This results in a range for the atomic C:N ratio, which was found to be 3.8 ± 0.1 under carbon limitation and 7.5 ± 1.2 under nitrogen limitation (Vrede et al. 2002). Since we worked with fixed C:N ratios, we chose the average of those two values, which yields a nitrogen content per cell of $\omega_{B,N} = 8.8 \times 10^{-10}\,\mu\mathrm{molN}$. Bacterial maximum growth rates cover wide ranges (Morris and Lewis 1992). In this study, the authors observed maximum growth rates as high as $1.7\,\mathrm{d}^{-1}$ during midsummer, but only $0.24\,\mathrm{d}^{-1}$ during winter. Bacteria are better competitors for phosphorus at low phosphorus concentrations, while *Monoraphidium* achieves higher uptake rates at high phosphorus concentrations (Rothhaupt 1992). Assuming that this coincides with growth rate and holds also for nitrogen, bacteria have a smaller maximum growth rate, but also a lower nitrogen half-saturation constant than *Monoraphidium*. Thus, again we chose the average of the above values and set the bacterial growth rate $\beta_A = 1\,\mathrm{d}^{-1}$, which ensures that *Monoraphidium* is able to outcompete the bacteria at high nutrient concentrations. We set the bacterial nitrogen half-saturation constant $H_{B,N}$ to $1/10$th of the algae, which yields $H_{B,N} = 4.9\,\mu\mathrm{molN/L}$ and makes the bacteria better competitors for nitrogen when it is scarce. The bacterial half-saturation for organic carbon was taken from literature, $H_{B,C} = 0.83\,\mu\mathrm{molC/L}$ (Tittel et al. 2012).

Zooplankton parameters

We chose the rotifer *Brachionus calyciflorus* as the model organism in our study as it is a commonly used predator in chemostat experiments (Fussmann et al. 2000; Shertzer et al. 2002; Becks et al. 2012; Declerck et al. 2015). In a typical chemostat with $N_I = 80\,\mu\mathrm{molN/L}$ and $\delta = 0.55\,\mathrm{d}^{-1}$ and population cycles, the predator reaches densities between 60 and $70\,\mathrm{Ind/mL}$ (unpublished data, personal communication G. Weithoff). Assuming that during such a peak all available nitrogen in the chemostat is concentrated in the predator, this results in a per-capita nitrogen content $\omega_{R,N} = 1.2 \times 10^{-3}\,\mu\mathrm{molN/L}$. Using a published C:N ratio for *B. calyciflorus* of 5.6 (Jensen et al. 2006), this results in a per-capita carbon content $\omega_{R,C} = 6.7 \times 10^{-3}\,\mu\mathrm{molC}$ which corresponds to $80\,\mathrm{ngC}$. The dry weights for this species range between 100 and $450\,\mathrm{ng}$ (Dumont et al. 1975). This fits with our assumption of $80\,\mathrm{ngC}$ as typically about half of the dry weight consists of carbon. The maximum ingestion rate was taken from literature as $288\,\mathrm{ngC/Ind/d}$ (Rothhaupt 1990a) and was converted to a maximum specific ingestion rate of $G = 3.6\,\mathrm{d}^{-1}$ using the per-capita carbon content. In approximate agreement with Fussmann et al. (2000), who chose a rotifer half-saturation constant $H_R = 15\,\mu\mathrm{molN/L}$, we set H_R to $195\,\mu\mathrm{molC/L}$, which can be translated to $18\,\mu\mathrm{molN/L}$ by using the C:N ratio of the algae in our study.

Derivation of the exudation

We assume that the rate r_{growth} at which an alga grows in units of carbon is determined by a three-step process. First, organic carbon has to be fixed which happens at rate r_{fix}. Secondly a portion of this organic carbon is exudated at rate $e_{\mathrm{dyn}}\,r_{\mathrm{fix}}$. Finally the remaining carbon $(1 - e_{\mathrm{dyn}})\,r_{\mathrm{fix}}$ may be used to build new biomass, depending on the nitrogen availability given by the Monod term $\frac{N}{H_A+N}$.

$$r_{\mathrm{growth}} = (1 - e_{\mathrm{dyn}})\,r_{\mathrm{fix}}\,\frac{N}{H_A + N} \tag{A4.1}$$

The portion of organic carbon that is exudated increases under nitrogen limitation, given by $\left(1 - \frac{N}{H_A+N}\right)$. We assume that the exudation e_{dyn} is a linear function of the nitrogen limitation and bounded between a minimum $e_{\min}$ and a maximum $e_{\max}$ (Fig. A4.1a).

$$e_{\mathrm{dyn}} = (e_{\max} - e_{\min}) \left(1 - \frac{N}{H_A + N}\right) + e_{\min} \tag{A4.2}$$

The flux of exudated carbon equals

$$r_{\mathrm{exud}} = e_{\mathrm{dyn}}\, r_{\mathrm{fix}} \tag{A4.3}$$

We assume that the production of organic carbon operates at a fixed rate. It is measured if nitrogen is not limiting, i.e. $\frac{N}{H_A+N} = 1$, as the maximum per capita growth rate in units of carbon and it follows from Eqs. A4.1 and A4.2 that

$$\begin{aligned} r_{\max\,\mathrm{growth}} &= \omega_{A,\,C}\, \beta_A \\ &= r_{\mathrm{fix}}\, (1 - e_{\min}) \end{aligned}$$

and therefore

$$r_{\mathrm{fix}} = \frac{1}{1 - e_{\min}} \omega_{A,\,C}\, \beta_A$$

With Eq. A4.3 the per capita exudation rate in unites of carbon becomes

$$r_{\mathrm{exud}} = \frac{e_{\mathrm{dyn}}}{1 - e_{\min}}\, \omega_{A,\,C}\, \beta_A$$

The per capita growth rate under nitrogen limitation with exudation included (Eq. A4.1) thus becomes

$$\begin{aligned} r_{\mathrm{growth}} &= \omega_{A,\,C}\, \beta_A \frac{1 - e_{\mathrm{dyn}}}{1 - e_{\min}}\, \frac{N}{H_A + N} \\ &= \omega_{A,\,C}\, F_A \end{aligned}$$

For plots of the exudation rate and growth rate at different maximal exudation ratios see Suppl. Fig. A4.1.

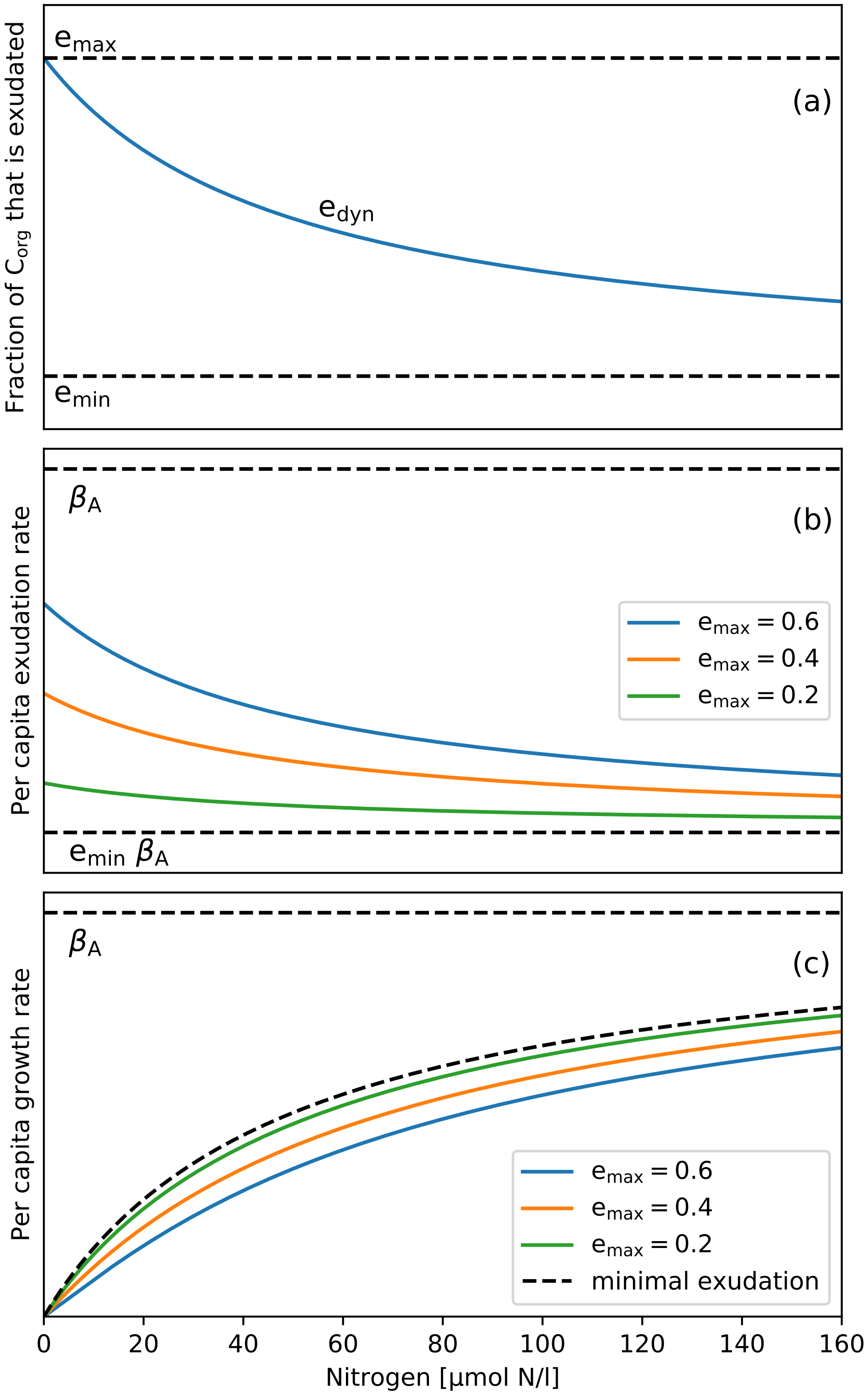

Figure A4.1 Effect of the exudation model for a half-saturation constant of $H_A = 49\,\mu\mathrm{mol N/L}$ and a minimal exudation of $e_{\min} = 0.1$. (a) Fraction of fixed carbon that is exudated. (b) Carbon exudation rate relative to the realized per-capita growth rate β_A. (c) Per capita growth rate. The dashed black line represents growth that is only affected by minimal exudation.

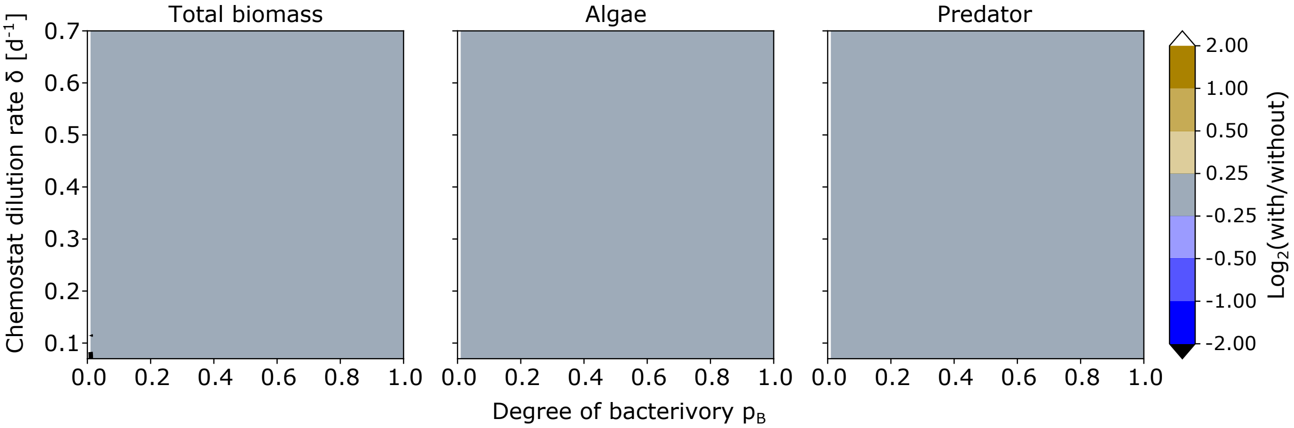

Figure A4.2 Effect size of bacterial presence under bacteria-suppressing conditions: $e_{\max} = 0.2$, $r_B = 0.7$ and $\varepsilon = 0.7$. The effect size is defined as the logarithmic ratio to base 2 of the mean biomasses with and without bacteria.

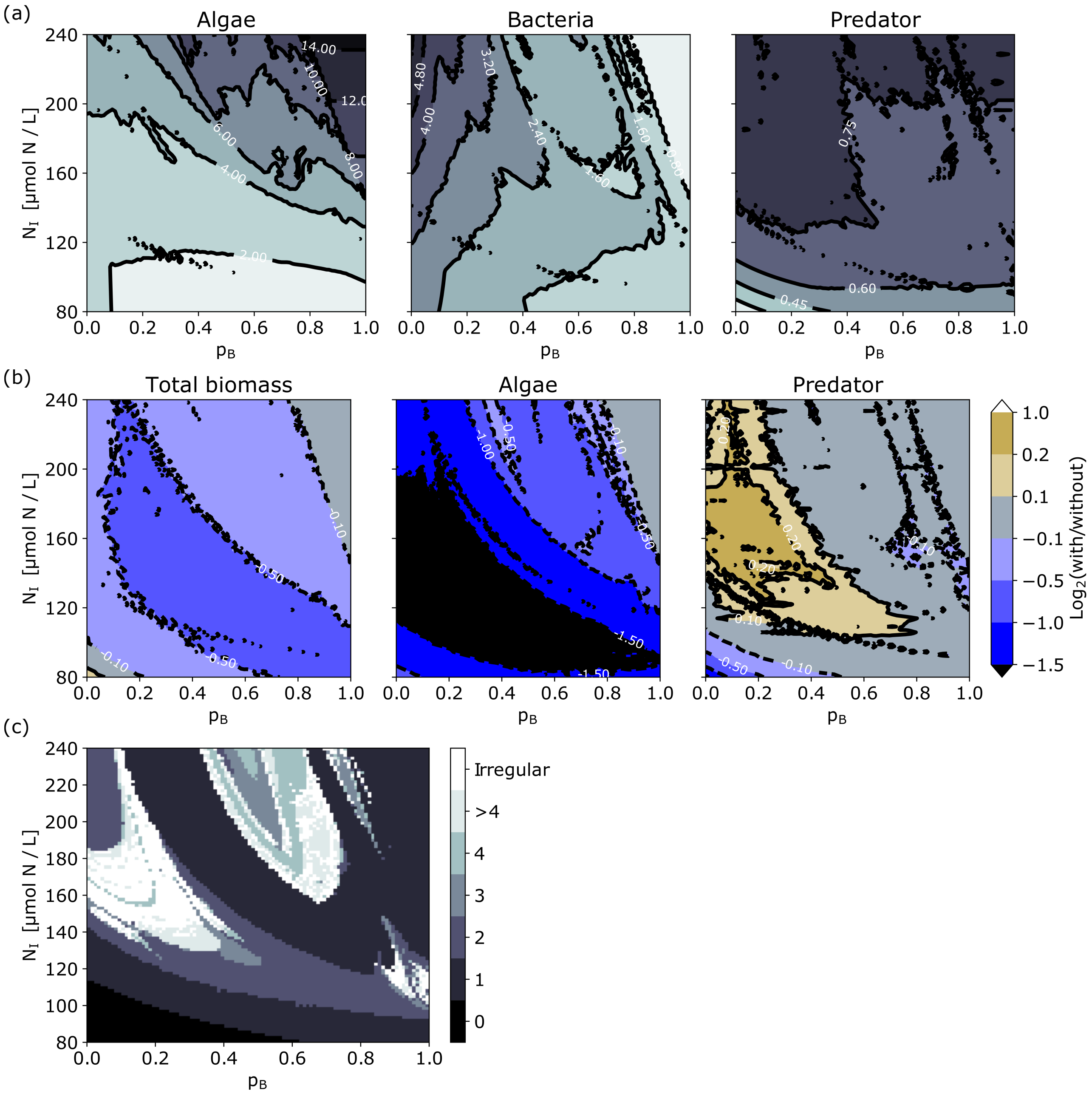

Figure A4.3 Parameter space spanned by degree of bacterivory p_B and nutrient inflow concentration N_I under favouring conditions at a dilution rate of $\delta = 0.35\,\mathrm{d}^{-1}$ for (a) mean biomasses, (b) effect size of bacterial presence and (c) types of dynamics characterized by the number of algae maxima per repetitive unit.

Bibliography

Baines, S. B. and Pace, M. L. (1991). The production of dissolved organic matter by phytoplankton and its importance to bacteria: Patterns across marine and freshwater systems. *Limnol. Oceanogr.* 36: 1078–1090.

Becks, L., Ellner, S. P., Jones, L. E., and Hairston Jr, N. G. (2010). Reduction of adaptive genetic diversity radically alters eco-evolutionary community dynamics. *Ecol. Lett.* 13: 989–997.

Becks, L., Ellner, S. P., Jones, L. E., and Hairston, N. G. (2012). The functional genomics of an eco-evolutionary feedback loop: Linking gene expression, trait evolution, and community dynamics. *Ecol. Lett.* 15: 492–501.

Declerck, S. A. J., Malo, A. R., Diehl, S., et al. (2015). Rapid adaptation of herbivore consumers to nutrient limitation: eco-evolutionary feedbacks to population demography and resource control. *Ecol. Lett.* 18: 553–562.

Dumont, H. J., Van de Velde, I., and Dumont, S. (1975). The dry weight estimate of biomass in a selection of Cladocera, Copepoda and Rotifera from the plankton, periphyton and benthos of continental waters. *Oecologia* 19: 75–97.

Fussmann, G. F., Ellner, S. P., Shertzer, K. W., and Hairston, N. G. J. (2000). Crossing the Hopf Bifurcation in a Live Predator-Prey System. *Science* 290: 1358–1360.

Gaedke, U., Seifried, A., and Adrian, R. (2004). Biomass Size Spectra and Plankton Diversity in a Shallow Eutrophic Lake. *Int. Rev. Hydrobiol.* 89: 1–20.

del Giorgio, P. A. and Cole, J. J. (1998). Bacterial growth efficiency in natural aquatic systems. *Annu. Rev. Ecol. Syst.* 29: 503–541.

Humphreys, W. F. (1979). Production and respiration in animal populations. *J. Anim. Ecol* 48: 427–453.

Jensen, T. C., Anderson, T. R., Daufresne, M., and Hessen, D. O. (2006). Does excess carbon affect respiration of the rotifer Brachionus calyciflorus Pallas? *Freshw. Biol.* 51: 2320–2333.

Morris, D. P. and Lewis, W. M. (1992). Nutrient limitation of bacterioplankton growth in Lake Dillon, Colorado. *Limnol. Oceanogr.* 37: 1179–1192.

Rothhaupt, K. O. (1992). Stimulation of phosphorus-limited phytoplankton by bacterivorous flagellates in laboratory experiments. *Limnol. Oceanogr.* 37: 750–759.

Rothhaupt, K. O. (1990a). Differences in particle size-dependent feeding efficiencies of closely related rotifer species. *Limnol. Oceanogr.* 35: 16–23.

Rothhaupt, K. O. (1990b). Population growth rates of two closely related rotifer species: effects of food quantity, particle size, and nutritional quality. *Freshw. Biol.* 23: 561–570.

Shertzer, K. W., Ellner, S. P., Fussmann, G. F., and Hairston, N. G. (2002). Predator-prey cycles in an aquatic microcosm: Testing hypotheses of mechanism. *J. Anim. Ecol.* 71: 802–815.

Straile, D. (1997). Gross growth efficiencies of protozoan and metazoan zooplankton and their dependence on food concentration, predator-prey weight ratio, and taxonomic group. *Limnol. Oceanogr.* 42: 1375–1385.

Tittel, J., Büttner, O., and Kamjunke, N. (2012). Non-cooperative behaviour of bacteria prevents efficient phosphorus utilization of planktonic communities. *J. Plankton Res.* 34: 102–112.

Vadstein, O., Olsen, L. M., Busch, A., Andersen, T., and Reinertsen, H. R. (2003). Is phosphorus limitation of planktonic heterotrophic bacteria and accumulation of degradable DOC a normal phenomenon in phosphorus-limited systems? A microcosm study. *FEMS Microbiol. Ecol.* 46: 307–316.

Vrede, K., Heldal, M., Norland, S., and Bratbak, G. (2002). Elemental Composition (C, N, P) and Cell Volume of Exponentially Growing and Nutrient-Limited Bacterioplankton. *Appl. Environ. Microbiol.* 68: 2965–2971.

Yoshida, T., Jones, L. E., Ellner, S. P., Fussmann, G. F., and Hairston, N. G. (2003). Rapid evolution drives ecological dynamics in a predator-prey system. *Nature* 424: 303–306.

B Further relevant publications

Different movement behaviour of male and female rotifers may be detected by video microscopy and machine learning

Ulrike Obertegger[1], Adam Cieplinski[2], Michael Raatz[3] and Pierluigi Colangeli[3]

[1] Department of Sustainable Agro-ecosystems and Bioresources, Research and Innovation Centre, Fondazione Edmund Mach, San Michele all'Adige, Italy; [2] Research Institute for Limnology, University of Innsbruck, Mondsee, Austria; [3] Department of Ecology and Ecosystem Modelling, University of Potsdam, Potsdam, Germany

Abstract

Swimming is of vital importance for aquatic organisms because it determines several aspects of fitness, such as encounter rates with food, predators, and mates. Generally, rotifer swimming speed is measured by manual tracking of the swimming paths filmed in videos. Recently, an open-source package has been developed that integrates different open-source software and allows direct processing and analysis of the swimming paths of moving organisms. Here, we filmed groups of females and males of *Keratella cochlearis* separately and in a mixed experimental setup. We extracted movement trajectories and swimming speeds and applied the classification method random forest to assign sex to individuals of the mixed setup. Finally, we used advanced statistical methods of movement ecology, namely a hidden Markov model, to investigate swimming states of females and males. When not discriminating swimming states, females swam faster than males, while when discriminating states males swam faster. Specifically, females and males showed two main states of movement with many individuals switching between states resulting in four modes of swimming. We suggest that switching between states is related to predator avoidance. Males of *K. cochlearis* especially exhibited switching between turning in a restricted area and swimming over longer distances. No mating or

other male–female interactions were observed. Our study elucidates the steps necessary for automatic analysis of rotifer trajectories with open-source software. Application of sophisticated software and analytical models will broaden our understanding of zooplankton ecology from the individual to the population level.

Obertegger, U., Cieplinski, A., Raatz, M., and Colangeli, P. (2018). Switching between swimming states in rotifers – case study Keratella cochlearis. *Mar. Freshw. Behav. Physiol.* 51: 159–173.

Estimating parameters from multiple time series of population dynamics using Bayesian inference

Benjamin Rosenbaum*[1][2], Michael Raatz*[3], Guntram Weithoff[3], Gregor F. Fussmann[4] and Ursula Gaedke[3]

[1] German Centre for Integrative Biodiversity Research (iDiv) Halle-Jena-Leipzig, Leipzig, Germany; [2] Institute of Biodiversity, Friedrich Schiller University Jena, Jena, Germany; [3] Department of Ecology and Ecosystem Modelling, Insitute for Biochemistry and Biology, University of Potsdam, Potsdam, Germany; [4] Department of Biology, McGill University, Montreal, Canada

* These authors contributed equally.

Abstract

1. Empirical time series of interacting entities, e.g. species abundances, are highly useful to study ecological mechanisms. Mathematical models are valuable tools to further elucidate those mechanisms and underlying processes. However, obtaining an agreement between model predictions and experimental observations remains a demanding task. As models always abstract from reality one parameter often summarizes several properties. Parameter measurements are performed in additional experiments independent of the ones delivering the time series. Transferring these parameter values to different settings may result in incorrect parametrizations. On top of that, the properties of organisms and thus the respective parameter values may vary considerably. These issues limit the use of a priori model parametrizations.

2. In this study, we present a method suited for a direct estimation of model parameters and their variability from experimental time series data. We combine numerical simulations of a continuous-time dynamical population model with Bayesian inference, using a hierarchical framework that allows for variability of individual parameters. The method is applied to a comprehensive set of time series from a laboratory predator-prey system that features both steady states and cyclic population dynamics.

3. Our model predictions are able to reproduce both steady states and cyclic dynamics of the data. Additionally to the direct estimates of the parameter values, the Bayesian approach also provides their uncertainties. We found that fitting cyclic population dynamics, which contain more information on the process rates than steady states, yields more precise parameter estimates. We detected significant variability among parameters of different time series and identified the

variation in the maximum growth rate of the prey as a source for the transition from steady states to cyclic dynamics.

4. By lending more flexibility to the model, our approach facilitates parametrizations and shows more easily which patterns in time series can be explained also by simple models. Applying Bayesian inference and dynamical population models in conjunction may help to quantify the profound variability in organismal properties in nature.

Rosenbaum, B., Raatz, M., Weithoff, G., Fussmann, G. F., and Gaedke, U. (2018). Estimating parameters from multiple time series of population dynamics using Bayesian inference. biorXiv.

C Curriculum vitae

Pages 170-173 contain private information and have thus been removed from this document.

Pages 170-173 contain private information and have thus been removed from this document.

Pages 170-173 contain private information and have thus been removed from this document.

Pages 170-173 contain private information and have thus been removed from this document.

Acknowledgements

I want to express my gratitude to both of my "PhD parents" Ursula Gaedke and Alexander Wacker for providing guidance where required, support where needed and freedom where wanted. You made this trip a challenging, but fruitful and enjoyable journey.

I am especially thankful to Elias Ehrlich for initiating this adventure into the field of Ecology, and providing invaluable help and advice once he had dragged me into it.

I am grateful for the successful collaboration with my Co-PhD student Svenja Schälicke that taught me to acknowledge how tricky experiments can be. I admire her endurance.

An often underappreciated aspect of modelling is that it can become very technical. I would like to thank Ruben Ceulemans for help with coding and the development of methods I could not have thought of alone. Such work often also requires profound technical support and Stefan Saumweber is to be praised for that – additionally to keeping the coffee supply chain running.

Often, valuable advice is received unconsciously in small but persistent doses. For this I would like to thank Toni Klauschies, Apostolos-Manuel Koussoroplis and Michael Sieber, who, during the many walks to and from the Mensa, provided me with a lot of guidance.

A special feature of our group is the combination of experimental and theoretical work. I tried to not only visit the laboratories for collecting money and signatures for gift cards, but also for practical insights to stitch my often patchy knowledge. Thus, I am grateful to Silvia Heim, Sabine Donath and Christina Schirmer for sharing their immense knowledge with me.

I also want to thank the so far unnamed co-authors of my papers, especially Pierluigi Colangeli, Guntram Weithoff, Ellen van Velzen and Benjamin Rosenbaum, for teaching me on topics ranging from rotifer physiology and life cycle over quantitative genetics to Bayesian statistics.

I have come to know that doing a PhD is hard work, but also a lot of fun. With many of the above people I got to enjoy intense Doppelkopf matches, emotional table football duels and convivial evenings in the pub. I want to thank everyone of them!

Often, doing a PhD also requires putting in long hours. Scheduling a family around this is challenging and I thank my parents and my parents-in-law for their efforts in making this work.

I am deeply grateful to my wife Larissa and my son Leon for being my harbour and my exhaustless source of energy.

Erklärung

Ich versichere hiermit, dass ich die vorliegende Arbeit selbstständig angefertigt und keine anderen als die angegebenen Hilfsmittel und Quellen verwendet habe.
Die Arbeit wurde an keiner anderen Hochschule im In- oder Ausland eingereicht.

Potsdam, 23. November 2018

Michael Raatz